AGES 437–548

ISSN 0003–2654

THE ROYAL SOCIETY OF CHEMISTRY

1841-1991

The Analyst

A monthly international journal dealing with all branches of the theory and practice of analytical chemistry, including instrumentation and sensors, and physical, biochemical, clinical, pharmaceutical, biological, environmental, automatic and computer-based methods

Vol.116 No.5 May 1991

The Analyst

The Analytical Journal of The Royal Society of Chemistry

The Analyst (ISSN 0003–2654) is published monthly by The Royal Society of Chemistry, Thomas Graham House, Science Park, Milton Road, Cambridge CB4 4WF, UK. All orders, accompanied with payment by cheque in sterling, payable on a UK clearing bank or in US dollars payable on a US clearing bank, should be sent directly to The Royal Society of Chemistry, Turpin Transactions Ltd., Blackhorse Road, Letchworth, Herts SG6 1HN, United Kingdom. Turpin Transactions Ltd., distributors, is wholly owned by the Royal Society of Chemistry. 1991 Annual subscription rate EC £246.00, USA $580, Rest of World £283.00. Purchased with *Analytical Abstracts* EC £551.00, USA $1299.00, Rest of World £634.00. Purchased with *Analytical Abstracts* plus *Analytical Proceedings* EC £648.00, USA $1527.00, Rest of World £745.00. Purchased with *Analytical Proceedings* EC £313.00, USA $738.00, Rest of World £360.00. Air freight and mailing in the USA by Publications Expediting Inc., 200 Meacham Avenue, Elmont, NY 11003.

USA Postmaster: Send address changes to: *The Analyst,* Publications Expediting Inc., 200 Meacham Avenue, Elmont, NY 11003. Second class postage paid at Jamaica, NY 11431. All other despatches outside the UK by Bulk Airmail within Europe, Accelerated Surface Post outside Europe. PRINTED IN THE UK.

Information for Authors

Full details of how to submit material for publication in *The Analyst* are given in the Instructions to Authors in the January issue. Separate copies are available on request.

The Analyst publishes papers on all aspects of the theory and practice of analytical chemistry, fundamental and applied, inorganic and organic, including chemical, physical, biochemical, clinical, pharmaceutical, biological, environmental, automatic and computer-based methods. Papers on new approaches to existing methods, new techniques and instrumentation, detectors and sensors, and new areas of application with due attention to overcoming limitations and to underlying principles are all equally welcome. There is no page charge.

The following types of papers will be considered:

Full research papers.

Communications, which must be on an urgent matter and be of obvious scientific importance. Rapidity of publication is enhanced if diagrams are omitted, but tables and formulae can be included. Communications receive priority and are usually published within 5–8 weeks of receipt. They are intended for brief descriptions of work that has progressed to a stage at which it is likely to be valuable to workers faced with similar problems. A fuller paper may be offered subsequently, if justified by later work. Although publication is at the discretion of the Editor, communications will be examined by at least one referee.

Reviews, which must be a critical evaluation of the existing state of knowledge on a particular facet of analytical chemistry.

Every paper (except Communications) will be submitted to at least two referees, by whose advice the Editorial Board of *The Analyst* will be guided as to its acceptance or rejection. Papers that are accepted must not be published elsewhere except by permission. Submission of a manuscript will be regarded as an undertaking that the same material is not being considered for publication by another journal.

Regional Advisory Editors. For the benefit of potential contributors outside the United Kingdom and North America, a Group of Regional Advisory Editors exists. Requests for help or advice on any matter related to the preparation of papers and their submission for publication in *The Analyst* can be sent to the nearest member of the Group. Currently serving Regional Advisory Editors are listed in each issue of *The Analyst.*

Manuscripts (four copies typed in double spacing) should be addressed to:

Harpal S. Minhas, Editor, *The Analyst,*
Royal Society of Chemistry,
Thomas Graham House,
Science Park, Milton Road,
CAMBRIDGE CB4 4WF, UK *or*:

Dr. J. F. Tyson
US Associate Editor, *The Analyst*
Department of Chemistry
University of Massachusetts
Amherst MA 01003, USA

Particular attention should be paid to the use of standard methods of literature citation, including the journal abbreviations defined in Chemical Abstracts Service Source Index. Wherever possible, the nomenclature employed should follow IUPAC recommendations, and units and symbols should be those associated with SI.

All queries relating to the presentation and submission of papers, and any correspondence regarding accepted papers and proofs, should be directed either to the Editor, or Associate Editor, *The Analyst* (addresses as above). Members of the Analytical Editorial Board (who may be contacted directly or via the Editorial Office) would welcome comments, suggestions and advice on general policy matters concerning *The Analyst.*

Fifty reprints are supplied free of charge.

PUBLISH IN THE ANALYST

Cambridge, 1991.

Dear Subscriber,

As a regular reader of *The Analyst* you probably know a fair amount about the journal. But did you know that *The Analyst*

- is the oldest English-language analytical science journal
- has the largest circulation of any European analytical science journal
- is truly international, going to over 90 countries worldwide, with US and Canadian sales equalling those in the UK
- accepts papers on all aspects of analytical chemistry
- is produced using full-time qualified professional editors, with a high standard of error detection (top in a recent independent survey of analytical chemistry journals)
- has no page or other charges, and provides authors with 50 free reprints
- uses peer review of submissions by two independent referees, and is backed by an internationally known editorial board
- now has a US Associate Editor, enabling North American submissions to be reviewed in their country of origin
- achieves rapid publication (5 months from acceptance to publication of papers, or 6–8 weeks for communications)?

If you did, you're probably already submitting your primary papers to *The Analyst*. If not, don't you think you should be? We welcome submissions in the areas stated below, and look forward to hearing from you.

Yours sincerely,

Harpal S. Minhas,
Editor

THE ANALYST
WELCOMES PAPERS ON:

- **Biochemical analysis**
- **Chemometrics**
- **Mass spectrometry**
- **Vibrational spectroscopy**
- **EPR and ESR**
- **Atomic & molecular absorption spectroscopy**
- **Chromatography**
- **Electrochemistry**

Editor, *The Analyst*, Harpal S. Minhas,
The Royal Society of Chemistry,
Thomas Graham House, Science Park,
Milton Road, Cambridge CB4 4WF, UK
Tel: 0223 420066. Fax: 0223 423623.
Tlx: 818293 ROYAL

US Associate Editor, Dr. J. F. Tyson,
Department of Chemistry,
University of Massachusetts, Amherst,
MA 01003, USA
Tel: 413 545 0195. Fax: 413 545 4490

ROYAL SOCIETY OF CHEMISTRY
Information Services

Editorial Manager, Analytical Journals: Judith Egan

Certification of a Reference Material for Aromatic Hydrocarbons in Tenax Samplers

Stefaan Vandendriessche and Bernardus Griepink
Commission of the European Communities, Community Bureau of Reference (BCR), Brussels, Belgium

Jacobus C. Th. Hollander, Johannes W. J. Gielen and Fred G. G. M. Langelaan
TNO, Division of Technology for Society, Delft, The Netherlands

Kevin J. Saunders
BP Research Centre, Sunbury-on-Thames, Middlesex TW16 7LN, UK

Richard H. Brown
OMHL3, Health and Safety Executive, 403 Edgware Road, London NW2 6LN, UK

A homogeneous and stable reference material consisting of aromatic hydrocarbons sorbed on Tenax in stainless-steel sample tubes has been prepared and certified. An initial feasibility trial established that a homogeneous and stable batch could be prepared. Part of this batch was used in an intercomparison, which allowed the identification of various sources of error. A second test batch was used in a second intercomparison in an attempt to improve the analytical performance of the participating laboratories. A third batch (of 1000 tubes) was then prepared and certified on the basis of analyses carried out in ten laboratories. The certified values for benzene, toluene and *m*-xylene are, respectively, 1.053 ± 0.014, 1.125 ± 0.015 and 1.043 ± 0.015 μg per tube. This Community Bureau of Reference (BCR) Certified Reference Material 112 is recommended for quality control and for calibration purposes.

Keywords: *Tenax; occupational hygiene; reference material; intercomparison; aromatic hydrocarbons*

National and international legislation prescribes that the exposure of individual workers to certain potentially harmful substances (defined as agents according to Directive 80/1107/EEC)[1] shall be assessed. If the assessment indicates that exposure is likely to be in the region of the relevant exposure limit, regular monitoring must be carried out.

Of the various techniques that are suitable for regular monitoring of personal exposure to a wide variety of organic vapours, a device commonly used is a sorption tube. In this technique a known volume of workplace air (usually from the worker's breathing zone) is drawn through the tube by means of a sampling pump, or a mass of analyte is collected by diffusion. The vapours collected are recovered by solvent or thermal desorption and determined, usually by gas chromatography (GC). The certified reference material (CRM) described [Community Bureau of Reference (BCR)[2]] is based on Tenax, a sorbent that is usually desorbed thermally. This is the first sorbent for which appropriate long-term stability has been demonstrated.

A CRM to be used for quality control or calibration should ideally closely match the material being analysed. However, it would be impractical to have CRMs to cover all possible combinations of organic solvents. A choice of representative analytes must therefore be made, and for the first certification, benzene, toluene and *m*-xylene have been chosen on the basis of their toxicity and wide usage throughout the world.

Experimental

Preparation of Homogeneously Charged Batches

The tubes used for the preparation of the test batches and for the production of CRM 112 were commercially available stainless-steel tubes which were cleaned and filled with Tenax as shown in Fig. 1. The tube dimensions were: length, 89 mm; o.d., 6.34 mm; and i.d., 5.0 mm. Proprietary brass caps with polytetrafluoroethylene (PTFE) ferrules were used to close the tubes. (Preliminary experiments had shown that the aluminium caps supplied with the tubes were inadequate for the purpose of long-term storage.)

The bed of Tenax (100 mg, 60–80 mesh) was 32 mm long and was retained at one end by a metal gauze and at the other end by a plug of quartz wool, a metal gauze and a spring.

All tubes were pre-conditioned for 16 h at 300 °C and with a helium flow of 30 ml min^{-1}. Each tube contained, before charging, less than 1 ng (the limit of detection of the method is 1 ng) of benzene, toluene and *m*-xylene.

Diffusion cells were used to blend known levels of benzene, toluene and *m*-xylene vapours into a stream of clean air. A known volume of this air was drawn through each tube. The apparatus used is represented schematically in Fig. 2.

The amounts of benzene, toluene and *m*-xylene (approximately 1 μg of each), the flow-rates and the volumes of air (approximately 1 l per tube) were such that saturation or breakthrough did not occur.

The following precautions were taken to ensure that all the tubes received the same mass of each vapour: (*i*) the temperature of diffusion cells was controlled to within ± 0.02 °C; (*ii*) the mass flows of air were controlled to within ± 0.2%; (*iii*) all tubes were charged in an uninterrupted period of time during which the atmospheric pressure (which influenced the rates of diffusion) varied only slightly (*e.g.*, the finally certified batch was charged in a period of 44 h in which the lowest and highest atmospheric pressures were 100.1 and 102.0 kPa); (*iv*) the total vapour content of the air was continuously monitored by use of a photoionization detector; and (*v*) the amount of air drawn through each tube was fixed by an electronic timer which operated the valves.

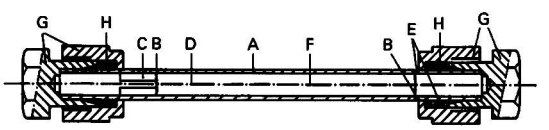

Fig. 1 Schematic representation of a sample of CRM 112. A, Stainless-steel tube; B, metal gauze; C, spring; D, quartz wool plug; E, grooves for O-rings; F, bed of Tenax (100 mg); G, Swagelok caps (brass); and H, PTFE ferrules

The volume flow-rates were measured at regular intervals using calibrated mercury sealed piston flow meters. The diffusion rates of the cells were known accurately from gravimetric determinations which were made weekly over a period of more than 3 months. The purity of the liquids in the diffusion cells was greater than 99.9%. On the basis of the measured flow-rates, rates of diffusion and times taken to charge the tubes, the amounts of vapour received by each tube could be calculated with an estimated uncertainty [a combination of precision (95% confidence limits) and bias] of 0.015 μg of each compound for individual tubes and 0.010 μg for the means of a batch. Assuming quantitative sorption on the Tenax, the amounts charged to each sample of CRM 112 were calculated to be: 1.054 μg of benzene; 1.123 μg of toluene; and 1.039 μg of *m*-xylene.

Homogeneity and Stability Tests

The homogeneity and stability of each batch studied were tested in the following manner: (*a*) a number of tubes (13 for the test batches, 40 for the reference material) were selected systematically so as to include all sampling units (see Fig. 2) and to include at least one in every four of each series of 12 tubes that were loaded simultaneously. These tubes were analysed in one laboratory on the same day. (*b*) Tubes stored under different conditions, *i.e.*, in a refrigerator (0–4 °C), at room temperature (19–23 °C) and at approximately 40 °C, were analysed at regular time intervals (in the same laboratory, the tubes stored under different conditions all being analysed on the same day). All these tests were carried out at the laboratory which prepared the batches.

Intercomparisons

For each round of analysis (two preliminary intercomparisons and the certification exercise), each participating laboratory analysed from four to ten tubes. The participating laboratories were as follows: Akzo Research (Arnhem, The Netherlands); BP Research (Sunbury-on-Thames, UK); Directoraat–Generaal Van de Arbeid (Voorburg, The Netherlands); Dow Chemical (Nederland) (Terneuzen, The Netherlands); Eolas (Dublin, Ireland); Health and Safety Executive, Occupational Medicine and Hygiene Laboratory (London, UK); ICI Chemicals and Polymers plc. (Runcorn, UK); Koninklijke–Shell Laboratorium (Amsterdam, The Netherlands); Laboratory of the Government Chemist (London, UK); Arbejdsmiljoinstituttet (Hellerup, Denmark); Rhone–Poulenc Industrialization(Decines-Charpieu, France); State Laboratory (Dublin, Ireland); and Universita Degli Studi di Urbino (Urbino, Italy).

In the following text, numerical codes (not related to the above alphabetical order) are used to refer to the analytical laboratories.

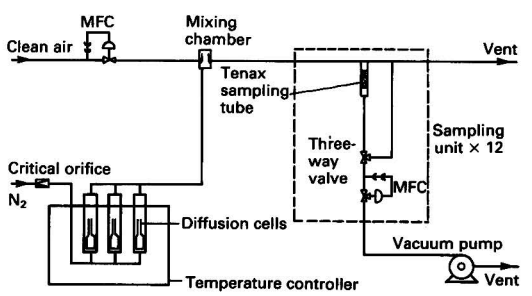

Fig. 2 Schematic representation of the vapour generating and tube charging apparatus; up to 12 tubes were charged in parallel. (MFC = mass flow controller)

All the laboratories but one used a procedure based on thermal desorption and gas chromatographic separation and detection (represented schematically in Fig. 3) as follows. (*a*) A carrier gas stream was passed through the tube to be analysed, which was held at approximately 250 °C (laboratory 9: 275 °C; laboratory 6: 280 °C) for 5–10 min (laboratory 10: 3 min; laboratory 6: 4 min; laboratory 8: 25 min). The gas stream was then passed into a cold trap which contained a small amount of Tenax (or similar sorbent) and which was held at approximately −30 °C (laboratory 8: −25 °C). (*b*) For the second step of the procedure (injection into the gas chromatograph), a valve was switched so that the gas flow was directed into the GC column and the cold trap was heated to 250–300 °C. (*c*) In the third step of the procedure (gas chromatographic separation and detection) the valve was switched to the original position and (unless the isothermal mode was used) the temperature programme of the chromatograph was started. Most of the laboratories used a capillary column (length, 25–60 m; i.d., 0.20–0.32 mm) coated with a non-polar stationary phase [*e.g.*, poly(dimethylsiloxane)]. Laboratory 6 used a packed column (2 m × 2 mm i.d.). A wide range of temperature programmes were used (chosen so as to complete the chromatogram in 5–20 min). A flame ionization detector was used in all instances.

The procedures used in laboratories 6, 11 and 12 differed significantly from that outlined above. Solvent desorption and mass spectrometric detection were used in laboratory 11. The Tenax powder was removed from the tube and transferred with 2 ml of hexane into a 5 ml flask which was occasionally shaken. After 30–60 min at room temperature, samples from the solution were injected into the gas chromatograph with a syringe. No cold-trap was used in laboratory 6; the vapours were sorbed directly on the GC column which was held at room temperature. Laboratory 12 transferred the Tenax from the tubes supplied into 18 cm tubes before desorption.

Certification of CRM 112

In the third round of analysis, the certification round, the participants had all re-evaluated their method of calibration. An example re-evaluation is given by Wright.[3] All syringes and volumetric glassware used were calibrated gravimetrically and the analytical balances were checked with certified weights.

The results were calculated from the GC detector response using calibration graphs based on three or more calibration solutions. These solutions were prepared by mixing accurately known volumes (laboratories 3 and 7) or masses (other laboratories) of pure benzene, toluene and *m*-xylene with an accurately known amount of solvent (methanol, cyclohexane or carbon disulphide), in systems designed so as to minimize losses through evaporation. Successive dilution was avoided. The purity of the products used was verified.

In laboratories 6 and 12, microlitre amounts of standard solutions were injected directly into the gas chromatograph for calibration. In other laboratories, similar amounts of standard solutions were added to clean Tenax tubes by injection in a flow of clean gas (injection of liquid on the Tenax powder was avoided) and these tubes were analysed in the same way as the samples.

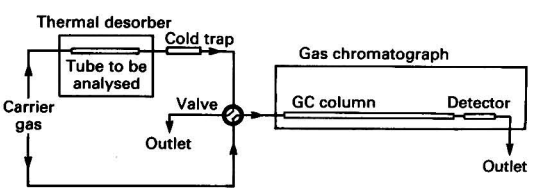

Fig. 3 Schematic representation of thermal desorption–gas chromatography equipment

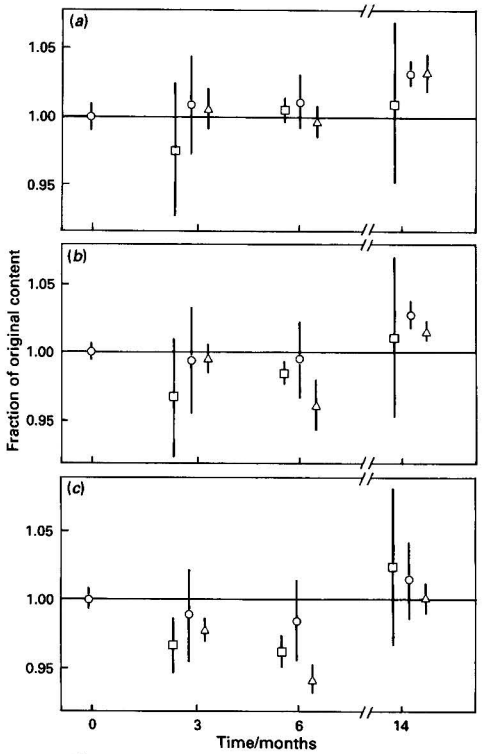

Fig. 4 Stability of a batch of charged tubes similar to CRM 112. Mean ± one standard deviation of a set of 5–13 analyses. (*a*) Benzene; (*b*) toluene; and (*c*) *m*-xylene. □, storage at 0–4 °C; ○, storage at ambient temperature; and △, storage at 40 °C

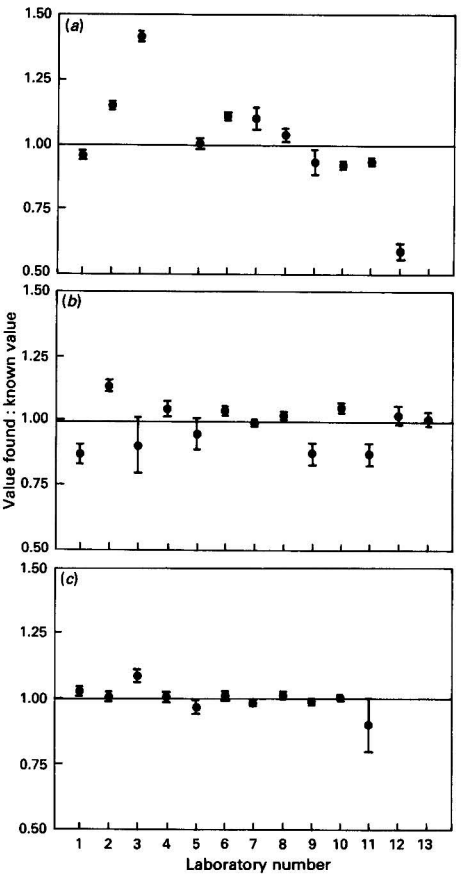

Fig. 5 Results of three successive intercomparisons for benzene on Tenax (mean value and standard deviation for each laboratory). 'Known value' = value calculated from charging data. (*a*) First round; (*b*) second round; and (*c*) third round

Results and Discussion

Homogeneity and Stability Tests

The homogeneity test yielded in all instances relative standard deviations (RSDs) of <1.5%; this corresponds with the RSD typical for the thermal desorption–gas chromatography procedure used by Brown *et al.*[4] It was concluded that no inhomogeneity could be detected.

The stability test outlined above was applied only to the first test batch. The results are presented graphically in Fig. 4. Significant systematic differences which correlated to the volatility of the compound or to the storage temperature were not observed; the long-term variation in the results is thus of analytical origin and not caused by losses through evaporation, chemical reactions or irreversible sorption.

The stability of CRM 112 has been monitored further by the periodic analysis of samples stored at room temperature (as the entire batch); no instability was detected after 25 months.

Intercomparisons

Figs. 5(*a*) and (*b*), 6(*a*) and (*b*), and 7(*a*) and (*b*) present the intercomparison results for individual laboratories in graphical form where the variable plotted is the ratio of the value found to the known value, and the means and standard deviations are shown.

In each instance, the mean values were close to the amounts with which the tubes were charged, but the confidence intervals were unsatisfactory as they were much larger than expected on the basis of the within-laboratory repeatability of the analysis.

After each of the preliminary intercomparisons, the results were discussed with all the participating laboratories. They explained in great detail how their analyses had been carried out. Consequently, various potential sources of error were identified and eliminated. Considerable progress was made between the second and the third round of analysis. This improvement resulted from measures being taken, from which some laboratories expected only a minor improvement (*e.g.*, calibration of volumetric glassware, preparation of calibration solutions in sealed systems in order to avoid losses through evaporation, gravimetric dilution and dispensing, weighing of the syringe before and after injection, and calibration and maintenance of the analytical balance).

As all participating laboratories were considered to be highly competent analytical laboratories, other laboratories are expected to experience similar difficulties and therefore some typical sources of error are listed below.

Errors due to the handling of the tubes

Errors arising from the handling of the tubes included: loss of sorbent when applying force to remove the cap from the grooved end of the tubes; and losses of vapour (or contamination risk) upon contact with the atmosphere when the tubes were opened in order to transfer the sorbent into another container for solvent desorption, or similar risks when caps

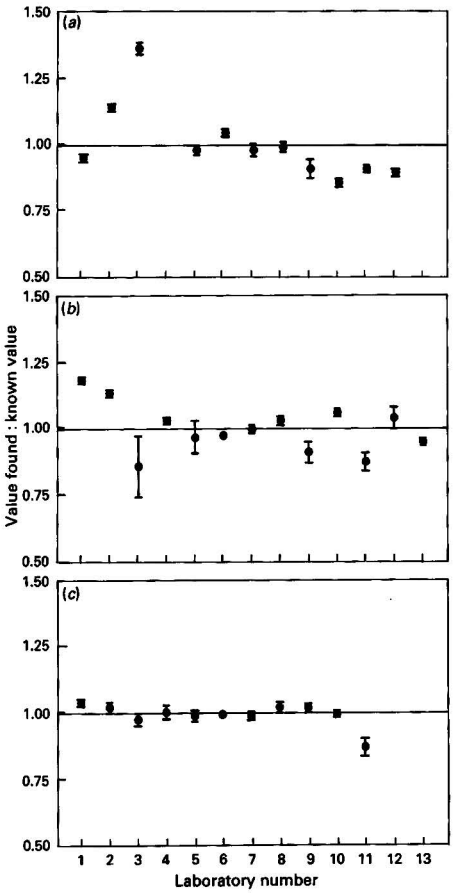

Fig. 6 Results of three successive intercomparisons for toluene on Tenax (mean value and standard deviation for each laboratory). 'Known value' = value calculated from charging data. (*a*) First round; (*b*) second round; and (*c*) third round

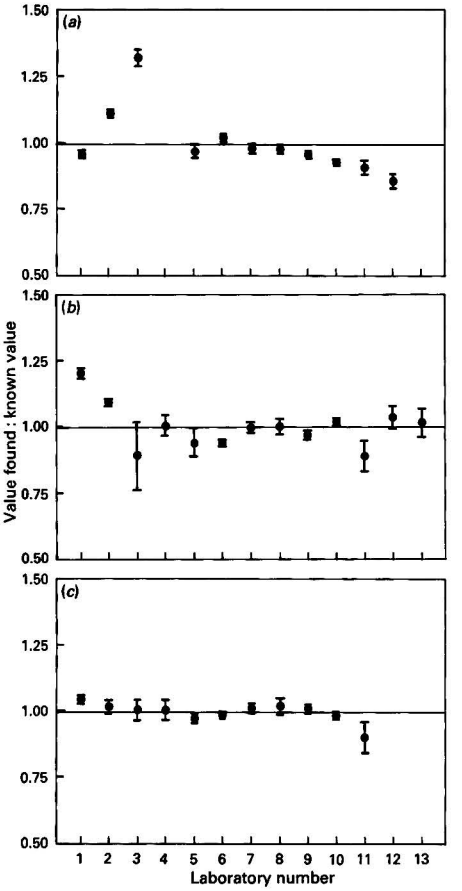

Fig. 7 Results of three successive intercomparisons for *m*-xylene on Tenax (mean value and standard deviation for each laboratory). 'Known value' = value calculated from charging data. (*a*) First round; (*b*) second round; and (*c*) third round

were removed a long time before the determinations were carried out.

Errors in the calibration

Errors in calibration resulted from: partial evaporation of volatile compounds of interest, or of the volatile solvent, between preparation and final use of the standard solutions (especially when syringes were being manipulated); relying on uncalibrated syringes or other glassware (errors of the order of 10% can be expected); and ignoring the water content of the solvents used.

Errors due to malfunctioning instruments

Errors caused by malfunctioning instruments were due to leaks in the connections of the tube in the thermal desorber; the use of a malfunctioning analytical balance (if the calibration is not checked periodically, an error may remain undetected as short-term repeatability may remain normal); and the use of an ionization detector that was not optimized (checking is required whenever the response factors for benzene, toluene and *m*-xylene differ by more than 2%).

Certification

The results of the certification (effectively a third intercomparison) are presented in Figs. 5(*c*), 6(*c*) and 7(*c*). For this intercomparison, the ten laboratories applying thermal desorption achieved excellent agreement. Only one result (laboratory 3, benzene) was identified as a straggler (Dixon test). As this result was associated with a calibration error, the result was rejected. The data obtained from laboratory 11 (which used solvent desorption) were also rejected, on the grounds either that solvent desorption had been used or that losses through volatilization had occurred when the Tenax was being transferred from the tube into the flask, or that desorption had been incomplete.

The mean of laboratory means and the halfwidth of its 95% confidence interval for each component are as follows: benzene, (1.053 ± 0.014) μg per tube; toluene, (1.125 ± 0.015) μg per tube; and *m*-xylene, (1.043 ± 0.015) μg per tube. If the interlaboratory standard deviation is significantly larger (as calculated using the *F*-test) than the intralaboratory standard deviation, the presence of remaining systematic errors in the participating laboratories is indicated. It is generally assumed that these errors are randomized, *i.e.*, they do not cause a

systematic error in the mean of means, if the interlaboratory standard deviation does not exceed the intralaboratory standard deviation by more than a factor of 2–3; in the present instance, the factor is <1.0 for each analyte.

In addition, the values measured correspond closely with the masses with which the tubes were charged (the difference being 0.1, 0.2 and 0.4% for benzene, toluene and *m*-xylene, respectively). These results were therefore considered to provide sufficient basis for certification.

Conclusions

The data presented in this paper demonstrate that a batch of Tenax tubes charged with benzene, toluene and *m*-xylene can be prepared and analysed to an uncertainty of better than 2%, provided the analytical laboratories apply due care and attention to detail. Initial intercomparisons gave results with much larger errors and some of the potential sources of such errors have been identified.

The absence of a detectable systematic error is a sufficient reason to declare the batch certified to BCR specifications and the batch is offered for sale for calibration and quality control. The uncertainty obtained renders the material useful for these purposes.

The certification of this reference material is the first major achievement in the BCR efforts to provide means of quality assurance in occupational health monitoring.

Work similar to that described here is in various stages of progress for: (*i*) aromatic hydrocarbons on active charcoal (for solvent desorption); (*ii*) chlorinated C_2 hydrocarbons on Tenax; and (*iii*) esters and ketones on Tenax.

Several other possible projects are in the discussion stage; feasibility studies on amines (including triethylamine), aldehydes (including formaldehyde) and isocyanates are planned for the near future.

References

1 Council of the European Communities, Directive 88/1107/EEC, *Official Journal of the European Communities*, 1980, No. L327/8.

2 Vandendriessche, S., and Griepink, B., *The Certification of Benzene, Toluene and* m-*Xylene Sorbed on Tenax in Tubes*, Report EUR 12308EN, Commission of the European Communities, Luxembourg (Office for Official Publications of the European Communities, 1989).

3 Wright, M. D., *BCR Certification of Reference Materials—Organics on Tenax—a Critical Examination of Sources of Calibration Error*, Health and Safety Executive (HSE) Internal Report IR/L/IA/90/3, HSE, London, 1990.

4 Brown, R. H., Cox, P. C., Purnell, C. J., West, N. G., and Wright, M. D., in *Identification and Analysis of Organic Pollutants in Air*, ed. Keith, L. H., Ann Arbor Science Publishers/Butterworth, Woburn, MS, 1984.

Paper 0/05393G
Received November 29th, 1990
Accepted December 12th, 1990

Investigation of the Quenching of Peroxyoxalate Chemiluminescence by Amine Substituted Compounds

Joseph K. DeVasto and Mary Lynn Grayeski*
Chemistry Department, Seton Hall University, South Orange, NJ 07079, USA

The role of amine compounds in quenched peroxyoxalate chemiluminescence was investigated. The mechanistic steps examined included (1) fluorescence quenching; (2) base hydrolysis of the oxalate; and (3) a competitive interaction between the quencher and fluorophore for the peroxyoxalate reaction intermediate(s). The results showed no evidence of amines causing fluorescence quenching. Base hydrolysis of the oxalate is significant only at high concentrations of amines. When the concentration of amines is greater than or equal to the level of oxalate, the amines can compete with the fluorophore for reaction with the intermediate(s). Because competitive effects were demonstrated, one analytical implication is that caution must be exercised in applications where more than one fluorophore is present. At low concentrations of fluorophores relative to the oxalate, chemiluminescence emission of both fluorophores will be observed. At higher levels, the fluorophores can compete for reaction with the intermediate(s). Finally, an important analytical implication of this study is that the quenching response can be used to quantify amines without the need for derivatization. The limitation is that the linear response is approximately one order of magnitude.

Keywords: *Peroxyoxalate chemiluminescence; aliphatic/aromatic amines; quenched chemiluminescence*

Rauhut *et al.*[1] first reported significant differences in quantum yields and chemiluminescence (CL) lifetimes when adding basic compounds to a peroxyoxalate reaction containing bis(2,4-dinitrophenyl) oxalate (DNPO) and 9,10-diphenylanthracene. Quenched peroxyoxalate CL was also observed in the reaction of hydrogen peroxide with bis(pentachlorophenyl) oxalate (PCPO) using sodium salicylate as a base catalyst.[2]

A number of substituted anilines, and organosulphur and ionic compounds have been analysed by high-performance liquid chromatography and flow injection with quenched peroxyoxalate CL detection.[3,4] A competitive quenching mechanism between easily oxidizable analytes and the peroxyoxalate reaction intermediate was initially proposed. A later report[4] suggested that the quencher is involved in radiationless deactivation of the fluorophore–charge-transfer complex.

The purpose of this study was to examine the role of aliphatic and aromatic amines in quenched peroxyoxalate CL, and to develop an analytical technique for measuring amine compounds by means of this quenching phenomenon. The advantage of this approach is that a derivatization step is not required prior to detection of the aliphatic amines. This is particularly important for tertiary aliphatic amines for which derivatization reactions are limited.

The mechanistic pathways that a quencher (Q) can follow in the reaction with bis(2,4,6-trichlorophenyl) oxalate (TCPO) and hydrogen peroxide are:

$$\text{TCPO} + \text{H}_2\text{O}_2 \rightarrow \text{intermediate(s) (I)} + 2[\text{2,4,6-trichlorophenol (TCP)}] \quad (1)$$

$$\text{TCPO} + \text{OH}^- \xrightarrow{\text{Q}} 2\text{TCP} \quad (1a)$$

$$\text{I} + \text{fluorophore (FL)} \rightarrow [\text{I}^{\bullet-}\text{FL}^{\bullet+}] \quad (2)$$

$$\text{I} + \text{Q} \rightarrow \text{non-CL} \quad (2a)$$

$$[\text{I}^{\bullet-}\text{FL}^{\bullet+}] \rightarrow \text{FL}^* \quad (3)$$

$$\text{FL}^* \rightarrow \text{FL} + h\nu \quad (4)$$

$$\text{FL}^* + \text{Q} \rightarrow \text{FL} \quad (4a)$$

The asterisk signifies the excited state of the fluorophore. Equations (1)–(4) [excluding (1a), (2a) and (4a)] are the proposed light producing pathways.[1] Hydrogen peroxide and TCPO react to form a high energy intermediate(s) that undergoes an electron charge transfer with a fluorophore. The charge-transfer process leads to radical ion annihilation and formation of an excited state fluorophore that fluoresces. The addition of an amine (or other quencher) can cause the reaction to proceed along dark pathways such as (*i*) base hydrolysis of the oxalate [equation (1a)], (*ii*) competitive interaction of the quencher and fluorophore for the intermediate [equation (2a)] and (*iii*) fluorescence quenching of the fluorophore [equation (4a)].

* To whom correspondence should be addressed.

Experimental

Chemicals

Triethylamine (TEA), *N*-propylamine (*N*-PA), *N*-isopropylcyclohexylamine (*N*-IPCA), 2-ethylaniline (2-EA), 4-toluidine (4-TOL), *N,N*-dimethylaniline (*N,N*-DMA) and 30% hydrogen peroxide were obtained from Aldrich. Analytical-reagent grade dibasic sodium phosphate was received from J. T. Baker and TCPO was obtained from A. Mohan (New Jersey Department of Health, Trenton, NJ, USA).

Spectrophotometric grade acetonitrile (Aldrich) and analytical-reagent grade anhydrous sodium perchlorate (GFS Chemicals) were used for determining the oxidation potentials of the fluorophores. The fluorophores used in the fluorescence and CL studies, *viz.*, 1-aminoanthracene, 1-aminopyrene, anthracene, pyrene, perylene, rubrene and 1-aminonaphthalene, were purchased from Aldrich. 2,4,6-Trichlorophenol (TCP) was obtained from Eastman Chemicals, and HPLC grade acetonitrile (Fisher) was used throughout. All chemicals were used as received without additional purification.

Static Chemiluminescence: Competitive and Quenching Experiments

A Turner Instruments Model TD-20e luminometer was used for CL measurements. In the competitive interaction experiments, the reagents were added to a 1.6 ml polypropylene cuvette in the following order: (*i*) 100 µl of H_2O_2 (490 mmol dm^{-3}); (*ii*) 100 µl of Na_2HPO_4 buffer (5 mmol dm^{-3}) (pH 6.2); and either (*iiia*) 40 µl of acetonitrile for a blank run, (*iiib*) 20 µl of solution for a single fluorophore

run plus 20 μl of acetonitrile or (*iiic*) 20 μl of each fluorophore solution with no acetonitrile added for runs with mixtures of two fluorophores. For the quenched CL experiments, steps (*i*) and (*ii*) were repeated and either (*a*) 20 μl of 1-aminopyrene (1 μmol dm^{-3}) plus 20 μl of quencher solution, (*b*) 20 μl of fluorophore solution plus 20 μl of acetonitrile, (*c*) 20 μl of quencher solution plus 20 μl of acetonitrile or (*d*) 40 μl of acetonitrile were added to the cuvette. The TCPO (2 mmol dm^{-3}) was injected last (50 μl) for either set of experiments into the reaction cuvette with the Turner apparatus. With the final addition of TCPO the total volume was 290 μl for each CL measurement.

The CL signal was monitored for 120 s with a Fisher Series 5000 strip-chart recorder, and the CL intensity areas were determined by electronic integration (0–120 s) with the Turner luminometer. The CL reagents were prepared in acetonitrile except for the aqueous phosphate buffer.

Relative Fluorescence Quenching Experiments

Fluorescence quenching was measured by using a Fluorolog 2 + 2 spectrofluorimeter with a 450 W Xe continuous source (Spex Industries). The fluorescence intensity of 1-aminopyrene (1 μmol dm^{-3}) was determined by adding 0.2 ml of the fluorophore to a cuvette containing 1.0 ml of sodium phosphate buffer (5 mmol dm^{-3}) (pH 6.2) and 1.7 ml of acetonitrile. Relative fluorescence quenching was measured by adding 0.2 ml of the quencher (at several concentrations examined in the quenched CL experiments) plus 0.2 ml of 1-aminopyrene (1 μmol dm^{-3}) to 1.0 ml of phosphate buffer (5 mmol dm^{-3}) (pH 6.2) and 1.5 ml of acetonitrile. Spectral peak areas were determined at an excitation wavelength of 360 nm and an emission wavelength range of 390–500 nm with a 1 nm bandpass.

Base Hydrolysis and Apparent pH

The formation of TCP from TCPO was measured at 298 nm by ultraviolet (UV) absorbance[5] using a Varian 2200 UV spectrophotometer. Absorbance readings were recorded 2 min after injecting the last reagent under two sets of run conditions. The injection volumes for each set of runs were: 0.5 ml of TCPO (2 mmol dm^{-3}) + 1.0 ml of Na_2HPO_4 buffer (5 mmol dm^{-3}) (pH 6.2) + 1.0 ml of H_2O_2 (490 mmol dm^{-3}) + (0.2 ml of 1-aminopyrene (1 μmol dm^{-3}) + 0.2 ml of acetonitrile; and the same sequence as for the first run but with 0.2 ml of quencher solution substituted for acetonitrile. The background absorbance readings of the fluorophore, H_2O_2, buffer and quencher solution components were subtracted from the values obtained from the two sets of runs. All reagents were prepared in acetonitrile (except for the aqueous buffer). The quartz cuvette was placed in the instrument prior to injecting the final reagent (TCPO) in order to improve the experimental precision.

Measurements of apparent pH were made on CL solutions that contained quenchers at concentrations ranging from 0.0069 to 6.9 mmol dm^{-3}. The injection order and concentrations of CL reagents were: 10 ml of H_2O_2 (490 mmol dm^{-3}); 10 ml of Na_2HPO_4 buffer (5 mmol dm^{-3}) (pH 6.2); 2 ml of 1-aminopyrene (1 μmol dm^{-3}); 2 ml of quencher solution; and 5 ml of TCPO (2 mmol dm^{-3}). Acetonitrile (2 ml) was substituted for the quencher solution when the apparent pH of the CL reaction was measured. The apparent pH was determined with an Orion Research Model 611 pH meter 2 min after adding the last reagent.

Oxidation Potentials

Oxidation potentials of 1-aminoanthracene and 1-aminopyrene were determined by cyclic voltammetry with an IBM EC/225 voltammetric analyser. Half-wave potentials were determined by using a platinum disc working electrode, a platinum wire auxiliary electrode and an $Ag–Ag^+$ reference electrode. The supporting electrolyte was 0.5 mol dm^{-3} sodium perchlorate in acetonitrile, and the sweep rate was 10 mV s^{-1}.

Results

Quenched peroxyoxalate CL in a buffered solution was investigated by measuring the CL response while varying the concentration of amines over several orders of magnitude (Figs. 1 and 2). The CL signal was quantified by determining the quenching ratio $I_Q : I_0$, where I_Q is the CL intensity with the quencher and I_0 is the intensity without a quencher in the CL reaction. Figs. 1 and 2 show that the aliphatic amines have a more significant quenching effect on the CL reaction in the 0.035–0.69 mmol dm^{-3} concentration range. Also, an increase in CL intensity is observed for 2-EA and 4-TOL at a concentration of 0.035 mmol dm^{-3}.

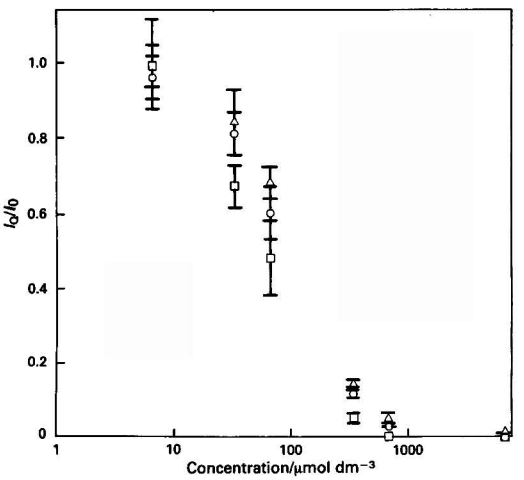

Fig. 1 Quenched peroxyoxalate CL ratios for the aliphatic amines TEA (○), *N*-IPCA (□) and *N*-PA (△). 1-Aminopyrene was used as the CL reaction fluorophore at a concentration of 0.069 μmol dm^{-3}. All points represent the average of three injections plus the standard deviation with the exception of some measurements where no light was observed. The concentrations of the amines are the final concentrations in the cuvette

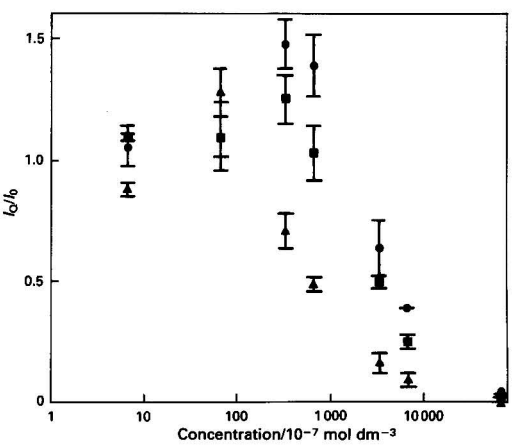

Fig. 2 Quenched peroxyoxalate CL ratios for the aromatic amines 2-EA (●), 4-TOL (■) and *N,N*-DMA (▲). Point representation and concentration of the fluorophore as in Fig. 1

Figs. 3 and 4 show typical quenched CL profiles of TEA and 2-EA, respectively. Two peaks are observed when a 0.69 mmol dm^{-3} TEA solution is added to the CL reaction without 1-aminopyrene (Fig. 3, B). No double peak is observed, however, when the fluorophore is included in the CL reaction. Also, double peaks are not observed when aromatic amines are added to the CL reaction. A decrease in the CL rate of decay occurs at relatively low concentrations (less than 0.069 mmol dm^{-3}) of aromatic amines, and an increase in CL emission is observed.

The quenched CL response is linear [analysis of variance (ANOVA) regression; $F = 0.975$] over a relatively narrow concentration range, *viz.*, 0.017–0.17 mmol dm^{-3} for TEA, and 0.045–0.17 mmol dm^{-3} for *N*-IPCA or *N*-PA. The CL response curve was calculated by taking the reciprocal value of the quenched CL signal *versus* concentration. The lowest levels of aliphatic amines measured ($n = 4$) by quenched CL were 0.017 ± 0.001 mmol dm^{-3} TEA, 0.045 ± 0.002 mmol dm^{-3} *N*-IPCA and 0.045 ± 0.003 mmol dm^{-3} *N*-PA.

Fluorescence Quenching

A relative comparison of fluorescence spectral peak areas of 1-aminopyrene was made with and without an amine in solution in order to determine fluorescence quenching (Table 1). No fluorescence quenching is observed when the amines are added to 1-aminopyrene in an acetonitrile–phosphate buffer solution. Also, there is no evidence of a shift in the spectral peaks of 1-aminopyrene at any concentration of the quenchers studied.

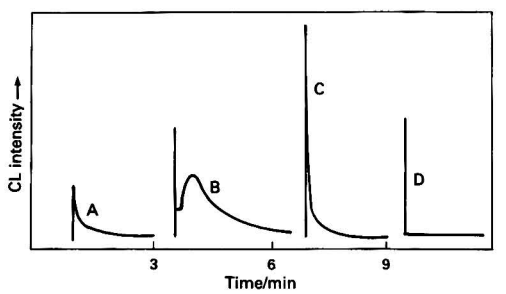

Fig. 3 Quenched peroxyoxalate CL with 0.69 mmol dm^{-3} TEA. Static CL curves: A, acetonitrile blank (CL solution without fluorophore or TEA); B, CL solution with TEA and no fluorophore; C, CL solution with 1-aminopyrene; and D, CL solution with 1-aminopyrene plus TEA. The sensitivity of the luminometer was increased 100-fold when recording CL curves A and B relative to curves C and D

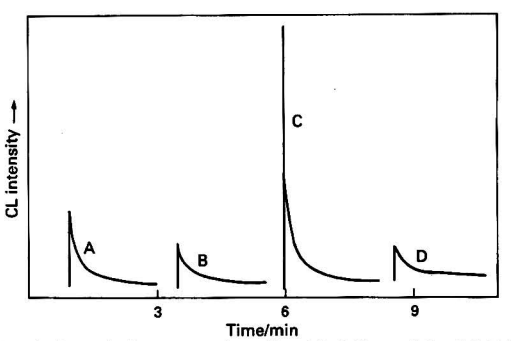

Fig. 4 Quenched peroxyoxalate CL with 0.69 mmol dm^{-3} 2-EA. Static CL curves A–D are as given for Fig. 3 with curves A and B measured at a 100-fold increase in sensitivity relative to curves C and D

Hydrolysis

The apparent pH of the quenched peroxyoxalate CL reaction was measured and compared with the CL reaction without a quencher. There is no significant increase in apparent pH of the quenched CL reaction, except for aliphatic amines added at concentrations greater than or equal to 0.069 mmol dm^{-3}. A similar experiment was conducted using UV absorbance to measure the change in the concentration of TCP in the CL reaction when adding TEA at several concentrations (Table 2). As the concentration of the aliphatic amine increases, an increase in the level of TCP relative to the CL reaction without TEA is observed. When absorbance measurements were made on the CL reaction with and without the addition of aromatic amines, there was no increase observed in the concentration of TCP.

Competitive Interaction

The competitive role of the quencher and fluorophore for the CL reaction intermediate(s) was examined by comparing the CL response of the reaction with one fluorophore with the CL response of the reaction with a mixture of two fluorophores. If the sum of the signals for the individual fluorophores is equivalent to the CL response of the mixture, then there is no competition between the fluorophores for interaction with the intermediate. If the CL signal of the mixture is not equivalent, the interaction with the peroxyoxalate intermediate(s) would be favoured for one fluorophore relative to the other.

Two sets of conditions were evaluated in the competitive interaction experiments: (*i*) the concentrations of the fluorophores were lower than the concentration of TCPO by approximately 2–5 orders of magnitude (except for pyrene); and (*ii*) the total concentration of amino substituted fluorophores was within one order of magnitude of the concentration of TCPO. These conditions include the entire range of concentrations of amines used in the quenching experiment.

If the two fluorophores react competitively with the intermediate(s), the reactivity of one fluorophore might be favoured based on its oxidation potential or concentration. Both of these parameters were evaluated for various fluorophores (Table 3). Sums of the CL signals were determined for pairs of fluorophores by using a central composite experimental design. The results showed that the CL signal ($n = 3$ injections) for a mixture of two fluorophores is equivalent

Table 1 Relative fluorescence quenching. The values are relative to the fluorescence intensity of 1-aminopyrene, which is equal to 1.00 in the absence of a quencher; relative standard deviation = 6.1% ($n = 7$)

Quencher	6.9 mmol dm^{-3}	0.69 mmol dm^{-3}	0.34 mmol dm^{-3}
TEA	1.06	1.08	1.00
N-PA	1.04	1.03	1.01
N-IPCA	0.95	—	—
2-EA	1.02	0.98	1.03
4-TOL	1.06	0.96	—
N,N-DMA	0.97	0.98	—

Table 2 TCP product formation during the peroxyoxalate CL reaction plus quencher

TEA concentration/mmol dm^{-3}	TCP/mmol dm^{-3}
0	0.54*
0.0069	0.55
0.034	0.56
0.069	0.57
0.34	0.60
0.69	0.60
6.9	0.66

* Average of duplicate injections; relative standard deviation = 1.3%.

Table 3 Oxidation potentials (E_1ox) and concentrations of fluorophores in the CL reaction. Final CL reagent concentrations in the static cell: TCPO, 0.34 mmol dm^{-3}; H_2O_2, 170 mmol dm^{-3}; and phosphate buffer, 1.7 mmol dm^{-3}

Fluorophore	E_1ox/ V *versus* Ag–Ag$^+$*	Concentration/ μmol dm^{-3}†		
Anthracene	+0.79	7.4	3.7	0.7
Pyrene	+0.86	69.7	34.8	7.0
1-Aminoanthracene	+0.10	0.08	0.04	0.008
1-Aminopyrene	+0.19	0.07	0.04	0.007
Perylene	+0.55	0.01	0.005	0.001
Rubrene	+0.52	0.02	0.01	0.002
1-Aminonaphthalene	+0.24	1.4	0.7	0.14

* References 6 and 7.

† Three concentration levels were studied with pairs of fluorophores mixed in solution.

(within a 95% confidence interval) to the sum of the CL signals for the individual fluorophores when measured at concentrations much lower than that of TCPO. The second set of conditions was examined by increasing the total concentration of the fluorophores and decreasing the level of TCPO by one order of magnitude. 1-Aminonaphthalene (13 μmol dm^{-3}) and 1-aminopyrene (0.71 μmol dm^{-3}) were measured in the experiment with TCPO (0.034 mmol dm^{-3}), H_2O_2 (170 mmol dm^{-3}) and phosphate buffer (1.7 mmol dm^{-3}) (pH 6.2). The CL signal of the mixed fluorophores ($n = 3$) is not equivalent to the sum of the CL responses of each fluorophore when compared within 95% confidence intervals.

Discussion

Role of the Quencher

The role of amines in a buffered peroxyoxalate reaction was examined through a number of possible quenching mechanisms. The non-chemiluminescent reaction pathways investigated included: fluorescence quenching of the fluorophore [equation (4a)]; base hydrolysis of the oxalate [equation (1a)]; and competitive interaction of the amine and fluorophore for the peroxyoxalate reaction intermediate(s) [equation (2a)].

The results in Table 1 show that there is no significant change in the fluorescence intensity of 1-aminopyrene at the higher concentrations of quenchers used in this study. Therefore, the amines are not causing fluorescence quenching [equation (4a)] of the fluorophore in the peroxyoxalate CL reaction.

The effect of TEA on the base hydrolysis of TCPO was determined at several concentrations of TEA in the CL reaction (Table 2). The formation of TCP is increased relative to the CL reaction without TEA at levels greater than or equal to 0.069 mmol dm^{-3}. Aliphatic amines also affect the apparent pH of the CL reaction at concentrations greater than 0.069 mmol dm^{-3}. These results indicate that aliphatic amines have sufficient basicity to exceed the buffer capacity of the CL reaction and cause the hydrolysis of TCPO. It has been speculated that the efficiency of the peroxyoxalate CL reaction decreases above pH 8 because of base hydrolysis of the oxalate.[8] In this study, base hydrolysis also appears to be part of the quenching mechanism when high concentrations of aliphatic amines are added.

There is no evidence of base hydrolysis when aromatic amines are added to the CL reaction. There is also no significant change in the apparent pH of the CL reaction when 2-EA, 4-TOL or *N,N*-DMA are added at a high concentration (6.9 mmol dm^{-3}). These aromatic amines are relatively weak bases compared with the aliphatic species studied, and do not exceed the buffer capacity of the CL reaction.

The possibility of a competitive quenching mechanism was investigated by measuring the CL response of pairs of fluorophores both as a mixture and separately (Table 3). If a competitive mechanism exists, then a decrease in CL intensity should be observed relative to the sum of the intensities for each species measured separately. There is no competitive interaction for the peroxyoxalate reaction intermediate(s) when the concentration of TCPO is several orders of magnitude greater than that of the fluorophores. Also, differences in the oxidation potentials of the two fluorophores do not contribute to a competitive interaction for the reaction intermediate(s).

There is evidence of a competitive mechanism when the total concentration of 1-aminopyrene or 1-aminonaphthalene is within one order of magnitude of the level of TCPO. As the concentration of the peroxyoxalate reaction intermediate(s) is limited relative to that of the fluorophores, one fluorophore acts as a competitive quencher of the CL reaction. The non-fluorescent amines used in the quenching study (Figs. 1 and 2) were added to the peroxyoxalate reaction at concentrations that were greater than or equal to the level of TCPO (0.34 mmol dm^{-3}). This implies that a competitive mechanism can occur between the quencher and fluorophore for the peroxyoxalate reaction intermediate(s) if the concentration ratio of quencher : TCPO is greater than or equal to unity. This is based on most of the TCPO reagent being converted into the high energy intermediate(s) in the peroxyoxalate reaction.

It is not clear which quenching mechanism operates when the concentration of the amine is significantly less than that of TCPO. An earlier report[4] on the role of a quencher in the peroxyoxalate reaction postulated that the fluorophore–charge-transfer complex undergoes radiationless deactivation. This suggests that a trimolecular interaction of the quencher, fluorophore and intermediate is favoured over a bimolecular light-producing fluorophore–intermediate reaction pathway.

It should be noted that fluorophores with broad emission bands and some spectral overlap were included in this study. Theoretically, it should be possible to measure the emission from one fluorophore in the presence of another if the two fluorophores are sufficiently spectrally resolved and exhibit efficient CL. This would require the use of a very long wavelength emitter relative to the fluorophores usually measured with this reaction.[9] For the fluorophores examined here, the emission levels were very low at all the concentrations studied and the total intensity was integrated over all wavelengths in order to collect an adequate signal.

Analytical Implications

Aliphatic and aromatic amines can be quantified by using quenched peroxyoxalate CL detection. An advantage of this technique is that aliphatic amines can be detected without derivatization. This is important in quantifying tertiary aliphatic amines where the choice of a derivatizing reagent is very limited.

There are limitations that must be considered in quantifying amines by quenched CL detection. Fig. 1 clearly shows a non-linear quenching response when aliphatic amines are measured over three orders of magnitude in concentration. This is the result of the quencher causing complex kinetics that change the CL peak shape and rate of decay. A probable cause of this phenomenon (Fig. 3, C and D) is that as the concentration of the aliphatic amine increases in the buffered CL reaction, it exceeds the buffer capacity and acts as a base catalyst thus increasing the CL rate of decay.[10] A linear response can only be observed over a range less than or equal to one order of magnitude in concentration.

The quenched CL response of the aromatic amines (Fig. 2) is also non-linear and shows an increase in CL emission at relatively low concentrations. The cause of the increase in CL

emission was not investigated, but a decrease in the CL rate of decay was observed. It is possible that the aromatic amines are increasing the formation of a second peroxyoxalate reaction intermediate.[11] Possible evidence for this mechanism was obtained qualitatively (Fig. 3, B). The CL intensity–time curve has two peaks, which indicates that two intermediates are formed when aliphatic amines are added to the CL reaction without a fluorophore. A burst of light generates the initial peak which might correspond to a reaction pathway in which an arylperoxyoxalic acid intermediate is formed rapidly together with a dioxetane dione or dioxetanone intermediate species. Although double peaks are not observed for the aromatic amines (Fig. 4), it is still possible that a second reaction intermediate is formed but cannot be observed. The addition of aromatic amines might generate a burst of light which is too rapid to measure, or a second low-level emission peak which cannot be detected above the main CL signal.

As competition occurs, the question about mixtures of fluorophores is raised. Is one fluorophore preferentially being measured when several fluorophores are present in a solution? This information was obtained by investigating the competitive role of a quencher in the peroxyoxalate CL reaction. A quenched CL signal could occur when determining the concentration of more than one fluorophore in a solution. One fluorophore can act as a quencher if the total concentration is within one order of magnitude of the level of the oxalate in the CL reaction. A quantitative CL signal should result from a mixture of fluorophores when the total concentration of the fluorophores is significantly less than that of the oxalate.

This research was supported through a grant from Research Corporation.

References

1 Rauhut, M. M., Bollyky, L. J., Roberts, G. B., Loy, M., Whitman, R. H., Iannotta, A. V., Semsel, A. M., and Clarke, R. A., *J. Am. Chem. Soc.*, 1967, **89**, 6515.
2 Catherall, C. L. R., Palmer, T. F., and Cundall, R. B., *J. Chem. Soc., Faraday Trans. 2*, 1984, **80**, 823.
3 van Zoonen, P., Kamminga, D. A., Gooijer, C., Velthorst, N. H., and Frei, R. W., *Anal. Chem.*, 1986, **58**, 1245.
4 van Zoonen, P., Bock, H., Gooijer, C., Velthorst, N. H., and Frei, R. W., *Anal. Chim. Acta*, 1987, **200**, 131.
5 Givens, R. S., Schowen, R. L., Matuszewski, B., Alvarez, F., Parekh, N., and Nakashima, K., paper presented at the Federation of Analytical Chemistry and Spectroscopy Societies Symposium, St. Louis, MO, September 1986.
6 Pysh, E. S., and Yang, N. C., *J. Am. Chem. Soc.*, 1963, **85**, 2124.
7 Siegerman, H., *Techniques of Electroorganic Synthesis, Part II*, Wiley, New York, 1975, vol. 5.
8 Weinberger, R., *J. Chromatogr.*, 1984, **314**, 155.
9 Mann, B., and Grayeski, M. L., *Anal. Chem.*, 1990, **62**, 1532.
10 Nozaki, O., Ohba, Y., and Imai, K., *Anal. Chim. Acta*, 1988, **205**, 255.
11 Alvarez, F. J., Parekh, N. J., Matuszewski, B., Givens, R. S., Higuchi, T., and Schowen, R. L., *J. Am. Chem. Soc.*, 1986, **108**, 6435.

Paper 0/03784B
Received August 17th, 1990
Accepted December 17th, 1990

Rapid Method for the Determination of the Major Components of Magnesite, Dolomite and Related Materials by X-ray Spectrometry

Michael H. Jones and B. William Wilson*
CSIRO Division of Mineral Products, P.O. Box 124, Port Melbourne, Victoria 3207, Australia

A new flux, MAG 5743, has been developed, which contains 57% m/m lithium tetraborate and 43% m/m lithium metaborate for use in the analysis of raw magnesite, caustic and dead burnt magnesia, (*i.e.*, magnesite heated to 700–1100 °C and >1400 °C, respectively) and dolomite. The flux can be used for the determination of loss on fusion followed by X-ray fluorescence analysis of the glass disc for its major component elements, as their oxides MgO, CaO, SiO_2, Al_2O_3 and Fe_2O_3, on the one sample. As the flux is both fluid and reactive at 1000 °C, fusion times are short (10 min) regardless of the reactivity of the sample. The results obtained from the analysis of three certified reference materials using the new flux were statistically indistinguishable at the 95% confidence level from the certificate values.

Keywords: *X-ray fluorescence; magnesia, magnesite and dolomite analysis; loss on fusion*

The rapid and accurate determination of the principal components of magnesite, magnesia, dolomite and calcite (as the oxides MgO, CaO, SiO_2, Al_2O_3, Fe_2O_3) and the loss on ignition (LOI) is necessary for quality control in mining and processing.

Current X-ray fluorescence (XRF) techniques require the sample to be calcined before fusion,[1,2] determine only one component[3,4] and/or require the use of high melting-point fluxes with relatively long fusion times. Overall, the techniques currently used, although accurate, are time consuming and labour intensive. In addition, making a separate measurement of the LOI has several disadvantages, these being: the time taken for measurement; the temperature of ignition being sometimes insufficient to break down any refractory constituents; and the possibility of re-adsorption of H_2O and/or CO_2 on cooling. These last two disadvantages can contribute to a low LOI measurement. Furthermore, the LOI temperatures in recommended methods range from 1000–1100 °C.[5–9]

The flux used to prepare discs for XRF analysis in most methods is lithium tetraborate.[1,2,4,10] An 'acidic' flux such as lithium tetraborate or sodium metaphosphate[10] is necessary for the dissolution of samples and production of stable discs. Lithium tetraborate at the usual fluxing temperature of 1100–1200 °C has such a high viscosity that even modern fluxing machines require dissolution times of 30 min or longer. Mixed lithium tetraborate–metaborate fluxes with melting-points of <1000 °C and a high fluidity are widely available but they usually contain a high proportion of lithium metaborate, which produces unstable discs when used with samples that have high concentrations of Mg or Ca.

This paper describes the development of a new flux, designated MAG 5743, with a composition of 57% m/m lithium tetraborate and 43% m/m lithium metaborate, which not only produces stable discs but is also sufficiently reactive so as to obtain the complete dissolution of magnesites, calcined magnesites and dolomites in 10 min at 1000 °C.

Two methods are described. The magnesite method, in which the glass disc composition has a flux to sample (FTS) ratio of 5 : 1, is used with samples for which the LOI is >40% (*i.e.*, uncalcined raw materials). This method provides oxide analysis and a loss on fusion (LOF) value simultaneously. The general method, in which the glass disc composition has an FTS ratio of 10 : 1, is essentially for samples where the LOI is <40%. (*i.e.*, calcined products). Certified reference materials (CRMs)[11] and four magnesite samples are analysed using the new flux.

* To whom correspondence should be addressed.

Experimental

Sample Preparation

The British Chemical Standard (BCS) CRMs magnesites 319 and 389, which are magnesias, were re-ignited at 1025 °C and the dolomite (BCS CRM 368) was oven dried at 110 °C before use. Three discs were prepared from each CRM for analysis and the results obtained were compared with the certificate values.

Four samples of magnesite (labelled magnesite A, B, C and D) from the Kunwarara deposit (Queensland, Australia) with a range of MgO, CaO and SiO_2 contents, were ground to a particle size of <150 μm (100%) for analysis by both the magnesite and general methods. Three glass discs were prepared from each of the magnesite samples using both methods, *i.e.*, the LOFs were determined simultaneously. Each disc was analysed separately over a period of 4 d. The data were compared with those obtained from the same magnesites after calcination at 1300 °C; the LOI was determined separately.

Preparation of MAG 5743 Flux

The flux was a mixture of 57% m/m lithium tetraborate and 43% m/m lithium metaborate. This flux can be obtained custom blended (by special order from suppliers such as Sigma or Johnson Matthey) or can be blended in the laboratory by mixing the constituents, which are then dried at 500 °C in a muffle furnace for at least 4 h. After removal from the furnace, the flux was cooled in a desiccator charged with a suitable desiccant. The flux should be stored in a capped jar in a desiccator. In order to test whether the flux was in a proper condition for use, a 3 g portion was fused at 1000 °C for 10 min to determine the LOF. (If the LOF exceeds 0.2% the flux must be re-dried at 500 °C.)

Preparation of Glass Discs

A 0.3000 ± 0.0005 g sample (general method) or, a 0.6000 ± 0.0010 g sample (magnesite method) was transferred into a 95% Pt–5% Au alloy crucible which had been previously heated to 1000 °C and cooled to constant mass. The sample masses were chosen in order to prepare 30–32 mm diameter discs. Larger diameter discs required larger masses of both sample and flux. The sample was then intimately mixed (by stirring thoroughly with a clean platinum rod) with 3.000 ± 0.001 g of dry flux and the total mass of the crucible and contents recorded. The crucible was placed in a muffle furnace

(containing an agitator mechanism) and the sample fused at 1000 °C for 10 min. Alternatively, any comercially available fusion device fitted with an agitator could be used under equivalent conditions. The crucible was removed from the furnace, cooled rapidly on an aluminium block heat sink contained in a desiccator and then re-weighed. The crucible and glass were returned to the furnace at 1000 °C, allowed to melt, and then poured into a casting mould (95% Pt–5% Au alloy, 30 mm i.d.), which had been pre-heated to at least 1000 °C over an oxygen–liquified petroleum gas (LPG) flame. A muffle furnace of appropriate size (set at 1000 °C) is a suitable alternative for casting the disc. The casting mould containing the molten glass was removed from the heat source and cooled rapidly on a graphite block or an air-cooled aluminium block. The disc was then available for analysis in a suitable X-ray spectrometer. [**N.B.** When a very large number of fusions are made daily, it might be desirable to give the aluminium block a ceramic coating to minimize the possibility of any aluminium adsorption.]

Measurement

The instrument conditions for the determination of the major components MgO, CaO, SiO_2, Al_2O_3 and Fe_2O_3 are listed in Table 1. A Philips PW 1404 wavelength dispersive, sequential X-ray spectrometer equipped with a scandium–molybdenum dual anode side-window X-ray tube (operated at 40 kV), with a flow-proportional counter, was operated under vacuum to measure the Kα lines of each element. A combination of flow-proportional and scintillation counters in tandem was used to measure the intensity of the iron Kα line. Pulse-height selection or line-overlap corrections can be used to reduce interference from the fifth-order calcium Kα line on the first-order magnesium Kα line for samples with a high-calcium and low-magnesium content.

Calibration measurements were carried out using high-purity oxides or carbonates. The calibration was not carried out utilizing CRMs because only three CRMs for this rock type were available, *viz.*, BCS CRMs 319, 368 and 389.

A series of fifteen calibrations on discs containing only single elements was used to calibrate the spectrometer. Multiple regression analysis was used to calibrate the concentration of the ignited oxide (the temperature of ignition was determined by the metal constituent) against intensity (count rate). The matrix interference correction for the element on itself was also calculated simultaneously utilizing the de Jongh equation,[12] which is provided in the Philips X40 software. A further ten discs were prepared with the elements paired as follows: MgO–CaO, MgO–SiO_2, MgO–Al_2O_3, MgO–Fe_2O_3, CaO–SiO_2, CaO–Al_2O_3, CaO–Fe_2O_3, SiO_2–Al_2O_3, SiO_2–Fe_2O_3, and Al_2O_3–Fe_2O_3. The inter-element matrix correction for the paired elements was calculated by regression analysis.[12]

The same series of discs was used for calibration using both the magnesite and general methods. The discs were originally used for the general method but, by using the following equations, the data were corrected for use with the magnesite method. Equation (1) is a general equation that, in this instance, becomes eqn. (2), which in turn, simplifies to eqn. (3)

$$C_{MAG} = C_{GEN} \times \frac{S_{GEN}}{S_{MAG}} \times \frac{T_{MAG}}{T_{GEN}} \quad (1)$$

$$C_{MAG} = C_{GEN} \times \frac{0.3000}{0.6000} \times \frac{3.600}{3.300} \quad (2)$$

$$C_{MAG} = 0.5455\ C_{GEN} \quad (3)$$

where, C_{MAG} is the calibration concentration for the magnesite method; C_{GEN} is the calibration concentration for the general method; S_{GEN} is the sample mass for the general method; S_{MAG} is the sample mass for the magnesite method; T_{MAG} is the sample plus flux mass for the magnesite method; and T_{GEN} is the sample plus flux mass for the general method.

Table 1 Instrumental parameters for Philips PW 1404

Element	Time/s	Crystal	Collimator	2θ/°
Fe	40	LiF 200	Fine	57.57
Ca	40	LiF 200	Fine	113.19
Si	40	PET*	Coarse	109.17
Al	40	PET*	Coarse	145.08
Mg	200	PX1†	Coarse	23.16

* PET = Pentaerythritol.
† PX1 = Synthetic layered crystal, $2d$ = 4.9800 nm.

Repeatability

The repeatability of the results using the two XRF methods was tested over a period of 2–3 d by analysing each of the three individual discs from magnesite sample C in sequence. This measurement sequence was repeated twice at daily intervals and finally one disc was analysed in triplicate. The result for an individual disc reading was compared with that from the group.

Effect of Initial Temperature on Loss on Fusion

Raw magnesite sample B was analysed using the magnesite method. The crucible and contents were placed in the fusion furnace, operating over a range of initial fusion temperatures (500–1000 °C), and the LOF was determined.

Results and Discussion

Development of Flux

Bennett and Oliver[13] have detailed the relative merits and disadvantages of existing fluxes, such as lithium tetraborate (100%) and mixtures with lithium metaborate, for forming fused glass discs. The MAG 5743 flux was developed from Norrish 1222 flux (a mixture of 35% m/m lithium tetraborate and 65% m/m lithium metaborate). Norrish 1222 is an alkaline flux with a low melting-point and a low solubility for oxides such as MgO, CaO and Al_2O_3 (the so-called basic oxides). Stable discs could not be produced with samples of a high magnesium or calcium content with Norrish 1222. The solubility of the basic oxides in Norrish 1222 flux can be increased by the addition of another oxide such as SiO_2, TiO_2 or B_2O_3 in order to decrease the basicity of the flux. Boron(III) oxide is a non-interfering oxide in XRF spectrometry and, when added as a modifier, increases the acidity and also the viscosity of the flux. A mixture of 100 g of Norrish 1222 flux plus 12 g of boron(III) oxide was considered to be necessary in order to obtain a suitable compromise of viscosity, high oxide solubility and low temperature of fusion. The use of this composite flux, however, was limited to pre-ignited samples because the mass of flux lost on fusion is approximately 15 mg g^{-1} which precludes its use for accurate LOF determinations. The variable water content of boron(III) oxide is the cause of the mass loss and makes the flux difficult to stabilize by heating or drying.

The Norrish 1222 flux has a $Li_2O : B_2O_3$ ratio of 20 : 80 and calculations showed that the same ratio could be achieved with a lithium tetraborate–lithium metaborate mixture of 57% m/m lithium tetraborate and 43% m/m lithium metaborate. This flux, which can be obtained custom mixed from a supplier or produced by the user, is stable long-term when dried by heating at 500 °C and stored in a desiccator.

The MAG 5743 is a reactive flux, which is fluid at 1000 °C, in contrast to the lithium tetraborate flux usually used for fusion

of carbonate rocks. The fusion of raw magnesite samples with the MAG 5743 at 1000 °C requires fluxing times (10 min) similar to those required when lithium tetraborate is used at 1100–1200 °C. This is a result of mixing due to the loss of volatiles on fusion. In contrast, caustic calcined and fused magnesia samples require 20–30 min for complete reaction with lithium tetraborate, but only 10 min with the MAG 5743 flux.

The MAG 5743 is a specialized flux, hence, matrix corrections were not possible using commercial calculation programs. Therefore, the corrections obtained for the elements were determined empirically and compared with those calculated using the modified NRL-XRF program[14] for lithium tetraborate and the Norrish 1222 flux, because the composition of the MAG 5743 flux is between these two fluxes. The values obtained empirically were within the range of the values of the program-calculated correction coefficients for Fe_2O_3, CaO, SiO_2, Al_2O_3 and MgO with the lithium tetraborate and Norrish 1222 flux.

Table 2 Repeatability (n = 4) of measurements on three glass discs prepared from sample C

Determinand	Concentration (%)	Standard deviation (%)	Relative standard deviation (%)
MgO	44.83	0.20	0.5
CaO	2.10	0.04	1.9
SiO_2	1.12	0.06	5.4
Fe_2O_3	0.05	0.01	20
Al_2O_3	0.04	0.01	25
LOF	51.80	0.13	0.3

Less than 1% of the beads produced from MAG 5743 cracked; these beads were, nevertheless, still usable.

Repeatability

Table 2 gives details of the results obtained from three separate discs prepared from the magnesite sample C.

The results obtained from the individual discs showed that reproducible, stable discs giving repeatable results could be prepared, for analysis by XRF using the rapid fusion method. The discs slowly absorb moisture (at a rate determined by the relative humidity), which decreases the intensity of the signal. Therefore, long-term storage of the discs in a desiccator is necessary. Determination of the five major components together with the LOF can be obtained within 35–40 min.

Analysis of CRMs

The values obtained using the two methods (*i.e.*, magnesite and general methods) are compared with the certificate values of a series of BCS CRMs in Table 3. As both magnesite standards had already been calcined only the general method could be used. The dolomite (BCS CRM 368) had not been calcined during preparation so it could be used as a basis for comparison of the two methods. Comparison of the results for pre-ignited dolomite (BCS CRM 368) by the general method was not considered valid because the recommended temperature of ignition (1025 °C) does not decompose the sample completely. The measured LOF of the pre-ignited sample was 1.1 ± 0.1%, which together with the measured LOI at 1025 °C of 46.5 ± 0.1% gave a total loss of 47.6 ± 0.2%. This value compares favourably with the LOF at 1030 °C of 47.5 ± 0.3%

Table 3 Comparison of XRF results (n = 12) with the certificate values for the CRMs (all values expressed as percentages)

	Certified reference material										
	BCS 319*			BCS 368†					BCS 389*		
		General method			General method		Magnesite method			General method	
Determinand	Certificate value	Concentration	Standard deviation	Certificate value	Concentration	Standard deviation	Concentration	Standard deviation	Certificate value	Concentration	Standard deviation
MgO	90.46	90.37	0.05	20.9	20.57	0.09	20.47	0.12	96.7	96.65	0.11
CaO	2.28	2.28	0.03	30.8	30.67	0.33	30.58	0.13	1.66	1.66	0.02
SiO_2	1.55	1.58	0.05	0.92	0.92	0.05	0.89	0.01	0.89	0.90	0.05
Al_2O_3	0.97	0.94	0.02	0.17	0.12	0.02	0.14	0.01	0.23	0.21	0.02
Fe_2O_3	4.63	4.58	0.05	0.23	0.24	0.02	0.20	0.02	0.29	0.32	0.03
LOF	NA‡	0.16	0.05	ND‡	47.27	0.15	47.50	0.28	NA	0.21	0.10
LOI	ND	ND	ND	46.7	ND	ND	ND	ND	ND	ND	ND

* Magnesite method not applicable to these samples; pre-treatment temperature, 1025 °C.
† Pre-treatment temperature, 110 °C.
‡ NA = not applicable, ND = not determined.

Table 4 Comparison of XRF results (n = 3) for fused-disc methods (all values expressed as percentages)

	Sample											
	A			B			C			D		
Determinand	1*	2†	3‡	1*	2†	3‡	1*	2†	3‡	1*	2†	3‡
MgO	46.21	46.16	46.30	45.12	45.19	45.35	45.12	45.15	45.08	46.69	46.63	46.53
CaO	1.28	1.25	1.27	2.32	2.31	2.35	2.08	2.07	2.11	1.00	0.98	1.00
SiO_2	0.20	0.20	0.18	0.27	0.25	0.23	1.24	1.17	1.16	0.12	0.12	0.10
Al_2O_3	0.04	0.03	0.03	0.08	0.04	0.05	0.06	0.04	0.05	0.02	0.03	0.01
Fe_2O_3	0.04	0.05	0.05	0.04	0.07	0.04	0.05	0.06	0.05	0.03	0.04	0.03
LOI§	52.23	NA¶	NA	52.03	NA	NA	51.55	NA	NA	52.15	NA	NA
LOF‖	NA	52.42	52.30	NA	52.07	52.05	NA	51.83	51.66	NA	52.43	52.44

* Results for ignited sample (0.3 g, 1300 °C) with values adjusted for LOI.
† Results for sample (0.3 g) with no adjustment, and LOF determined using the general method.
‡ Results for sample (0.6 g) with no adjustment, and LOF determined using the magnesite method.
§ LOI determined by igniting sample at 1300 °C before fusion.
¶ NA = not applicable.
‖ LOF determined after fusion at 1000 °C.

(Table 3). Loss on ignition results are always lower because of incomplete decomposition. The LOI results are only comparable to LOF results if the magnesite dolomite has been ignited at 1300 °C to constant mass. Certified reference materials (BCS CRMs 319, 368 and 389) can only be used for comparison (Table 3) because CRMs 319 and 389 are burnt magnesites and 368 is a dolomite.

Analysis of Magnesites

Originally, the flux was developed for the rapid analysis of calcined magnesia but, because the flux was so stable, it was decided that the method could be modified and applied to unignited samples, thus including LOF in the analysis. The LOF value was therefore included as a correction factor in the de Jongh equation.[15]

With unignited samples, the LOF can be as much as 52% for magnesite and 42% for calcite which means that, if a 10 : 1 FTS ratio is used, the line intensities are reduced to about half those produced using a disc prepared from ignited material. In order to compensate for this loss in signal, the mass of sample was doubled thus halving the FTS ratio. The alternative method of maintaining the signal, *i.e.*, by doubling the count time, was rejected because of the concomitant increase in analysis time. A further benefit was achieved by increased accuracy in weighing.

Table 4 shows a comparison of the results obtained for the four magnesite samples, using the conventional, general and magnesite methods. As with the results for the CRMs, agreement was achieved between the conventional analysis and the two proposed methods.

Effect of Initial Fusion Temperature on LOF Value

Loss on fusion values for magnesite sample B of 52.03, 52.07, 52.10, 52.16 and 52.11% were obtained for initial fusion temperatures of 500, 600, 700, 800 and 1000 °C, respectively. The LOF value obtained using the magnesite method was 52.09 ± 0.13%.

The results show that there was virtually no sample loss during the fusion. If any loss of mass had occurred owing to decrepitation of the sample, as opposed to loss due to CO_2 and H_2O evolution, the LOF value would have been greater at higher initial fusion temperatures.

Conclusion

A rapid fusion technique has been developed for the determination by XRF of the major oxides in magnesites, magnesias and dolomites. The total analysis time is as short as 40 min. The flux used in the fusion (MAG 5743), if prepared properly, has no LOI and produces stable discs. Thus it can be used for the accurate and rapid simultaneous determination of the major oxides and the LOF.

The validity of the method was checked by comparison of the results with the certificate values of three CRMs.

The work reported here was sponsored by Queensland Magnesia Pty. Ltd.

References

1 King, B.-S., and Vivit, D., *X-Ray Spectrom.*, 1988, **17**, 85.
2 King, B.-S., and Vivit, D., *X-Ray Spectrom.*, 1988, **17**, 145.
3 Simonov, K. V., Zos'ka, A. V., Polovinkina, R. S., and Dremina, V. A., *Ind. Lab. (Engl. Transl.)*, 1979, **44**, 1026.
4 Prager, M. F., and Graves, D., *J. Am. Oil Chem. Soc.*, 1977, **60**, 1386.
5 British Chemical Standard, Certificate of Analysis.
6 Standards Association of Australia, AS2503.4, 1987.
7 International Standards Organization/Draught International Standard, 10058.
8 American Society for Testing and Materials, C574, 1982.
9 Deutsche Industrie Norm, 273, 1981.
10 Pertl, A., Lehmann, H., and Grubitsch, H., *Radex Rundsch.*, 1976, **1**, 639.
11 Govindaraju, K., *Geostand. Newsl.*, 1989, **XIII** (Special Issue), Appendix 1, p. 27.
12 de Jongh, W. K., *X-Ray Spectrom.*, 1973, **2**, 151.
13 Bennett, H., and Oliver, G. J., *Analyst*, 1976, **101**, 803.
14 Norrish, K., Commonwealth Scientific and Industrial Research Organization (CSIRO), Adelaide, South Australia, Australia, personal communication, 1990.
15 de Jongh, W. K., *X-Ray Spectrom.*, 1979, **8**, 52.

Paper 0/04412A
Received October 1st, 1990
Accepted December 19th, 1990

Kinetic Model of pH-based Potentiometric Enzymic Sensors

Part 1. Theoretical Considerations

Stanisław Glab, Robert Koncki and Adam Hulanicki
Department of Chemistry, University of Warsaw, Pasteura 1, 02-093 Warsaw, Poland

A theoretical, kinetic model for a pH-based potentiometric enzymic sensor has been developed. It has been shown that the response of these sensors is governed by the pH, the buffering capacity of solutions analysed, and also the stirring rate. This model takes into account the variability of the kinetics of the enzymic reaction. The final equation is presented in an algebraic form and can be used in both fitting and optimization procedures.

Keywords: *Potentiometric enzymic pH sensor; kinetic model; steady-state response*

Enzymic sensors are important analytical devices used for the determination of substances that often cannot be determined by conventional methods of analysis.[1] In these devices a substrate-active enzyme layer is placed directly on the surface of a classical sensor that measures the concentration of the products formed in the enzymic reaction. In a large number of enzymic reactions, substances having protolytic properties are either formed or consumed. This explains why the pH-based potentiometric enzymic sensors are probably among the most versatile of the potentiometric enzymic sensors. Development of this group of biosensors has stimulated studies on the formulation of a mathematical model, describing the physico-chemical phenomena responsible for the formation of the analytical signal.

Until now, mainly diffusion models for the enzymic electrodes have been presented.[2–6] These models lead to equations that can only be solved by assuming that the kinetics of the enzymic reaction are of first or zero order.[2] Owing to the form of the Michaelis–Menten equation, in general non-linear parabolic differential equations are obtained, which cannot be solved simply. The solution of these equations can be presented either as a definite integral in a non-elementary form or as an expansion of a power series.[3,4] Therefore, sometimes, instead of these equations extrapolation methods are used.[5]

Diffusion models can be applied in order to describe the response of electrodes with a thick layer of enzyme and with defined geometry. These models do not take into account the influence of the rate of stirring on the analytical signal, commonly observed in practical measurements with enzymic electrodes. In order to explain this effect, the diffusion coefficients inside the enzyme sensing layer are assumed to vary with the rate of stirring.[3,4] This assumption is also made by other authors[7] for electrodes with liquid-state membranes. Another treatment of this problem is based on the consideration of the changes of concentration in a hypothetical interfacial zone between the enzyme layer and the bulk solution.[6] From a mathematical point of view this model is very complicated and special numerical procedures have to be used.

The papers mentioned above deal with models of the enzymic electrode response when the potentiometric sensor is sensitive to the product of an enzymic reaction. Modifications of these diffusion models for pH-metric sensors lead to more complicated equations. Combination of the equations describing the diffusion of the respective species, with equations describing the kinetics of the protolytic reactions[8,9] or acid–base equilibria[10–15] leads to a set of non-linear partial differential equations of the second order. These equations can be transformed, in special instances, into a rather complicated algebraic form.[8–11] For example, when the kinetics of a protolytic reaction are taken into consideration, the enzymic reaction is assumed to be first order and any acid product assumed to be fully dissociated.[8,9] Combination of the kinetic constants of the enzymic and protolytic reactions in the same equation also seems to be unjustified, because the magnitudes of these parameters are not comparable.[16] Combination of equations describing diffusion with equations describing dissociation leads to algebraic equations only when it is assumed that the substrate is totally transformed into protolytic products.[10,11] This drastic assumption is equivalent to a situation, considered by a classical equation, describing the pH of a mixture of weak acids and bases.[17] Varanasi and co-workers[10,11] have taken into account the influence of stirring with an assumption that the concentrations of all of the species at the surface of the electrode and in the bulk solution are different.

The diffusion model in the general form without the assumptions mentioned above and, in addition, considering the modification of the kinetics of the enzymic reaction by inhibitors or pH, leads to a very complicated expression. Therefore, special numerical procedures have to be used.[12–15]

The mathematical complexity of the models presented above, and the difficulties with the interpretation of the influence of the rate of stirring on measurements, are caused by an assumption that the transport rate is proportional to the gradient of the concentration. This inconvenience can be ignored if, as assumed by Morf,[18] the transport rate is proportional to the concentration of the species. In this instance, the derived equations are analogous to the kinetic equations. These equations take into account the influence of stirring, which causes the change in the rate constant. The model by Morf describes an enzymic layer on the potentiometric electrode, which is sensitive to the product of the enzymic reaction.

The aim of this paper is to present a simple model of the response of a pH-based potentiometric enzymic sensor. The proposed model is a modification of the substrate–enzyme electrode model of Morf.[18]

Description of the Model

The layer on the surface of a pH sensor contains an enzyme that catalyses the reaction of the substrate, S, leading to the formation of an acid, HA, a base, B, and a non-protolyic product, Z:

$$S + n_X X \xrightarrow{\text{Enzyme}} n_A HA + n_B B + n_Z Z \qquad (1)$$

where, n denotes the respective stoichiometric coefficients and X refers to other reaction substrates present.

The rate, V, of the over-all enzymic reaction is given by the equation:

$$V = \frac{V_{max}[S]}{K_m + [S]} \quad (2)$$

where V and [S] denote the actual rate and concentration of the substrate in the enzymic layer, K_m is the Michaelis–Menten constant and V_{max} the maximum reaction rate. It is possible to take into account the variability of the kinetic parameters V_{max} and K_m [in eqn. (2)] as a function, for example, of pH, as discussed later.

The protolytic equilibria in the sensing layer for the reaction products, HA and B, and for the buffer system HW–W, are described by the corresponding acid dissociation constants, K_{aX}, these constants are assumed to be equal to those in the bulk of the solution:

$$K_{aA} = \frac{[H][A]}{[HA]} \quad (3a)$$

$$K_{aB} = \frac{[H][B]}{[HB]} \quad (3b)$$

$$K_{aW} = \frac{[H][W]}{[HW]} \quad (3c)$$

The mass balances in the enzymic layer and in the bulk solution, marked with the superscript B, are given by eqns. (4a)–(4e):

$$c_W^B = [W]^B + [HW]^B \quad (4a)$$

$$c_W = [W] + [HW] \quad (4b)$$

$$c_A = [A] + [HA] \quad (4c)$$

$$c_B = [B] + [HB] \quad (4d)$$

$$c_H = [H] + [HW] + [HA] + [HB] \quad (4e)$$

In these equations the symbols c_X correspond to total concentration in the sensing layer, or c_X^B, the concentration, in the bulk solution. All of the protolytic species can diffuse in either direction across the hypothetical semi-permeable membrane which separates the bulk of the analyte solution from the enzyme-containing sensing layer. The transport of the respective species is described by the transport rate constants, k_W, k_{HW}, *etc.* It is assumed that there is no preconcentration of substances in the enzymic layer. This means that the transport rate constants in both directions are equal.

The scheme presented in Fig. 1 illustrates the proposed model for the response of pH-based potentiometric enzymic sensors. The substrate having concentration $[S]^B$ in the bulk of the analysed solution diffuses into the enzymic layer with a transport rate constant, k_S, and can pass out again with the same rate constant. A decrease in the substrate concentration of the enzymic layer is a result of the enzymic reaction occurring with the rate described by the Michaelis–Menten equation [in eqn. (2)].

The rate of changes of the total concentration of substances [eqns. (4a)–(4e)] in the enzymic layer are represented by a set of equations, which take into account the rate of transport of respective species into and out of the sensing layer, and also the rate of the following enzymic reactions:

$$\frac{d[S]}{dt} = k_S[S]^B - k_S[S] - \frac{V_{max}[S]}{K_m + [S]} \quad (5a)$$

$$\frac{dc_W}{dt} = k_W[W]^B + k_{HW}[HW]^B - k_W[W] - k_{HW}[HW] \quad (5b)$$

$$\frac{dc_A}{dt} = n_A\frac{V_{max}[S]}{K_m + [S]} - k_A[A] - k_{HA}[HA] \quad (5c)$$

$$\frac{dc_B}{dt} = n_B\frac{V_{max}[S]}{K_m + [S]} - k_B[B] - k_{HB}[HB] \quad (5d)$$

$$\frac{dc_H}{dt} = k_H[H]^B + k_{HW}[HW]^B + n_A\frac{V_{max}[S]}{K_m + [S]} - k_H[H] - k_{HW}[HW] - k_{HW}[HW] - k_{HA}[HA] - k_{HB}[HB] \quad (5e)$$

At steady state, the conversion of substrate and the formation of product is compensated for by the interfacial mass transfer, and consequently the concentrations of all of the substances are constant. Therefore, the derivatives are equal to zero and eqns. (5a)–(5e) can be re-written in the forms given by eqns. (6a)–(6e):

$$k_S[S]^B = k_S[S] + \frac{V_{max}[S]}{K_m + [S]} \quad (6a)$$

$$k_W[W]^B + k_{HW}[HW]^B = k_W[W] + k_{HW}[HW] \quad (6b)$$

$$n_A\frac{V_{max}[S]}{K_m + [S]} = k_A[A] + k_{HA}[HA] \quad (6c)$$

$$n_B\frac{V_{max}[S]}{K_m + [S]} = k_B[B] + k_{HB}[HB] \quad (6d)$$

$$k_H[H]^B + k_{HW}[HW]^B + n_A\frac{V_{max}[S]}{K_m + [S]} = k_H[H] + k_{HW}[HW] + k_{HA}[HA] + k_{HB}[HB] \quad (6e)$$

The eqns. (6a)–(6e) are based on the assumption of a steady state, which means that the rate of increase of the concentration in the enzymic layer (the left-hand sides of the equations) is the same as the rate of decrease (the right-hand sides of the equations). The sets of eqns. (3a)–(3c), (4a)–(4c) and (5a)–(5e) give the solution in an algebraic form [eqn. (7)] which shows the dependence of the hydrogen ion concentration, inside the enzymic layer, on the substrate concentration, $[S]^B$, in the bulk solution.

$$k_H([H]^B - [H]) + k_{HW}\left([HW]^B - \frac{k_{HW}[HW]^B + k_W[W]^B}{k_{HW} + k_W K_{aW}/[H]}\right) + \frac{V_{max}[S]}{K_m + [S]}\left[n_A\left(1 - \frac{k_{HA}}{k_{HA} + k_A K_{aA}/[H]}\right) - n_B\left(\frac{k_{HB}}{k_{HB} + k_B K_{aB}/[H]}\right)\right] = 0 \quad (7)$$

In the derivation of the final equation the transport rate for the species is assumed not to depend on protonation, *i.e.*, k_A =

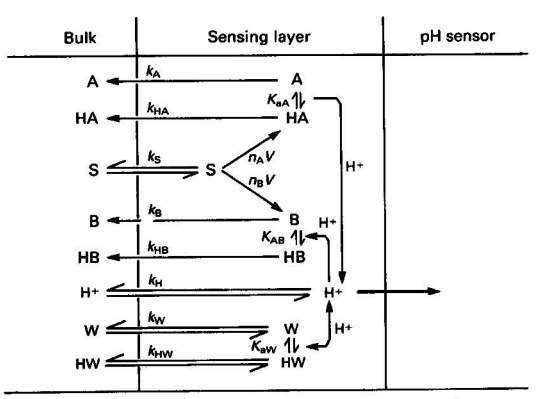

Fig. 1 Scheme of the pH-based potentiometric enzymic sensor. Where: k and K_a, with corresponding subscripts, are transport rate constants and acid dissociation constants, respectively, for species indicated by the subscripts; and HW–W is a pH buffer system. Other symbols as in eqns. (1) and (2)

k_{HA} *etc.* This is, most probably, a sufficiently good approximation, but the differences can also be taken into account, thus making the final equation more complicated, but still solvable. With the assumptions mentioned above it is possible to transform eqn. (7) into:

$$k_H([H]^B - [H]) + k_W c_W^B \left[\frac{1}{1 + K_{aW}/[H]^B} - \frac{1}{1 + K_{aW}/[H]}\right] + \frac{V_{max}[S]}{K_m + [S]}\left(\frac{n_A}{1 + [H]/K_{aA}} - \frac{n_B}{1 + K_{aB}/[H]}\right) = 0 \quad (8)$$

where [S], obtained by solving eqn. (6a), is given by:

$$[S] = \frac{1}{2}\left[[S]^B - \frac{V_{max}}{k_S} - K_m + \sqrt{\left([S]^B - \frac{V_{max}}{k_S} - K_m\right)^2 + 4K_m[S]^B}\right] \quad (9)$$

From eqns. (8) and (9), using normalized rate constants defined by eqns. (10a)–(10c),

$$\bar{k}_H = \frac{k_H}{k_S} \quad (10a)$$

$$\bar{k}_W = \frac{k_W}{k_S} \quad (10b)$$

$$\bar{k}_V = \frac{V_{max}}{k_S} \quad (10c)$$

a general algebraic equation describing the proposed model is obtained:

$$\bar{k}_H([H]^B - [H]) + \bar{k}_W c_W^B\left[\frac{1}{1 + K_{aW}/[H]^B} - \frac{1}{1 + K_{aW}/[H]}\right] + \frac{1}{2}\left[[S]^B + \bar{k}_V + K_m \sqrt{([S]^B - \bar{k}_V - K_m)^2 + 4K_m[S]^B}\right]\left[\frac{n_A}{1 + [H]/K_{aA}} - \frac{n_B}{1 + K_{aB}/[H]}\right] = 0 \quad (11)$$

This equation can be transformed into simple linear relationships *versus* analyte concentration and/or normalized rate constants for the following situations:

firstly, for $[S]^B \gg [S]$,

$$\bar{k}_H([H]^B - [H]) + \bar{k}_W c_W^B\left[\frac{1}{1 + K_{aW}/[H]^B} - \frac{1}{1 + K_{aW}/[H]}\right] + [S]^B\left[\frac{n_A}{1 + [H]/K_{aA}} - \frac{n_B}{1 + K_{aB}/[H]}\right] = 0 \quad (12a)$$

secondly for, $K_m \ll [S]$

$$\bar{k}_H([H]^B - [H]) + \bar{k}_W c_W^B\left[\frac{1}{1 + K_{aW}/[H]^B} - \frac{1}{1 + K_{aW}/[H]}\right] + \bar{k}_V\left[\frac{n_A}{1 + [H]/K_{aA}} - \frac{n_B}{1 + K_{aB}/[H]}\right] = 0 \quad (12b)$$

and thirdly for, $K_m \gg [S]$

$$\bar{k}_H([H]^B - [H]) + \bar{k}_W c_W^B\left[\frac{1}{1 + K_{aW}/[H]^B} - \frac{1}{1 + K_{aW}/[H]}\right] + \frac{\bar{k}_V[S]^B}{K_m + \bar{k}_V}\left[\frac{n_A}{1 + [H]/K_{aA}} - \frac{n_B}{1 + K_{aB}/[H]}\right] = 0 \quad (12c)$$

Because of the simplicity of the form of eqns. (11) and (12a)–(12c) it is not difficult to take into account the influence of inhibitors.[1,19] For this purpose the Michaelis–Menten equation [eqn. (2)] should only be modified to include the concentrations of the competitive, $[I_c]$, and non-competitive, $[I_{nc}]$, inhibitors [eqn. (13a)].[1,19]

$$V = \frac{V_{max}[S]}{K_m(1 + [I_c]/K_{I_c}) + [S](1 + [I_{nc}]/K_{I_{nc}})} \quad (13a)$$

where K_{I_c} and, $K_{I_{nc}}$ are the respective inhibition constants.

In a similar way to the influence of the substrate and the products, inhibitors can also be taken into account:

$$V'_{max} = \frac{V_{max}}{1 + [P]/K_{I_p}} \quad (13b)$$

$$K'_m = K_m(1 + [S]^2/K_{I_s}) \quad (13c)$$

The kinetic parameters of the enzymic reaction, K'_m and V'_{max} strongly depend on pH. The influence of pH on these parameters can be described by a simple protolytic model proposed by Waley.[1,19,20] This model (Fig. 2) assumes that only one protolytic form of the enzyme can form an activated complex with the substrate, and only one protolytic form of this complex is irreversibly decomposed upon the formation of the enzyme and products. On the basis of this model the following relationships can be obtained:

$$V'_{max} = \frac{V_{max}\,pH_{opt}}{1 + K_{a1}/[H] + [H]/K_{b1}} \quad (14a)$$

$$K'_m = K_m\,pH_{opt}\frac{1 + K_{a2}/[H] + [H]/K_{b2}}{1 + K_{a1}/[H] + [H]/K_{b1}} \quad (14b)$$

where pH_{opt} denotes the pH at which the enzyme activity is at a maximum. K_{a1}, K_{a2}, K_{b1} and K_{b2} are acidic and basic dissociation constants, respectively (see Fig. 2). These relationships, can easily be introduced into the general equation [eqn. (11)] or into the approximate forms of the equation [eqns. (12a)–(12c)]. These modifications allow the variability of the enzymic reaction kinetics, influenced by local changes of pH inside the enzymic layer, to be taken into account.

Discussion

The model presented in this work for the response of the pH-based potentiometric enzymic sensors assumes that the enzymic layer is separate from the bulk solution. All of the components of the solution and the enzyme layer, except for the enzyme molecules are able to diffuse through the membrane in both directions. Realistic examples which can be described by the proposed model are enzymic sensors with pseudo-immobilized enzymes connected to the surface of the pH sensor by means of a dialysis membrane. However, the application of the model is not limited to this instance only. In several situations (including that for the hydrogen ion because of the enzymic reaction), such a membrane does not exist at all, and there is only a hypothetical border between the bulk solution and the zone where the local concentration changes, which alter the analytical signal, occur. The thickness of the enzymic layer is not defined in the proposed model. Contrary to the previously described diffusion models,[12–15] this means that this model is not applicable for use in describing the concentration profiles inside the sensing layer. On the other hand, the geometry of the sensing layer does not have to be known, and this is a major advantage of the proposed model. Diffusion models cannot be used for describing the response of enzymic sensors with a monomolecular sensing layer of enzyme. Because the geometry of the enzymic layer is not

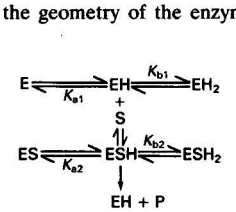

Fig. 2 Scheme of the protolytic model by Waley to describe the enzymic reaction. Where S = substrate; P = product; and E = enzyme

known it is not important to know the exact concentration of the enzyme in this layer. The enzyme concentration in the sensing layer, however, is required for a diffusion model. This becomes impossible when the enzyme is covalently bound to the surface of the sensor. Therefore, electrodes with thin enzymic layers can also be described by the proposed model.

Diffusion models adequately describe the pH response of sensors with thick enzymic layers, whereas for electrodes with thin sensing layers the use of the model proposed by Morf is more plausible,[18] after the appropriate modification for pH-based sensors. This is confirmed by the observation that the response of thin-layer sensors depends on the stirring rate, whereas with thick enzyme film electrodes this effect is not seen. The proposed model takes the stirring effect into account, as stirring modifies the respective transport rate constants.

Apart from the fundamental differences in the treatment of the transport phenomena, the diffusion and kinetic models lead to the same conclusions. However, the model proposed in this paper appears to be more practicable because of the mathematical simplicity. The general equation [eqn. (11)] can be modified without increasing the mathematical complexity. This model can also be used when a polyprotic acid is used as a component of the buffer system and/or polyprotic products are formed in the enzymic reaction. This requires only small changes in eqns. (3a)–(3c), (4a)–(4c) and (5b)–(5c). The proposed model also allows for differences between the transport rate constants, which depends both on the type of substance and the type of protolytic form [eqn. (7)]. Similarly an assumption that the transport rates both to and from the sensing layer are different does not exclude the use of the equation. In this instance, only the distribution coefficients will quantitatively describe the process of species concentration. These modifications complicate the general equation [eqn. (11)] but do not cause difficulties in its use. The same modifications, when introduced to the diffusion model, markedly increase the mathematical complexity.

On the other hand, some simplifications of the general equation [eqn. (11)] are possible when proper approximations [eqns. (12a)–(12c)] are accepted. If the concentration of the substrate in the sensing layer is assumed to be much smaller than that in the bulk solution, *i.e.*, $[S] \ll [S]^B$, hence, only the transport phenomena govern the response, then an equation [eqn. (12a)] is obtained, which is an explicit algebraic function $[S]^B = f[H]$. This relationship is linear *versus* the transport parameters and the buffer concentration, but owing to the assumption that the substrate is totally transformed into products in the enzymic reaction, the kinetic parameter does not appear in this equation. This equation is identical with one of the equations for the diffusion model, derived with the same assumptions[10,11] when the kinetic parameters, $\bar{k}_H$ and $\bar{k}_W$, are replaced by the partition coefficients (defined as the concentration ratio of the species at the sensing layer and in the bulk solution). An additional assumption that the transport rate constants for all species are the same ($\bar{k}_H = \bar{k}_W = 1$) leads to the transformation of eqn. (12a) into the classical equation describing the pH value of a mixture of acids and bases.[17]

Equation (12a) can be used for describing the response of pH-based sensors when the concentration of the substrate, $[S]^B$, is low. The response calculated by using the equation agrees with the experimental response[10,11] for urea[21] and penicillin[14] sensors at low concentrations of substrate. The differences at higher concentrations of the substrate (the lack of the upper limit of determination) appear because the kinetic parameters of the enzymic reaction are not taken into account. The proposed model allows the pH at the upper determination limit to be calculated, on the basis of eqn. (12b), which was obtained with the assumption that the kinetics of the enzymic reaction are of zero order. For zero order kinetics ($[S] \gg K_m$), eqn. (12b) is obviously independent of the substrate concentration and describes only the maximum value of the analytical signal, *i.e.*, the pH which corresponds to the concentration at the upper limit of determination. The derivation of eqn. (12c) is based on the approximation of the Michaelis–Menten non-linear equation by a kinetic equation, for the first-order reaction, ($[S] \ll K_m$). It should be noted that for large values of $\bar{k}_V$, *i.e.*, for a high level of enzyme activity, the simplified equation [eqn. (12c)] approaches that for the diffusion model, where $[S] \ll [S]^B$.

In all the instances mentioned, as for the general equation, the bisection method can be applied. The equations are linear *versus* the various parameters, which makes the use of linear algebra possible, and in consequence, simple numerical optimization and fitting procedures. The calibration graphs calculated for any given experimental conditions, approximate the general equation relationships in particular regions (Fig. 3).

As mentioned earlier it is not difficult to take into account the influence of inhibitors on the kinetics parameter [eqns. (11), (12b), (12c) and (13a)]. Because inhibitors are neither consumed nor formed it can be assumed that their concentrations in the bulk solution are equal to that in the enzyme layer. When the solutions to be analysed contain inhibitors at equal concentrations, the use of eqn. (2) without modification except for the apparent kinetic parameters K_m and V_{max} (*i.e.*,

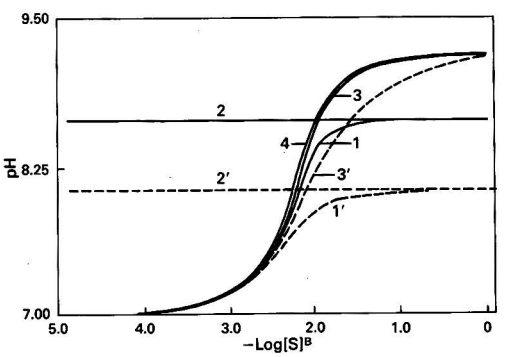

Fig. 3 Theoretical response of pH-based sensor. As an example the urea sensor is used. Phosphate buffer, pH 7.0, 0.01 mol dm^{-3}. The curves were calculated from the general equation describing the proposed model: 1 and 1′, without any approximations (general equation); 2 and 2′, with the assumption that $K_m \ll [S]$ (zero order); 3 and 3′, with the assumption that $K_m \gg [S]$ (first order); and 4, with the assumption that $[S] \ll [S]^B$ (substrate concentration in the sensing layer negligible). Lines 1′, 2′ and 3′, the influence of pH on enzyme kinetics was taken into account

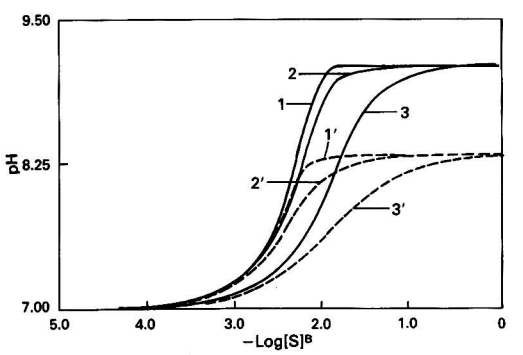

Fig. 4 Influence of the value of the Michaelis–Menten constant, K_m, on the response of the pH-based urea sensor. Phosphate buffer, pH 7.0, 0.01 mol dm^{-3}. Where $\bar{k}_V = 0.01$; 1 and 1′, $K_m = 0.0001$ mol dm^{-3}; 2 and 2′, $K_m = 0.001$ mol dm^{-3}; and 3 and 3′, $K_m = 0.01$ mol dm^{-3}. Lines 1′, 2′ and 3′, the influence of pH on enzyme kinetics was taken into account

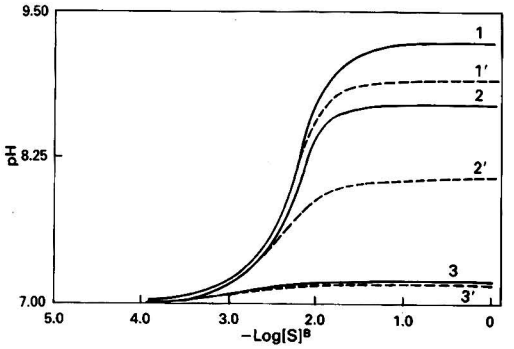

Fig. 5 Influence of normalized rate constant of enzymic reaction, k_v, on the response of the pH-based sensor (urea sensor). Phosphate buffer, pH 7.0, 0.01 mol dm^{-3}; K_m = 0.001 mol dm^{-3}. 1 and 1′, $\bar{k}_V$ = 0.1; 2 and 2′, $\bar{k}_V$ = 0.01; and 3 and 3′, $\bar{k}_V$ = 0.001. 1′, 2′ and 3′, the influence of pH on enzyme kinetics was taken into account

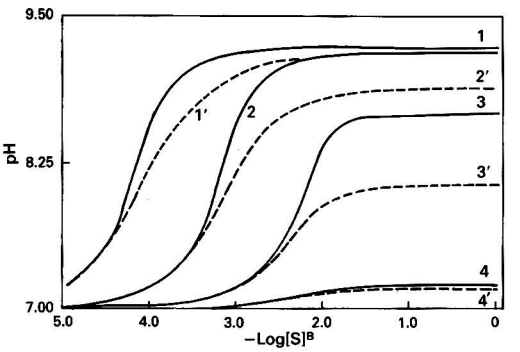

Fig. 6 Influence of buffer concentration, c_W^B on the response of the pH-based urea sensor. Phosphate buffer, pH 7.0; K_m, 0.001 mol dm^{-3}; and $\bar{k}_V$, 0.01. 1 and 1′, $c_W^B = 1 \times 10^{-4}$ mol dm^{-3}; 2 and 2′, $c_W^B = 1 \times 10^{-3}$ mol dm^{-3}; and 3 and 3′, $c_W^B = 1 \times 10^{-2}$ mol dm^{-3}. 1′, 2′ and 3′, the influence of pH on enzyme kinetics was taken into account

$\bar{k}_v$), is possible. The response of the pH-based potentiometric enzymic sensor is affected by local changes of pH within the sensing layer, because of the change of enzymic reaction kinetics. This is taken into account in eqns. (14a) and (14b) (Fig. 3). The introduction of all of the modifications discussed above causes an increase in the complexity of the final relationships, but as previously stated there are simple algebraic equations in either non-explicit [eqn. (11)] or explicit [eqns. (12a)–(12c)] forms. The introduction of these modifications to the equations describing the diffusion models requires the use of complicated numerical methods which can give only approximate solutions.

By using eqns. (11), (12b) and (12c) it is possible to anticipate the influence of kinetic parameters on the shape of the calibration graphs. The value of the Michaelis–Menten constant affects mainly the upper limit of determination and only slightly changes the analytical signal. The larger the value of K_m, the further the upper limit of determination is extended, but the sensitivity decreases (Figs. 4 and 5). The parameter $\bar{k}_V$ indicates the influence of the enzyme activity on the calibration graph (Fig. 5) because it has the same function as the 'loading factor' in the diffusion models. An increase of $\bar{k}_V$ causes an increase in the sensitivity of the sensor over a range of concentrations.

For all of the substances, the transport rate constants [eqns. (10a)–(10c)] depend on the stirring rate to the same extent, therefore, only $\bar{k}_V$ takes into account the effect of stirring. An increase in the stirring rate decreases the value of $\bar{k}_V$ and consequently, also the sensitivity of the detector (Fig. 5).

The proposed model allows a prediction to be made regarding the influence of the concentration and pH of the buffer used, on the shape of the calibration graph for the pH-based potentiometric enzymic sensor (Figs. 6 and 7). An increase in the concentration of the buffer, c_W^B, shifts the calibration graph towards the higher concentration range and decreases the sensitivity (Fig. 6). The sensitivity of the sensor is mainly dependent on the pH in the bulk solution, pH^B. When, owing to the enzymic reaction, the pH increases, a decrease in the sensitivity of the sensor is observed for a pH-based potentiometric enzymic electrode for urea (Fig. 7). A small influence on the detection limit is primarily connected with the changes in buffering capacity. Therefore, at a pH close to the pK_a of the buffer (*i.e.*, for maximum buffering capacity) the sensor shows the worst detection limit.

All of the effects mentioned above were experimentally investigated in detail and will be submitted for publication at a later date.

The considerations presented in this paper refer to the steady state. When a non-steady state is considered the

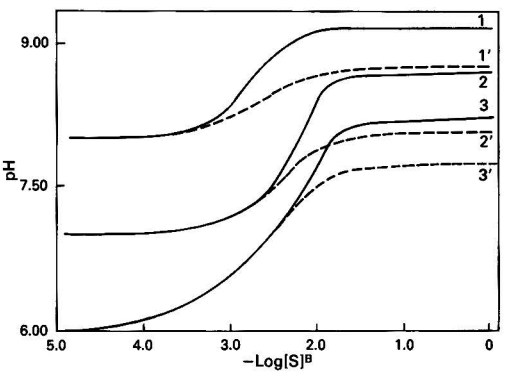

Fig. 7 Influence of pH of the analysed solution, pH^B, on the response of the pH-based urea sensor. Phosphate buffer, 0.01 mol dm^{-3}; K_m = 0.001 mol dm^{-3}; and $\bar{k}_V$ = 0.01. 1 and 1′, pH = 8.0; 2 and 2′, pH = 7.0; and 3 and 3′, pH = 6.0. 1′, 2′ and 3′, the influence of pH on enzyme kinetics was taken into account

differential equations [eqns. (5a)–(5e)] have to be solved. Because the magnitude of the transport rates, for all of the substances, and the rate of the enzymic reaction are of the same order, and because the rates of protolytic reactions are much higher,[16] the consideration may be limited to a discussion of eqn. (5a) as carried out by Morf.[18]

Conclusion

The proposed kinetic model for the response of the pH-based potentiometric enzymic sensor has the following advantages in comparison to earlier published models. (*i*) The model is mathematically simple, and in order to describe it only algebraic equations are required. (*ii*) The geometry of the enzymic sensing layer need not be defined. (*iii*) Stirring effects are taken into account. (*iv*) Modifications of the model are possible, without further complications, and which take into account: the differences in the transport rates of the respective species; the process of concentrating the species in the enzymic layer; the decrease in enzyme activity caused by local changes in pH or by the presence of inhibitors; and all protolytic equilibria.

The proposed model also leads to conclusions similar to those of the previously described diffusion models.

This model can be applied not only to potentiometric sensors but generally to systems where hydrogen ions are monitored such as ISFETs (ion selective field effect transistor) and optodes.

References

1 Carr, P. W., and Bowers, L. D., *Immobilized Enzymes in Analytical and Clinical Chemistry. Fundamentals and Applications*, Wiley, New York, 1980.
2 Blaedel, W. J., Kissel, T. R., and Boguslaski, R. C., *Anal. Chem.*, 1972, **44**, 2030.
3 Hameka, H. F., and Rechnitz, G. A., *Anal. Chem.*, 1981, **53**, 1586.
4 Hameka, H. F., and Rechnitz, G. A., *J. Phys. Chem.*, 1983, **87**, 1235.
5 Brady, J. E., and Carr, P. W., *Anal. Chem.*, 1980, **52**, 977.
6 Jochum, P., and Kowalski, B. B., *Anal. Chim. Acta*, 1982, **144**, 25.
7 Morf, W. E., Lindner, E., and Simon, W., *Anal. Chem.*, 1975, **47**, 1596.
8 Eddowes, M. J., *Sens. Actuators*, 1985, **7**, 97.
9 Eddowes, M. J., Pedley, D. G., and Webb, B. C., *Sens. Actuators*, 1985, **7**, 233.
10 Varanasi, S., Stevens, R. L., and Ruckenstein, E., *AIChE J.*, 1987, **33**, 558.
11 Varanasi, S., Ogundiran, S. O., and Ruckenstein, E., *Biosensors*, 1988, **3**, 269.
12 Caras, S. D., Janata, J., Saupe, D., and Schmitt, K., *Anal. Chem.*, 1985, **57**, 1917.
13 Caras, S. D., Petelenz, D., and Janata, J., *Anal. Chem.*, 1985, **57**, 1920.
14 Caras, S. D., and Janata, J., *Anal. Chem.*, 1985, **57**, 1924.
15 Moynihan, H. J., and Wang, N.-h. L., *Biotechnol. Progr.*, 1987, **3**, 90.
16 Bell, P. R., *Acids and Bases: Their Quantitative Behaviour*, Methuen, London, 1969.
17 Hulanicki, A., *Reactions of Acids and Bases in Analytical Chemistry*, Ellis Horwood, Chichester, 1989.
18 Morf, W. E., *Mikrochim. Acta*, 1980, **2**, 317.
19 *The Enzymes*, ed. Boyer, P. D., Academic Press, New York, vol. 1, 1970.
20 Waley, S. G., *Biochim. Biophys. Acta*, 1953, **10**, 27.
21 Nilsson, H., Akerlund, A. C., and Mosbach, K., *Biochim. Biophys. Acta*, 1975, **320**, 529.

Paper 0/03136D
Received July 12th, 1990
Accepted January 14th, 1991

Studies on Enzyme Electrodes With Ferrocene and Carbon Paste Bound With Cellulose Triacetate

S. K. Beh, G. J. Moody and J. D. R. Thomas*
School of Chemistry and Applied Chemistry, University of Wales College of Cardiff, P.O. Box 912, Cardiff CF1 3TB, UK

A ferrocene-based chemically modified electrode has been prepared from a mixture of carbon paste and ferrocene, bound with cellulose triacetate. Glucose oxidase immobilized onto nylon net placed over the chemically modified indicator electrode completed the assembly of a robust ferrocene-mediated enzyme electrode. This was housed in a three-electrode Stelte micro-cell modified for flow injection according to previous studies, and further modified by introducing a viscose acetate exclusion membrane between the outermost nylon–enzyme mesh and the ferrocene–carbon paste layer. Glucose was determined amperometrically by monitoring the product of hydrogen peroxide enzymolysis at +160 mV *versus* a silver–silver chloride reference electrode. The enzyme electrodes showed a detection range of 0.01–70 mmol dm^{-3} glucose and the lifetime of the chemically modified electrode exceeded 24 months with intermittent use. Interference from ascorbic acid was minimal, while the maximum useful range was extended to 100 mmol dm^{-3} glucose by simply covering the electrode surface with an exclusion membrane. A simplex optimization procedure was employed in evaluating electrodes without the use of an exclusion membrane.

Keywords: *Chemically modified glucose enzyme electrode; ferrocene; flow injection; simplex optimization*

The use of electron-transfer mediators has significantly improved the scope and performance of amperometric probes. These mediators are redox couple agents of low relative molecular mass, which shuttle electrons from the redox centre of the enzyme catalyst to the surface of the indicator electrode. During the catalytic cycle, the mediator, M_{ox}, reacts with the reduced enzyme, and then undergoes rapid charge transfer at the electrode surface as illustrated for adenine flavin dinucleotide (FAD):

$$\text{Glucose} + \text{FAD} \rightarrow \text{gluconic acid} + \text{FADH}_2 \quad (1)$$

$$\text{FADH}_2 + M_{ox} \rightarrow \text{FAD}^{2+} + M_{red} + 2\text{H}^+ \quad (2)$$

$$M_{red} \rightarrow M_{ox} + ne^- \quad (3)$$

Provided M_{ox} does not react with oxygen, it substitutes for oxygen in the classical enzymic reaction [eqns. (1)–(3)], and the rate at which the reduced mediator, M_{red}, is produced can be measured amperometrically at a suitable electrode.

A practical mediator needs to be of low relative molecular mass, easily adsorbed onto an electrode surface, reversible, fast reacting, regenerated at low potential, pH independent, stable in both oxidized and reduced forms, unreactive with oxygen and non-toxic. Among the most successful mediators are those based on ferrocene [bis(*n*-cyclopentadienyl)iron] and its derivatives,[1] all of which fulfil the stated criteria, and those with a standard electrode potential (E°) ≈160 mV *versus* a saturated calomel electrode.

The first successful mediated enzyme electrode was based on 1,1-dimethylferrocene which was adsorbed onto a graphite electrode with the enzyme having been chemically immobilized using the carbodiimide route.[1] The upper linear detection limit was 30 mmol dm^{-3} glucose, and response times were 60–90 s. A variety of oxidoreductases[2] have since been used in association with the ferrocene-modified electrode. The method seems to be generally applicable[3] and mediators other than ferrocene have been used but generally they do not have the versatility of ferrocene. Dimethylferrocene-mediated electrodes are the most developed and form the basis of a commercial glucose monitor.[2]

Traditionally, graphite with immobilized glucose oxidase and coated with a ferrocene redox mediator has been used as a dip-type glucose sensor,[1] but for flow injection (FI), the modified electrode needs to be more robust. Covalent binding onto polymer film has been studied, but the system is relatively unstable.[4] Another approach is the use of a carbon paste electrode, where a quinone[5,6] or dimethylferrocene[7,8] mediator is mixed with the carbon–binder matrix to form the working electrode. In the present study the carbon powder and mediator are bound together with cellulose triacetate, and the enzyme is chemically immobilized with the use of a nylon mesh matrix.

Experimental

Reagents and Materials

Glucose oxidase (E.C. 1.1.3.4, 1.667 μkat mg^{-1}, purified from *Aspergillus niger*), *p*-benzoquinone, lysine, 25% glutaraldehyde solution and β-D-(+)-glucose were all obtained from Sigma (Poole, Dorset, UK). Nylon net was obtained from Henry Simon (Stockport, Cheshire, UK), viscose acetate (Visking tubing, 0.32 mm thickness and of relative molecular mass > 150000) was obtained from Gallenkamp (Loughborough, Leicestershire, UK), cellulose triacetate from Kodak (London, UK) and carbon powder from Goodfellow Metals (Cambridge, UK).

The enzyme was stored desiccated in a freezer (−5 °C). All other reagents used were of the best analytical grade available and were used without further pre-treatment.

Sodium dihydrogen orthophosphate buffer (0.1 mol dm^{-3}, pH 4.5 when freshly prepared) was of pH 4 when used. This was adjusted to the appropriate higher pH values by spiking with 4 mol dm^{-3} sodium hydroxide.

Glucose standards were prepared from fresh β-D-(+)-glucose (0.1 mol dm^{-3}) in sodium dihydrogen orthophosphate buffer (0.1 mol dm^{-3}, pH 7) which was also used in the FI carrier stream.

Immobilization of Enzyme

The chemical immobilization of glucose oxidase onto nylon net was carried out as previously described.[9] Nylon net (95–150 μm mesh size, 1 × 1 cm) was treated with dimethyl sulphate (30 cm^3) in a boiling-tube, and placed in a water-bath at 75 ± 3 °C for exactly 5 min with constant swirling. The

* To whom correspondence should be addressed.

boiling-tube was immersed in ice to stop the reaction. After cooling, the membrane was washed twice (or more if necessary) with methanol (30 cm^3) until the methanol washings became clear. The lysine spacer molecule was attached by immersing the membrane in 30 cm^3 of 0.5 mol dm^{-3} lysine for 2 h at ambient temperature.[9] After rinsing with 0.1 mol dm^{-3} sodium chloride the membrane was placed in a saturated solution of *p*-benzoquinone for 2 h at ambient temperature. Finally, in order to attach the enzyme, the membrane was dipped into a solution of glucose oxidase (50 mg) in 5 cm^3 of phosphate buffer (100 mmol dm^{-3}, pH 7) for 2 h at ambient temperature, or overnight at 4 °C.

Electrode Fabrication

The chemically modified electrode material was prepared by thoroughly mixing carbon powder and ferrocene, and was bound with 20% cellulose triacetate (1 + 2 + 1 m/m) in 1,2-dichloroethane. The ferrocene, carbon powder and polymer mixture was then packed into the well of an electrode holder and smoothed over with a clean flat spatula. A small drop of the cellulose triacetate solution was then placed on the electrode surface to form a protective covering. The electrode was oven-dried for 24 h at 50 °C and smoothed using very fine emery paper.

Flow Injection Apparatus

The FI system described previously[9] was used to evaluate the ferrocene-type glucose oxidase electrode using glucose standards. For this, the mediated glucose oxidase electrode was completed by placing the nylon net with immobilized glucose oxidase over the chemically modified carbon paste indicator electrode. This was then set up in a modified three-electrode Stelte micro-cell (Metrohm EA 1102) assembly.[10] The electrode potential was controlled and the current was monitored by using a Metrohm (Herisau, Switzerland) VA-detector E611 potentiostat in conjunction with a Linear Model 500 *y–t* chart recorder. The carrier stream and sample propulsion were driven by a four-channel Watson-Marlow (Falmouth, Cornwall, UK) peristaltic pump, and an Omnifit (Atlantic Reach, NY, USA) sample injection valve was used. All connecting tubes were of either silicone rubber or polytetrafluoroethylene with a nominal i.d. of 1.27 mm. A pulse suppressor was fitted between the pump and the injection valve.

The indicator electrode was set at +160 mV *versus* a silver–silver chloride reference electrode. The following scheme illustrates the reaction sequence:[1]

$$\text{Glucose} + \text{GOD}_{ox} \rightarrow \text{gluconolactone} + \text{GOD}_{red} \quad (4)$$

$$\text{GOD}_{red} + 2\text{Fecp}_2\text{R}^+ \rightarrow \text{GOD}_{ox} + 2\text{Fecp}_2\text{R} + 2\text{H}^+ \quad (5)$$

$$2\text{Fecp}_2\text{R} - 2e^- \rightarrow 2\text{Fecp}_2\text{R}^+ \quad (6)$$

where GOD_{ox} and GOD_{red} are the oxidized and reduced forms of glucose oxidase, respectively, and R represents substituents in the $Fecp_2$ ring system for $Fecp_2R^+$ and $Fecp_2R$.

Results and Discussion

Optimization of the FI System for Glucose Determination

Optimization of reaction pH

Each enzyme electrode was optimized by varying the pH between 5 and 9 through increments of 0.5 pH unit. The resulting peak height *versus* pH plots reached a plateau at pH 6.8–7.2. All further work was therefore carried out at pH 7. Other workers have reported a broad pH range of 4.0–7.0 with a maximum response at about pH 5.5 for solubilized glucose oxidase.[11,12] However, the optimum pH range is a direct result of the micro-environment of the enzyme and is related to the immobilization technique and the nature of the support material, and for immobilized glucose oxidase an optimum pH of 7.0 is normal.

Effect of temperature

The effect of temperature on glucose sensing was studied by slowly raising the temperature from 5 to 75 °C over a period of 2 h. The sample solution and carrier stream were kept at the same temperature in a water-bath for each run. The glucose signal rose from 154 nA at 5 °C to a maximum of 280 nA at 38–42 °C; thereafter the signal decreased (to 230 nA at 75 °C), presumably due to denaturation of the enzyme. A repeat run on the same electrode gave a similar profile, but with a reduced glucose signal for temperatures ranging from 5 to 75 °C; the signal was reduced by 27 nA at 5 °C, 52 nA at 35–42 °C and 41 nA at 75 °C.

Optimization of flow conditions

The sample volume and carrier solution flow-rate were optimized for electrodes without the use of viscose acetate membranes, and on 100 mmol dm^{-3} glucose standards, using an additional modified simplex optimization procedure,[13] this being an adaptation of the modified simplex optimization algorithm.[14,15] For this, the control parameters of flow-rate and sample volume were examined with respect to the response criteria of peak height and run time, *i.e.*, the time taken from sample injection to the attainment of the maximum current signal and a return to the baseline. The bias of the optimization in previous studies[13–15] was maximization of the peak height with minimization of the run time. Different degrees of importance can be placed on the various response criteria according to the requirement expected of the enzyme electrode.

The criteria of convergence for the simplex occur when the standard deviation (SD) of the signal responses of its vertices is less than five times the signal fluctuation (noise) of the system. The signal fluctuation can be determined by taking the SD of the signals of ten runs; this is necessary to prevent degeneracy of the simplex caused by the signal fluctuation. It is important to note that with the search method of optimization the data need to be verified, as the computation of each search point, and its direction, is dependent on the previous point. Therefore, a minimum of three runs was carried out for each subsequent cycle, the data being accepted only when there were three points with a percentage SD : signal ratio within the corresponding ratio of the original ten runs.

If large signals are required, regardless of the run time, then greater weighting is placed on signal size rather than on run time. At the other extreme a system may be required that can

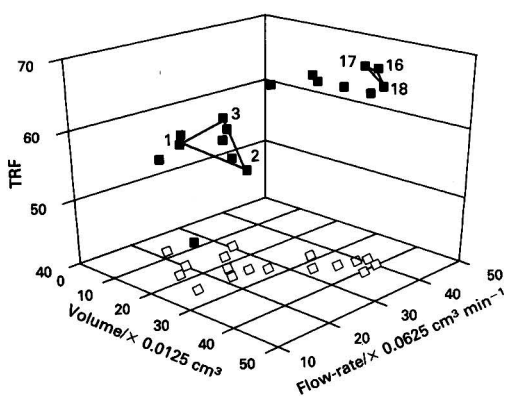

Fig. 1 Simplex optimization of enzyme electrode without viscose acetate membrane. Open squares represent the experimental conditions; closed squares represent the normalized response of peak height and experimental run time, *i.e.*, the TRF

Table 1 Study of the interference of organic acids on the glucose sensor with and without a viscose acetate exclusion membrane

	Separate injection			Mixed injection		
	Δ*i*/nA			Δ*i*/nA		
	+160 mV		+600 mV	+160 mV		+600 mV
Organic acid	Without membrane	With membrane	Without membrane	Without membrane	With membrane	Without membrane
Ascorbic	0.05	0.03	3.00	1.05	1.03	4.00
Gluconic	0.00	0.00	0.00	1.00	1.00	1.00
Lactic	0.00	0.00	0.00	1.00	1.00	1.00
Citric	0.00	0.00	0.00	1.00	1.00	1.00
Acetic	0.00	0.00	0.00	1.00	1.00	1.00

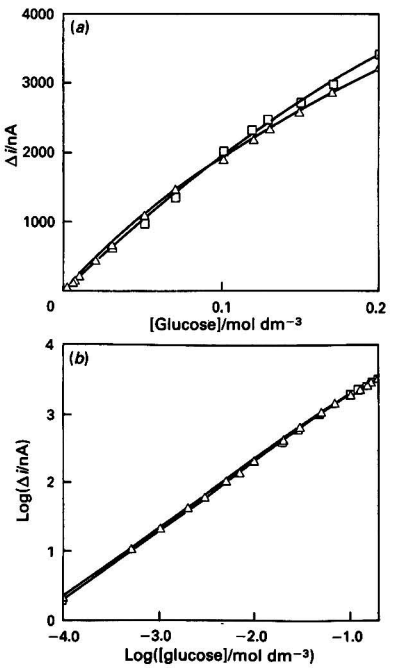

Fig. 2 (*a*) Glucose calibration plots for electrodes with (□) and without (△) viscose acetate exclusion membranes. (*b*) Log–log glucose calibration plots for electrodes with (□) and without (△) viscose acetate exclusion membranes

Table 2 Response parameters of the two enzyme electrodes at +160 mV *versus* silver–silver chloride reference electrodes. *F*-factor obtained when comparing the two electrode systems = 26.67 at p = 0.01, denominator = 8, numerator = 1 with critical value = 8.29, shows that the two electrode systems gave significantly different signals

Electrode	Linear detection range/ mmol dm^{-3}	Δ*i* for 1 mmol dm^{-3} glucose/ nA	SD*/nA	Response time/s	Washout time/s
Without	0.10–70	22.0	0.791	15	30
With	0.10–100	20.0	0.354	25	45

* n = 5.

handle a large throughput of sample, thus placing greater emphasis on minimizing the run time. Operating conditions of sample volume and flow-rate for the systems in this study were optimized with equal emphasis being placed on the two response criteria, namely peak height and run time, which together make up the total response function (TRF) (Fig. 1). The open squares represent the experimental conditions and the closed squares represent the normalized response of peak height and experimental run time, *i.e.*, the TRF. The initial search starts from iterations 1, 2 and 3, and the optimum range occurs at iterations 16, 17 and 18 as shown in Fig. 1. The optimum range was the same for different search starting points.

As a result of the optimization, the carrier stream flow-rate adopted was 2.3 cm^3 min^{-1} and the corresponding sample size was 0.5 cm^3, based on 100 mmol dm^{-3} glucose standards so as to realise large currents (≈ 2000 nA) without recourse to the use of instrumental noise adjustments.

Sensor Selectivity

The possible interference of ascorbic, gluconic, lactic, citric and acetic acids, particularly important in the analysis of food, was assessed by using two different techniques. In the first, 1 mmol dm^{-3} of interferent was injected directly into the system and in the other a mixture of substrate and interferent, both at a concentration of 1 mmol dm^{-3}, was injected into the sensing system. The signal was normalized with respect to the signal obtained for 1 mmol dm^{-3} glucose which was taken as zero (Table 1). Ascorbic acid interfered very slightly but this interference was further reduced by covering the indicator electrode with a viscose acetate membrane. However, this acid causes severe interference even at +300 mV with the analogous glucose electrode, described by Wang *et al.*,[8] where the enzyme is physically, rather than chemically, immobilized.

Electrode Calibration

The electrodes were calibrated by FI with glucose standards over the range 0.01–200 mmol dm^{-3} using the optimized conditions. The lowest detectable concentration of glucose was 0.1 mmol dm^{-3}, while the calibration was linear to 70 mmol dm^{-3} glucose (Fig. 2).

Sensitivity analysis was carried out to determine the linear portion of the calibration plot because at higher concentrations the tailing-off effect of the signal from the system was caused by a physical phenomenon rather than by random error. The non-linear portion of the calibration plot cannot therefore be rejected on the basis that the points on this part of the graph are simply outliers.

The sensitivity analysis was performed by determining the coefficient of regression (r^2) of the calibration plot, wherein each point is the mean signal for three replicate determinations. The point representing the highest concentration is rejected and the value of r^2 obtained from the remaining points is compared with the previous value. If the value of r^2 does not approach unity, the remaining final point of the calibration plot is again rejected and the r^2 of the calibration determined rejecting the point of highest concentration each time until r^2 approaches unity. This procedure is carried out because the 'outliers' are not caused by noise (or random

error), but are the result of phenomena concerning the electrode itself.

After optimization, the inclusion of the viscose acetate membrane over the electrode surface extended the linear detection range to between 0.01 and 100 mmol dm^{-3} (Fig. 2). The inclusion of the membrane over the electrode surface probably promotes this by limiting mass transfer to the electrode surface. This effect can be seen by comparing the time of response of the electrode system without the exclusion membrane (≈15 s) and that with the exclusion membrane in place (≈20 s); respective washout times were ≈30 and ≈45 s (Table 2). These times compare favourably with those of the analogous glucose electrode described by Wang *et al.*,[8] whose linear range, however, is inferior, namely, 0.5–8.0 mmol dm^{-3}.

Membrane Lifetimes

Membrane lifetimes and storage stability are significant factors with regard to a wider practical role for biosensors. In order to determine membrane lifetime with respect to substrate, a 1 mmol dm^{-3} glucose solution was continuously pumped (2.3 cm^3 min^{-1}) over the immobilized glucose oxidase electrode. At daily intervals the electrode was washed and re-calibrated. The study showed that the membrane could withstand at least 24 h of glucose flow before any loss of enzyme activity was detected. After 7 d the signal had fallen by 25%.

It was also noted that membranes stored at 4 °C in buffer gave electrodes that responded well to glucose; after frequent intermittent use (1 h per week) over 4 months the signal was 70% of that for a new electrode.

Electrode Lifetimes

The carbon–ferrocene chemically modified electrodes are highly stable with lifetimes of >2 years with intermittent use. The immobilized enzyme membrane can be changed when there is a signal loss due to enzyme deterioration. To achieve this long lifetime the electrodes are stored in a cool, dry and dark place when not in use. This indicates that the electrode lifetime is independent of the immobilized enzyme, the long life being attributed to the carbon paste being bound with a porous polymer matrix rather than the Nujol used by other workers.[16]

Conclusion

Cellulose triacetate is sufficiently porous to permit electrical contact between the reaction substrate and the electrode material, and the pores are small enough to prevent the electrode modifying material from leaching away. This is indicated by the long lifetimes of the electrodes used under tortuous FI conditions. The maximum linear limit can be extended, and interference from ascorbic acid minimized, by placing a viscose acetate membrane over the electrode surface, as the mass transfer to the electrode surface is thus reduced.

The authors thank the Trustees of the Analytical Chemistry Trust Fund of the Royal Society of Chemistry for the award of an SAC Research Studentship and the Committee of Vice Chancellors and Principals for a concurrent Overseas Research Scheme Studentship (both to S. K. B.).

References

1 Cass, A. E. G., Davis, G., Francis, G. D., Hill, H. A. O., Aston, W. J., Higgins, I. J., Plotkin, E. V., Scott, L. D. I., and Turner, A. P. F., *Anal. Chem.*, 1984, **56**, 667.
2 D'Costa, E. J., Higgins, I. J., and Turner, A. P. F., *Biosensors*, 1986, **2**, 71.
3 Mattews, D. R., Holman, R. R., Brown, E., Steemson, J., Watson, A., Hughes, S., and Scott, D., *Lancet*, 1987, **1**, 778.
4 Foulds, N. C., and Lowe, C. R., *Anal. Chem.*, 1988, **60**, 2473.
5 Ikeda, T., Hamada, H., Miki, K., and Senda, M., *Agric. Biol. Chem.*, 1985, **49**, 541.
6 Senda, M., Ikeda, T., Miki, K., and Hasa, H., *Anal. Sci.*, 1986, **2**, 501.
7 Dicks, J. M., Aston, W. J., Davis, G., and Turner, A. P. F., *Anal. Chim. Acta*, 1986, **182**, 103.
8 Wang, J., Wu, L.-H., Lu, Z., Li, R., and Sanchez, J., *Anal. Chim. Acta*, 1990, **228**, 257.
9 Beh, S. K., Moody, G. J., and Thomas, J. D. R., *Analyst*, 1989, **114**, 1421.
10 Moody, G. J., Sanghera, G. S., and Thomas, J. D. R., *Analyst*, 1986, **111**, 605.
11 Bright, H. J., and Appleby, M. J., *J. Biol. Chem.*, 1969, **244**, 3625.
12 Weibel, M. K., and Bright, H. J., *J. Biol. Chem.*, 1971, **246**, 2734.
13 Beh, S. K., Moody, G. J., and Thomas, J. D. R., *Anal. Proc.*, 1990, **27**, 82.
14 Beh, S. K., Moody, G. J., and Thomas, J. D. R., *Anal. Proc.*, 1989, **26**, 290.
15 Beh, S. K., Moody, G. J., and Thomas, J. D. R., *Analyst*, 1989, **114**, 29.
16 Gunasingham, H., and Tan, C.-H., *Analyst*, 1990, **115**, 35.

Paper 0/02581J
Received June 11th, 1990
Accepted January 1st, 1991

pH Dependence of Hydrochloric Acid Diffusion Through Gastric Mucus: Correlation With Diffusion Through a Water Layer Using a Membrane-mounted Glass pH Electrode

C. V. Nicholas, M. Desai and P. Vadgama
Department of Medicine (Clinical Biochemistry), University of Manchester, Clinical Sciences Building, Hope Hospital, Salford M6 8HD, UK

M. B. McDonnell
Department of Chemistry, University of Southampton, Southampton SO9 5HH, UK

S. Lucas
Computational Group, Computing Department, University of Manchester, Stopford Building, Manchester M13 9PT, UK

Solute diffusion coefficients (D) can indicate a dependence upon actual solute concentrations. Here a single compartment has been utilized, in which effective HCl diffusion to a membrane-mounted glass pH electrode can be measured across the pH spectrum. The study has investigated HCl diffusion through both mucus and water layers as a function of HCl concentration. The observed dynamic responses of a liquid-film and mucus-coated electrodes over a range of HCl concentrations suggest that the speed at which equilibrium is attained is pH dependent; equilibrium was reached rapidly under more acidic and alkaline conditions. Estimated values of D_{HCl} also indicate a strong pH dependence for both liquid film and mucus. In both instances, a >10-fold reduction in D_{HCl} at pH 7.5 as compared with that at pH 3.5 has been demonstrated. Furthermore, estimated values of D_{HCl} are approximately 4-fold smaller through the mucus gel, as compared with a water layer. The findings indicate that the most powerful influence on diffusional resistance is pH itself, whereby a marked drop in H^+ diffusion is likely to occur towards neutral pH irrespective of the composition of the gel barrier. Possible implications of the findings are discussed in relation to mucosal protection from acid.

Keywords: *Hydrochloric acid diffusion; gastric mucus; pH electrode*

Mucus forms a continuous, adherent visco-elastic gel layer over the gastrointestinal mucosa, which in man has an estimated depth of 50–450 μm (Kress *et al.*[1]). In the stomach and duodenum, mucus has been considered to play an important role in protecting the mucosa from damage by luminal acid (Allen and Garner[2]). Studies of its diffusional resistance to HCl have revealed a resistance that is 4–5-fold greater than that of an equivalent unstirred layer of water (Williams and Turnberg,[3] Pfeiffer[4] and Turner *et al.*[5]). Furthermore, steep pH gradients have been observed within mucus, across intact gastric mucosa, by means of implanted micro-pH electrodes (Williams and Turnberg,[6] Bahari *et al.*,[7] Takeuchi *et al.*[8] and Flemstrom and Kivilaakso[9]). These have been explained on the basis of an intra-gel neutralization of HCl with hydrogen carbonate secreted by the surface epithelium (Allen and Garner[2] and Flemstrom and Kivilaakso[9]). In this concept of the mucus–hydrogen carbonate barrier, the neutralizing action of HCO_3^- is considered to be potentiated by neutralization occurring in the restricted volume of the mucus gel phase. A mathematical model developed by Engel *et al.*[10] for intra-mucus neutralization, however, suggested that a relatively minor (5 mmol dm^{-3}) drop in H^+ concentration was likely to be generated across the mucus layer based on existing, reported values for gel layer thickness, hydrogen carbonate flux and HCl diffusion.

Solute diffusion coefficients can show a dependence upon actual solute concentrations (Crank[11]) and in the present study HCl diffusion through both mucus and water layers as a function of HCl concentration has been examined. A significant change from earlier reported values for HCl diffusion could provide further information concerning the resistive contribution made by mucus in its protective role over the gastroduodenal mucosa. A more detailed profiling of hydrogen ion diffusion is warranted, as its diffusion is unique in involving passage from one water molecule to the next, through the formation of a sequence of hydrogen bonds (Robinson and Stokes[12]). In a previous study, HCl diffusion through water was observed to be retarded by a factor of 100, as compared with earlier reported values, when conditions approached neutrality (Nicholas *et al.*[13]). The correlation between diffusion through water and mucus layers is reported here, and possible implications of these findings for mucosal protection from acid are discussed.

Theory

The two-compartment diffusion chamber is appropriate for the study of most solute species (IUPAC[14]). However, for H^+ diffusion, measurement requires highly acidic (pH<2) conditions (Williams and Turnberg,[6] Robinson and Stokes[12] and Slomiany *et al.*[15]) if buffering is to be avoided. A one-compartment system based on the glass pH electrode, which allows measurements under acidic through to neutral and alkaline conditions, was used in the present study.

The dynamic response of a pH electrode and its approach to an equilibrium may be modelled in terms of diffusion through a stagnant, unstirred layer over the sensor surface (Morf and Simon[16]). Provided that the diffusion layer, and not the intrinsic electrode response, is rate limiting, the change in the electrode e.m.f. showed the following dynamic time dependence in its approach to an equilibrium response:

$$E_t = E_{eq} + S\log\left[1 - \left(1 - \frac{[H^+]_0}{[H^+]_{eq}}\right)\frac{4}{\pi}e^{-t/\tau}\right] \quad (1)$$

Here, E_t is the electrode e.m.f. at any given time t, E_{eq} is the electrode equilibrium response, S is the slope of the pH calibration graph (mV per decade), $[H^+]_0$ is the H^+ concentration at time zero, $[H^+]_{eq}$ is the H^+ concentration at the final equilibrium response and τ is the time constant for the system. The value of τ is governed by both the thickness of the

unstirred layer, d, and by the H^+ diffusion coefficient, D, within that layer:

$$\tau = \frac{4d^2}{\pi^2 D} \quad (2)$$

The measurement of τ permits the calculation of D provided d is known. Alternatively, mucus and liquid films have been created over the glass surface of a pH electrode (Nicholas *et al.*[13]), which provided a well-defined boundary layer in a stirred solution and which, furthermore, were of sufficient depth both to define the dynamic response of the pH electrode according to eqns. (1) and (2) and eliminate the effects of an external Nernst diffusion layer.

Experimental

The measuring glass pH electrode (Type CETL; Russell, Fife, UK) was used in conjunction with a saturated calomel reference electrode (Microelectrodes, Londonderry, NH, USA). Electrode e.m.f. was measured using a pH meter (PCMKI, Newcastle upon Tyne, UK) and output recorded at a strip-chart recorder (Linseis, Selb, Germany). A combination pH electrode served as a follower electrode to monitor bulk solution pH during the addition of HCl in the pH jump experiments. All standard reagents were of AnalaR grade and purchased from BDH (Poole, Dorset, UK); bovine serum albumin (BSA) was obtained from Sigma (Poole, Dorset, UK). Native pig gastric mucus was removed as described previously (Williams and Turnberg[3]), from the stomachs of abattoir animals that had been killed recently.

Mucus was applied to the tip of the measuring glass pH electrode which had a pre-mounted 135 μm nylon netting that acted as a spacer. A uniform gel or mucin layer was then created by stretching an external 10 μm Cuprophan dialysis membrane layer, using a Cuprophan from a haemodialysis cartridge (Gambro, Lund, Sweden). For measurements through aqueous films the nylon spacer and dialysis membrane were used alone. Measuring and follower electrodes were immersed in a chamber containing 175 ml of solution that was stirred rapidly (Vadgama and Alberti[17]), and 1 mol dm^{-3} HCl was injected *via* an automatic pipette over a period of 1–2 s in order to create a change in the pH of the bulk solution of about 1 pH unit; the temperature of the solution was 21 ± 2 °C.

Results

The dynamic response of the uncovered glass pH electrode in stirred solution, as monitored at the strip-chart recorder, was complete within 2 s of the addition of HCl over the entire pH range used in these studies. The magnitude and dynamic response were unaffected by either previous contact with mucus gel or with the bulk solutions used. Dynamic response profiles were reproducible to within 5% with respect to e.m.f. The observed dynamic responses of a liquid-film and mucus-coated electrodes over a range of pH values in the presence of albumin, as a non-diffusible buffer, are shown in Fig. 1(*a*) and (*b*), respectively. These suggest that the speed at which equilibrium is attained depends upon pH, with equilibrium being reached more rapidly under more acidic and alkaline conditions; this would not be expected on the basis of eqn. (1) (Morf and Simon[16]), which predicts similar dynamic responses across the pH spectrum, provided the magnitude of the pH jump is uniform. However, when eqn. (1) was used to calculate the dynamic electrode response, it showed good agreement with observed e.m.f changes, both for liquid-film electrodes (Fig. 2) and the mucus-coated electrodes (Fig. 3) over a range of pH changes. This indicates a change in effective diffusion coefficients for HCl (D_{HCl}) over a range of pH values. The value of D_{HCl} was estimated using BSA as a non-diffusible buffer to assist in the pH stabilization of the bulk solution. The results are shown in Fig. 4; these indicate a strong pH dependence for D_{HCl} for both a liquid film and mucus. In both situations there is a >10-fold reduction in D_{HCl} at pH 7.5, as compared with pH 3.5. In addition, estimated diffusion coefficients are approximately 4-fold smaller through the mucus gel, as compared with a water layer. Interestingly, as conditions are made more alkaline, D_{HCl} is seen to increase again. A reliable estimation of D_{HCl} at pH <2 was precluded by the very rapid responses of the film-coated electrode. For the citrate buffer examined here, background ionic strength had no apparent effect on the trend in D_{HCl} values observed over the pH range investigated, as shown in Fig. 5. However, results obtained using different concentrations of glucosamine as a diffusible buffer in the presence of albumin (Fig. 6) suggest that there may be an effective increase in D_{HCl}, particularly at more acidic and alkaline pH values when a high concentration of such a diffusible buffer is used. This possibility receives some support from the finding of a higher D_{HCl} with a mucus-coated electrode at pH 10.5 in the presence of 30 mmol dm^{-3} salicylate and albumin (Fig. 7) as compared with albumin alone.

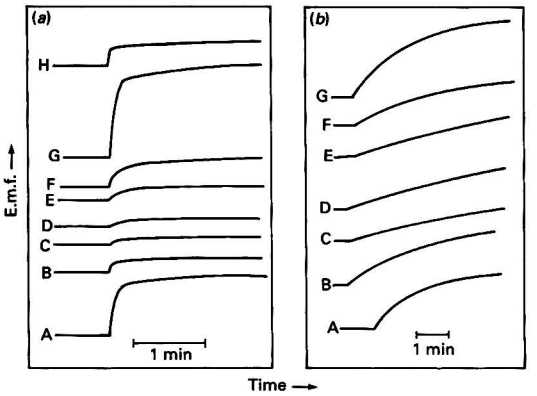

Fig. 1 Dynamic responses of a pH electrode mounted with a 135 μm nylon spacer and dialysis membrane. (*a*) Liquid film; pH change: A, 8.70–7.42; B, 7.42–7.07; C, 6.83–6.64; D, 6.46–6.29; E, 5.89–5.59; F, 5.59–4.98; G, 4.98–3.07; and H, 3.07–2.51. (*b*) Mucus layer; pH change: A, 10.02–9.08; B, 9.08–7.80; C, 7.80–6.73; D, 6.73–5.62; E, 5.62–4.72; F, 4.72–4.00; and G, 4.00–2.88. Albumin (20 g l^{-1}) was used as a non-diffusible buffer

Discussion

The concept of the mucus–hydrogen carbonate barrier (Allen and Garner[2] and Flemstrom and Kivilaakso[9]) has received important supportive evidence (Williams and Turnberg[6] and Flemstrom and Kivilaakso[9]), and continues to attract interest (Munster *et al.*[19]). The effectiveness of this barrier would be critically affected by the rate at which protons approach the surface epithelium from the lumen. A mucus gel layer with a high diffusional resistance would appear to be ideal for such a system; however, the retardation of the diffusion of H^+ in mucus would appear to be insufficient to explain the type of pH gradients observed (Engel *et al.*[10]). Part of the explanation for the retardation of the diffusion of the H^+ ion in mucus is the net negative charge of the constituent glycoprotein. This may operate by means of a Donnan exclusion mechanism, although comparison with uncharged gel suggest that the effect is minor (Lee and Nicholls[20]). Any specific ordering of water molecules around the glycoprotein structure is likely to be minimal (Soggett[21]) and, therefore, unlikely to result in significant additional diffusional resistance, particularly in view of the low (<5%) concentration of the glycoprotein in the gel (Allen and Garner[2]). For native mucus, particulate

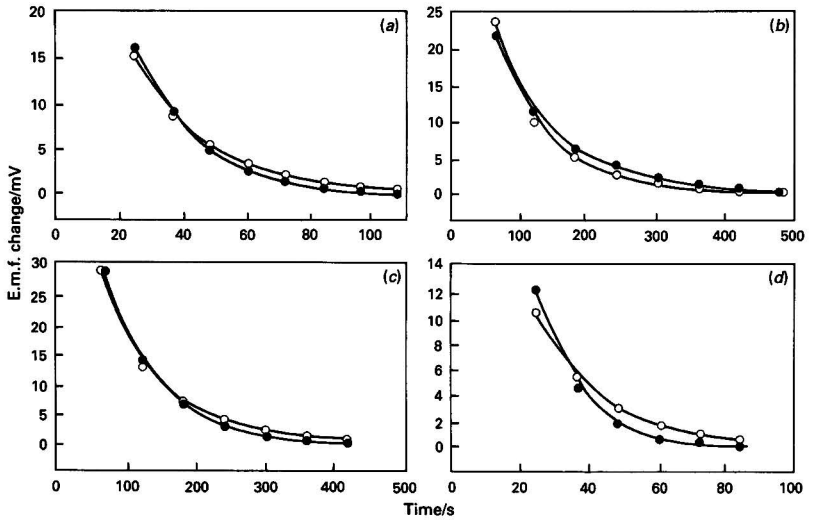

Fig. 2 Spacer and dialysis membrane mounted pH electrode response profiles for a liquid film at various pH jumps. (*a*) pH 10.99–9.99; (*b*) 9.00–7.4; (*c*) 6.97–5.91; and (*d*) 4.03–2.96. Calculated (○) and measured (●) e.m.f. values are compared

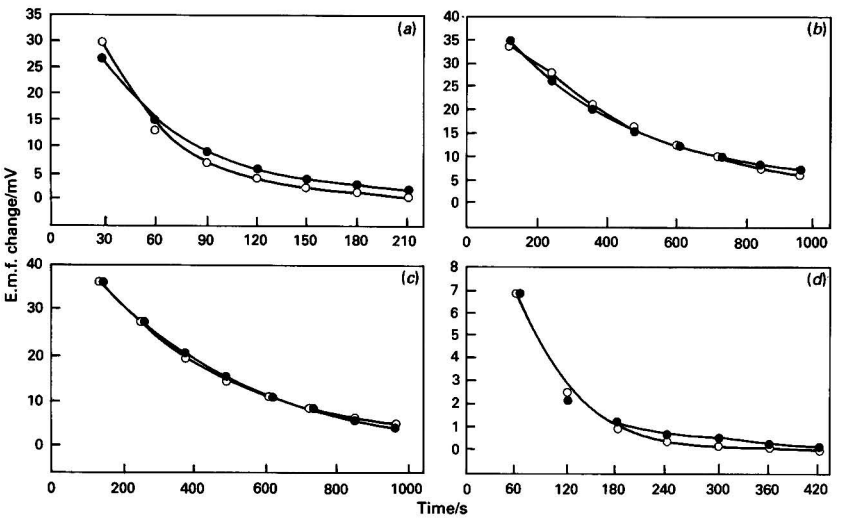

Fig. 3 Spacer and dialysis membrane mounted pH electrode response profiles for a mucus layer at various pH jumps. (*a*) pH 11.5–9.98; (*b*) 7.98–7.03; (*c*) 6.11–5.04; and (*d*) 3.98–2.93. Calculated (○) and measured (●) e.m.f. values are compared.

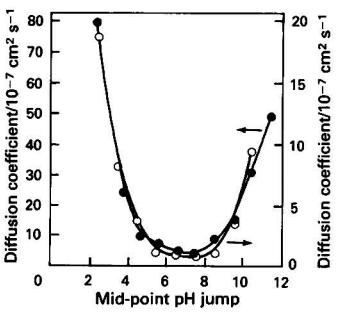

Fig. 4 Effective D_{HCl} calculated from dynamic responses of a spacer and dialysis membrane mounted pH electrode in albumin buffer: ●, liquid film only; and ○, liquid film with mucus. pH values are the mid-points of pH jumps of magnitude about 1

material, protein and lipid, do appear to confer additional diffusional resistance (Slomiany *et al.*[22]).

The summation of all the above effects is undoubtedly important in reducing D_{HCl} relative to that of a liquid film. The effect observed in this study is consistent with that reported previously by Williams and Turnberg,[3] who used a classical two-compartment diffusion chamber. However, the present work would appear to indicate that the most powerful influence on diffusional resistance is pH itself, whereby a marked drop in H^+ diffusion is likely to occur towards neutral pH irrespective of the composition of a gel barrier (Fig. 4).

The D_{HCl} has not previously been measured directly, largely because of the problems of achieving a stable pH under near neutral conditions without buffering. As a result, all previous studies of D_{HCl} in mucus have been limited to using HCl at a pH of about 1. The technique reported here permits determination of D_{HCl} in mucus over most of the pH spectrum. In the present study, the small unbuffered compartment, *i.e.*, the

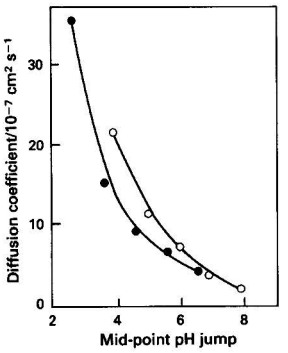

Fig. 5 Effective D_{HCl} calculated from dynamic responses of a liquid film mounted pH electrode for solutions containing 10 mmol dm^{-3} citrate in ○, 10 mmol dm^{-3} NaCl; and ●, 300 mmol dm^{-3} NaCl (the latter data are redrawn from reference 18 for comparison)

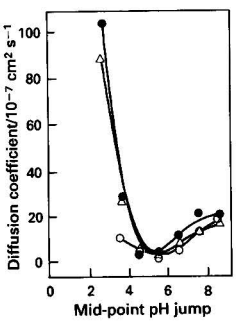

Fig. 6 Effective D_{HCl} calculated for a liquid film electrode from dynamic responses in glucosamine solutions at various concentrations: ○, 10 mmol dm^{-3} (redrawn from reference 18 for comparison); △, 30 mmol dm^{-3}; and ●, 60 mmol dm^{-3} in albumin buffer

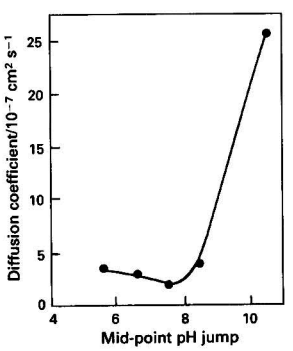

Fig. 7 Effective D_{HCl} for a mucus-coated electrode calculated from dynamic responses for 30 mmol dm^{-3} salicylate in albumin buffer for a range of pH changes

liquid or mucus layer over the pH electrode, was more readily controlled with regard to pH by incorporation of a non-diffusible buffer in the much larger external compartment, *i.e.*, the bulk solution. The effective D_{HCl} values at about neutral pH would appear to have major implications for H^+ diffusion in biological systems generally. The mechanism for such pH dependence remains to be elucidated; however, one possibility is the unique mechanism for proton transfer through water, involving multiple hydrogen bonding.

The effect of a diffusible buffer (B) in solution is to augment proton transfer by means of a buffer shuttle (Engasser and Horvath[23]):

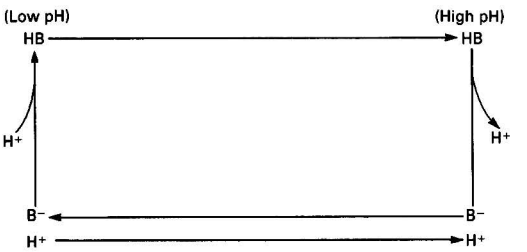

This system would be expected to operate in a concentration-dependent manner and also to have maximal effect at a pH close to the pK_a of the buffer (Vadgama and Alberti[24]). Both phenomena have been observed previously to affect the dynamic response of a pH glass electrode mounted with immobilized protein (Deem *et al.*[25]), and also native gastric mucus (Vadgama and Alberti[17]). Over the buffer concentrations used in the present study, any possible effect was minor, except when a high concentration of buffer was used (Figs. 6 and 7). The over-all reduction of D_{HCl} at low glucosamine concentration may have been the result of buffer shuttling, although this could have been affected by the binding of glucosamine to albumin. Estimated D_{HCl} values obtained in different low ionic strength buffers of low relative molecular mass[18] demonstrated some differences between citrate, ascorbate and glucosamine, but these were relatively minor as compared with the steep drop in D_{HCl} as neutral pH was approached. Values of D_{HCl} were also lower for the diffusible buffers as compared with the albumin system. This raises the possibility that in the total absence of a buffer effect, values of D_{HCl} may be even lower than reported here, as neutrality is approached. The results augment considerably the postulated resistive property of the surface mucus layer; for a relatively small rise in pH, H^+ diffusion may be reduced by a factor of $\approx$10.

A possible implication of the present findings for the mucus–hydrogen carbonate barrier is that HCO_3^- secretion into mucus may be designed to adjust the pH of the mucus to a range were D_{HCl} is reduced, rather than to effect complete neutralization. Indeed, at the equivalence point HCO_3^- cannot neutralize HCl; for 100 mmol dm^{-3} HCl the final pH would be 3–5 (Vadgama and Alberti[24]). It is even conceivable that a high concentration of buffer within the mucus layer, including the HCO_3^-/CO_2 buffer system, would actually accelerate proton fluxes to the surface epithelium by the operation of a buffer shuttle. Thus, while the high urease activity of *Heliobacter pylori* generates ammonia which can neutralize H^+ within mucus (Thompson *et al.*[26]), there may be significant associated shuttling of H^+ along the pH gradient in mucus which might actually contribute to mucosal damage associated with this organism.

The present studies reconcile the idea of mucus as a resistive barrier (Williams and Turnberg[6]) with that of mucus as simply an unstirred water layer (Morris[27]). In conclusion, the results obtained should be regarded as effective D_{HCl} values, but ones which nevertheless reflect the diffusion behaviour of the physiological system. Further comparative studies are in progress for other ion and solute species using the coated electrode technique described.

References

1 Kress, S., Allen, A., and Garner, A., *Clin. Sci.*, 1982, **63**, 187.
2 Allen, A., and Garner, A., *Gut*, 1980, **21**, 249.

3 Williams, S. E., and Turnberg, L. A., *Gastroenterology*, 1980, **79**, 299.
4 Pfeiffer, C. J., *Am. J. Physiol.*, 1981, **240**, B176.
5 Turner, N. C., Martin, G. P., and Marriott, C., *J. Pharm. Pharmacol.*, 1985, **37**, 776.
6 Williams, S. E., and Turnberg, L. A., *Gut*, 1981, **22**, 94.
7 Bahari, H. M. M., Ross, I. N., and Turnberg, L. A., *Gut*, 1982, **23**, 513.
8 Takeuchi, K., Magee, D., Critchlow, J., Matthew, J., and Gilen, W., *Gastroenterology*, 1982, **84**, 331.
9 Flemstrom, G., and Kivilaakso, E., *Gastroenterology*, 1983, **84**, 787.
10 Engel, E., Peskoff, A., Kauffman, G. L., and Grossman, M. I., *Am. J. Physiol.*, 1984, **247**, G321.
11 Crank, J., *The Mathematics of Diffusion*, Oxford University Press, Oxford, 1959.
12 Robinson, R. A., and Stokes, R. H., *Electrolyte Solutions*, Butterworth, London, 1955.
13 Nicholas, C. V., McDonnell, M. B., and Vadgama, P., *J. Chem. Soc., Chem. Commun.*, 1990, **4**, 320.
14 IUPAC, Conditional Diffusion Coefficients of Ions and Molecules in Solution. An Appraisal of the Conditions and Methods of Measurements, *Pure Appl. Chem.*, 1979, **51**, 1575.
15 Slomiany, B. L., Laszewicz, W., and Slomiany, A., *Digestion*, 1986, **33**, 146.
16 Morf, W. F., and Simon, W., in *Ion-Selective Electrodes in Analytical Chemistry*, ed. Freiser, H., Plenum, New York, 1978, vol. 1, p. 211.
17 Vadgama, P., and Alberti, K. G. M. M., *Experientia*, 1983, **39**, 573.
18 Vadgama, P., Nicholas, C. V., McDonnell, M. B., Lucas, S., and Desai, M., *J. Chem. Soc., Faraday Trans.*, 1991, **87**, 293.
19 Munster, D. J., Robertson, A. M., and Bagshaw, P. F., *N. Z. Med. J.*, 1989, **102**, 607.
20 Lee, S. P., and Nicholls, J. F., *Biotechnology*, 1987, **24**, 565.
21 Soggett, A., in *Water: A Comprehensive Treatise*, ed. Franks, F., Plenum, New York, 1980, vol. 4, p. 519.
22 Slomiany, B. L., Piasek, A., Sarasick, J., and Slomiany, A., *Scand. J. Gastroenterol.*, 1985, **20**, 1191.
23 Engasser, J. M., and Horvath, C., *Biochim. Biophys. Acta*, 1974, **358**, 178.
24 Vadgama, P., and Alberti, K. G. M. M., *Digestion*, 1983, **27**, 203.
25 Deem, G. S., Zabusky, N. J., and Sternlicht, H., *J. Membr. Sci.*, 1978, **4**, 61.
26 Thompson, L., Tasman-Jones, C., Morris, A., Wiggins, P., Lee, S., and Furlong, L., *Scand. J. Gastroenterol.*, 1989, **24**, 761.
27 Morris, G. P., *Gastroenterol. Clin. Biol.*, 1985, **9**, 106.

Paper 1/00132I
Received January 11th, 1991
Accepted January 23rd, 1991

Comparative Barium Ion Sensing Qualities of Planar and Tetrahedral Tripodal Receptor Molecules

Y. P. Feng, G. Goodlet, N. K. Harris, M. M. Islam*, G. J. Moody and J. D. R. Thomas
School of Chemistry and Applied Chemistry, University of Wales College of Cardiff, P.O. Box 912, Cardiff CF1 3TB, UK

Nine acyclic polyethers, representing examples of planar and tripodal 'scorpion-like' molecules, each with oligoether 'tails' and a pair of anionic 'pincers', were evaluated as possible barium ion-selective electrodes (ISEs) when incorporated into a poly(vinyl chloride) matrix membrane with 2-nitrophenyl phenyl ether as the solvent mediator. The general performance was inferior to a traditional ISE based on the tetraphenylborate salt of the barium complex with α-(nonylphenyl)-ω-hydroxy-*catena*-poly(oxyethylene) (Antarox CO-880 with 30 oxyethylene units). However, a general barium ion response seems to be favoured by a tetrahedral tripodal structure (sensor C, electrode 3), with its design promoting good ion–dipole interactions, as seen in another study on the association constants of these acyclic polyethers with barium ions. A more extensive study of the effect of methoxylated benzyl groups on similar type groups in the pincer positions for the tetrahedral tripodal structures is indicated.

Keywords: *Receptor molecule; polyether; ion-selective electrode; barium; planar and tetrahedral tripodal structures*

Examples of strong stoichiometric complexes between alkali and alkaline earth metal cations and neutral carriers are well established.[1–6] In ion-selective electrode (ISE) terms, an early example is based on the naturally occurring ionophore, valinomycin, which forms the basis of the highly selective potassium ISE.[7,8] However, such a rigid cyclic arrangement is not necessary for complexation, and ionophores with a more open structure have selective ion sensing capabilities.[9] Systems based on complexes between polyalkoxylate systems and alkaline earth metal cations, especially barium, have been exploited for their potentiometric response in ISE membranes.[10–15] The tetraphenylborate salt of a barium complex with α-(nonylphenyl)-ω-hydroxy-*catena*-poly(oxyethylene) (with 30 oxyethylene units) [Ba^{2+} (Antarox CO-880)] [BPh_4^-]$_2$, when incorporated with 2-nitrophenyl phenyl ether as the plasticizing solvent mediator in a poly(vinyl chloride)(PVC) support matrix, yields electrodes with a near Nernstian response, giving a slope of 28 mV decade^{-1}, for concentrations of barium ions between 1×10^{-1} and 1×10^{-4} mol dm^{-3}.[13]

As a result of an investigation on the complexation of dibenzo-30-crown-10,[16–19] a regio-selective synthesis of acyclic polyether (based on the oxyethylene units) intermediates was devised.[16] In due course, this led to the synthesis of a series of 'scorpion-like' ligands, each with oligoether 'tails' and a pair of anionic 'pincers'.[20] These were shown to be capable of metal encapsulation with the association of some members of the alkali and alkaline earth metals, with the affinity for barium being relatively strong compared with the other alkali and alkaline earth metals.[20] Some possible technological benefits were indicated, such as the use of these materials to overcome clogging, *e.g.*, by barium sulphate scale formation during oil production from oil wells.[20] Additionally, there was the prospect of the application of these scorpion-like ligands as potentiometric ion sensors. Thus, some of these ligands (sensors A–I in Fig. 1 and Table 1) were studied for their suitability as possible selective sensors in PVC matrix membranes incorporating 2-nitrophenyl phenyl ether as the solvent mediator, and their performance was compared with that of a traditional barium sensor using [Ba^{2+} (Antarox CO-880)][BPh_4^-]$_2$ (sensor J, Table 1).

* Present address: Chemistry Department, Bangladesh University of Engineering and Technology, Dhaka, Bangladesh.

Experimental

Reagents

Sensors A–I (Fig. 1, Table 1) were donated and synthesized by Stoddart and co-workers at the University of Sheffield, Sheffield, UK,[20] and Antarox CO-880 was donated by GAF Chemicals, Manchester, UK. The [Ba^{2+} (Antarox

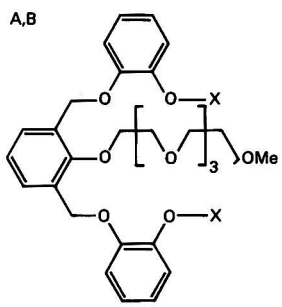

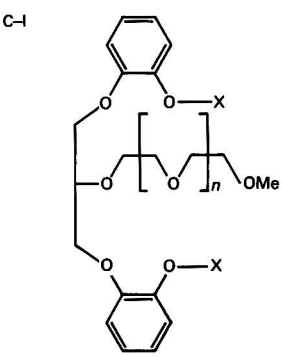

J = [$C_9H_{19}C_6H_4(OCH_2CH_2)_{30}OH$]$Ba_{2.5}$[$BPh_4^-$]$_5$

Fig. 1 Structural details of sensors. A and B are planar tripodal structures, whereas C–I are tetrahedral tripodal structures. For key see Table 1

CO-880)][BPh_4^-]$_2$ was prepared as described previously,[13] 2-nitrophenyl phenyl ether was supplied by Eastman Kodak, Rochester, NJ, USA and PVC Breon Resin II EP by BP Chemicals, Barry, UK. Otherwise, analytical-reagent grade reagents were used, including the chlorides of barium, calcium, magnesium, lithium, sodium, potassium, caesium and rubidium (BDH, Poole, Dorset, UK).

PVC Membrane Fabrication and E.m.f. Measurements

The PVC matrix membrane ISEs were fabricated from membranes containing a sensor (2.5 mg), 2-nitrophenyl phenyl ether (360 mg) and PVC (170 mg), and assembled according to established procedures.[21,22] The internal filling solution was barium chloride (0.1 mol dm^{-3}), and all the electrodes were conditioned in barium chloride (0.1 mol dm^{-3}) prior to use.

The e.m.f measurements were made with a Radiometer PHM64 pH-millivoltmeter (Radiometer A/S, Copenhagen, Denmark) in conjunction with a saturated calomel reference electrode (EIL Model 1370-710). A Corning pH meter and a glass electrode (EIL Model 740748) were used for pH measurements. Electrode calibrations were carried out by spiking with successive aliquots of known concentrations of the sample into doubly de-ionized water thermostated at 25 ± 0.1 °C. When not in use, the electrode membranes were stored in barium chloride (0.1 mol dm^{-3}).

Selectivity Coefficient Determination

Potentiometric selectivity coefficients, ($k^{pot}_{Ba,B}$) were determined using the separate solution method:

$$\log k^{pot}_{Ba,B} = \frac{E_2 - E_1}{S} + \left[1 + \frac{z_{Ba}}{z_B}\right] \log a_{Ba} \qquad (1)$$

where E_1 and E_2 are the electrode responses to the barium and interferent ion, respectively, each at a barium concentration of 1×10^{-2} mol dm^{-3}, S is the calibration slope and z_{Ba} and z_B are the charges of the barium and interferent ions, respectively. For divalent interferent ions, eqn. (1) simplifies to

$$\log k^{pot}_{Ba,B} = \frac{E_2 - E_1}{S} \qquad (2)$$

For determination of the pH interference-free ranges, e.m.f. measurements were made on solutions of barium chloride in a 0.01 mol dm^{-3} tris(hydroxymethyl)aminomethane (Trizma) buffer (obtained from Sigma, Poole, Dorset, UK), whose pH values were adjusted with 0.1 mol dm^{-3} hydrochloric acid.

Table 1 Structural characteristics of the planar and tetrahedral molecules used and electrode numbers (PVC matrix membrane type based on 2-nitrophenyl phenyl ether plus sensor)

Sensor	No. of oxyethylene units	Nature of X in Fig. 1	ISE No.
A	3	p-OMe-benzyl	1
B	3	Benzyl	2
C	3	Benzyl	3
D	2	H	4
E	3	H	5
F	4	H	6
G	5	H	7
H	3	CH_2COOH	8
I	4	CH_2COOH	9
J	30	—	10*

* This electrode is based on a sensor of the tetraphenylborate salt of the barium complex with Antarox CO-880.

Results and Discussion

A number of points are relevant for discussion with regard to both the performance characteristics (calibration slope and $k^{pot}_{Ba,B}$ values) of these materials as potentiometric barium ion sensors, and their selectivity characteristics, namely: (*i*) a general comparison of the barium ion sensing qualities of the sensors formed from compounds A–I with the traditional systems of J; (*ii*) a comparison of the planar tripodal (B) and the corresponding tetrahedral tripodal structure (C); (*iii*) the dependency of the number of oxygen atoms in the oxyethylene chain of the diphenol structures (D–G), and of the carboxylates (H and I); (*iv*) the effect of substituting the phenolic groups of E and F by carboxylic groups (H and I), and for E by benzyl (C); and (*v*) a comparison of the methoxylated benzyl derivative (A) with the benzyl derivative (B) for the planar tripodal structure.

Barium Ion Sensing Qualities

The calibrations for barium of the various ISEs were evaluated and compared with the [Ba^{2+}(Antarox CO-880)][BPh_4^-]$_2$ model,[13] ISE 10 (Fig. 2). All of the electrodes responded to barium ions, but to different degrees (Fig. 2); each of the new planar and tetrahedral molecule types (Fig. 1 and Table 1) were inferior to the previously established ISE 10 (Fig. 2).

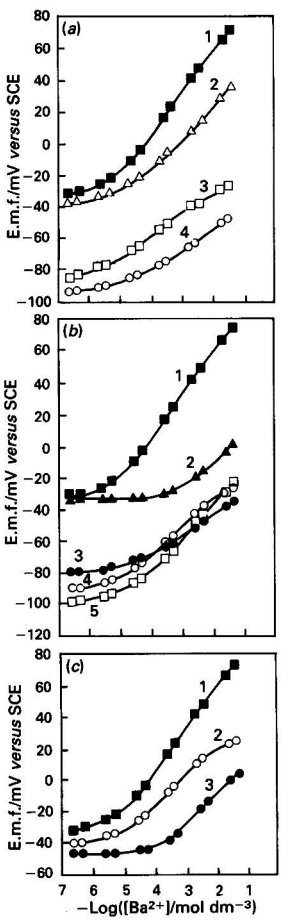

Fig. 2 Barium ion responses of various PVC matrix membrane electrodes. (*a*) 1, ISE 10; 2, ISE 3; 3, ISE 1; and 4, ISE 2: (*b*) 1, ISE 10; 2, ISE 7; 3, ISE 4; 4, ISE 6; and 5, ISE 5: and (*c*) 1, ISE 10; 2, ISE 8; and 3, ISE 9. For key see Table 1

In general terms, of the electrodes based on the planar and tetrahedral scorpion-like polyethers under investigation, it is ISE 3 (sensor C) that most closely resembles the calibration characteristics of ISE 10. This is because it has a higher (near-Nernstian) e.m.f. response than any of others. The next, in order of response, are ISEs 8 (sensor H), 9 (sensor I) and 7 (sensor G). Ion-selective electrode 5 showed the best slope, and has a reasonable linear range (2.6×10^{-4}–4.3×10^{-2} mol dm^{-3}), but its overall response characteristics are greatly inferior to that of ISE 10.

Sensor B (ISE 2) is inferior to C (ISE 3) and points to the tetrahedral tripodal structure being a favourable system for forming a pseudo-cavity around the metal ion in order to maximize the number of stable ion–dipole interactions as previously intimated from data for the association constants of these acyclic polyethers with barium ions.[20] Association constants (K_a) in tetrachloromethane of sensors B and C with alkali and alkaline earth metal cations as measured by the picrate extraction technique are as follows (data from reference 20). For sensor B: Li^+, 160; Na^+, 1300; K^+, 1600; Rb^+, 610; Cs^+, 220; Mg^{2+}, 140; Ca^{2+}, 500; Sr^{2+}, 900; and Ba^{2+}, 1500. For sensor C: Li^+, 670; Na^+, 1100; K^+, 3800; Rb^+, 1100; Cs^+, 800; Mg^{2+}, 180; Ca^{2+}, 700; Sr^{2+}, 1700; and Ba^{2+}, 24 000.

Regarding the effect of the dependency of the number of oxygen atoms in the oxyethylene chain, there is little difference between ISEs 4, 5 and 6 (sensors D, E and F), but ISE 7, although of short calibration (Fig. 2), indicates the extra effect of ion–dipole interaction promoted by the oxyethylene units. This is not so when ISEs 8 and 9 (sensors H and I) are compared (Fig. 2), but here the carboxylate group may have a modifying steric influence impressed on the extended oxyethylene chain (from 3 to 4 units). Appropriate groups in the 'pincer' positions certainly seem to promote barium ion-sensing (ISEs 3 and 8).

After comparing the effect of the methoxylated benzyl group in the pincer positions of the planar tripodal structure (ISE 1) with just the benzyl group for ISE 2, it would seem [Fig. 2(a)] that there is some virtue in a future study of the methoxylated benzyl derivative with the tetrahedral tripodal structure.

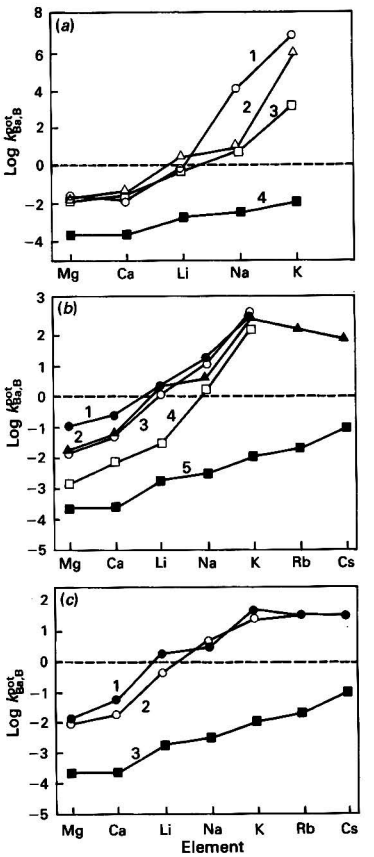

Fig. 3 Summary of selectivity coefficient data for various PVC matrix membrane electrodes. (*a*) 1, ISE 2; 2, ISE 3; 3, ISE 1; and 4, ISE 10: (*b*) 1, ISE 4; 2, ISE 7; 3, ISE 6; 4, ISE 5; and 5, ISE 10: and (*c*) 1, ISE 9; 2, ISE 8; and 3, ISE 10. For key see Table 1

Selectivity Characteristics

The selectivity features of ISEs 1–10 for barium with respect to selected alkali and alkaline earth metal cations are summarized in Fig. 3. Again, the superiority of ISE 10 (sensor J) is demonstrated. However, it is less easy to distinguish the trends between the various other electrodes.

It is of interest to note that ISE 5 (sensor E) is more selective [Fig. 3(b)] than ISE 4 (sensor D), 6 (sensor F) and 7 (sensor G). The structural reason for this is unclear. More obvious is that ISE 1 (sensor A) is more selective than ISE 2 (sensor B) [Fig. 3(a)], and ISE 3 (sensor C) is marginally more selective than ISE 2 (sensor B).

For the alkali metal cations, the interferences are not as significant as indicated by the positive values for log $k^{pot}_{Ba,B}$ in Fig. 3, as even when $k^{pot}_{Ba,B} > 1$ there can be a selectivity towards barium if B is a univalent cation.[23] Nevertheless, a value of log $k^{pot}_{Ba,K} = 6$ for ISE 3 is considerably greater than the threshold value of ≈ 2, which is necessary for the complete loss of selectivity towards barium over potassium for sensor C, and raises the question of whether the system yields a credible potassium ISE. Experiments indicated that potassium ISEs do result from the system, but they are of inferior quality to the well established ISE based on valinomycin. However, there was insufficient sensor material to permit a full definitive study, and the matter merits further investigation. With regard to barium ion selectivity, ISE 10 is still the best.

Conclusion

Although the general performance of ISEs, based on sensors of the planar and tetrahedral receptor molecules studied here, is inferior to that of barium ISEs based on an α-(nonylphenyl)-ω-hydroxy-*catena*-poly(oxyethylene) system, an extended study of the effect of methoxylated benzyl or similar type groups in the 'pincer' positions of the tetrahedral tripodal structures is indicated.

Hunan University, China, and the British Council are thanked for supporting visiting research associateships for Y.P.F. and M.M.I., respectively. The Science and Engineering Research Council is thanked for generous financial support under their Chemical Sensors research initiative which has made possible the support of N.K.H. and of the provision of the new type receptor molecule sensors from Dr. J. F. Stoddart (University of Sheffield). Discussions with Dr. Stoddart and Dr. J. F. Costello (University of Sheffield), and with Dr. D. J. Williams (Imperial College, London) are much appreciated.

References

1 Moore, C., and Pressman, B. C., *Biochem. Biophys. Res. Commun.*, 1964, **15**, 562.
2 Pedersen, C. J., *J. Am. Chem. Soc.*, 1967, **89**, 7017.
3 Eisenman, G., Ciani, S., and Szabo, G., *J. Membrane Biol.*, 1969, **1**, 294.

4 Truter, M. R., *Struct. Bonding*, 1973, **16**, 72.
5 Simon, W., Morf, W. E., and Meier, P. Ch., *Struct. Bonding*, 1973, **16**, 113.
6 Midgley, D., *Chem. Soc. Rev.*, 1975, **4**, 549.
7 Pioda, L., Stankova, B., and Simon, W., *Anal. Lett.*, 1969, **2**, 665.
8 Frant, M. S., and Ross, J. W., *Science NY*, 1970, **167**, 987.
9 Ammann, D., Morf, W. F., Anker, P., Meier, P. C., Pretsch, E., and Simon, W., *Ion-Sel. Electrode Rev.*, 1983, **5**, 3.
10 Levins, R. J., *Anal. Chem.*, 1971, **43**, 1045.
11 Levins, R. J., *Anal. Chem.*, 1972, **44**, 1544.
12 Bauman, E. W., *Anal. Chem.*, 1975, **47**, 959.
13 Jaber, A. M. Y., Moody, G. J., and Thomas, J. D. R., *Analyst*, 1976, **101**, 179.
14 Jaber, A. M. Y., Moody, G. J., and Thomas, J. D. R., *J. Inorg. Nucl. Chem.*, 1977, **39**, 1973.
15 Levins, R. J., *Ger. Offen.*, 2264721, 1973.
16 Allwood, B. L., Kohnke, F. H., Slawin, A. M. Z., Stoddart, J. F., and Williams, D. J., *J. Chem. Soc., Chem. Comm.*, 1985, 311.
17 Kohnke, F. H., and Stoddart, J. F., *J. Chem. Soc., Chem. Comm.*, 1985, 314.
18 Allwood, B. L., Kohnke, F. H., Stoddart, J. F., and Williams, D. J., *Angew. Chem., Int. Ed. Engl.*, 1985, **24**, 581.
19 Colquhoun, H. M., Goodings, E. P., Maud, J. M., Stoddart, J. F., Wolstenholme, J. B., and Williams, D. J., *J. Chem. Soc., Perkin Trans. 2*, 1985, **2**, 607.
20 Bartlett, J. S., Costello, J. F., Mehani, S., Ramdas, S., Slawin, A. M. Z., Stoddart, J. F., and Williams, D. J., *Angew. Chem., Int. Ed. Engl.*, 1990, **29**, 1404.
21 Moody, G. J., Oke, R. B., and Thomas, J. D. R., *Analyst*, 1970, **95**, 910.
22 Craggs, A., Moody, G. J., and Thomas, J. D. R., *J. Chem. Educ.*, 1974, **51**, 541.
23 Craggs, A., Kiel, L., Moody, G. J. and Thomas, J. D. R., *Talanta*, 1975, **22**, 907.

Paper 0/04934D
Received November 2nd, 1990
Accepted January 10th, 1991

Response Characteristics of Conductive Polymer Composite Substrate All-solid-state Poly(vinyl chloride) Matrix Membrane Ion-selective Electrodes in Aerated and Nitrogen-saturated Solutions

Salvador Alegret
Departament de Química, Universitat Autònoma de Barcelona, E-08193 Bellaterra, Spain
Antonio Florido
Departament d'Enginyeria Química, Escola Tècnica Superior d'Enginyers Industrials de Barcelona, Universitat Politècnica de Catalunya, E-08028 Barcelona, Spain

The characterization of a perchlorate ion-selective electrode, with a poly(vinyl chloride) matrix membrane on a conductive silver–epoxy composite, showed that electrodes with this type of internal solid contact have virtually the same electrochemical properties as electrodes constructed with the same sensor system (methyltri-*n*-octylammonium perchlorate and 2-nitro-*p*-cymene as mediator solvent) or commercially available electrodes for perchlorate ion, both of which have internal liquid contacts. The constructed all-solid-state electrodes were studied under a variety of experimental conditions (sodium perchlorate solutions of different concentrations, pH and extent of aeration) in order to determine the actual limitations of electrodes based on conductive plastic composites. Owing to the internal solid contact, these electrodes give rise to small drifts in continuously de-aerated solutions. However, this disadvantage does not hinder direct potentiometric measurements.

Keywords: *Ion-selective electrode; perchlorate; conductive epoxy composite-based ion-selective electrode; conducting filled polymer-based ion-selective electrode; all-solid-state poly(vinyl chloride) membrane electrode*

Potentiometric transducers consisting of poly(vinyl chloride) (PVC) membranes directly applied on to electrically conducting composite materials with no internal reference solutions are a viable alternative for implementing ion-selective electrodes (ISEs). Their construction is based on the formation and *in situ* application of a mobile carrier membrane on to a polymer substrate loaded with conductive material particles, which acts as an internal solid contact. This type of composite material is known as conducting filled polymer.

The procedure involved is straightforward and easily implemented, and has so far been used to construct various electrodes, selective for ions such as nitrate,[1–4] chloroacetate,[5] perchlorate,[6] benzoate,[7] calcium,[4,8,9] barium,[10] potassium[4,11] and ammonium,[12–14] by using different types of charged and neutral mobile carriers, mediator solvents and internal solid contacts (epoxy resin loaded with silver or graphite). The absence of an internal solution allows this type of electrode to be used in any position (horizontally, inverted, *etc.*) and in a variety of situations (microgravity, rotation, vibration, agitation, *etc.*).

The main advantage of this type of transducer is the possibility of readily constructing potentiometric devices in a variety of shapes and dimensions, as these are dictated by the design of the conductive plastic support,[15] which, unlike normal solid contacts, can be easily moulded. Hence, microelectrodes[9] and different types of flow-through detectors[1,2,8,11,12,14] have been constructed in this fashion; the latter devices allow the sequential detection of several analytes in flow injection[8] and the implementation of flow-through potentiometric biosensors by using additional membranes.[12–14]

In principle, all-solid-state PVC membrane electrodes having conducting filled polymers, but no internal-reference solution, belong to the same class as coated-wire ion-selective electrodes[16] and carbon-substrate ion-selective electrodes,[17] in which the interface between the membrane (an ionic conductor) and the internal solid contact (an electronic conductor) is theoretically blocked to a reversible electron or ion transfer,[18,19] *i.e.*, there is no well-defined internal reference potential, hence these transducers do not provide very reproducible results. However, in practice, the results presented here show that electrodes based on conducting filled polymers (silver[1–10] and graphite[11–14] composites) provide reproducible potentials, and especially good lifetimes, which are better than those of conventional electrodes having internal reference solutions,[5,6,10] as the occurrence of a single solution–membrane interface in the all-solid-state electrodes diminishes the risk of leaching of the sensing system confined within the membrane.

In this work, these novel ISEs, constructed by the above-mentioned procedure, are evaluated by focusing on the stability of their potential response, which determines their alternative practical applications as they resemble electrodes with internal reference solutions in every other aspect. For this purpose, a perchlorate ion-selective electrode, reported previously,[6] based on a silver–epoxy composite that accommodates a methyltri-*n*-octylammonium perchlorate–2-nitro-*p*-cymene sensor for perchlorate immobilized on a PVC membrane, was studied. The stability of the electrode response with time was studied under various conditions in sodium perchlorate media, which are typically used in solution equilibria chemistry. Finally, the use of these ISEs as reference electrodes for perchlorate media in potentiometric cells with no liquid junction was evaluated.

Experimental

Apparatus

Potential measurements were effected by means of Crison Digilab 517 digital potentiometers connected to an electrode switch, also from Crison, or to a customized automated titration system capable of commanding up to four autoburettes (Crison 738). All potentiometric measurements were carried out at 25 ± 0.2 °C under mild stirring. The coulometric titration was carried out with a Promax FAC-230 power supply, with its positive terminal immersed in a coulometric bridge containing 3.0 mol dm^{-3} $NaClO_4$.

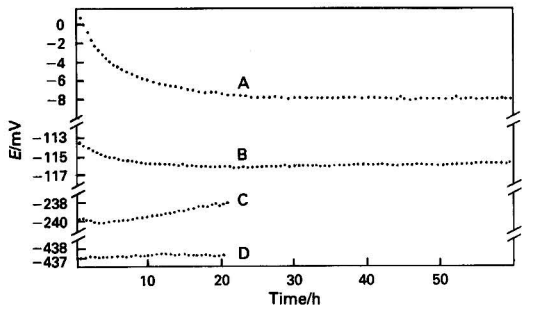

Fig. 1 Potential response of the conductive polymer composite based perchlorate ion-selective electrodes as a function of time at different perchlorate concentrations (A, 0.001; B, 0.1; and C, 3.0 mol dm^{-3}) compared with an Ag–AgCl reference electrode (D) (placed in a Wilhelm bridge of I = 3.0 mol dm^{-3}) in 3.0 mol dm^{-3} sodium perchlorate medium. All measurements were made by using an Orion 92-02-00 reference electrode. The calibrations were carried out after conditioning the electrodes with 3.0 mol dm^{-3} sodium perchlorate

Electrodes

The electrodes, accommodating a PVC membrane applied on to a conductive composite support (EPO-TEK 410 silver–epoxy resin from Epoxy Technology), were constructed as described in the literature.[4,6,10] The solution used to apply the membrane was prepared from 0.04 g of methyltri-*n*-octylammonium chloride (Fluka), 0.40 g of 2-nitro-*p*-cymene (Aldrich, technical grade) and 0.16 g of PVC (Fluka 81392, high relative molecular mass) in 6 ml of tetrahydrofuran (THF) (Merck). Those with internal reference solutions required preparation of a master membrane from the same solution, according to the method of Moody and Thomas.[20] For comparison, we also used a commercially available perchlorate electrode (Orion 93-81), an Ag–AgCl reference electrode with a Wilhelm salt bridge[21] containing a solution consisting of 10 mmol dm^{-3} $AgClO_4$, 2.99 mol dm^{-3} $NaClO_4$–3.0 mol dm^{-3} $NaClO_4$, and a commercially available Orion 90-02-00 Ag–AgCl electrode housing an Orion 90-00-02 solution in its inner compartment plus 3.0 mol dm^{-3} sodium nitrate when the ionic strength was adjusted to this value and 0.1 mol dm^{-3} ammonium fluoride when it was adjusted to 0.1 or 0.001 mol dm^{-3} in the external compartment. The pH measurements were carried out by means of an Ingold 102013031 glass electrode.

Reagents

Pro analisi grade reagents were used throughout. Sodium perchlorate solutions were prepared by successive dilution from a stock solution of about 7 mol dm^{-3}, prepared and standardized according to recommended procedures.[22]

Results and Discussion

Evaluation of the Perchlorate-selective Electrode Based on Silver–Epoxy Composite Substrate

The all-solid-state ISE, an ISE based on the same type of membrane, but including an internal reference solution, and also a commercially available perchlorate ISE (Orion), were calibrated simultaneously and periodically over a period of a few weeks. The three electrodes showed similar sensitivity to perchlorate and similar reproducibility over time. In fact, the average slope for a period of 8 weeks was −58.3 mV $decade^{-1}$ [standard deviation (SD) = 1.1 mV $decade^{-1}$] for the all-solid-state ISE with the internal liquid contact, −57.2 mV $decade^{-1}$ (SD = 1.2 mV $decade^{-1}$), and −58.9 mV $decade^{-1}$ (SD = 1.1 mV $decade^{-1}$) for the Orion ISE. These values were obtained from 20 calibrations on separate solutions with an ionic strength of 0.1 mol dm^{-3}, adjusted with ammonium fluoride.

The three electrodes also exhibited the same lower limits of linear response (5×10^{-5} mol dm^{-3}), response times (< 20 s), constant-response pH range (3–11.5 at an ionic strength of 0.05 mol dm^{-3}) and interference pattern.[6] The similarity between the responses of the three types of electrode confirms the suitability of conductive-epoxy composite ISEs with no internal reference solution. The potential readings of the all-solid-state electrodes described here were relatively stable over short periods of time (0.1 mV over a few minutes), which allowed reproducible linear calibration graphs [correlation coefficient (r) = 0.9999] to be obtained.[6] Nevertheless, the potential stability over relatively long periods of time was studied in detail, as this determines the practical application of the electrodes.

Potential Stability over Long Periods of Time

The stability of the electrode potential over a few days was determined by measuring potentials at pre-set time intervals using 3.0, 0.1 and 0.001 mol dm^{-3} perchlorate solutions thermostated at 25 °C after conditioning the electrodes with 3.0 mol dm^{-3} sodium perchlorate. For comparison, in the assay with 3.0 mol dm^{-3} perchlorate the stability over time of the potential provided by an Ag–AgCl reference electrode, including a Wilhelm salt bridge, was studied.

Fig. 1 shows the variation of the measured potential with time (every 30 min) at the three perchlorate concentrations stated above. The potential data, obtained in 3.0 mol dm^{-3} sodium perchlorate, reveal that the electrodes based on a conductive composite substrate provide apparently stable potentials within the first 6 h of operation, and afterwards to have constant potential drifts of about 2 mV for 20 h. The Ag–AgCl reference electrodes with a Wilhelm salt bridge and a double liquid junction (Orion 90-02-00) provided a more stable response as their potential response varied by only 0.5 mV over the same period of time. As can also be seen in Fig. 1, the responses of the electrodes based on a conducting composite at perchlorate concentrations of 0.1 and 0.001 mol dm^{-3} were different as they showed an initial drift of 3 and 9 mV, respectively, and stabilized after about 8 and 20 h, respectively. After that, the electrodes showed variations in the potential of less than 0.5 mV until the assays were finished, about 60 h after the start. The initial potential drifts were found to be readily avoidable, even in the 3.0 mol dm^{-3} perchlorate, by pre-conditioning the electrodes with solutions containing similar concentrations to that of the working solution to be used.

The slow initial drift, which disappeared a few hours after the electrodes were immersed in the solution, can be partly ascribed to the typical asymmetrical arrangement of membrane electrodes with internal solid contacts (metal|membrane|solution). It is known that the equilibration of the water content in one such membrane takes a few hours.[23] The equilibrium is appreciably altered between measurements when the electrodes are immersed in working solutions of very different water activities such as those studied here.

Potential Stability over Time in an Inert Nitrogen Atmosphere

Precise potentiometric determinations (*e.g.*, those carried out in studies on solution equilibria) are usually enacted in inert atmospheres, particularly when acid–base or redox equilibria are involved. Hence, some preliminary assays were carried out in order to determine the effect of nitrogen on the electrode potential. Three PVC membrane electrodes with a conductive epoxy resin composite support, previously conditioned in 0.1 mol dm^{-3} sodium perchlorate, were immersed in a solution of the same species at the same concentration, and

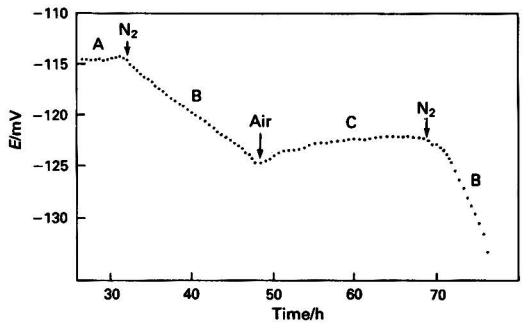

Fig. 2 Influence of de-aeration of the assayed solution with nitrogen on the potential response of a perchlorate ion-selective electrode based on a PVC membrane applied onto a conductive polymer composite support immersed in a 0.1 mol dm^{-3} sodium perchlorate solution, as a function of time. A, Solution at equilibrium with the atmosphere; B, bubbling nitrogen through the solution; and C, replacing nitrogen by bubbling with air

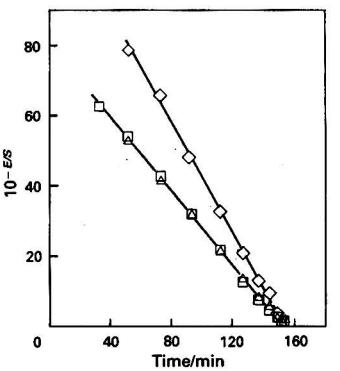

Fig. 3 Gran functions obtained in the potentiometric titration of the free acidity of a 3.0 mol dm^{-3} sodium perchlorate solution with coulometric generation of the hydroxyl ions and simultaneous acquisition of potential data for a glass electrode, using a perchlorate ion-selective electrode based on the conductive polymer composite substrate (◇), a commercially available perchlorate ISE (Orion) (△) and an Ag–AgCl electrode with a Wilhelm bridge (□) as reference electrodes

potential readings were recorded every 30 min. After a few hours of operation, a stream of nitrogen was passed through the solution and potentials were again recorded; the solution was then re-oxygenated by bubbling air through it, after which more nitrogen was bubbled through again.

The results obtained, representative of the three electrodes investigated, are shown in Fig. 2. Once immersed in the perchlorate solution, the electrodes reached a stable potential in a relatively short time, a potential that remained stable until the nitrogen was bubbled after 30 h. At that point there was a gradual drift in the potentials until the nitrogen was replaced with air, this caused the drift to progress in the opposite direction until a stable potential was reached. Further bubbling of nitrogen produced the effect observed initially.

The results obtained indicate that PVC membrane electrodes with conductive epoxy composite supports are not fully appropriate for use in a nitrogen atmosphere with continuous de-aeration. However, it should be noted that the variation in the potential caused by nitrogen bubbling was only about 5 mV every 10 h, which does allow the use of this type of electrode over short periods of time.

According to Cattrall *et al.*[24] and others,[25–27] electrodes with metal contacts and no internal reference solution provide an internal reference potential yielded by an oxygen half-cell, the gas of which comes from aerated working solutions and

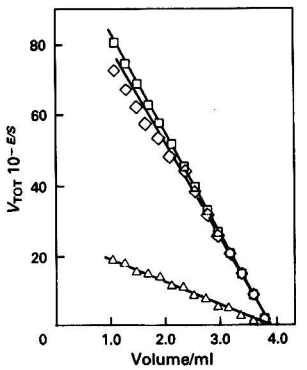

Fig. 4 Gran functions obtained in the potentiometric titration of the free acidity of a 3.0 mol dm^{-3} sodium perchlorate solution, with volumetric addition of hydroxyl ions and simultaneous acquisition of potential data from a glass electrode using a perchlorate ion-selective electrode based on the conductive polymer composite substrate (◇), a commercially available perchlorate ISE (Orion) (△) and an Ag–AgCl electrode with a Wilhelm bridge (□) as reference electrodes

diffuses across the PVC membrane to stabilize the electrode potential. The presence of an inert atmosphere altered the internal oxygen membrane environment and hence caused the additional drifts observed in the potentials.

Effect of pH on the Electrode Potential at High Perchlorate Concentrations

Metal–O_2 electrodes are notoriously irreversible, although they can provide relatively stable internal potentials if the oxygen system is coupled with another appropriate redox system, provided that the mass transport conditions for oxygen remain constant.[23] Sometimes oxidizable impurities included in the membrane (matrix, solvent mediator or additives, THF) might be responsible for the establishment of a stabilizing mixed internal potential.[23] For this reason, the presence of a possibly competitive acid–base equilibrium led to the reconsideration of the stability of the electrodes in solutions of a given perchlorate concentration at different pH values. This was determined as described elsewhere.[3,6] The potential response and stability of the electrodes were pH independent over the range 1.5–10.5 in 3.0 mol dm^{-3} $NaClO_4$.

The broad operational pH range suggests that the internal reference system is not dependent on an acid–base equilibrium.

Use of the Proposed Electrodes as Reference Electrodes in Direct Potentiometry. Determination of the Acidity of Concentrated Perchlorate Solutions

In order to test the applicability of the proposed electrodes as reference electrodes, the acidity of a 3.0 mol dm^{-3} sodium perchlorate solution was determined by direct potentiometry. For this purpose, an automated titration system was assembled, with a glass electrode as indicator, a perchlorate ISE based on a conducting composite substrate, and the commercially available Orion 90-02-00 Ag–AgCl electrode and an Ag–AgCl electrode with a Wilhelm salt bridge as reference electrodes.

The acidity of the aforesaid solution was determined by potentiometric titration with end-point detection by graphical extrapolation of Gran functions.[28] The titrant was added by generating, *in situ*, hydroxyl ions coulometrically, which resulted in no dilution of the ionic medium, or by using pure solutions of NaOH from an auto-burette, which gave rise to small changes in the ionic strength of the sodium perchlorate (10–15% at most).

In the coulometric titration, the above electrodes and a platinum plate connected to the negative terminal of the power supply, and one end of a coulometric bridge connected to the positive terminal, were immersed in 15 ml of the 3.0 mol dm^{-3} sodium perchlorate acidic solution. The coulometric titration was carried out by passing a current of 1 mA for different periods of time, between 5 and 20 min for each addition, in an inert nitrogen atmosphere. From the potential data, the corresponding Gran functions were calculated. The expression $10^{-E/S}$ (where E is the potential and $S = 59.16$ mV $decade^{-1}$ for the indicating glass electrode) was plotted against time (in minutes) (Fig. 3).

The volumetric titration was performed by immersing the electrodes in 25 ml of the same perchlorate solution under nitrogen, to which 42.6 mmol dm^{-3} NaOH was added. In this instance $V_{TOT}10^{-E/S}$ *versus* V_T, namely, the volume of NaOH added was plotted (Fig. 4).

According to the results shown in Figs. 3 and 4, the end-point was detected with a precision (relative standard deviation) of less than 1%, with no difference between the three electrode systems investigated. When applying the Gran functions to the volumetric titration (Fig. 4) the electrodes did deviate, although scarcely significantly, from the Nernstian response assumed. In any event, this did not prevent the determination of the end-point. This deviation can be ascribed to the continuous change in the perchlorate level in the titration medium arising from the titrant addition.

Part of this work was carried out under a research programme supported by the Comisíon Interministerial de Ciencia y Technologia (CICyT), Madrid, through Grant MAT 89-0246.

References

1 Alegret, S., Alonso, J., Bartrolí, J., Paulís, J. M., Lima, J. L. F. C., and Machado, A. A. S. C., *Anal. Chim. Acta*, 1984, **164**, 147.
2 Alegret, S., Alonso, J., Bartrolí, J., Lima, J. L. F. C., and Machado, A. A. S. C., *Anal. Lett.*, 1985, **18**, 2291.
3 Lima, J. L. F. C., Machado, A. A. S. C., Florido, A., Alegret, S., and Paulís, J. M., *Quím. Anal.*, 1985, **4**, 145.
4 Lima, J. L. F. C., and Machado, A. A. S. C., *Analyst*, 1986, **111**, 799.
5 Montenegro, M. C. B. S., Lima, J. L. F. C., and Machado, A. A. S. C., *Rev. Port. Quím.*, 1984, **26**, 197.
6 Alegret, S., Florido, A., Lima, J. L. F. C., and Machado, A. A. S. C., *Quím. Anal.*, 1986, **5**, 36.
7 Lima, J. L. F. C., Montenegro, M. C. B. S., Alonso, J., Bartrolí, J., and García-Raurich, J., *J. Pharm. Biol. Anal.*, 1989, **7**, 1499.
8 Alonso, J., Bartrolí, J., Lima, J. L. F. C., and Machado, A. A. S. C., *Anal. Chim. Acta*, 1986, **179**, 503.
9 Khalil, S. A. H., Moody, G. J., Thomas, J. D. R., and Lima, J. L. F. C., *Analyst*, 1986, **111**, 611.
10 Moody, G. J., Thomas, J. D. R., Lima, J. L. F. C., and Machado, A. A. S. C., *Analyst*, 1988, **113**, 1023.
11 Alegret, S., Alonso, J., Bartrolí, J., Lima, J. L. F. C., and Machado, A. A. S. C., in *Proceedings of the Second International Meeting of Chemical Sensors*, ed. Auconturier, J. L. Cauhapé, J. S., Destriau, M., Hagenmuller, P., Lucat, C., Méril, F., Portier, J., and Salardenne, J., Bordeaux Chemical Sensors, Bordeaux, Talance, 1986, p. 751.
12 Alegret, S., and Machado, A. A. S. C., *Analytical Uses of Immobilized Biological Compounds*, eds. Guilbault, G. G., and Mascini, M., Reidel, Dodrecht, 1988, p. 309.
13 Palleschi, G., Mascini, M., Martínez-Fàbregas, E., and Alegret, S., *Anal. Lett.*, 1988, **21**, 115.
14 Alegret, S., and Martínez-Fàbregas, E., *Biosensors*, 1989, **4**, 287.
15 Alegret, S., Alonso, J., Bartrolí, J., Lima, J. L. F. C., Machado, A. A. S. C., and Paulís, J. M., *Quím. Anal.*, 1987, **6**, 278.
16 Freiser, H., in *Ion-selective Electrodes in Analytical Chemistry*, ed. Freiser, H., Plenum, New York, 1980, vol. 2, p. 85.
17 Midgley, D., and Mulcahy, D. E., *Ion-Sel. Electrode Rev.*, 1983, **5**, 165.
18 Buck, R. P., in *Ion-selective Electrodes in Analytical Chemistry*, ed. Freiser, H., Plenum, New York, 1980, vol. 2, p. 1.
19 Nikolskii, B. P., and Materova, E. A., *Ion-Sel. Electrode Rev.*, 1985, **7**, 3.
20 Moody, G. J., and Thomas, J. D. R., in *Ion-selective Electrodes in Analytical Chemistry*, ed. Freiser, H., Plenum, New York, 1978, vol. 1, p. 287.
21 Forsling, W., Hietanen, S., and Sillén, L. G., *Acta Chem. Scand.*, 1952, **6**, 1952.
22 *Some Laboratory Methods*, Mimeograph, Department of Inorganic Chemistry, The Royal Institute of Technology, Stockholm, 1959.
23 Cattrall, R. W., and Hamilton, I. C., *Ion-Sel. Electrode Rev.*, 1984, **6**, 125.
24 Cattrall, R. W., Drew, D. M., and Hamilton, I. C., *Anal. Chim. Acta*, 1975, **76**, 269.
25 Hulanicki, A., and Trojanowicz, M., *Anal. Chim. Acta*, 1976, **87**, 411.
26 Schindler, J. G., Stork, G., Strüh, H. J., Schimid, W., and Karaschinski, K. D., *Fresenius Z. Anal. Chem.*, 1979, **295**, 248.
27 Heidecke, G., Kropf, J., Stork, G., and Schindler, J. G., *Fresenius Z. Anal. Chem.*, 1980, **303**, 364.
28 Gran, G., *Analyst*, 1952, **77**, 661.

Paper 0/02583F
Received June 11th, 1990
Accepted January 3rd, 1991

Simplified Sample Preparation for Fluoride Determination in Biological Material

Mirjana Nedeljković, Biljana Antonijević and Vesna Matović
Department of Toxicological Chemistry, School of Pharmacy, University of Belgrade, dr Subotića 8, 11000 Belgrade, Yugoslavia

A simple and rapid preparation method for the determination of fluoride in biological materials (blood and food) of various origins, is described. A homogenized sample was placed in a plastic diffusion cell and calcium phosphate added, it was then dried at 55 °C and treated with 70% $HClO_4$ and 40% $AgClO_4$. After digestion for 24 h at 55 °C, the fluorides released were fixed on the upper part of a diffusion cell containing a thin layer of NaOH. The analyses of the diffused fluoride were carried out with an ion-selective electrode. The proposed microdiffusion method, without mineralization, enables quantitative separation of the fluoride from the biological samples.

Keywords: *Sample preparation; biological material; fluoride determination; fluoride ion-selective electrode*

Fluoride is known to affect various types of plants, thus both man and animals are susceptible to poisoning by fluoride-contaminated food or feedstuffs. The complexity of the composition of vegetation and other biological materials presents many problems to the analyst, especially the isolation of fluoride from interfering material prior to determination.

Different procedures and methods for the isolation and determination of fluoride in biological materials have been proposed. The Willard and Winter distillation process[1] is a valuable technique that has been in use for a long time. Other workers have suggested mineralization in alkaline medium,[2] acid digestion,[3] and microdiffusion, either with or without ashing of the biological material.[4–6] However, the determination of fluoride in various biological materials is now based on the application of an ion-selective electrode.[7]

The aim of this study was to determine the conditions for a simple preparation method for biological materials in order to ensure the quantitative separation of the fluoride from the samples.

Experimental

Apparatus

Plastic diffusion cell (Fig. 1).

Fluoride ion selective electrode and reference calomel electrode.

pH meter.

Reagents

All reagents were of analytical-reagent grade. Solutions were prepared using re-distilled or de-ionized water.

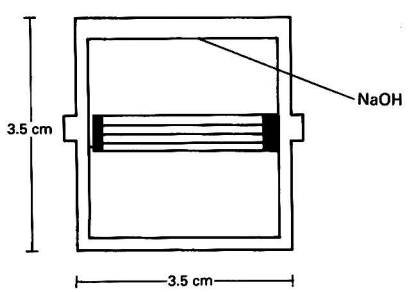

Fig. 1 Diffusion cell

NaOH solution, 1 mol l^{-1} *in ethanol.*

$HClO_4$, 70%.

$AgClO_4$, 40%. Ag_2O (22.5 g) dissolved in 100 ml of 60% $HClO_4$.

Total ionic strength adjustment buffer (TISAB).[8] Glacial acetic acid (57 ml), 58 g of NaCl and 300 mg of sodium citrate are added to 500 ml of water. After dissolution, the solution is neutralized to pH 5–5.5 with 5 mol l^{-1} NaOH, while immersed in a cooling water-bath. The buffer is then diluted to 1 l with water.

Procedure

Samples of cabbage, carrot, wheat, grass and apple were ground to produce a homogeneous mix (particle size of less than 3 mm). A 2–5 g portion of these homogenized samples, or 5 ml of the blood or milk specimens, were transferred into the diffusion cells (Fig. 1) and 0.1 g of $Ca_3(PO_4)_2$ added. The samples were dried in a laboratory oven at 55 °C. On the diffusion cell covers, thin layers were formed by the evaporation of 0.5 ml of 1 mol l^{-1} NaOH in ethanol in a laboratory oven at 55 °C. After the addition of 1.5 ml of 40% $AgClO_4$ and 1.5 ml of 70% $HClO_4$, to the samples, the diffusion cells were immediately covered. During the microdiffusion process (for 24 h at 55 °C) the fluorides, released under the influence of 70% $HClO_4$, reacted with the NaOH to form NaF. The constituents of the thin layers coating the diffusion cell covers were dissolved in 5 ml of de-ionized water, then quantitatively transferred into a polyethylene dish and mixed with the TISAB reagent in a 1:1 ratio. The separated fluorides were subsequently determined by a fluoride ion selective electrode.[7]

In order to define the accuracy of the proposed method of preparation, recoveries were calculated using two different samples originating from an industrially un-polluted region. An aqueous solution of NaF was added to 5 ml of the blood specimens and 5 g of homogenized mangel samples to give concentrations of 10, 50 and 100 μmol of F^- per litre or kilogram, respectively. The methods of preparation and determination used were the same as those described above. Various statistical parameters were calculated from the results obtained.

The method was used in order to determine the fluoride level in the samples obtained from an industrially polluted area, within a radius of 100–1000 m from a glass factory. (The samples from the un-polluted area were also analysed.) The fluoride level was determined in the following foodstuffs, cabbage, mangel, carrot, wheat, apple, milk and grass.

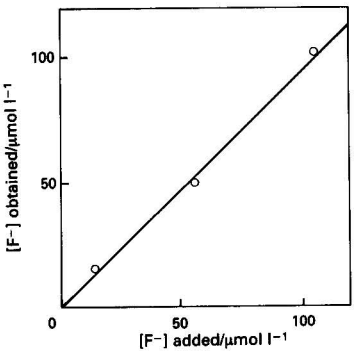

Fig. 2 Recovery of fluoride from blood specimens; $y = 0.534 + 0.957x$, regression coefficient = 0.999

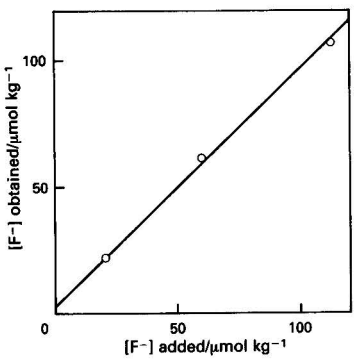

Fig. 3 Recovery of fluoride from mangel sample; $y = 1.52 + 0.96x$, regression coefficient = 0.9999

Results and Discussion

The results of the investigations are presented in Figs. 2 and 3 and Tables 1 and 2.

Figs. 2 and 3 and Table 1 show the high recovery values obtained by using the proposed microdiffusion method. The statistical parameters in Table 1 demonstrate the precision of the method.

The fluoride levels in the food and feedstuff samples taken from the polluted area are several times greater than those from an un-polluted region (Table 2).

Determination of fluoride in a biological material is a very complex analytical procedure with regard to sample preparation, and the procedure should be adapted according to the properties of the fluoride ion.

The results of comparative studies of various procedures for the preparation of biological material carried out by van den Heede *et al.*[3] show that the highest sensitivity and reproducibility were achieved by low-temperature ashing (50–60 °C), in an atmosphere of oxygen. Concentrated acid digestion also produced minimal losses of fluoride.

The method of sample preparation for the determination of fluoride in biological material presented here, combines the favourable points from both procedures. A digestion procedure using 70% $HClO_4$ at 55 °C in a closed diffusion cell, was used in order to eliminate the fluoride losses due to mineralization at high temperature.

On the basis of the recoveries and other statistical parameters, it is concluded that the proposed method is suitable for the determination of fluoride in biological materials. The advantages of the procedure are the accuracy, precision, reproducibility and ease of operation.

Table 1 Precision and recoveries obtained using the microdiffusion method for the determination of fluoride in biological samples, (n = 8)

	Blood		
Fluoride added/ μmol l^{-1}	$\bar{X} \pm$ SD/ μmol l^{-1}	RSD† (%)	Recovery (%)
0	4.61 ± 0.286	6.2	—
10	15.35 ± 0.801	5.2	104.9
50	51.35 ± 3.770	7.3	94.0
100	101.35 ± 3.990	3.9	96.9
	Mangel		
Fluoride added/ μmol kg^{-1}	$\bar{X} \pm$ SD/ μmol kg^{-1}	RSD (%)	Recovery (%)
0	11.12 ± 0.876	7.9	—
10	21.56 ± 0.417	1.9	102.1
50	60.50 ± 0	0	98.9
100	108.12 ± 5.14	4.71	97.3

* $\bar{X} \pm$ SD = mean ± standard deviation.
† RSD = relative standard deviation.

Table 2 Fluoride content in different samples, Results given are in μmol kg^{-1} (except for milk, μmol l^{-1}) n = 8

Sample	Fluoride contaminated area	Uncontaminated area
Cabbage	227.0 ± 1.27	3.6 ± 1.05
Mangel	71.0 ± 3.38	11.1 ± 1.18
Carrot	5.8 ± 0.31	4.7 ± 0
Wheat	45.0 ± 2.33	9.6 ± 0
Apple	5.3 ± 0.39	4.8 ± 0.12
Milk	9.8 ± 0.34	3.5 ± 0.10
Grass	208.0 ± 6.93	12.8 ± 0.88

The proposed method was used to determine the fluoride contents of different samples of food and feedstuffs originating from an area in the vicinity of a glass factory and from a region without fluoride contamination. Levels of fluoride several times higher were found in the samples from the fluoride polluted area, most markedly elevated in the cabbage, mangel and grass, thus influencing the high fluoride content of milk. Everyday control of the content of fluoride in air in this area shows that the average fluoride concentrations are frequently above the permitted values[9] resulting in an increased fluoride content in foodstuffs, as confirmed in this investigation.

It is concluded that the proposed sample preparation for the determination of fluoride, represents a suitable and reliable method for use in the routine analysis of biological materials.

References

1 Willard, H. H., and Winter, O. B., *Ind. Eng. Chem. Anal. Ed.*, 1933, **5**, 7.
2 Matthey, E. F., Fassa, F., and Demole, V., *Mitt. Geb. Lebensmittelunters. Hyg.*, 1960, **51**, 339.
3 van den Heede, M. A., Heyndrickx, A. M., van Peteghem, C. H., and van Zele, W. A., *J. Assoc. Off. Anal. Chem.*, 1975, **58**, 1135.
4 Bäumler, J., *Caries Res.*, 1967, **1**, 281.
5 Soldatović, D., Nedeljković, M., and Kuh, S., *Arh. Farm.*, 1975, **5**, 419.
6 Soldatović, D., and Nedeljković, M., *Hrana Ishrana.*, 1969, **10**, 448.
7 Tuši, J., *Clin. Chim. Acta*, 1970, **27**, 216.
8 Frant, M. S., and Ross, J. W., *Anal. Chem.*, 1968, **40**, 1169.
9 Tasić, M., and Nedeljković, M., *Hrana Ishrana.*, 1984, **25**, 201.

Paper 0/03294H
Received July 23rd, 1990
Accepted December 14th, 1990

Trifluoromethanesulphonate-selective Liquid Membrane Electrode

Frederic Favier and Jean Louis Pascal*
Laboratoire des Agrégats Moléculaires et Materiaux Inorganiques (URA 79 CNRS), Université Montpellier II, Sciences et Techniques du Languedoc, 34095 Montpellier Cedex 5, France

A liquid membrane electrode that is sensitive to trifluoromethanesulphonate (triflate) ions has been developed. It incorporates the ion-exchanging compound, $Ni(bphen)_3^{2+}\cdot 2(CF_3SO_3^-)$ (bphen = 4,7-diphenyl-1,10-phenanthroline), dissolved in the organic solvent 2-nitro-*p*-cymene. The electrode exhibits a near-Nernstian response for triflate concentrations greater than 1×10^{-4} mol dm^{-3}, with a slope of 59.5 mV per concentration decade at 25 °C. The limit of detection is 1.5×10^{-4} mol dm^{-3} triflate. The response time is about 5 s and the working pH is in the range 4–9. The electrode has a reasonably high selectivity towards the triflate ion relative to other common organic and inorganic ions. It can be used for the potentiometric determination of triflate. The triflate anion is a useful alternative to perchlorate in studies of monovalent ligands with poor coordination properties.

Keywords: *Ion-selective liquid membrane electrode; trifluoromethanesulphonate ion; triflate determination; selectivity coefficient*

The trifluoromethanesulphonate (triflate) ligand provides a good alternative to perchlorate or difluorophosphate groups in studies of monovalent ligands with poor coordination properties. Moreover, unlike perchlorates, triflates are not highly reactive or explosive compounds; they also form metallic complexes with similar geometries to those of perchlorates because of the very low basicities of both the ClO_4^- and the $CF_3SO_3^-$ anions.[1]

To our knowledge, there is no non-destructive method for the determination of triflates. One destructive approach, for example, consists of the determination of the percentage of the elemental constituents (C, S, O, F) after decomposition. This elemental analysis will only be satisfactory if the counter cationic group does not contain either C, S, O or F, so that the respective element can be determined. It therefore seemed worthwhile to develop a triflate-selective electrode.

The literature[2–4] contains descriptions of numerous specific membrane electrodes used in the determination of the concentration of ionic or molecular species. The working principle of this type of electrode, and the general arrangement and nature of the components, have been reviewed.[2]

This paper describes a liquid membrane electrode, incorporating a nickel–phenanthroline[5]–triflate complex, which is sensitive to the triflate anion. This electrode can be used for the potentiometric determination of triflate over a wide concentration range; it has a fast response, wide pH and temperature ranges and good selectivity.

Experimental

Measurements and Apparatus

All potentiometric measurements were carried out with continuous stirring at room temperature with a Tacussel ionometer containing TT100 and TT200 units. The TT100 unit allows the measurement of the actual value of the potential of glass, specific or metallic electrodes by means of a digital display, while the TT200 unit attached to the TT100 unit is an entrance amplifier of high impedance to which the electrodes are connected.

An Ag–AgCl electrode was used as the reference electrode, as for some commercial electrodes.[6]

Synthesis of the Organometallic Ion-exchange Material

A 0.0617 g (2.6×10^{-4} mol) amount of $NiCl_2\cdot 6H_2O$ (Merck, *pro analysi*) was dehydrated in $CHCl_3$ under reflux (24 h). Then 0.2513 g (7.6×10^{-4} mol) of 4,7-diphenyl-1,10-phenanthroline (bphen) (Aldrich, 97%) was added to the solution and refluxing was continued until the solution became orange, indicating the formation of $Ni(bphen)_3^{2+}\cdot 2Cl^-$. After cooling, 10 ml of 2-nitro-*p*-cymene (Aldrich, 90%) were added and the $CHCl_3$ was pumped out on a vacuum line (1×10^{-2} Torr). The remaining solution was shaken in a separating funnel with a 0.25 mol dm^{-3} aqueous NaOTf (OTf$^-$ = the trifluoromethanesulphonate anion) solution in order to exchange Cl^- for OTf$^-$. The mixture was decanted and the procedure was repeated until a test with $AgNO_3$ indicated the absence of Cl^- in the aqueous layer. The final solution, containing the $Ni(bphen)_3^{2+}\cdot 2(OTf^-)$ complex in 2-nitro-*p*-cymene, was used as the triflate liquid exchanger.

Cell Assembly

Potentiometric measurements were carried out with the following general electrode arrangement:

Ag–AgCl	Internal reference solution (0.14 mol dm^{-3} aqueous NaOTf)	$Ni(bphen)_3^{2+}\cdot 2(OTF^-)$ dissolved in 2-nitro-*p*-cymene	Test solution

The hydrophobic membrane,[6] a commercial polymeric membrane with a thickness of 100 μm, was simultaneously in contact with the internal reference and exchanger solutions.

In each instance, in order to obtain accurate readings, Na_2SO_4 (1 mol dm^{-3}), currently used as a fixed ionic strength buffer[7] with commercial liquid membrane electrodes, was added to the test solution prior to the measurement.

Results and Discussion

Potential Response

A graph of potential *versus* triflate concentration is given in Fig. 1, which shows the Nernstian potential response of the electrode over the range from 1×10^{-1} to 3×10^{-4} mol dm^{-3}. The slope, measured at 25 °C, of 59.5 mV per concentration decade is consistent with those observed for similar electrodes.[4] The graph is reproducible with a variation in the slope of less than 0.8%. The point L in Fig. 1 shows that the limit of detection of the electrode is 1.5×10^{-4} mol dm^{-3}.[8] This limit should attain 1×10^{-5} mol dm^{-3} with higher concentrations of the ion exchanger as observed for the perchlorate-selective electrode.[3]

* To whom correspondence should be addressed.

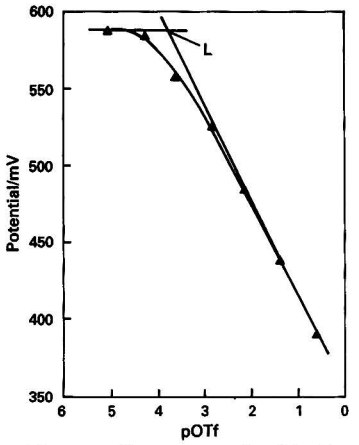

Fig. 1 Potential *versus* triflate concentration. Liquid membrane = 2-nitro-*p*-cymene containing $Ni(bphen)_3^{2+}\cdot 2(OTf^-)$ (2.6×10^{-2} mol dm^{-3}). Slope = 59.5 mv $decade^{-1}$. L = the limit of detection

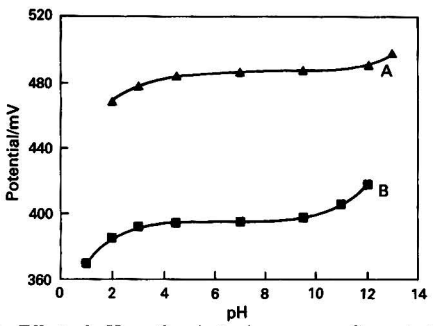

Fig. 2 Effect of pH on the electrode response. Concentration of OTf^-: A, 5×10^{-3}; and B, 2.5×10^{-1} mol dm^{-3}

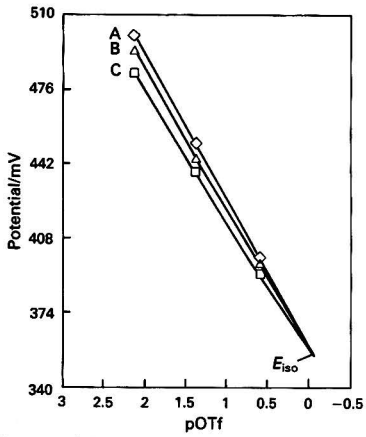

Fig. 3 Influence of the temperature on electrode response. E_{iso} = 352 mV (at intersection of isothermic lines). Temperature: A, 23; B, 45; and C, 55 °C

Table 1 Selectivity coefficients

Interfering ion (B)	$k^{pot}_{OTf^-,B}$ Mixed solutions method	$k^{pot}_{OTf^-,B}$ Separate solutions method
Br^-	3.8×10^{-3}	3.0×10^{-3}
Cl^-	3.1×10^{-3}	8.8×10^{-4}
F^-	1.4×10^{-3}	4.5×10^{-4}
IO_3^-	4.2×10^{-4}	9.0×10^{-5}
SO_4^{2-}	3.2×10^{-4}	2.3×10^{-3}
NO_2^-	7.0×10^{-3}	7.8×10^{-3}
CO_3^{2-}	1.3×10^{-4}	1.8×10^{-4}
ClO_3^-	1.3×10^{-2}	9.0×10^{-3}
ClO_4^-	0.16	6.8×10^{-2}
$Cr_2O_7^{2-}$	7.8×10^{-4}	1.1×10^{-3}
MnO_4^-	1.15	0.15
$[Fe(CN)_6]^{4-}$	1.3×10^{-5}	1.0×10^{-5}
Oxalate	4.6×10^{-5}	1.5×10^{-4}
Acetate	5.6×10^{-3}	2.7×10^{-4}

Response Time

The static response time[9,10] (the time required to attain a potential within 1 mV of the equilibrium value) was found to be about 10 s for a triflate concentration greater than 1×10^{-3} mol dm^{-3} and to vary from 30 s to 2 min for lower concentrations. Optimum conditions were attained when the concentration of the solution was greater than 1×10^{-3} mol dm^{-3}, the ionic strength was fixed, stirring was continuous and when the more strongly interfering ions (ClO_4^-, MnO_4^-, *etc.*) were not present in solution (see below).

Effect of pH and Temperature

The use of a specific electrode depends on the pH range. There are two effects of pH on the potential response of an electrode; in an acidic medium, H^+ complexes the anion whereas in a basic medium, OH^- complexes the organometallic cation. The measurements were carried out at two different triflate concentrations in the test solution, and the variation of pH was obtained by the addition of HCl or NaOH solution (0.1 mol dm^{-3}). It can be seen from Fig. 2 that the useful pH range is 4.5–7.5 at 2.5×10^{-1} mol dm^{-3} triflate and 4–9 at 5×10^{-3} mol dm^{-3} triflate.

Fig. 3 shows the Nernstian response of the electrode for test solutions at different temperatures: E_{iso}[11] was determined by extrapolation at the intersection of the three isothermic straight lines. For the triflate-selective electrode, a value of 352 mV was obtained.

Selectivity

The selectivity coefficients ($k^{pot}_{OTf^-,B}$) for a number of anions were evaluated using the mixed solutions and separate solutions methods.[12] For the mixed solution method, triflate activities were calculated after the addition of a 6.25×10^{-3} mol dm^{-3} $Cd(OTf)_2$[13] solution to a 0.1 mol dm^{-3} solution of the interfering ion. The results are reported in Table 1. The selectivity towards the triflate ion is reasonably high and common organic and inorganic anions, except MnO_4^- and ClO_4^- ions, cause no significant interference.

Determination of Triflates

A calibration graph of potential *versus* concentration (see Fig. 1) was obtained by recording the potential of solutions of NaOTf of known concentration. Sample solutions were prepared with 2 ml of the unknown test solution, 2 ml of 1 mol dm^{-3} Na_2SO_4 and 50 ml of water. The corresponding concentration of triflate in the test solution was read directly from the calibration graph after its potentiometric measurement.

The performance of the electrode described here is comparable to that of its commercial counterparts. It can be used successfully with a resonably fast response, at different temperatures and/or pH values, for the potentiometric determination of triflate in the presence of organic and inorganic species commonly present in the synthesis of triflato complexes.

We thank Professor J. Sarrazin for helpful suggestions and useful discussion and Dr. D. J. Jones for linguistic corrections to the manuscript. Financial support from the CNRS (France) is gratefully acknowledged.

References

1 Boumizane, K., Herzog, M. H., Jones, D. J., Pascal, J. L., Potier, J., and Roziere, J., in *Proceedings of the Second European Conference on Progress in X-Ray Synchrotron Radiation Research*, eds. Balerna, A., Bernieri, E., and Mobilio, S., Societa Italiana di Fisíca, Bologna, 1990, vol. 25, p. 903, and references cited therein.
2 Durand, G., *Tech. Ing. Mes. Phys.*, 1986, **P2**, p-2115.
3 Backzuk, R. J., and Dubois, R. J., *Anal. Chem.*, 1968, **40**, 685.
4 Jain, A. K., Jahan, M., and Tyagi, V., *Analyst*, 1989, **114**, 1155.
5 Case, J., *J. Org. Chem.*, 1951, **16**, 1541.
6 Durand, G., *Tech. Ing. Mes. Anal.*, 1986, **P2**, p-2115, 1-12.
7 *Analytical Methods Guide*, Orion Research, Cambridge, MA, 6th edn., 1974, pp. 12–23.
8 IUPAC, *Compendium de la Nomenclature en Chimie Analytique, Règles, Définitives de 1977*, Societe Chimique de France, 1980, ch. 21, pp. 215 and 216.
9 Moody, G. J., and Thomas, J. D. R., *Talanta*, 1972, **19**, 623.
10 Buck R. P., in *Ion Selective Electrodes in Analytical Chemistry*, ed. Frieser, H., Plenum, New York, 1978, ch. 1, pp. 117–127.
11 Durand, G., *Tech. Ing. Mes. Anal.*, 1986, **P2**, p-2115, 1-5.
12 Moody, G. J., and Thomas, J. D. R., *Selective Ion Sensitive Electrodes*, Merrow, Watford, 1971, ch. 2, pp. 9–32.
13 Boumizane, K., Thesis, Universite des Sciences et Techniques du Languedoc, Montpellier, 1989.

Paper 0/05066K
Received November 12th, 1990
Accepted January 3rd, 1991

Application of Flow-through Techniques to Drug Dissolution Studies

Zsófia Fehér, Ilona Kolbe and Ernő Pungor
Technical Analytical Research Group of the Hungarian Academy of Sciences, Institute for General and Analytical Chemistry, Technical University of Budapest, Gellért tér 4, 1502 Budapest XI, Hungary

Two flow-through techniques, *i.e.*, flow injection and triangle programmed flow titrimetry, have been used to follow the dissolution of drugs from pharmaceutical preparations. The applicability of direct ultraviolet spectrophotometry as a detection technique in flow injection was demonstrated for dissolution studies of nitrazepam- and metronidazole-containing pharmaceutical preparations. In the application of the triangle programmed titration technique, the dissolution of promethazine and ampicillin from pharmaceutical preparations was studied.

Keywords: *Drug dissolution study; nitrazepam, metronidazole, promethazine and ampicillin dissolution; flow injection with ultraviolet spectrophotometry; flow titration; electrolytic reagent generation*

Flow-through techniques are used mainly for the analysis of a series of individual samples. Continuous-flow analysis and flow injection (FI) techniques are useful tools in analytical laboratories handling a large number of samples. Several papers have been published also on the application of flow-through techniques in process monitoring (see, for example, references 1–3).

The need to determine the rate of drug dissolution from pharmaceutical preparations is becoming more frequent in quality control and pharmaceutical laboratories.[4–8] During the course of dissolution studies the concentration of the drug in question has to be determined in the dissolution medium continuously or at certain time intervals. In the automated systems used for this purpose the sampling and analysis can be carried out in a number of different ways. The most commonly used techniques are: continuous sampling and analysis; sequential sampling and analysis; and off-line sampling and subsequent analysis.

In commercially available systems, ultraviolet (UV) spectrophotometry is used almost exclusively as the analytical technique. A high-performance liquid chromatograph has also been coupled to these systems as a detector for dissolution rate studies (see, for example, references 9 and 10), which enables these studies to be performed even for complex pharmaceutical preparations.

Flow injection[11,12] is a frequently used analytical tool in many different fields of chemistry. In previous work,[13,14] FI coupled with voltammetric detection was used for the on-line determination of the drug-dissolution rate from pharmaceutical preparations. In the six-channel dissolution analysis system constructed in these laboratories,[13] six injectors were incorporated in order to inject portions of the dissolution medium arising from the dissolution vessels into the background electrolyte in succession.

Koupparis and co-workers[15–18] have also used FI to follow the dissolution process. Samples taken during the course of the dissolution process were analysed on-line using spectrophotometric detection following a chemical reaction between the sample and a carrier stream. Bigley and Grob[19] applied FI to the off-line analysis of samples taken during the course of the dissolution process.

Of those papers dealing with FI, few describe the direct application of UV spectrophotometry. Karlberg and co-workers[20,21] used FI with UV detection after the extraction of organics from different samples. However, for the analysis of pharmaceutical materials and preparations, UV spectrophotometry can advantageously be used directly as the detection technique in FI systems.

A triangle programmed titration technique has been developed in these laboratories.[22] In the course of this work it was shown that this technique is highly suitable for performing titrations in flow-through systems. The triangle programmed titration technique combines the advantages of flow-through analysis and the reliability of the titration.

The principle of the technique is as follows[22]: the sample solution of concentration c_s is streaming in the flow-through analytical channel at a constant flow-rate (v_s). It meets the appropriate titrant, the mass flow of which is changing with time according to an isosceles triangle shaped program (Fig. 1). After the two flows have merged, the segments of the flowing solution correspond to different degrees of titration. By ensuring an overtitration of the sample solution, the titration end-point is reached twice during the triangle-shaped mass flow *versus* time program. The titration process is followed by means of an appropriate detector. The relationship between the concentration of the sample solution and the time interval elapsing between the two equivalence points (Q) is given by:

$$Q = 2\tau - \frac{2a}{b} \cdot \frac{v_s}{n} \cdot c_s \qquad (1)$$

where 2τ is the time interval (in seconds) of the reagent addition program, a/b is the stoichiometric factor assuming a titration reaction of the type $aS + bR \rightarrow fP_1 + gP_2$ (S is the sample, R the reagent, and P_1 and P_2 are the products), c_s is the concentration of sample solution (in mol dm^{-3}) and n is the slope of the reagent mass flow *versus* time function (see Fig. 1).

An advantageous way of generating the titrant for triangle programmed titrations is current programmed electrolysis. In previous work, hydrogen and hydroxide,[23,24] silver,[25] mercury[24] and hypobromite[26] ions and also iodine[27] and bromine[28] were generated for carrying out acid–base, argentimetric, mercurimetric, iodimetric and bromimetric titrations.

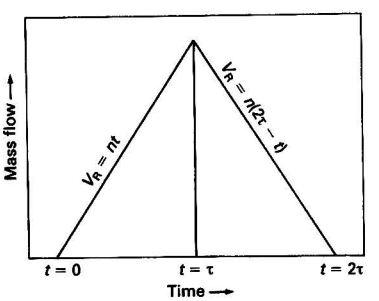

Fig. 1 Reagent mass flow *versus* time program of the triangle programmed titration technique (for details see text)

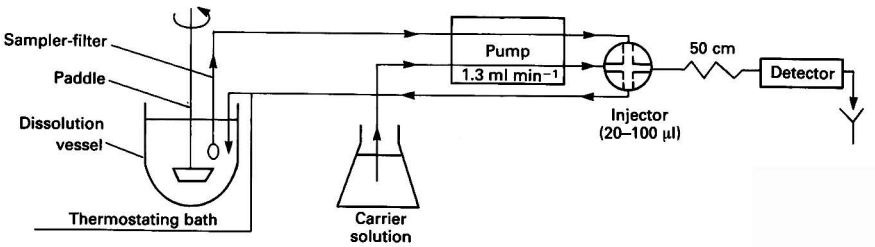

Fig. 2 Experimental set-up used for drug dissolution studies by FI

For electrolytic reagent generation the basic relationship is as follows:

$$Q = 2\tau - \frac{2a}{b} \cdot \frac{v_s \mu F \tau}{i_{max}} \cdot c_s \qquad (2)$$

where μ is the number of electrons involved in the reagent generating electrode process, F is the Faraday constant and i_{max} is the maximum value of the reagent generating current.

In this paper the application of FI with UV spectrophotometric detection and triangle programmed flow titration with amperometric detection as analytical techniques is demonstrated for on-line drug dissolution studies. During the course of measurements with the triangle programmed titration technique the dissolution characteristics of pharmaceutical preparations containing a phenothiazine derivative (promethazine hydrochloride) and of preparations containing a penicillin compound were studied.

The determination of different phenothiazine derivatives[25] and penicillins[27] has been described previously. Samples containing phenothiazine derivatives were titrated with electrolytically generated hypobromite ions and solutions containing the penicillin compound were titrated with iodine after a hydrolysis step using amperometric detection in the triangle programmed titrations.

Experimental

Apparatus and Procedure

Dissolution studies by FI were carried out in most instances with the experimental arrangement shown in Fig. 2. As can be seen, recycling is employed, *i.e.*, the solution is sucked continuously through a sampler-filter from the dissolution vessel by means of a peristaltic pump and returns to the dissolution vessel. The recycling solution flows through the loop of the injector and is injected into the carrier stream at certain time intervals.

A UV spectrophotometer fitted with a flow-through cell, placed behind the dispersion section, served as the detector.

A multi-channel peristaltic pump (Model OL-602, Labor-MIM, Esztergom, Hungary), a chromatographic injector (Model OE-320, Labor-MIM) with loops of 20, 50, 100 and 250 µl volume were used. A Liquodet Model 308 UV detector (Labor-MIM) with a Z-type flow-through cell of 8 µl volume was employed for measuring the absorbance values. The absorbance *versus* time profiles were recorded with an Omniscribe D 5000 *x–t* recorder (Houston, TX, USA).

For the triangle programmed flow titration technique the set-up shown in Fig. 3 was used. The sample solution is sucked continuously from the dissolution vessel and meets the titrant in the flow-through titration vessel. The titrant is generated electrolytically in the electrolysis cell. The two compartments of the reagent generating cell contain the generator and the auxiliary electrodes. The dialysis membrane separating the two compartments ensures electrical contact between the two compartments, but prevents mixing of the products of electrolysis. Platinum electrodes were used as the generator

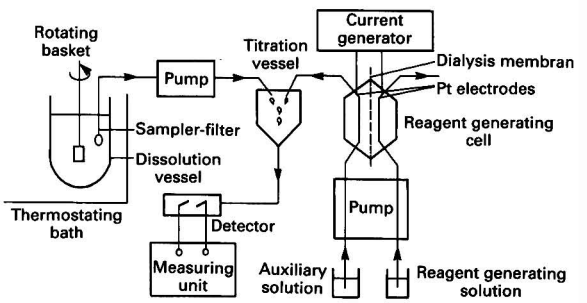

Fig. 3 Experimental set-up used for drug dissolution studies by triangle programmed titrimetry

and auxiliary electrodes. The titrant solution containing the hypobromite ion was generated from a 0.5 mol dm^{-3} potassium bromide solution (pH = 9.0) (reagent generating solution). Britton–Robinson buffer solution of pH 9.0 was used in the auxiliary line of the reagent generating cell.

For the determination of the penicillin compound, 0.5 mol dm^{-3} potassium iodide in a phosphate buffer of pH 7 was used for reagent generation, whereas a pH 7 phosphate buffer served as the reagent generating auxiliary solution.

The detector cell containing two platinum electrodes is connected to the titration vessel through a delay coil of 0.7 ml volume (w = 0.7 ml). A potential difference of 0.4 V was applied between the two platinum electrodes for the determination of the phenothiazine compound, whereas for the determination of the penicillin compound, the potential difference was 0.15 V. Owing to the relatively high potassium bromide/iodide concentration of the streaming solution, the potential of one of the platinum electrodes is constant during the course of the titration; hence the cathodic current flowing between the two platinum electrodes is proportional to the concentration of the titrant.

A laboratory-built programmable current generator was used for reagent generation, while a recording polarograph (Model OH-105, Radelkis, Budapest, Hungary) was employed for detection and recording of the titration curves (measuring unit).

Chemicals

Preparations containing nitrazepam and metronidazole were used as models for the FI study of the dissolution process, while those containing a phenothiazine derivative or a penicillin compound served as models for the triangle programmed titration technique.

Nitrazepam and metronidazole and the tablets containing these drugs were provided by Gedeon Richter Pharmaceutical Works (Budapest, Hungary) while the promethazine hydrochloride drug and the coated tablet containing 25 mg of promethazine were a gift from the EGIS Pharmaceutical Factory (Budapest, Hungary). The penicillin compound

(ampicillin) and the capsule containing 250 mg of ampicillin were provided by the Chinoin Pharmaceutical Factory (Budapest, Hungary). The drugs fulfilled the requirements of the Pharmacopoeia Hungarica VII.[29]

The chemicals used were of analytical-reagent grade.

Results and Discussion

Dissolution Studies by FI

The optimum parameters for FI were first determined. It seemed to be desirable to find suitable conditions for the dissolution analysis of pharmaceutical preparations containing active ingredients of different specific absorbance and different amounts of the active ingredient. The aim was also to achieve a relatively high sampling-analysis rate.

By studying the effect of the length and the diameter of the delay coil (dispersion section), the volume of the injected sample (V_{inj}) and the flow-rate of the carrier solution, the following parameters were chosen for the analysis of the dissolution medium by FI: diameter of the dispersion coil, 0.5 mm; length of the dispersion coil, 50 cm; and flow-rate of the carrier solution, 1.3 ml min^{-1}.

The injected volume was varied according to the specific absorbance and the amount of the drug present in the pharmaceutical preparation. Under the conditions mentioned above, an analysis rate of 1 sample min^{-1} was achieved.

A linear relationship was obtained between the signal measured (height of the injection peak) and the concentration of the solution injected for the drugs studied. The equations giving the relationship between the peak height and concentration and also the regression coefficients are as follows. Nitrazepam: $y = 12.12x + 0.32$; $r^2 = 0.9997$. Metronidazole: $y = 0.195x - 0.093$; $r^2 = 0.9990$.

Typical recorder traces obtained by injection of metronidazole solutions are shown in Fig. 4. The linear dependence of the signal on the concentration of the analyte permits the determination of the concentration of the drugs studied. Relative standard deviation (RSD) data obtained are presented in Tables 1 and 2. Data shown in Table 2 were obtained by injecting solutions of different concentration in succession.

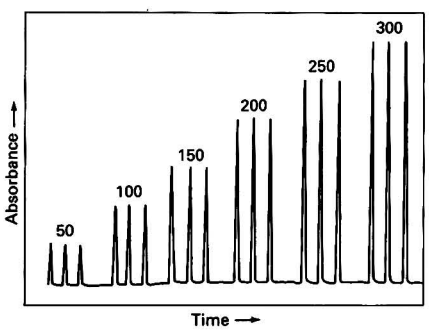

Fig. 4 Recorder traces obtained by injection of metronidazole solutions of different concentration. Values above the peaks are metronidazole concentrations in mg l^{-1}

Various pharmaceutical preparations were used in the dissolution studies. For example, a tablet containing 10 mg of nitrazepam and a tablet containing 250 mg of metronidazole were tested. Initially, it was shown that none of the ingredients present in the preparation interfered with the measurement of the absorbance of the active ingredient.

For this purpose, a mixture was prepared containing all the ingredients of the preparation under study except the active ingredient. After addition of the appropriate amount of water, a suspension was obtained which was filtered. The absorbance of the solution thus obtained was then measured.

The pharmaceutical preparation to be studied was dropped into 900 ml of 0.1 mol dm^{-3} hydrochloric acid in the dissolution vessel. The temperature of the dissolution medium was kept at 37.0 ± 0.1 °C using a thermostatically controlled water-bath. The paddle was rotated at a speed of 100 ± 3 rev min^{-1}. The shape and size of the dissolution vessel and those of the paddle fulfilled the requirements of the United States Pharmacopeia (USP XXII).[4]

The sample loop of the injector was filled continuously with the dissolution medium which was sucked from the dissolution vessel through a filter[30] (see Fig. 2). The contents of the loop were injected into the 0.1 mol dm^{-3} HCl carrier stream at 1 min intervals. (The volume of the loop employed was 100 µl for the preparation containing nitrazepam and 20 µl for the tablet containing 250 mg of metronidazole.) The absorbance was measured at 277 nm for the nitrazepam-containing tablet, and at 274 nm for the metronidazole-containing preparation.

The volume of the connecting tubes between the sampler and the injector was 0.9 ml, which corresponds to a delay time of about 40 s. The contents of the loop reach the detector 20 s after the injection has been performed. Hence, by carrying out the first injection 40 s after the start of the dissolution process, the first signal obtained can be assigned as the start of this process.

Figs. 5 and 6 show the dissolution curves for the two preparations studied. Fig. 5(*b*) shows a typical recorder trace for the nitrazepam-containing preparation.

It should be noted that the six-channel dissolution analysis system recently developed at this Institute[30,31] is a computerized system that allows sequential sampling and analysis by using an electropneumatically controlled six-way valve, the outlet of which is connected to the flow-through cell of a spectrophotometer. The FI technique can also be applied to this dissolution analysis system by incorporating the injector and delay coil between the six-way valve and the cell of the spectrophotometer. Hence, sequential analysis of the contents of the six dissolution vessels by FI can be performed.

It must be emphasized that FI with direct UV spectrophotometric detection can be used for the analysis of pharmaceutical preparations only in situations where the components accompanying the active ingredient do not interfere with the measurement of the absorbance.

Dissolution Studies by Triangle Programmed Titrimetry

For performing dissolution studies using the triangle programmed titration technique, the optimum measuring parameters have to be determined. It should be noted that

Table 1 Relative standard deviation (RSD) data for the analysis of a nitrazepam-containing solution by FI; $n = 7$

V_{inj}/µl	RSD (%)		
	v_s/ml min^{-1}		
	0.6	1.0	1.9
50	<1	<1	<1
100	—	—	<0.5
250	<0.4	<0.6	<0.6

Table 2 Relative standard deviation (RSD) data for the analysis of metronidazole-containing solutions by FI; $n = 5$, $v = 1.3$ ml min^{-1}

c/mg l^{-1}	RSD (%)
25	1.05
50	1.19
100	0.52
150	1.10
200	0.15
250	0.12
300	0.35

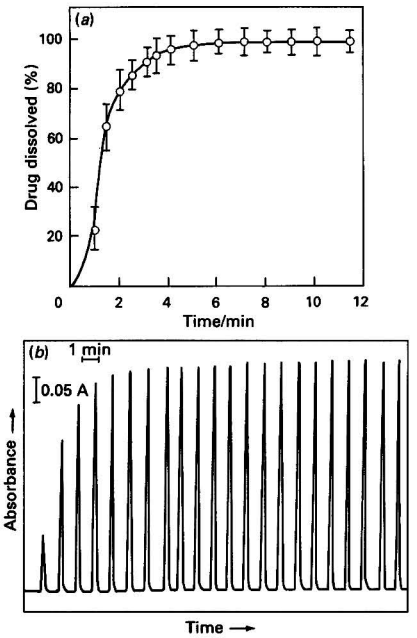

Fig. 5 (*a*) Dissolution curve (n = 3) and (*b*) recorder traces (λ = 277 nm; injection volume = 100 μl) obtained for the nitrazepam-containing pharmaceutical preparation

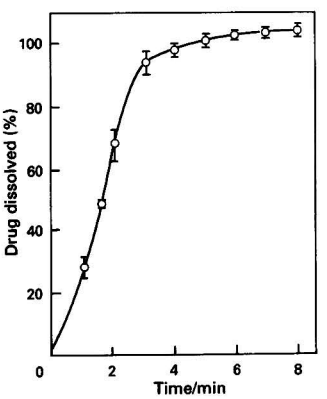

Fig. 6 Dissolution curve (n = 3) obtained for the metronidazole-containing pharmaceutical preparation

with this titration technique the actual values of the measuring parameters (i_{max}, 2τ and v_s) are not determined; instead a calibration graph constructed during the course of the experiments is used for the determination of concentrations.

As can be seen from eqn. (2) the slope of the calibration graph (Q *versus* c_s), and hence the reliability of the measurement, increases as the maximum value of the reagent generating current (i_{max}) decreases, and as the flow-rate and duration of the triangle-shaped current *versus* time program (titration time) increase.

The measuring parameters were selected experimentally according to the above correlations and by considering the following points. (1) The generating current has to be sufficient to ensure that there is an overtitration of the solution containing the drug content of the pharmaceutical preparation

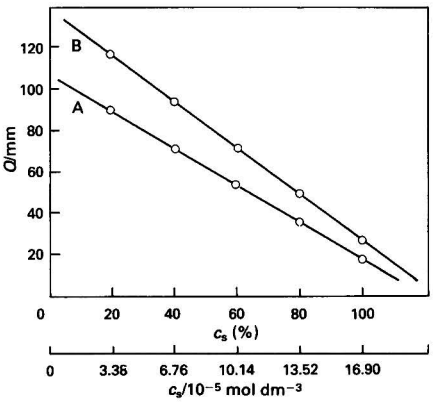

Fig. 7 Calibration graphs (Q *versus* c_s) for promethazine hydrochloride obtained by the triangle programmed titration technique. i_{max} = 2 mA; v_s = 1.0 ml min^{-1}; and w = 0.7 ml. A, 2τ = 40 s; and B, 2τ = 80 s

Table 3 Relative standard deviation (RSD) data for triangle programmed titration of promethazine-containing solutions; n = 5

$c/10^{-4}$ mol dm^{-3}	RSD (%)
1	1.02
3	0.97
5	1.16
7	0.86
10	0.79

Table 4 Relative standard deviation (RSD) data for triangle programmed titration of ampicillin-containing solutions; n = 5

$c/10^{-4}$ mol dm^{-3}	RSD (%)
1	1.75
3	1.82
5	1.27
7	1.19
10	1.45

to be studied; (2) as the sample solution being sucked from the dissolution vessel is not recycled, and hence passes to waste after the titration, the application of a high sample flow-rate is disadvantageous; (3) an increase in the time duration of the current *versus* time program (titration time) decreases the sampling frequency.

Calibration graphs for promethazine hydrochloride are shown in Fig. 7. Similar graphs were also obtained for ampicillin. The RSD data obtained for the determination of the two compounds are presented in Tables 3 and 4. The linear relationship between the analytical signal (Q-value) and the concentration of the sample solution permits the determination of concentrations during the course of the dissolution measurements.

It should be noted that during the course of the dissolution measurements a sample solution of changing concentration is flowing into the titration cell. Hence it is desirable to apply as short a reagent generating time interval (titration time) as possible.

For the titration of the solution sucked from the dissolution vessel, the result of the determination can be considered to be an average concentration characteristic of the time interval of the titration. The result (the amount of drug dissolved) was assigned to the middle of the time interval of the titration.

The assignment of the concentration data measured to the real time of the dissolution process was performed by

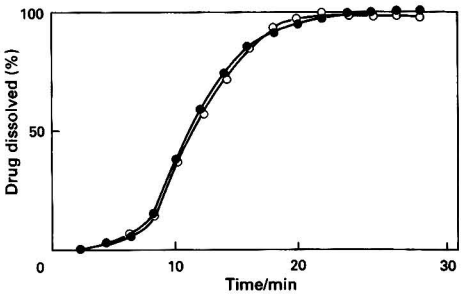

Fig. 8 Dissolution curve of a coated tablet containing promethazine hydrochloride, obtained by on-line analysis applying the triangle programmed titration technique: HCl (0.1 mol dm^{-3}, 900 ml); rotating basket; 100 ± 3 rev min^{-1}; $T = 37.0 \pm 0.1$ °C; $i_{max} = 2.0$ mA; $v_s = 1.0$ ml min^{-1}; and $2\tau = 40$ s. ○, Spectrophotometry; and ●, titration

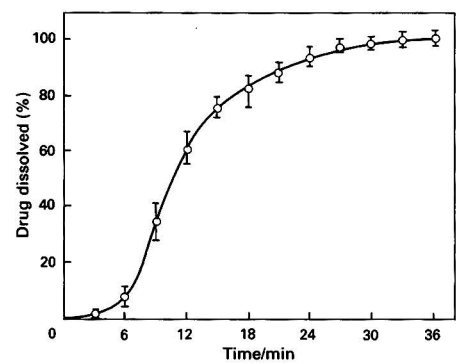

Fig. 9 Dissolution curve ($n = 3$) of the ampicillin-containing capsule. Distilled water, 900 ml; paddle method; 100 rev min^{-1}; $i_{max} = 1.0$ mA; $v_s = 0.05$ ml min^{-1}; and $2\tau = 100$ s

considering the volume of the connecting tubes for the determination of promethazine. For the determination of ampicillin the volume of both the hydrolysis section[27] and the connecting tubes was taken into consideration.

Fig. 8 shows the dissolution curves of a coated tablet containing promethazine hydrochloride; the result of three measurements performed by triangle programmed titrimetry can be seen. Fig. 8 also shows the dissolution curve obtained with the dissolution analysis system described earlier.[30,31] In the latter instance, UV spectrophotometric detection was used and the absorbance was measured at 249 nm. The correlation coefficient for the plot of the results of one method *versus* those of the other is 0.9985.

The advantage of the use of the triangle programmed titration technique is evident in those instances where direct spectrophotometric determination cannot be carried out. This is the situation with penicillin compounds. Fig. 9 shows the dissolution curve of an ampicillin-containing capsule.

In conclusion, it has been shown that flow-through techniques such as FI and triangle programmed titrimetry can be used advantageously for dissolution studies of pharmaceutical preparations. It should be noted that FI can be used with UV spectrophotometric detection in pharmaceutical analysis.

References

1 van der Linden, W. E., *Anal. Chim. Acta*, 1986, **179**, 91.
2 Frenzel, W., *Fresenius Z. Anal. Chem.*, 1988, **329**, 668.
3 Thommen, C., Garn, M., and Gisin, M., *Fresenius Z. Anal. Chem.*, 1988, **329**, 678.
4 *United States Pharmacopeia XXII*, United States Pharmacopeial Convention, Rockville, MD, 1988.
5 *British Pharmacopoeia 1988*, HM Stationery Office, London, 1988.
6 Gänshirt, H., Tessun, G., and Wolfschütz, R., *Drugs Made Ger.*, 1986, **29**, 93.
7 Wolfschütz, R., Gänshirt, H., and Tessun, G., *Pharm. Ind.*, 1987, **49**, 393.
8 McCarthy, J. P., *Pharm. Technol.*, 1988, **12**, 72, 74 and 80.
9 Wurster, D. E., Wargin, W. A., and de Berardinis, M., *J. Pharm. Sci.*, 1981, **70**, 764.
10 Doug, M. W., and Hockman, D. C., *Pharm. Technol.*, 1987, **11**, 70.
11 Nagy, G., Fehér, Zs., and Pungor, E., *Anal. Chim. Acta*, 1970, **52**, 47.
12 Růžička, J., and Hansen, E. H., *Flow Injection Analysis*, Wiley, New York, 1981.
13 Tóth, K., Fehér, Zs., Lindner, E., Nagy, G., and Pungor, E., *Magy. Kém. Lapja*, 1979, **34**, 77.
14 Kolbe, I., and Fehér, Zs., in *Modern Trends in Analytical Chemistry*, ed. Pungor, E., Akadémiai Kiadó, Budapest, 1984, p. 341.
15 Koupparis, M., Macheras, P., and Reppas, C., *Int. J. Pharm.*, 1984, **20**, 325.
16 Koupparis, M., Macheras, P., and Tsaprounis, C., *Int. J. Pharm.*, 1985, **27**, 349.
17 Koupparis, M. A., and Sarantonis, E. G., *J. Pharm. Sci.*, 1986, **75**, 800.
18 Koupparis, M. A., and Barcuchová, A., *Analyst*, 1986, **111**, 313.
19 Bigley, F. P., and Grob, R. L., *Anal. Chim. Acta*, 1986, **181**, 241.
20 Karlberg, B., and Thelander, S., *Anal. Chim. Acta*, 1978, **98**, 1.
21 Sahleström, Y., and Karlberg, B., *Anal. Chim. Acta*, 1986, **179**, 315.
22 Nagy, G., Fehér, Zs., Tóth, K., and Pungor, E., *Anal. Chim. Acta*, 1977, **91**, 87.
23 Nagy, G., Fehér, Zs., Tóth, K., Pungor, E., and Ivaska, A., *Talanta*, 1979, **26**, 1143.
24 Nagy, G., Fehér, Zs., Tóth, K., and Pungor, E., *Hung. Sci. Instrum.*, 1979, **46**, 5.
25 Nagy, G., Fehér, Zs., Tóth, K., and Pungor, E., *Anal. Chim. Acta*, 1977, **91**, 97.
26 Fehér, Zs., Kolbe, I., and Pungor, E., *Fresenius Z. Anal. Chem.*, 1988, **332**, 345.
27 Fehér, Zs., Kolbe, I., and Pungor, E., *Analyst*, 1988, **113**, 881.
28 Nagy, G., Fehér, Zs., Tóth, K., and Pungor, E., *Anal. Chim. Acta*, 1978, **100**, 181.
29 *Pharmacopoeia Hungarica*, Medicina, Budapest, 7th edn., 1986.
30 Fehér, Zs., Kolbe, I., Lindner, E., Tóth, K., Horvai, Gy., Nagy, G., Sárkány, P., and Pungor, E., *Gyógyszerészet*, 1990, **34**, 189.
31 Kolbe, I., Fehér, Zs., and Pungor, E., *Acta Pharm. Technol.*, in the press.

Paper 0/04747C
Received October 23rd, 1990
Accepted January 23rd, 1991

Extending On-line Dilution Steady-state Concentration Range by Modification of the Merging Stream and Tandem Injection Continuous-flow Methods

Yecheskel Israel* and Ramon M. Barnes†
Department of Chemistry, Lederle Graduate Research Center, University of Massachusetts, Amherst, MA 01003-0035, USA

The range of steady-state concentrations, which had been achieved previously by on-line dilution constant-flow methods including flow injection, has been extended by the introduction of new flow configurations. The extent of dilution achieved depends on their combined arrangement. The replacement of constant-flow channels by either completely or partially variable flow channels has extended the dilution range. Moreover, a flexible flow approach for on-line dilution is also achieved. With a totally variable speed flow, an on-line dilution system can be operated at a constant over-all flow-rate over all of the achievable dilutions. Hence the precision of the steady-state concentration section is improved, as the choice of a single efficient coil or coil assembly becomes possible. The most effective means of extending the dilution range is stream flow splitting of the diluted sample produced by the merging stream or tandem injection approach followed by remerging the split stream with the diluent. This combination can in practice provide any desired dilution irrespective of whether constant or partially variable speed flow is adopted. On-line dilution of more than 300 000 is demonstrated. Hydrodynamic injection was as effective in performing tandem injection on-line dilution as conventional tandem injection and yielded identical precision of the steady-state concentration. Each of these dilution techniques can be treated as a module with specific dilution features which can be combined with each other to provide specific steady-state concentration on-line dilution.

Keywords: *Tandem injection and hydrodynamic tandem injection; merging stream; on-line dilution; stream flow splitting and remerging; inductively coupled plasma atomic emission spectrometry*

Israel *et al.*[1] recently developed on-line dilution methods with steady-state concentrations by exploiting continuous-flow configurations including flow injection (FI). Israel and Barnes[2] applied these on-line dilution methods to sequential, multi-element analysis of soil sample digests with inductively coupled plasma atomic emission spectrometry (ICP-AES).

The basic requirement of these methods is to produce on-line dilutions with reproducible steady-state concentrations for both standard and sample solutions. For these conditions the precision and accuracy of the results depend solely on sample preparation and detector measurements. The expected on-line dilution at pre-set conditions can be calculated from derived relationships.[1,2] As the sample and standard solutions in any determination series undergo identical dilution, knowledge of the exact dilution has no consequence on the precision and accuracy of the results. The steady-state concentration on-line dilution approach is especially suited for operation with sequential detectors when multi-component determinations are sought, because these determinations require a finite measurement time. Therefore, these determinations can be implemented only with steady-state concentration dilutions.

In addition to increasing the speed of analyses, on-line dilution reduces the dangers of handling hazardous materials and permits in-line conditioning of the diluted sample (*i.e.*, adding acids, bases or buffers to adjust the pH; salts to maintain the ionic strength; and reagents to produce chemically active specific detectors, or to improve the accuracy of the results by either the addition of an internal reference standard or by performing standard additions). These operations can be performed simultaneously with on-line dilution, and they contribute to the reproducibility and flexibility of analytical determinations.

The dilution factors realized by the merging stream principle are limited and depend on the total stream to sample flow-rate ratios. In this approach, the sample solution is merged with the diluent in a single (Fig. 1) or double confluence (Fig. 2) junction(s). Efficient mixing coils are employed, which must have dimensions matched to the over-all flow-rate to the detector. In addition, a flow-rate interfacing device for the on-line manifold and the detector is important.[1,2]

The merging stream configurations do not require time-based control devices and are usually simple to construct. For this reason the merging stream principle is very attractive. An early example with FI was described by van Staden.[3] The prospect of extending its dilution capabilities is tempting, and two approaches are examined here to facilitate expanded on-line dilution.

The use of a variable- instead of a constant-speed peristaltic pump was suggested previously to simplify merging-stream manifold manipulations and to implement the design of a laboratory-built manifold module which can produce all possible dilutions without any alterations.[2] Often, FI systems employ a fixed-speed pump and require that the pump tubing diameter be changed to alter the stream flow-rate. Generally, a variable-speed pump is capable of attaining higher dilutions than a constant-speed pump.

For a constant-speed peristaltic pump operating with a flow manifold of constant dimensions including the mixing coil(s), the residence time of the sample–diluent mixture between each confluence junction and the detector will vary according to the over-all flow-rate. Conceivably, an efficient mixing coil for a certain over-all flow-rate range can become less effective when the flow-rate exceeds this range. The precision of the steady-state concentration section will deteriorate owing to the low residence time, which requires the use of a more efficient coil assembly. Further, excessive flow-rates generate high back-pressure. These considerations limit the applicable flow-rate and the extent of dilution. The flow-rate ratio of the diluent to sample must also be considered.

In order to minimize some of these limitations, a variable-speed peristaltic pump is employed. Hence, the over-all

* Present address: 39 Palmach Street, Haifa 34558, Israel.
† To whom correspondence should be addressed.

flow-rate can be maintained constant by operating the variable-speed pump motor at some controlled fraction of its maximum. This facilitates an increase in the dilution limit by increasing the diluent to sample flow-rate ratio. The consequence of operating at a constant over-all flow-rate is that an efficient mixing coil for one dilution is efficient for all dilutions, as the residence time is the same. Therefore, the precision of the steady-state concentration is uniform for all dilutions.

In order to extend the dilution limit significantly the most promising approach usually is to split a small volume fraction of the sample–diluent mixed stream and to remerge it typically with a large volume ratio of the diluent (*i.e.*, cascade dilution). The flow-rate ratio at remergence of the diluent with the diluted sample is high in order to effect a secondary high dilution with this stream flow splitting and remerging (SFS-RM) step. This approach was suggested previously[1] and was simultaneously employed by Whitman and Christian[4] for FI applications that produced transient concentration profiles.

The SFS-RM device is illustrated in Fig. 3, in which a T-junction and two peristaltic pump channels are needed to carry out this operation. The resulting dilution factor of this proposed technique is equal to the product of the dilution factors of the consecutive merging operations. If the SFS-RM step is repeated, any desired dilution can be achieved conceptually. When SFS-RM is also combined with a variable-speed flow or a combination of a constant- and variable-speed flow, a wide range of dilutions can be produced.

Stream splitting has been suggested for various FI applications.[4–10] Basson and van Staden[5] applied stream splitting alone for the simultaneous determination of Na, K, Ca and Mg with a flame photometer. Fernandez *et al.*[6] used stream splitting for the simultaneous determination of a specific analyte under various dispersion conditions and suggested that the approach could be adapted for differential kinetic analysis. Mindel and Karlberg,[7] Whitman and Christian,[4] and Clark *et al.*[8] applied the split zone technique in a sample pre-treatment system with much the same arrangement as suggested here. In effect, SFS-RM is analogous to FI dilution by the re-injection of the split sample zone.[9,10] However, re-injection of a split sample yields transient concentration profiles and requires the use of an additional valve synchronized with the conventional FI valve.

A novel approach was adopted earlier, employing tandem injection.[1] A discrete sample volume, V_i, was injected in tandem into a continuously flowing diluent stream. In order to obtain adequate precision of the resulting steady-state concentration section, the injection cycle volume was the sum of V_i and the cycle diluent volume, V_D.[1] However, V_D must not be unduly extended. In addition, the flow manifold must be designed for medium to high dispersion conditions. Diverse dilutions can then be achieved to produce steady-state concentrations by varying V_i and V_D. The dilution factor achieved by tandem injection is dependent on the volume ratio of the injection cycle to the sample injection. With time-based FI equipment, substituting times t_i and t_D instead of V_i and V_D, respectively, is appropriate, as the sample injection in a plug form conventionally is affected by the diluent flow.

In practice, only a combination of tandem injection with merging stream was applied to steady-state concentration on-line dilutions in order to avoid temporal concentration ripples.[1] The resulting dilution factor is, therefore, the product of the dilution factors achieved with each of the independent methods. Henceforth, in this paper, 'tandem injection' will refer to the combination of both methods.[2]

Růžička and Hansen[11,12] introduced hydrodynamic injection, which involves intermittently operated dual pumps. Unlike FI equipment, no moving parts are involved, but time-based equipment is required to synchronize the operation of the pumps. In the conventional FI time-based operation, only a single valve is necessary. One important feature of hydrodynamic injection is that it permits a considerable saving of sample volume. With tandem injection, sample economy is pronounced especially when the ratio of the tandem injection cycle period to the injection time (t_{TI}/t_i) is high.[1] For both methods the sample must fill the dead volume. However with hydrodynamic injection the sample flow stops as the diluent flow starts.

The use of hydrodynamic injection for tandem injection on-line applications offers an additional incentive in sample conservation. No sample loop must be filled repeatedly. However, the flow manifold for 'hydrodynamic tandem injection' contains more T-junctions than are needed for conventional tandem injection. Otherwise, the use of hydrodynamic tandem injection instead of conventional tandem injection for steady-state concentration on-line dilution is expected to yield identical results.

The same modifications which are examined here for extending the merging stream on-line dilution range can also be applied to tandem injection or hydrodynamic injection. The use of a variable- instead of a constant-speed peristaltic pump promises to extend the upper dilution limit achievable with a constant-speed pump. A considerable simplification of the flow manifold for both methods can result. Stream flow splitting and remerging is expected to improve the tandem injection approach as with the merging stream method, *i.e.*, to extend the dilution limit significantly. However, the application of a single SFS-RM module to hydrodynamic tandem injection would require additional T-junctions compared with the same manifold operated in the absence of SFS-RM. This complicates the flow manifold design and can make its operation difficult.

The purpose of this study was to examine the feasibility of applying hydrodynamic injection for use as a tandem injection device in order to conserve sample. The utility and advantages of replacing a constant- by a variable-speed peristaltic pump were also studied for the merging stream and tandem injection steady-state on-line dilution configurations. In addition, the feasibility of applying SFS-RM and its combination with a variable-speed peristaltic pump or with constant- and variable-speed pumps was examined for all the on-line dilution steady-state concentration methods. These experiments were performed mainly to extend the dilution range and to eliminate unnecessary sample manipulations. In this study, the application of hydrodynamic tandem injection is the only modification that does not aim at extending the dilution range.

Experimental

Flow Manifolds for Merging Stream Dilution

A four-channel, variable-speed peristaltic pump, P_1 (Rainin Rabbit), coupled with three different flow manifolds was used for each of the merging stream on-line dilution configurations (Figs. 1–3). Laboratory-built flow modules were prepared for each application, and each was connected to the peristaltic pump tubes on one side and to the nebulizer peristaltic pump, P_2, of an ICP-AES detector on the other. Y-Connectors were used for confluence junctions, and T-connectors for both the SFS and the SFS-RM devices. The first serves as a flow-rate interface between the flow manifold and the ICP-AES detector.[1,2] Both P_1 and P_2 were operated simultaneously, and the diluted sample total flow-rate was always maintained in excess of the optimum nebulizer flow-rate. Therefore, SFS is necessary to divert to waste (W) the excess of diluted sample that does not flow through P_2.

Two channels of P_1 were employed for the sample (S) and diluent (D_1) streams followed by mixing in an efficient coil (a) for the single confluence junction illustrated in Fig. 1. An additional channel of P_1 was required to achieve a second confluence junction with the diluent (D_2) followed by mixing in two additional coils (b and c) as illustrated in Fig. 2. For the

SFS-RM flow manifold illustrated in Fig. 3, four channels of P_1 were utilized. Two channels were used for a single confluence merging of the sample with the diluent. One channel was employed to withdraw a fraction of the diluted sample through P_1 at a usually low flow-rate to be remerged with a fourth channel of the diluent (D_2) through P_1 at a usually high flow-rate ratio of the diluent to the split diluted sample. Flow module tubing [Fisherbrand Accu-Rated poly(vinyl chloride)] was used, and the flow-rates in the peristaltic pump tubing were measured at 100% of the pump motor speed to allow the calculation of the expected dilutions.[1,2]

In order to calculate accurately the anticipated dilutions from the flow-rates, the flow-rate in each tube must be determined repeatedly and the mean values used. Tubing with the same nominal dimensions can produce different flow-rates. These measurements must also be carried out at the same motor speed and at about the same time as the on-line dilution operations. Also, the flow-rate continuously changes as the tubing fatigues, and the fraction of the pump motor speed does not yield precisely the same flow-rate fraction. As these considerations were not implemented in this study, the flow-rate values indicated must be considered to be approximate and serve only for rough evaluation of the expected dilutions.

Experimental dilutions were usually determined from intensity measurements at the maximum Sc II 361.384 nm emission.[1] The total flow-rate of the diluted sample at 100% motor speed was able to exceed 1 ml min^{-1}, the flow-rate used for P_2. However, if it exceeded 2.0 ml min^{-1}, the motor speed was decreased accordingly to keep the flow-rate to below 2.0 ml min^{-1}.

This arrangement is advantageous in facilitating the selection of an effective mixing coil assembly for each configuration.

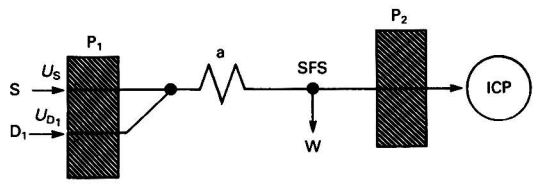

Fig. 1 Schematic diagram of a single merging stream on-line configuration: P_1, four-channel variable-speed peristaltic pump; P_2, peristaltic pump of the ICP-AES detector (ICP) with a flow-rate of approximately 1.0 ml min^{-1}; SFS, interfacing stream flow splitting T-junction; W, waste and a, coil (length in cm/i.d. in mm) 40/1.42. Flow-rates, U, in ml min^{-1}; U_S and U_D are the sample and diluent, respectively (*cf.* Table 1)

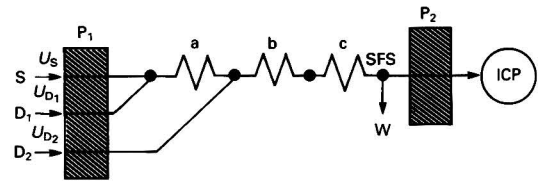

Fig. 2 Schematic diagram of a double merging stream on-line dilution configuration: flow-rates, U, in ml min^{-1}; U_{D_1} and U_{D_2}, first and second diluent merging streams, respectively (*cf.* Table 1). Coils: b, 41/0.75; and c, 41/1.42. Other notations as in Fig. 1

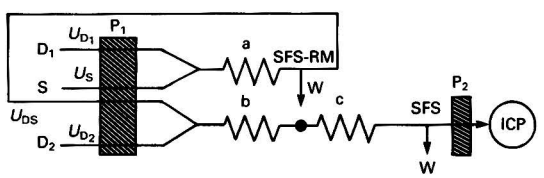

Fig. 3 Schematic diagram of a single merging stream, stream flow splitting of the diluted sample and remerging and remerging on-line dilution configuration (SFS-RM). U_{DS}, flow-rate on splitting of the diluted sample (*cf.* Table 2). Other notations as in Fig. 2

Flow Manifolds for Tandem Injection Dilution

Three types of tandem injection flow manifold were adopted for the following applications: conventional with a combination of a constant- and a variable-speed peristaltic pump; hydrodynamic with a constant-speed peristaltic pump; and conventional with SFS-RM modification with either a constant- or a combination of constant- and variable-speed peristaltic pumps.

A commercial FI instrument (Tecator FIAstar 5020 analyser) with a four-channel, constant-speed peristaltic pump was used for all these tandem injection configurations.[2,13] However, a four-channel, variable-speed peristaltic pump (Rainin Rabbit) was coupled with the operation of the FI instrument, when variable-speed flow channels were partially used for conventional injection with or without an SFS-RM device.

Replicate determinations at the steady-state section of on-line dilutions were performed following the same procedures as applied previously.[1] However, both scandium and lanthanum were used for intensity measurements at Sc II 361.384 nm and La II 379.478 nm lines.

Conventional Tandem Injection Configuration With a Variable-speed Peristaltic Pump

The flow configuration, illustrated in Fig. 4, is essentially identical with the previously described flow arrangement[1] except that a single instead of a double confluence, a variable-speed pump for the diluent channel (D_1) and minor coil assembly modifications were made.

Hydrodynamic Tandem Injection With Dual Constant-speed Peristaltic Pumps

The conventional tandem injection configuration can be reproduced by the application of an intermittent pumping configuration illustrated schematically in Fig. 5. A time-based control device (T) was programmed to operate the dual constant-speed pumps (P_1 anmd P_2) in an intermittent stopped-flow mode. The pump, P_1 was operated for a period of time t_1, while P_2 was stopped for the same period of time, and *vice versa*, for a period of time, t_2. This cycle was repeated at will by programming the timer, T. During the time period

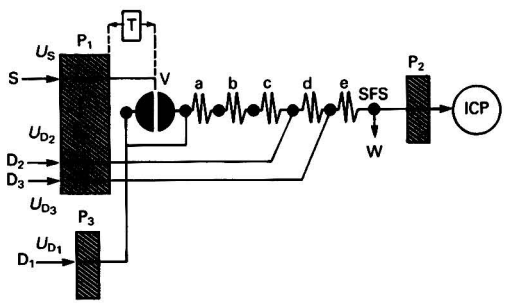

Fig. 4 Schematic diagram of tandem injection on-line dilution with double merging stream and a variable-speed flow through the diluent (D_1). P_1 and P_2, pumps (*cf.* Fig. 1); P_3, variable-speed peristaltic pump; T, timer; and V, injection valve. Flow-rates in ml min^{-1}: U_S, 1.21; and U_{D_1}, 0.32 (at 100% motor speed). Three flow configurations were used: a, U_{D_2} and U_{D_3}, 0.65; b, U_{D_2}, 1.21; and U_{D_3}, 2.42; c, U_{D_2} and U_{D_3}, 2.42. Coils: a, 40/1.42; b, 50/0.7; c, 40/1.0; d, 50/0.7; and e, 40/1.42

t_1, the sample (S) and the diluent streams [D_2 in Fig. 5(*a*) or D_2 and D_4 in Fig. 5(*b*)] flow continuously through the respective channels, while the diluent streams [D_1 and D_3 in Fig. 5(*a*) or D_1, D_3 and D_5 in Fig. 5(*b*)] are idle. However, during time period t_2 the sample (S) and the diluents (D_2, or D_2 and D_4) are idle, while the diluent streams (D_1 and D_3, or D_1, D_3 and D_5) flow continuously through the respective channels. This intermittent flow is repeated a pre-set number of times. As soon as the sample crosses junction A′, one sample zone after another will be sandwiched between the diluent zones, thus triggering dispersion between adjacents layers. This pattern is identical with that which occurs in the tandem injection approach.[1] A flow-rate interfacing SFS junction was inserted for every configuration. Tandem hydrodynamic injection with a variable-speed peristaltic pump was not attempted owing to the absence of suitable equipment.

The sample channel S is designed to be as short as possible in order to confine the dead volume before reaching the confluence junction A′. As described above, the sample flow stops during time period t_2 in contrast to conventional tandem injection operation wherein the sample continues to flow to the valve loop to waste or directly to waste during both the run and injection periods. Hence, a considerable saving in sample volume results when intermittent pumping is employed for steady-state concentration on-line dilution. When the ratio $t_2:t_1$ is high, the sample volume is a minimum. A preliminary study to apply SFS-RM to hydrodynamic injection using constant-speed peristaltic pumps was carried out; however, the high back-pressure created hindered regular manifold operation.

Tandem Injection Dilution With SFS-RM Device With Constant- and Variable-speed Peristaltic Pump Operation

Tandem injection was examined using a single confluence with the diluent prior to SFS-RM. Five channels were devoted to the sample and diluent streams as illustrated in Fig. 6. The variable-speed peristaltic pump P_3 was utilized to drive the diluent channel D_1 and the diluted sample stream split, while the constant-speed peristaltic pump of the FI instrument was used for driving the sample S and the diluent channels D_2 and D_3.

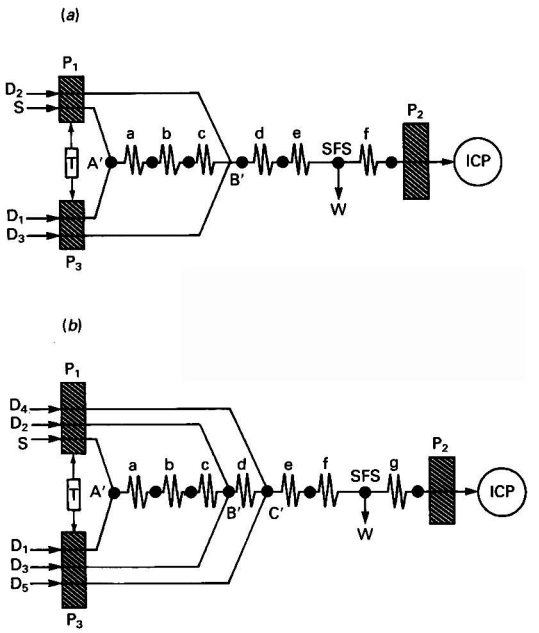

Fig. 5 Schematic diagram of hydrodynamic tandem injection on-line dilution using intermittent pumping, with (*a*) single- and (*b*) double-confluence stream junction(s) A′, B′ and C′. P_1 and P_2, dual four-channel constant-speed peristaltic pumps operating in the intermittent pumping mode. Coil f, 40/1.0. Flow-rates (in ml min^{-1}): U_S, 1.21; U_{D1}, 0.21, 0.34 or 0.45; U_{D2}, 1.21 or 2.41; U_{D3}, 1.21, 2.41 or 3.71; U_{D4} and U_{D5}, 2.41 or 3.71. Other notations as in Fig. 4

ICP-AES Detector

A sequential ICP-AES system (Perkin-Elmer Plasma II) with the same operating conditions described previously was employed.[2]

Solutions

A stock standard solution of Sc (1000 mg l^{-1}) was prepared in 5% v/v nitric acid,as described previously.[1,2] A stock solution of 8000 mg l^{-1} of La in 5% v/v nitric acid was also prepared by the dissolution of 6.235 g of $La(NO_3)_3.6H_2O$ in 250 ml of 5% v/v nitric acid. Various dilutions of both stock solutions were made as necessary.

Results and Discussion

The procedures applied previously to establish the dilution factor and the precision of the steady-state section using replicate determinations[1] were employed in this study. The results obtained for each of the arrangements are discussed in the following sections.

Dilution by Single and Double Confluence Junction(s) With a Variable-speed Peristaltic Pump

The flow systems illustrated in Figs. 1 and 2 were employed for examination of the single- and double-merging stream configurations, respectively. The results obtained are listed in Table 1. The various flow-rates employed resulted in dilutions in the range 1.33–42. The relative standard deviations (RSDs) obtained (0.6–1.3%) are satisfactory, and no significant difference exists compared to the precision of replicate determinations of directly nebulized, pre-diluted standard solutions.

The upper dilution limit obtained by using the double-confluence junction configuration (Fig. 2) was only slightly higher than the corresponding dilution obtained with the single-confluence junction. Therefore, a single merging stream was adopted for other modifications whenever some or all of the channels were operated with a variable-speed pump.

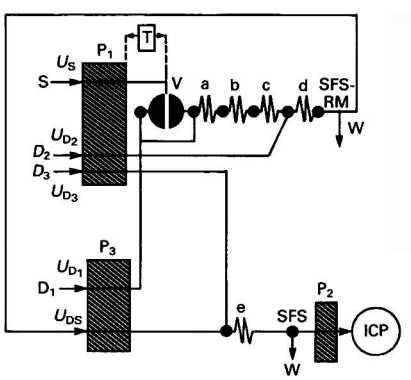

Fig. 6 Schematic diagram of tandem injection on-line dilution with a single confluence junction, followed by SFS-RM, and a combination of constant- and variable-speed flow channels. All notations as in Fig. 4

The ability to attain these dilutions for a single merging stream is due to the application of a variable-speed pump. Under these conditions, the flow manifold module was considerably simplified. The maximum dilution reported in previous work employing two confluence junctions of the sample with the diluent and a constant-speed peristaltic pump was approximately 15.[1]

One configuration that was not studied combines two peristaltic pumps, at least one of which has a variable speed, and is believed to be more flexible and might deliver slightly higher dilutions. This might be achieved by utilizing a variable-speed pump for driving the sample channel while the diluent channels are driven by either a constant- or a variable-speed pump.

Single-confluence Junction Dilution, Splitting the Diluted Sample and Remerging, With a Variable-speed Peristaltic Pump

With the flow configuration illustrated in Fig. 3, the results obtained for the single-confluence junction dilution, splitting the diluted sample and remerging, with a variable-speed peristaltic pump are listed in Table 2. Only a few flow-rate combinations of the flow channels were examined to demonstrate high dilutions. Both intermediate and low dilutions are possible with this configuration.

The range of dilutions investigated was approximately 400–2500 with signal precision of 0.73–1.1%. These RSD values are essentially the same as the precision obtained by direct aspiration of the pre-diluted samples. The signal reproducibility achieved with a variable-speed peristaltic pump was uniform for all dilutions. Repeated experiments shown in Table 2 yield satisfactory results and indicate the reliability of using this steady-state concentration on-line dilution method for performing a series of determinations at the same flow configuration. The application of SFS-RM has proved to be a powerful tool for extending the dilution range by almost 50-fold.

Table 1 Single and double merging stream on-line dilution using a variable-speed peristaltic pump (*cf.* Figs. 1 and 2). Single and double merging stream configurations using a variable-speed peristaltic pump to keep the overall flow-rate at less than 2 ml min^{-1} by varying the motor speed. The mean flow-rates are U_S (sample) and U_{D_1} and U_{D_2} (the first and second diluent merging steams, respectively). The flow-rates used for each experiment are quoted at 100% motor speed. Twenty replicate intensity measurements of Sc II 361.384 nm were made[1] either at the steady-state concentration section for each on-line dilution experiment or for the direct aspiration of a pre-diluted sample

Mean flow-rates*			Motor speed†	Dilution‡	RSD§
U_S	U_{D_1}	U_{D_2}	(%)	(found)	(%)
1.41	1.25	—	50	1.87	0.83
1.25	1.41	—	50	2.12	0.99
0.457	1.41	—	75	4.27	0.62
1.41	0.457	—	75	1.33	0.90
0.457	2.28	—	50	5.45	0.93
0.457	4.14	—	30	9.44	0.92
0.457	7.75	—	18	16.8	1.3
0.20	2.28	—	60	12.0	0.85
0.20	7.75	—	20	39.8	1.3
0.20	2.28	4.14¶	25	34.2	1.0
0.20	4.14	4.14¶	20	42	1.1

* Flow-rates are given in ml min^{-1} at 100% motor speed. The actual flow-rate is the product of the quoted flow-rate and the motor speed divided by 100.

† Time delay to reach steady-state concentration is 3–4 min.

‡ Mean value of 20 replicate measurements.

§ Relative standard deviation of 20 replicate measurements.

¶ Double confluence junction configuration.

Conventional Tandem Injection With Double-confluence Junctions

Conventional tandem injection with double-confluence junctions operated by a combination of constant- and variable-speed peristaltic pumps is illustrated in Fig. 4. Operation of tandem injection is similar to a previous study.[1] However, the diluent D_1 flows in a variable-speed channel, which enables the dilution to be increased by simply lowering the flow-rate. The results are listed in Table 3 and demonstrate satisfactory precision for a dilution range of 65–2400.

The increase in the upper dilution limit was facilitated by the use of a variable-speed channel for D_1. The main effect of the application of fractional motor speed to this channel in particular is to enhance the dilution limit. However, the time delay in achieving the steady-state concentration section is dependent on the flow-rate of channel D_1 in particular. The time delay to obtain the steady-state concentration at 20% motor speed is about 20 min. In order to limit this time delay, one of the three coils (*i.e.*, coil c) used for the tandem injection section can be removed without influencing the efficiency of mixing, because the flow-rate of channel D_1 in this example is very low.

Hydrodynamic Tandem Injection

Hydrodynamic injection on-line dilution operating dual constant-speed peristaltic pumps with intermittent pumping and using a single- [Fig. 5(*a*)] and double- [Fig. 5(*b*)] confluence junction(s) was demonstrated with tandem injection on-line dilution for a range of dilutions up to about 900 (Table 4) with similar results to those obtained previously for tandem injection.[1] The only advantage of hydrodynamic tandem injection over conventional tandem injection is conservation of the sample volume.

Tandem Injection

Results for tandem injection on-line dilution with a single merging stream, followed by SFS-RM using constant-speed flow channels are given in Table 5. Data for variable-speed flow for a number of channels are summarized in Table 6. Operation of this flow configuration is identical with the operation of tandem injection shown in Fig. 4. However, in practice the dilution capabilities of these arrangements handle

Table 2 Single merging stream coupled with SFS-RM using a variable-speed peristaltic pump (*cf.* Fig. 3). A single-confluence junction of the sample and the diluent followed by SFS of the diluted sample (DS) and remerging using a variable-speed peristaltic pump. U_{DS}, Flow-rate of the diluted sample from the first confluence

Mean flow-rate*				Motor speed†	Dilution‡	RSD§
U_S	U_{D_1}	U_{DS}	U_{D_2}	(%)	(found)	(%)
0.20	7.75	0.46	4.14	40	432	0.79
0.20	7.75	0.46	4.14	35	425	0.93
0.20	7.75	0.46	4.14	45	435	0.73
0.20	7.75	0.46	7.75	45	884	0.91
0.20	7.75	0.46	7.75	35	848	1.06
0.20	7.75	0.20	4.14	45	873	0.91
0.20	7.75	0.20	7.75	25	2525	1.02
0.20	7.75	0.20	7.75	25	2527	0.80

* Flow-rates are given in ml min^{-1} at 100% motor speed. The actual flow-rate is the product of the quoted flow-rate and the motor speed divided by 100.

† Time delay to reach steady-state concentration is 3–4 min.

‡ Mean value of 20 replicate measurements.

§ Relative standard deviation of 20 replicate measurements.

any required dilution, even when a constant-speed peristaltic pump is used (Table 5). Dilutions as high as 23000 were realized with the constant-speed peristaltic pump. Very high dilutions of about 300000 were attained with variable-speed flow channels used for the diluent D_1 and the diluted split sample. The influence of using a variable-speed pump for these two channels is significant for extending the maximum attainable dilution. However, achievement of the steady-state concentration is compromised by the resulting time delay in the absence of SFS-RM. This delay is reduced considerably if only the diluted and split sample channel flow is variable. For this arrangement the maximum attainable dilution is about 70000.

Table 3 Conventional tandem injection on-line dilution with a double-confluence junction and partially variable speed channels (*cf.* Fig. 4). Dilution of the sample by tandem injection with a double merging with the diluent; the constant-speed peristaltic pump P_1 drives the sample S and the diluent D_2 streams. Only the diluent D_1 stream is driven by the variable-speed peristaltic pump, and the per cent. motor speed refers only to the last channel

Flow configuration*	Injection time/s	Injection period/s	Motor speed† (%)	Dilution‡ (found)	RSD§ (%)
a	2	25	100	65	1.3
a	2	25	50	128	1.0
a	2	25	30	218	0.9
a	1	25	100	125	1.5
a	1	25	50	255	1.2
a	1	25	30	435	1.1
a	1	30	100	145	1.8
a	1	30	50	297	1.3
a	1	30	30	530	1.3
b	2	25	100	140	1.1
b	2	25	50	290	1.0
b	2	25	30	480	1.1
b	1	25	100	268	1.8
b	1	25	50	595	1.2
b	1	25	30	920	0.9
c	2	25	100	206	2.2
c	1	25	100	414	1.9
c	1	25	50	805	1.3
c	1	25	25	1620	0.7
c	1	30	20	2410	1.1

* Flow-rates of the various channels: a, U_{D_2} and U_{D_3}, 0.65; b, U_{D_2}, 1.21; and U_{D_3}, 2.42; c, U_{D_2} and U_{D_3}, 2.42 ml min^{-1}. Pump tubing diameters given in Fig. 4.

† Time delay to reach steady-state concentration is approximately 6 min at 100%, 12 min at 50% and 20 min at 25% motor speed.

‡ Mean value of 20 replicate measurements.

§ Relative standard deviation of 20 replicate measurements.

Table 4 Hydrodynamic tandem injection on-line dilution of the sample with a single- and double-confluence junction with the diluent with constant-speed operation. Time delay to reach steady-state concentration is approximately 5–6 min

Injection time/s	Injection period/s	Dilution* (found)	RSD† (%)
25	35	6.8	2.0
10	15	8.8	1.0
10	20	12.6	0.9
5	20	24.2	1.2
2	20	59.1	1.2
1	20	114	1.8
1	25	224	2.1
1	30	272	1.9
1	20	610	2.3
1	30	910	3.0

* Mean value of 20 replicate measurements.

† Relative standard deviation of 20 replicate measurements.

Conclusions

Modifications of the merging stream and tandem injection steady-state concentration on-line dilution method were examined. Hydrodynamic injection using intermittent pumping with dual pumps can achieve tandem injection in an identical manner to conventional FI, and enable dilutions of up to about 1000 to be obtained with a double merging stream configuration. This method was examined with only constant-speed peristaltic pumps, but it should be possible to combine it with variable-speed flow channels.

The upper dilution range was extended for both the merging stream and the tandem injection configurations to cover all on-line dilutions that might be required practically. Variable-speed channels were either incorporated totally or only in part and permitted an increase in dilutions by a factor of about 2.5 over a constant-speed flow. However, when the variable-speed pump is used for all channels, all dilutions at the same over-all flow-rate can be achieved. The consequence of this approach is that the choice of an efficient mixing coil assembly can result in uniform precision, and a single flow module can produce any dilution over the whole range of dilutions. With partially variable flow channels, the over-all flow-rate becomes variable from one range of dilutions to another. Although a higher gain in the dilution factor is possible over a constant-speed flow, the repercussion is a considerable delay

Table 5 Conventional tandem injection with a single-confluence junction followed by SFS-RM and constant-speed peristaltic pump operation. Time delay to reach steady-state concentration is 5–6 min.

Flow configuration*	Injection time/s	Injection period/s	Dilution† (found)	RSD‡ (%)
a	10	30	1120	1.6
a	5	30	2890	1.7
a	2	27	6240	1.4
a	2	27	6120	1.2
a	1	26	8990	1.8
a	1	26	8830	1.4
b	15	40	1680	1.5
b	15	40	1640	1.3
b	10	35	2380	1.5
b	10	35	2390	1.6
c	2	27	12480	1.5
c	2	27	12330	1.4
d	1	26	23200	1.1
d	1	27	23070	1.4

* Flow-rates: a, U_{D_2} and U_{D_3}, 0.65; b, U_{D_2}, 1.21; and U_{D_3}, 2.42; c, U_{D_2} and U_{D_3}, 2.42; d, U_{D_2}, 2.42 and U_{D_3}, 3.71 ml min^{-1}. Pump tubing diameters given in Fig. 4.

† Mean value of 20 replicate measurements.

‡ Relative standard deviation of 20 replicate measurements.

Table 6 Conventional tandem injection with a single-confluence junction followed by SFS-RM using a partially variable speed operation of a number of flow channels (*cf.* Fig. 6) for an injection time of 1 s and an injection period of 26 s

Motor speed* (%)	Dilution† (found)	RSD‡ (%)
75	16100	2.3
75	16770	2.9
50	35230	2.2
50	38060	4.8
30	148700	1.4
28	168900	1.3
20	331900	1.0
20	305700	1.4

* Time delay to reach steady-state concentration is approximately 7–8 min at 75%, 12–14 min at 50% and 25–30 min at 20% motor speed.

† Mean value of 20 replicate measurements.

‡ Relative standard deviation of 20 replicate measurements.

in the attainment of the steady-state concentration section, which may be partially overcome by several operating procedures.

The simplest and most powerful means of increasing on-line dilution is cascade dilution by stream flow splitting of the diluted sample solution, either by the merging stream approach or by tandem injection, followed by remerging with the diluent. A single SFS-RM operation can contribute as much as a dilution factor of 50 to the over-all dilution. Stream flow splitting and remerging is usually carried out smoothly, except for its combination with hydrodynamic tandem injection, where high back-pressure developed as a result of the large number of T-junctions required to carry out this combination.

In conclusion distinct units of flow systems that can contribute to steady-state concentration on-line dilution have been developed and were combined in a modular fashion to produce various dilutions. These combinations have the capability to cover, in practice, any required on-line dilution range.

This research was supported by the *ICP Information Newsletter*.

References

1 Israel, Y., Lásztity, A., and Barnes, R. M., *Analyst*, 1989, **114**, 1259.
2 Israel, Y., and Barnes, R. M., *Analyst*, 1990, **115**, 1411.
3 van Staden, J. F., *Fresenius Z. Anal. Chem.*, 1985, **322**, 36.
4 Whitman, D. A., and Christian, G. D., *Talanta*, 1989, **36**, 205.
5 Basson, W. D., and van Staden, J. F., *Fresenius Z. Anal. Chem.*, 1980, **302**, 370.
6 Fernandez, A., Gomez-Nieto, M. A., Luque De Castro, M. D., and Valcarcel, M., *Anal. Chim. Acta*, 1984, **165**, 217.
7 Mindel, B. D., and Karlberg, B., *Lab, Pract.*, 1981, **30**, 719.
8 Clark, G. D., Růžička, J., and Christian, G. D., *Anal. Chem.*, 1989, **61**, 1773.
9 Mindegaard, J., *Anal. Chim. Acta*, 1979, **104**, 185.
10 Garn, M. B., Gisin, M., Gross, H., King, P., Schmidt, W., and Thommen, C., *Anal. Chim. Acta*, 1988, **207**, 225.
11 Růžička, J., and Hansen, E. H., *Anal. Chim. Acta*, 1980, **114**, 19.
12 Růžička, J., and Hansen, E. H., *Anal. Chim. Acta*, 1983, **145**, 1.
13 Israel, Y., *Anal. Chim. Acta*, 1988, **206**, 313.

Paper 0/04515B
Received October 8th, 1990
Accepted January 3rd, 1991

Studies on the Application of Photochemical Reactions in a Flow Injection System

Part 1. Determination of Trace Amounts of Nitrite, Based on Its Inhibitory Effect on the Photochemical Reaction Between Iodine and Ethylenediaminetetraacetic Acid

Ren-Min Liu and Dao-Jie Liu
Department of Chemistry, Liaocheng Teachers College, Liaocheng, Shandong, People's Republic of China

An automated procedure for the photochemical determination of nitrite has been developed, involving use of a laboratory-built flow-through photochemical reactor and a laboratory-built flow-through amperometric detector in a flow injection system, based on the inhibitory effect of nitrite on the photochemical reaction between iodine and ethylenediaminetetraacetic acid. Optimum analytical conditions were established. Nitrite can be determined in the range from 1×10^{-7} to 4×10^{-6} mol dm^{-3}, with a sampling frequency of 60–80 h^{-1} and a relative standard deviation of less than 1%. The method has been applied to the determination of nitrite in natural water samples, and recoveries of at least 91% have been attained.

Keywords: *Photochemical analysis; flow injection; nitrite determination*

Studies on the application of photochemical reactions in analytical chemistry have become more common during the 1980s,[1–7] together with the development of the theory of photochemical reactions. The analytical methods based on photochemical reactions are of high sensitivity and selectivity. More than 30 elements can be determined by using photochemical reactions at different stages. Photochemical analysis has opened up a new field of analytical chemistry. However, the photochemical reactions have mainly been used at a certain stage of the analytical process. Few have been combined with modern analytical techniques.[8]

Faure and co-workers[9,10] have studied the photochemical reaction between I_2 and ethylenediaminetetraacetic acid (EDTA). This reaction is a chain reaction, and the mechanism is as follows:

$$I_2 \xrightarrow{h\nu} 2I$$

$$I + >NCH_2COO^- \rightarrow >NCH_2 + I^- + CO_2$$

$$>NCH_2 + I_2 \rightarrow >NCH_2I + I$$

Nitrite has a strong inhibitory effect on the reaction. The mechanism is:

$$I + NO_2^- \rightarrow I^- + NO_2$$

The chain reaction between I_2 and EDTA is terminated by nitrite. Hence, the concentration of nitrite is related to the concentration of the residual I_2, and nitrite can be determined by the determination of the residual I_2. Sánchez-Pedreño *et al.*[1] have determined trace amounts of nitrite by using this photochemical reaction. However, the determination was time consuming (usually more than 10 min).

In the present paper, the photochemical reaction between I_2 and EDTA is applied to a flow injection (FI) system involving use of a laboratory-built flow-through photochemical reactor and a flow-through amperometric detector. Iodine, EDTA and pH buffer and sample solutions are pumped into the photochemical reactor and react therein. The reaction solution is then introduced into an amperometric detector by means of an injection valve, and nitrite is determined by measurement of the concentration of residual I_2. The proposed method is of high sensitivity, selectivity and speed of analysis (40–60 s), and provides a novel means for realizing the automation of photochemical analysis.

Experimental

Apparatus

The peristaltic pump and sampling system were supplied by the Jiangsu Electroanalytical Instrument Plant. A flow-through photochemical reactor (made in this laboratory; shown in Fig. 1) and a flow-through amperometric detector (shown in Fig. 2) were used in the FI system. The working electrode was polarized with a 79–1 voltammeter (The Fourth Radio Plant of Jinan), and the current signal was recorded with an XWT-S platform recorder (The Third Automatic Instrument Plant of Shanghai).

Reagents

Ethanolic iodine stock solution (0.01 mol dm^{-3}).

NaH_2EDTA stock solution (0.01 mol dm^{-3}).

pH buffer solutions. Prepared by mixing 0.1 mol dm^{-3} sodium acetate and 0.1 mol dm^{-3} acetic acid, adjusting with 0.1 mol dm^{-3} NaOH, and correcting with a pH meter.

Nitrite stock standard solution (0.01 mol dm^{-3}). Prepared with sodium nitrite and standardized with potassium permanganate.

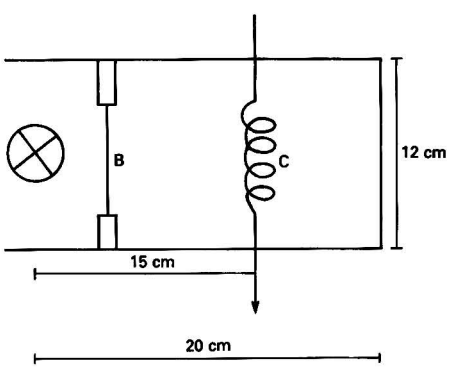

Fig. 1 Schematic diagram of the flow-through photochemical reactor. A, Light source; B, quartz window for heat insulation; and C, reaction tube (silicone rubber, 45 cm × 0.8 mm i.d.)

All the solutions were prepared with analytical-reagent grade chemicals.

Procedure

The FI system is connected up with polyethylene tubing (0.8 mm i.d.) according to the arrangement shown in Fig. 3. The peristaltic pump is started and the flow-rates of reagents and sample solutions are adjusted according to the parameters given in Fig. 3. Iodine, EDTA, and pH buffer and sample solutions are pumped into the photochemical reactor and react therein. The reactants are then injected into another channel of buffer solution, and the residual I_2 is determined in the flow-through amperometric detector (the working electrode is polarized at 100 mV *versus* an SCE with a 79–1 voltammetric analyser). The current signal is recorded. The nitrite is determined from the difference in peak heights between the sample and blank, with a sampling frequency of 60–80 h^{-1}.

Results and Discussion

Power of the Light for the Photochemical Reactor

An incandescent lamp was used as the source of light. The extent of the reaction depends not only on the power of the light bulb, but also on the distance of the lamp from the reaction coil. The effect of the lamp on the photochemical reaction was studied by keeping the distance constant as shown in Fig. 1. The results show that, in the laboratory-built photochemical reactor, the reaction cannot take place when a 25 W lamp is used; a weak reaction can be seen when a 40 W lamp is used; a notable reaction can be seen when a 60 W lamp is used; and when a 100 W lamp is used, the reaction takes place violently and is difficult to control by adjusting the length of the reaction tube. Therefore, a 60 W incandescent lamp was chosen as the source of light for the photochemical reactor.

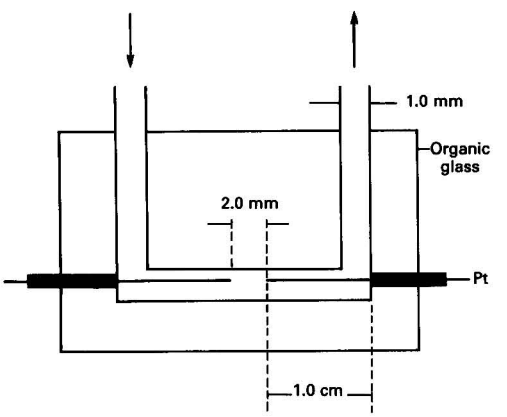

Fig. 2 Schematic diagram of the flow-through amperometric detector (platinum wire, 1.0 cm × 0.5 mm)

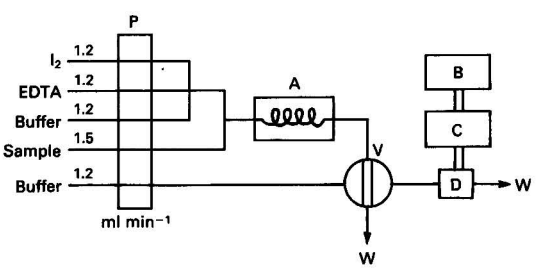

Fig. 3 Schematic diagram of the FI apparatus. P, Peristaltic pump; V, injection valve (loop volume, 100 µl); A, photochemical reactor; B, recorder; C, 79–1 voltammeter; D, detector; and W, waste. I_2, 5.0 × 10^{-4} mol dm^{-3}; EDTA, 1.5 × 10^{-3} mol dm^{-3}; and buffer, pH 7.0

Length of Reaction Tube

The length of the reaction tube has a significant effect on the photochemical reaction between I_2 and EDTA. The extent of the reaction can be controlled by adjusting the length of the reaction tube when the power of the lamp and the distance of it from the reaction coil are kept constant. Under the experimental conditions employed, a 45 cm reaction tube is suitable for the determination when 5.0 × 10^{-4} mol dm^{-3} I_2 and 1.5 × 10^{-3} mol dm^{-3} EDTA are used.

Effect of pH

The peak heights for the blank solution and 1.0 × 10^{-6} mol dm^{-3} nitrite at various pH values were measured when 5.0 × 10^{-4} mol dm^{-3} I_2 and 1.5 × 10^{-3} mol dm^{-3} EDTA were used (Fig. 4). Fig. 4 shows that the peak height is not affected by pH values >6.5. A buffer solution with a pH of 7.0 was used for the determination.

Concentration of I_2 and EDTA

The stability and sensitivity were studied with various concentrations of I_2 and EDTA. The results show that when the ratio of the concentration of I_2 to EDTA is 1:1 to 1:4, good sensitivity and stability are attained. Optimum results are obtained when 5.0 × 10^{-4} mol dm^{-3} I_2 and 1.5 × 10^{-3} mol dm^{-3} EDTA are used.

Interference of Foreign Ions

The interference of a number of foreign ions was studied by the addition of such ions to 1.0 × 10^{-6} mol dm^{-3} nitrite. The results listed in Table 1 show the high selectivity of the method (with a relative error of less than 5%).

Calibration Graph

According to the proposed procedure, the calibration graph was established with standard solutions of nitrite (Fig. 5). The linear range for nitrite is from 1.0 × 10^{-7} to 4.0 × 10^{-6} mol dm^{-3}.

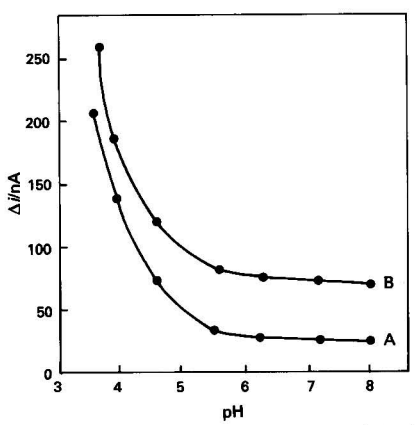

Fig. 4 Influence of pH. A, Without nitrite; and B, with 1.0 × 10^{-6} mol dm^{-3} nitrite

Table 1 Effect of foreign ions on the determination of 1.0×10^{-6} mol dm^{-3} nitrite

Foreign ion	Tolerated molar ratio (ion : NO_2^-)
Cl^-, SO_4^{2-}, NO_3^-, F^-, Br^-, CO_3^{2-}, $H_2PO_4^-$, NH_4^+, K^+, Na^+	No influence
Ca^{2+}, Mg^{2+}, Ba^{2+}, Al^{3+}, Ni^{2+}, Zn^{2+}, Cd^{2+}, Pb^{2+}, Cu^{2+}	1500
Fe^{3+}, Mn^{2+}, Hg^{2+}	150
S^{2-}	10
$Cr_2O_7^{2-}$	6
SO_3^{2-}, $S_2O_3^{2-}$	2

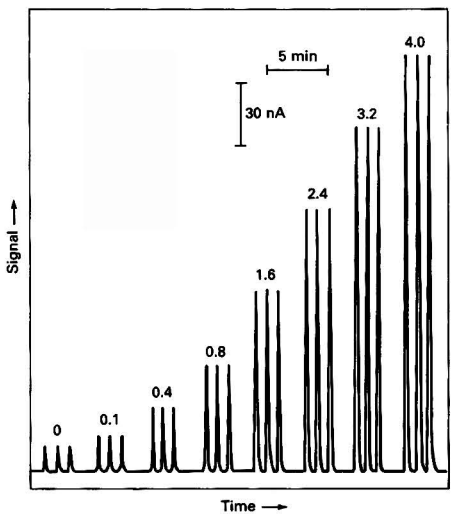

Fig. 5 Recorder signals for standard solutions of NO_2^- under optimized conditions. Values above peaks are concentrations of NO_2^- in μmol dm^{-3}

Applications

Table 2 shows the results obtained with the proposed method for natural water samples to which 1.0×10^{-5} mol dm^{-3} nitrite was added. The precision for the determination of nitrite was measured by analysing each of the samples listed in Table 2 six times. The relative standard deviations for samples of tap, rain, well and lake water were 0.91, 0.84, 0.93 and 0.87%, respectively.

Natural water samples were treated as described previously[11] and the nitrite was determined by the proposed method and by a spectrophotometric method using α-naphthylamine.[11] The results are listed in Table 3.

Table 2 Recovery of nitrite from natural water samples

Sample	Nitrite found/ mol dm^{-3}	Total nitrite present after addition/ mol dm^{-3}	Recovery (%)
Tap water	8.62×10^{-6}	19.22×10^{-6}	106
Rain water	7.87×10^{-5}	8.83×10^{-5}	96
Well water	5.04×10^{-6}	15.43×10^{-6}	104
Lake water	1.39×10^{-5}	2.30×10^{-5}	91

Table 3 Concentration of nitrite in natural water samples

Sample	Data obtained by the proposed method/ mol dm^{-3}	Data obtained by α-naphthylamine spectrophotometry/ mol dm^{-3}	Relative error (%)
Tap water	8.62×10^{-6}	9.07×10^{-6}	−5.0
Rain water	7.87×10^{-5}	7.71×10^{-5}	+2.1
Well water	5.04×10^{-6}	5.21×10^{-6}	−3.1
Lake water	1.39×10^{-5}	1.34×10^{-5}	+3.7

The photochemical reaction capabilities of an FI system ensure high sensitivity, selectivity and speed of analysis. Photochemical analysis can be performed easily and rapidly when in combination with the FI technique. The proposed method provides a novel means for studies on photochemical analysis.

References

1 Sánchez-Pedreño, C., Sierra, M. T., Sierra, M. I., and Sanz, A., *Analyst*, 1987, **112**, 837.
2 Zhang, Y., and Wu, L., *Analyst*, 1986, **111**, 767.
3 Sánchez-Pedreño, C., Sierra, M. T., Sierra, M. I., and Sanz, A., *Analyst*, 1988, **113**, 145.
4 Aaron, J. J., Fidanza, J., and Gaye, M. D., *Talanta*, 1983, **30**, 649.
5 Liu, S., Men, R., and Pu, T., *Chem. J. Chin. Univ.*, 1987, **8**, 226 (Chinese edition).
6 Men, R., *Fenxi Huaxue*, 1986, **14**, 126.
7 Men, R., Liu, S., and Yu, Y., *Fenxi Huaxue*, 1987, **15**, 77.
8 Men, R., *Metall. Anal.*, 1989, **9**, 40 (in Chinese).
9 Faure, J., and Joussot-Dubien, J., *Bull. Soc. Chim. Fr.*, 1967, 3064.
10 Faure, J., and Fornier de Violet, P., *J. Chim. Phys. Chim. Biol.*, 1972, **69**, 996.
11 The Compiling Group of Analytical Methods for Environmental Monitoring, *Analytical Methods for Environmental Monitoring*, Bureau of Environment Protection Under Ministry of Urban and Rural Construction and Environment Protection, Beijing, 1983, p. 125 (in Chinese).

Paper 0/03768K
Received August 16th, 1990
Accepted November 23rd, 1990

Determination of Ultra-trace Amounts of Uranium and Thorium in High-purity Aluminium by Inductively Coupled Plasma Mass Spectrometry

Kikuo Takeda, Tokio Yamaguchi, Hideaki Akiyama and Toshihiko Masuda
Ehime Research Laboratory, Sumitomo Chemical Co. Ltd., 5-1 Soubiraki-cho, Niihama, Ehime 792, Japan

A sensitive method is decribed for the simultaneous determination of ultra-trace amounts of uranium and thorium in high-purity aluminium by inductively coupled plasma mass spectrometry (ICP-MS). Uranium and thorium were separated from a sample solution of 10 mol dm^{-3} hydrochloric acid by extraction with a 10% v/v solution of tributyl phosphate in cyclohexane. The internal standard method was used for quantification by ICP-MS. For a sample mass of 10 g, the detection limits for uranium and thorium are 7 and 8 pg g^{-1}, respectively.

Keywords: *Uranium and thorium determination; inductively coupled plasma mass spectrometry; high-purity aluminium; extraction with tributyl phosphate*

Because of the problem of 'soft errors',[1] which can occur owing to changes of potential in electronic memory units by the ejection of α-particles from uranium and thorium, the determination of trace amounts of uranium and thorium in materials used in electronic devices is important. In particular, with the trend towards increased storage capacity in highly integrated chips, a reduction in the permissible concentration of these elements is necessary.

Many methods have been described for the determination of uranium and thorium in high-purity aluminium, for example, neutron activation analysis (NAA),[2–4] glow discharge mass spectrometry,[4] secondary ion mass spectrometry,[5] inductively coupled plasma atomic emission spectrometry,[6] polarography,[6] spectrofluorimetry[4] and spectrophotometry.[4] However, these methods lack satisfactory sensitivity for the determination of uranium and thorium. In order to increase the sensitivity of the determination of uranium and thorium, NAA methods combined with chemical separation of ^{239}Np and ^{233}Pa using ion-exchange chromatography[7,8] or extraction with thenoyltrifluoroacetone[9] have been proposed. It is, however, difficult to conduct these methods in an ordinary laboratory, because NAA requires irradiation in a nuclear reactor.

On the other hand, inductively coupled plasma mass spectrometry (ICP-MS) has superior limits of detection and permits the determination of ultra-trace amounts of uranium and thorium. However, a solution with a high salt content causes plugging of the orifice which can result in a decrease in signal intensities. If the solution is diluted, the concentrations can become insufficient for trace element analysis. This problem can be overcome by separating the analytes from the matrix. For this purpose, Saisho *et al.*[4] reported a method for extracting uranium and thorium individually from a nitric acid medium. Uranium was extracted with a solution of tributyl phosphate (TBP) in carbon tetrachloride and thorium with 4-methylpent-3-en-2-one (mesityl oxide). However, only ng g^{-1} levels of uranium and thorium could be determined.

This paper describes the determination of pg g^{-1} levels of uranium and thorium in high-purity aluminium by ICP-MS after extraction of the elements from a hydrochloric acid medium with a solution of TBP in cyclohexane.

Experimental

Apparatus

All inductively coupled plasma mass spectrometric measurements were carried out with a VG PlasmaQuad II instrument (VG Elemental) installed in a clean room (Class 1000). The instrumental conditions are shown in Table 1. The nebulizer uptake rate was controlled by a Minipuls 3 peristaltic pump (Gilson). All of the analytical procedures prior to ICP-MS measurements were performed in a clean hood (Class 100) installed in a clean room (Class 1000).

Reagents

All the chemicals used were of analytical-reagent grade, unless specified otherwise. De-ionized water (>18 MΩ cm) was produced by a Milli-Q water purification system (Millipore). The uranium and thorium contents were each less than 0.5 pg ml^{-1} by ICP-MS measurements.

Uranium standard solution, 1 mg ml^{-1}. Prepared by dissolving 89.1 mg of uranyl acetate dihydrate in 5 ml of concentrated hydrochloric acid and diluting to 50 ml with water.

Thorium standard solution, 1 mg ml^{-1}. Prepared by dissolving 119.0 mg of thorium nitrate tetrahydrate in 5 ml of concentrated hydrochloric acid and diluting to 50 ml with water.

Bismuth internal standard solution, 1 mg ml^{-1}. Prepared by dissolving 232.1 mg of bismuth nitrate pentahydrate in 100 ml of 0.5 mol dm^{-3} nitric acid.

Copper solution, 1 mg ml^{-1}. Prepared by dissolving 100 mg of copper metal (99.99%, Wako Chemical) in 10 ml of 3.5 mol dm^{-3} nitric acid, heating to dryness, dissolving the residue in 10 ml of concentrated hydrochloric acid, heating to dryness again and dissolving the residue in 100 ml of 1 mol dm^{-3} hydrochloric acid.

Hydrochloric acid. Prepared with a PTFE sub-boiling distillation apparatus (Fujihara Seisakusyo). The contents of uranium and thorium were each less than 0.5 pg ml^{-1} by ICP-MS measurements.

Sulphuric and nitric acid. Super-analytical grade (Tama Pure AA-100, Tama Chemical).

Table 1 ICP-MS operating conditions

Plasma	Argon
Forward power	1.35 kW
Coolant flow-rate	14.0 l min^{-1}
Auxiliary flow-rate	0.5 l min^{-1}
Carrier flow-rate	0.7 l min^{-1}
Solution uptake rate	0.6 ml min^{-1}
Sampling aperture	Nickel, diameter 1.0 mm
Skimmer aperture	Nickel, diameter 0.8 mm
Ion lens settings	Maximum signal, ^{115}In or ^{208}Pb
Data acquisition	Pulse counting; multi-channel scaling (MCS) 2048 MCS channels; 0.64 ms dwell time; 50 sweeps

Table 2 Recoveries of uranium and thorium from hydrochloric acid containing aluminium. Hydrochloric acid (10 mol dm^{-3}, 200 ml) containing 1 ng each of uranium and thorium and 10 g of aluminium was shaken with 50 ml of each extractant containing 10% v/v TBP

Extractant	Recovery (%)	
	Uranium	Thorium
TBP–cyclohexane	95	91
TBP–carbon tetrachloride	71	83
TBP-chloroform	31	5
TBP–xylene	85	62
TBP–hexane	62	81
TBP–kerosene	52	76
TBP–IBMK	—*	—*

* Separation of the two phases could not be achieved.

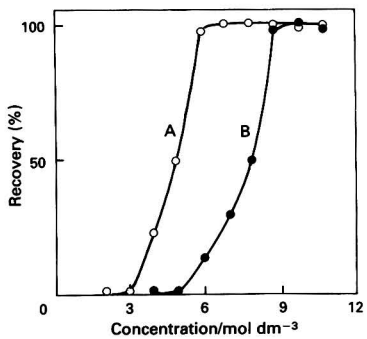

Fig. 1 Effect of the concentration of hydrochloric acid on the recoveries of uranium and thorium by extraction with 10% v/v TBP solution in cyclohexane. A, 1 ng of uranium; and B, 1 ng of thorium

Procedure

A drilled high-purity aluminium sample (10 g) was placed in a 250 ml quartz beaker. A 200 ml volume of 10 mol dm^{-3} hydrochloric acid and 0.1 ml of copper solution (1 mg ml^{-1}) (as an accelerator) were added. The beaker was covered with a quartz watch-glass and heated on a hot-plate. A 0.2 ml volume of hydrogen peroxide (3%) was added carefully in small portions. After dissolution was complete, the beaker was allowed to cool and the contents were transferred into a 500 ml separating funnel. A 10% v/v TBP solution in cyclohexane (50 ml) was added. The separating funnel was shaken for 3 min and then allowed to stand in order to separate the two phases. The aqueous phase was transferred into another 500 ml separating funnel and extracted with a further 50 ml of 10% v/v TBP solution in cyclohexane. The two organic phases were combined and shaken with 50 ml of 0.1 mol dm^{-3} hydrochloric acid for 30 s to strip uranium and thorium from the organic phase. The aqueous phase was transferred into a 200 ml quartz beaker. The stripping procedure was repeated with a further 50 ml of 0.1 mol dm^{-3} hydrochloric acid and the two aqueous phases were combined in the beaker. After the addition of 0.5 ml of the bismuth internal standard solution (100 ng ml^{-1}) and 20 μl of sulphuric acid, the contents were evaporated on a hot-plate held at 90 °C until only sulphuric acid remained in the beaker. A 3 ml volume of concentrated nitric acid was added and the evaporation process was repeated. After the addition of 3 ml of 0.27 mol dm^{-3} nitric acid, the contents of the beaker were warmed gently for a few minutes and allowed to cool. The solution was transferred into a test-tube and diluted to 5 ml with 0.27 mol dm^{-3} nitric acid. The signal intensities of ^{238}U, ^{232}Th and ^{209}Bi were measured by ICP-MS. The signal intensities of uranium and thorium were corrected to that of bismuth.

A blank analysis of 200 ml of 10 mol dm^{-3} hydrochloric acid was carried out in parallel with the sample procedure.

Results and Discussion

Extraction of Uranium and Thorium

It is known that uranium and thorium are extracted by various oxygen-containing extractants, such as diethyl ether and isobutyl methyl ketone (IBMK), from aqueous solutions having a high nitrate ion concentration.[10] Tributyl phosphate has also been proposed as an extractant for nitrate solutions.[10–12] On the other hand, high-purity aluminium can easily be dissolved in hydrochloric acid, whereas it is only dissolved in nitric acid with difficulty. For this reason, it is desirable that uranium and thorium are extracted from hydrochloric acid solutions. There are, however, few studies on the separation of these elements from a hydrochloric acid medium. Sato[13] discussed the extraction of high concentration levels of uranium and thorium from hydrochloric acid for preparative purposes, using TBP solutions in benzene and kerosene, and showed that thorium could not be extracted quantitatively. However, the extraction behaviour has not been studied at ultra-low concentration levels nor from hydrochloric acid solutions containing high concentration levels of aluminium. In the present work, the extraction of ultra-trace amounts of uranium and thorium from hydrochloric acid solutions containing aluminium by using TBP as the extractant was investigated.

Selection of the solvents

In order to examine the effect of the solvent for TBP on the efficiency of the extraction of uranium and thorium, tests were carried out with 50 ml of 10% v/v TBP solutions in several organic solvents, such as cyclohexane, carbon tetrachloride, chloroform, xylene, hexane, kerosene and IBMK, by extracting 1 ng each of uranium and thorium from 200 ml of 10 mol dm^{-3} hydrochloric acid solutions containing 10 g of aluminium. The results are shown in Table 2. It was found that cyclohexane was the most effective solvent; the other solvents had poor extracting ability. When IBMK was used, separation of the two phases could not be achieved. It was also found that quantitative recoveries were achieved by extraction with two 50 ml portions of a 10% v/v TBP solution in cyclohexane. A shaking time of 2 min was sufficient for the extraction.

Effect of the concentration of hydrochloric acid

The optimum concentration range of hydrochloric acid was examined by extracting 1 ng each of uranium and thorium from 200 ml of hydrochloric acid solutions of different concentrations containing 10 g of aluminium. It was found that quantitative recoveries of uranium and thorium were achieved with hydrochloric acid concentrations greater than 6 and 9 mol dm^{-3}, respectively. The results are shown in Fig. 1.

Effect of the concentration of TBP

In order to study the effect of the concentration of TBP, 1 ng each of uranium and thorium was extracted from 200 ml of 10 mol dm^{-3} hydrochloric acid containing 10 g of aluminium into 50 ml of 5–20% v/v TBP solutions in cyclohexane. It was found that the concentration of TBP used had no influence on the recoveries of the analytes.

Back-extraction

For the back-extraction of uranium and thorium from the organic phase into the aqueous phase, 50 ml of 0.1 mol dm^{-3} hydrochloric acid were used based on the results shown in Fig. 1. Quantitative stripping was achieved with two extractions for a period of 30 s each.

Effect of Sulphuric Acid on the Vaporization Step

The aqueous solution obtained by back-extraction was vaporized in a 200 ml quartz beaker by heating on a hot-plate controlled at 90 °C. A serious loss of uranium and thorium was observed at ultra-low concentration levels as shown in Table 3. It was assumed that this phenomenon was caused by adsorption on the walls of the quartz beaker. In order to prevent the formation of insoluble substances drying on the wall of the beaker, a small amount of sulphuric acid was added to the aqueous solution prior to heating. It was found that the addition of 20 μl of sulphuric acid led to improved recoveries of uranium and thorium. The results are summarized in Table 3.

ICP-MS Measurements

In order to determine the optimum sample flow-rate for ICP-MS measurements, the relationship between sample flow-rate and the signal intensities of uranium and thorium was studied using a 0.27 mol dm^{-3} nitric acid solution containing 0.2 ng ml^{-1} each of the analytes. The signal intensities gradually increased with an increase in sample flow-rate and reached almost constant values at flow-rates greater than 0.5 ml min^{-1} as shown in Fig. 2. From these results, the sample flow-rate was fixed at 0.6 ml min^{-1}.

It was recognized that variation of the signal intensities could not be ignored, particularly at low concentration levels of the analytes. Therefore, the reproducibility of the measurements of uranium and thorium was improved by using the internal standard method. To a sample solution were added 50 ng of bismuth and the signal intensities of uranium and thorium were corrected to the signal intensity of bismuth. When the corrected intensities of 0.2 ng ml^{-1} each of uranium and thorium were measured ten times, the relative standard deviations for uranium and thorium were 4.1 and 4.3%, respectively, compared with 9.8 and 10.7% for measurements in the absence of the bismuth internal standard. The other conditions for ICP-MS measurements are as shown in Table 1.

Table 3 Effect of sulphuric acid on the vaporization step. Hydrochloric acid (0.1 mol dm^{-3}, 100 ml) containing uranium and thorium was vapourized on a hot-plate held at 90 °C

		Recovery (%)	
Element	Added/ng	Without sulphuric acid	Addition of sulphuric acid*
Uranium	50	105	102
	0.5	61	94
Thorium	50	90	95
	0.5	47	96

* 20 μl of sulphuric acid were added prior to vaporization.

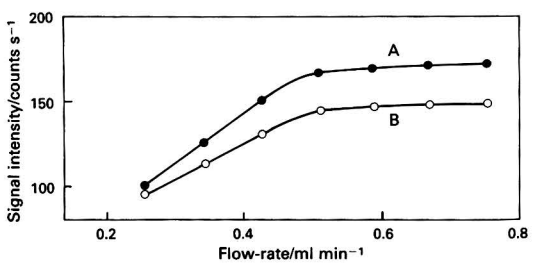

Fig. 2 Relationship between sample flow-rate for ICP-MS and signal intensities of uranium and thorium. A, 0.2 ng ml^{-1} of uranium; and B, 0.2 ng ml^{-1} of thorium

Interference

Although residual impurities in high-purity aluminium are less than 1 μg g^{-1}, the influence of these impurities on the extraction of uranium and thorium was studied. To 200 ml of 10 mol dm^{-3} hydrochloric acid, 1 ng each of uranium and thorium and 10 μg each of 35 elements (Ag, As, Au, B, Ba, Be, Ca, Cd, Co, Cr, Fe, Ga, Ge, In, K, Li, Mg, Mo, Mn, Na, Nb, Ni, P, Pb, Sb, Se, Si, Sn, Sr, Ta, Ti, Tl, V, Zn and Zr) were added. The analytes were then extracted with 50 ml of 10% v/v TBP solution in cyclohexane. No interference with the extraction of uranium and thorium was found for any of the elements added. On the other hand, gallium and molybdenum were almost completely co-extracted under the conditions used, and gold, niobium, tin and zirconium were partly co-extracted. However, mass spectra interferences from polyatomic ions such as AuCl (*m/z* 232) were not observed.

Blank Contamination and Detection Limits

In order to evaluate the blank contamination and the detection limits, ten replicate blank procedures were carried out. The blank values (average of ten measurements) for uranium and thorium were 0.05 and 0.04 ng, respectively. On the other hand, the detection limits, expressed as three times the standard deviation of the blank, were 0.07 ng of uranium and 0.08 ng of thorium. These detection limits are equivalent to 7 pg g^{-1} of uranium and 8 pg g^{-1} of thorium, when a 10 g amount of sample is used.

Calibration Graphs

The relationship between the signal intensities and the concentrations of uranium and thorium was examined by taking various amounts of uranium and thorium through the procedure described above. Linear relationships were obtained over the range 0.05–50 ng each of uranium and thorium.

Recoveries of Uranium and Thorium

The recoveries of uranium and thorium were examined. A drilled high-purity aluminium sample (10 g) was dissolved in 200 ml of 10 mol dm^{-3} hydrochloric acid and uranium and thorium (0.5–5 ng) were added to the solutions. The subse-

Table 4 Recoveries of uranium and thorium

	Uranium			Thorium		
Aluminium sample	Added/ng	Found/ng	Recovery (%)	Added/ng	Found/ng	Recovery (%)
A	--	ND*	—	—	ND*	—
	0.50	0.49	98	0.50	0.50	100
B	—	0.34	—	—	0.16	—
	1.00	1.27	93	1.00	1.15	99
	2.00	2.28	97	2.00	2.02	93
C	—	1.25	—	—	1.02	—
	5.00	6.43	104	5.00	5.83	96

* ND = not determined.

Table 5 Results of the analysis of high-purity aluminium

High-purity aluminium sample	Proposed method		Conventional method	
	Uranium/ ng g^{-1}	Thorium/ ng g^{-1}	Uranium/ ng g^{-1}*	Thorium/ ng g^{-1}†
A	1.06	1.31	1.0	1
B	0.35	0.29	0.4	<1
C	0.02	0.02	<0.1	<1
D	ND‡	ND‡	<0.1	<1

* Spectrofluorimetric analysis.[4]
† Spectrophotometric analysis with Arsenazo III.[4]
‡ ND = not determined.

quent procedure was as described above. The results obtained are shown in Table 4. It was found that recoveries of uranium and thorium of more than 93% could be obtained and the procedure was verified as practical and effective.

Analysis of High-purity Aluminium

The proposed method was applied to the analysis of several different types of high-purity aluminium samples used in micro-electronic devices. The results were compared with those obtained by conventional methods and are summarized in Table 5. From these results it can be seen that the determination of ultra-trace amounts of uranium and thorium in high-purity aluminium using the proposed method is feasible.

Conclusion

Ultra-trace amounts of uranium and thorium in high-purity aluminium were determined simultaneously by ICP-MS combined with an extraction technique. The extraction of uranium and thorium with a 10% v/v TBP solution in cyclohexane was satisfactory. Reproducibility was improved by using the internal standard method. For a sample mass of 10 g, the detection limits of uranium and thorium were 7 and 8 pg g^{-1}, respectively.

References

1 May, T. C., and Wood, M. H., *Annu. Proc. Reliab. Phys. (Symp.)*, 1978, **16**, 33.
2 Kudo, K., Shigematsu, T., Yonezawa, H., and Kobayashi, K., *J. Radioanal. Chem.*, 1981, **63**, 345.
3 Dyer, F. F., Emery, J. F., Northcutt, K. J., and Scott, R. M., *J. Radioanal. Chem.*, 1982, **72**, 53.
4 Saisho, H., Tanaka, M., Nakamura, K., and Mori, E., *J. Res. Natl. Bur. Stand.*, 1988, **93**, 398.
5 Honma, N., Kurosawa, S., and Kawashima, I., *Rev. Electr. Commun. Lab.*, 1982, **30**, 503.
6 Kudermann, G., and Blaufuss, K.-H., *Mikrochim. Acta, Part II*, 1985, 85.
7 Egger, K. P., and Krivan, V., *Fresenius Z. Anal. Chem.*, 1987, **327**, 119.
8 Hirai, S., and Hayakawa, Y., *Bunseki Kagaku*, 1987, **36**, 284.
9 Yonezawa, C., Hoshi, M., Tachikawa, E., and Kamioki, H., *Bunseki Kagaku*, 1988, **37**, 7.
10 Sandell, E. B., *Colorimetric Determination of Traces of Metals*, Interscience, New York, 1959.
11 Warf, J. C., *J. Am. Chem. Soc.*, 1949, **71**, 3257.
12 Sato, T., *J. Appl. Chem.*, 1965, **15**, 489.
13 Sato, T., *J. Appl. Chem.*, 1966, **16**, 53.

Paper 0/02217I
Received May 21st, 1990
Accepted December 21st, 1990

Evaluation of Microwave Digestion and Solvent Extraction for the Determination of Trace Amounts of Selenium in Feeds and Plant and Animal Tissues by Electrothermal Atomic Absorption Spectrometry

Pierre Hocquellet and Marie-Paule Candillier
Institut Municipal de Recherches sur l'Alimentation Humaine et Animale, Laboratoire Municipal, rue du Professeur Vèzes, 33300 Bordeaux, France

A sensitive method for the accurate determination of Se in agricultural products at sub-ppm levels is described. The proposed procedure involves the wet oxidation of samples by using a mixture of nitric, sulphuric and perchloric acids, co-extraction of Se and added Pd with diethylammonium *N,N*-diethyldithiocarbamate in chloroform, and electrothermal atomic absorption spectrometric determination of Se in the organic extract. Atomization and extraction conditions are discussed. Special attention is given to the wet oxidation step, and its advantages in speed and simplicity over conventional heating have been evaluated using an automated microwave digestion system. The results reported, obtained from several reference materials, confirm the accuracy of the method with which a detection limit of 0.002 μg g^{-1} of Se can be achieved.

Keywords: *Selenium determination; electrothermal atomic absorption spectrometry; solvent extraction; microwave digestion; feed and plant and animal tissue*

Selenium is an essential element in living organisms. It is now recognized that deficiencies of selenium, which are widespread in France and in some other European countries, are responsible for cardiomyopathy, muscular dystrophy and reproductive disorders in a variety of animal species.[1] Concentrations of selenium of less than 30 ng g^{-1} of feed lead to severe losses of livestock, whereas concentrations between 0.1 and 0.4 μg g^{-1} are considered to be optimum[2] and can be achieved in most instances by the addition of Se compounds. Owing to the dual nature of this element which is both essential and toxic, depending on the concentration at which it is supplied, routine but reliable methods are needed in order to determine the Se content of mixed feeds and plant and animal tissues with the sensitivity and accuracy required for the detection of deficiencies and for the strict control of supplements in feeding.

The best analytical technique for this purpose seems to be electrothermal atomic absorption spectrometry (ETAAS) with which a low limit of detection can be achieved. Its sensitivity, generally reported in terms of a characteristic mass, is about 30 pg of Se, which produces an integrated absorbance signal whose net area is equal to 0.0044 A s.[3] This implies, however, that at least 2 mg of dry sample should be atomized in order to determine precisely a concentration value near or below the threshold of deficiency. In this instance the determination of Se is subject to strong spectral and chemical interferences from the highly concentrated matrix, which are not completely overcome by chemical modifiers and atomization from a L'vov platform. Therefore, direct application of this technique cannot be the most convenient way of quantifying Se at low concentrations. Extraction of the element prior to its atomization remains the only alternative allowing accurate determinations at sub-ppm levels and providing the lowest limit of detection whatever the nature and the matrix composition of the materials being analysed.

The procedure proposed in this paper has been developed from an earlier method involving a fast extraction of Se by use of a 2% diethylammonium *N,N*-diethyldithiocarbamate (DDDC) solution in chloroform.[4] Further improvements have been achieved. All the operating conditions have been optimized in order to minimize sample handling, reduce analysis time and particularly to automate the wet oxidation pre-treatment of samples by means of a microwave digestion technique.

Experimental

Apparatus

A Perkin-Elmer Model 4000 atomic absorption spectrometer with a PRS 10 printer sequencer was used for atomic absorption measurements. The transient signal was also recorded with a Perkin-Elmer Model 56 strip-chart recorder. Selenium was determined at the 196.0 nm wavelength with an electrodeless discharge lamp as the source. A slit setting of 0.7 nm and simultaneous background correction with a deuterium arc lamp device were used.

Electrothermal atomization was performed by using a Perkin-Elmer Model HGA-500 graphite furnace equipped with a Model AS-40 auto-sampler. Argon was used as the purge gas. The graphite tubes were coated with tantalum carbide according to the procedure described previously[5]: a mixture containing 1 g of Ta_2O_5 and 0.2 ml of glycerol diluted with a 10% gum arabic aqueous solution was applied to both the inside and the outside surface of the graphite tube, which was then heated very slowly to 2700 °C.

Conventional sample decompositions were carried out in a borosilicate glass digestion apparatus such as that described by Pien[6] and Gorsuch[7], which consists of a 150 ml Kjeldahl flask topped with a 50 ml reservoir and a vertical condenser. A stopcock between the flask and the reservoir allows refluxing or distillation of the acid mixture. Automated sample decompositions were performed by means of a Prolabo A-300 microwave digestion system equipped with two pumps for the addition of reagents. Glass-stopped tubes (120 × 15 mm) were used for the reduction and extraction of Se. All glassware was cleaned with hot 10% HNO_3 and rinsed with de-ionized water before use.

Reagents

Ascorbic acid solution. Prepare fresh daily by dissolving 2.5 g of ascorbic acid (analytical-reagent grade) in 50 ml of water.

Palladium solution, 1000 mg l^{-1}. Dissolve 85 mg of $PdCl_2$ (anhydrous for synthesis, Merck) in 5 ml of hot 12 mol dm^{-3} HCl, then dilute to 50 ml with water.

Diethylammonium N,N-*diethyldithiocarbamate solution.* Dissolve 2 g of DDDC (Merck) in 100 ml of chloroform.

Selenium stock solution (1000 mg l^{-1}). Dissolve 281 mg of SeO_2 (analytical-reagent grade) in 200 ml of 0.5 mol dm^{-3} HCl. Dilute daily with 0.5 mol dm^{-3} HCl as required to obtain a working standard solution containing 1 mg l^{-1} of Se.

Procedure

Sample decomposition

Conventional method. Weigh 2 g of sample into the Kjeldahl flask of the digestion apparatus. Add two glass beads and 25 ml of HNO_3 [relative density (d) = 1.38]. Connect the flask to the apparatus and heat gently until the sample is dissolved, then reflux for at least 15 min. Let the mixture cool. Add 3 ml of $HClO_4$ (d = 1.67) and 2 ml of H_2SO_4 (d = 1.84). Heat to boiling and distil HNO_3 into the reservoir until the digest turns yellow, not brown or black; avoid charring of the sample by adding the distillate drop by drop until the digest remains colourless after prolonged heating. Carefully allow all the distillate to run back into the flask and distil again until white fumes appear. Let the digest cool. Disconnect the flask, add about 10 ml of de-ionized water and heat until fumes of $HClO_4$ are produced. After cooling, add 30 ml of water and transfer into a 50 ml calibrated flask. Rinse the Kjeldahl flask and make up to volume with water.

Microwave method. Accurately weigh 0.5–1 g of sample into the 50 ml conical flask, or 2 g into the 100 ml cylindrical flask of the apparatus. Add one glass bead and 20 ml of HNO_3 (d = 1.38). Connect the flask to the A-300 microwave system and start the digestion programme described in Table 1. Dilute the final digest to 50 ml with water.

Reduction of Se^{VI} to Se^{IV}

Pipette 5 ml of the sample digest into a glass-stoppered tube. Add 2 ml of 12 mol dm^{-3} HCl, mix thoroughly and place the tube in a boiling water-bath for 20 min. Cool to room temperature (20 °C).

Table 1 Microwave digestion programme

	Step		
	1	2	3
Reagent	A*	B†	C‡
Volume/ml	20	5	5
Power (%)	15	30	40
Time/min	15	10	8
Power (%)	25	40	0
Time/min	10	35	0
Wait/min	0	3	0

* HNO_3 previously added to the sample.
† H_2SO_4 + $HClO_4$ (2 + 3).
‡ De-ionized water.

Standard solutions

Pipette 0, 50, 100 and 200 μl of the 1 mg l^{-1} Se standard solution into separate glass-stoppered tubes. Add 5 ml of an acid mixture containing 4% (v/v) H_2SO_4 and 6% (v/v) $HClO_4$ in water, then add 2 ml of 12 mol dm^{-3} HCl. Mix thoroughly. The series contains 0.0, 0.05, 0.10 and 0.20 μg of Se.

Extraction of Se–DDDC complex

Pipette 100 μl of the Pd solution and 200 μl of the ascorbic acid solution into each sample and standard tube and mix thoroughly. After 1 min add exactly 1 ml of the DDDC solution and shake vigorously for 30 s. Allow the layers to separate. Remove the aqueous layer until about 1 cm of aqueous solution remains above the level of the organic solution.

Measurements

By using a long micropipette, transfer 400 μl of each organic extract into the autosampler cups into which 0.5 ml of water has been previously dispensed; the upper aqueous layer will prevent the evaporation of chloroform and therefore any change in the concentration of the organo-selenium compound while measurements are being made. Inject 30 μl of the extracts into the furnace and atomize according to the electrothermal programme given in Table 2. Read both the maximum and integrated absorbances; the very low concentrations are calculated from peak height measurements while the peak area is used to quantify high concentrations of Se. In both instances, accurate measurements require that a baseline offset correction is made immediately before the atomization is carried out.

Results and Discussion

Atomization Programme

The volatility of Se is one of the major problems encountered in the determination of this element by ETAAS. Premature losses of Se occur during the charring step at temperatures as low as 300 °C, whereas a complete destruction of the DDDC matrix cannot be achieved below 600 °C. Ediger[8] first reported that the addition of Ni or Cu as a chemical modifier made it possible to prevent the volatilization of Se until a temperature of 1200 °C was reached. The formation of more thermally stable metal selenides was postulated. More recently, it has been shown that Pd produces a similar thermal stabilization of Se[9,10] and it has been suggested that Pd might be a better modifier than Ni or any of the other metals having a similar effect. Palladium was also successfully used in the determination of several other volatile elements, particularly Hg,[11] Bi[12] and As,[13,14] and it was therefore recommended as a universal chemical modifier.[15] Since 1982, Pd has been selected instead of Ni, which was used previously[4] because, unlike Ni, Pd can be quantitatively and readily co-extracted with Se using the DDDC reagent. A comparison of curves 1 and 2, Fig. 1, shows that the addition of Pd markedly improves the thermal stabilization of Se which, however, is partly maintained in the furnace to a temperature of 1700 °C in the absence of a

Table 2 Electrothermal programme for the determination of Se

	Step				
Parameter	Dry	Char 1	Char 2	Atomize	Clean
Temperature/°C	120	300	700	2500	2700
Ramp time/s	30	10	10	0	1
Hold time/s	10	10	20	5	4
Internal gas (flow-rate/ml min^{-1})	Air (300)	Air (300)	Ar (300)	Ar (0)	Ar (300)
Read command	—	—	—	—	—

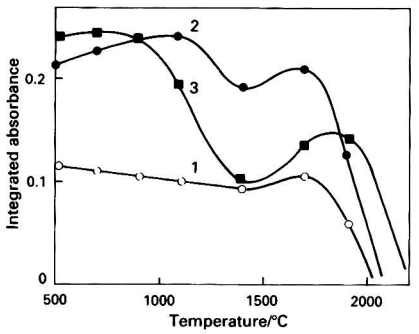

Fig. 1 Study of charring for 3 ng of Se in the DDDC extract. Atomization from a tantalum carbide coated tube. Furnace conditions as in Table 2: 1, without air and chemical modifier; 2, without air and with 6 μg of Pd; and 3, with air and 6 μg of Pd

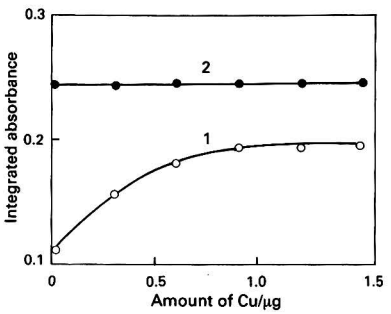

Fig. 2 Thermal stabilization effect of Cu for 3 ng of Se in the DDDC matrix: 1, without Pd; and 2, in the presence of 6 μg of Pd. Furnace conditions as in Table 2

chemical modifier, owing to the use of a tantalum carbide coated tube. The efficiency of atomization is enhanced more than 2-fold. The amount of Pd added was optimized experimentally for 3 ng of Se and a charring temperature of about 700 °C; peak heights and peak areas reached maximum values for about 1 μg and remained constant for up to 10 μg of Pd. It was found that 6 μg of Pd was adequate to compensate for the additional thermal stabilization effect from Cu, which is co-extracted with Se (see Fig. 2).

Surface interaction can be another factor in the thermal stabilization of Se,[16] which explains why this element is not completely lost despite charring temperatures of the order of 1800 °C when a tantalum carbide coated surface is used without any chemical modifier. It has been pointed out that ordinary[17] or porous[18] graphite and graphite surfaces treated with refractory metals such as Ta, Zr or Nb[19,20] provide a higher atomization efficiency for Se than pyrolytic graphite. As can be seen from Fig. 1, curve 2, the integrated absorbance slightly decreases at temperatures above 1100 °C, then increases again and, near 1700 °C, reaches a maximum which indicates a strong retention of Se by the tantalum carbide coated surface. This observation might be due to the formation of selenide at the coated surface, whose characteristic behaviour is fairly similar to that of tantalum salts tested as chemical modifiers by Alexander *et al.*[21] Owing to the relatively high temperature required to destroy the matrix, the tantalum carbide coated surface cannot be used without the presence of Pd, as indicated above, but its additional thermal stabilization effect prevents any loss of Se which might occur at temperatures between the charring and atomization temperatures. However use of a tantalum carbide coated surface leads to memory effects when large amounts of Se are introduced into the furnace.

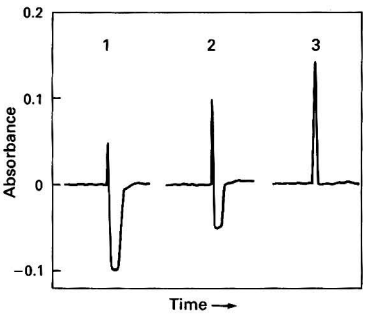

Fig. 3 Determination of Se in vine leaves containing 1000 μg g^{-1} of Cu. Comparison of absorbance profiles for the thermal conditions given in Table 2 with: 1, atomization from a graphite surface without air; 2, atomization from a tantalum carbide surface without air; and 3, with air

The determination of Se by ETAAS is affected by several spectral interferences. The extent of such interferences greatly depends on both the performance of the background corrector and the atomization conditions used. The narrow band spectral interferences of phosphorus species and Fe on the Se 196 nm line are well known.[22,23] They cannot be suppressed by the continuum background correction devices with which the majority of AA instruments are equipped, although Zeeman-effect systems can cope with the problem.[24] When using a classical deuterium arc corrector, P and Fe produce a large negative signal due to over-compensation of the background. The same effect was observed when Pd and other metals such as Cu or Ni were added to the DDDC or to any digestion mixture containing sulphuric acid, whereas the same metals in dilute nitric or hydrochloric acid did not cause a negative signal. This suggests, therefore, that sulphides, which are formed during the pyrolysis of such matrices in an argon atmosphere, *i.e.*, under reducing conditions, might be responsible for a structured band spectral interference near the 196.0 nm line. This assumption is supported by the fact that it is possible to suppress over-compensation of the background by using air as an alternate internal gas during a first charring step at 300 °C, in order to prevent or to minimize the formation of sulphides when the thiocarbamate is decomposed. Fig. 3 shows that the combination of atomization from a tantalum carbide coated surface and the use of air allows the complete elimination of the very important negative signal generated in a graphite furnace by the large amount of Cu co-extracted with Se and Pd when materials containing a significant amount of Cu, such as vine leaves, have to be analysed. However, the addition of air appears to be a factor in the thermal destabilization of Se, as can be seen in Fig. 1, curve 3, by the decrease in integrated absorbance at temperatures above 800 °C. Consequently, the maximum temperature during the charring must not exceed 700 °C, which is sufficient to destroy the DDDC matrix.

Extraction of Selenium

The use of DDDC in chloroform offers two important advantages over some of the reagents previously proposed by other workers, such as aromatic *ortho*-diamines[25–29] or other thiocarbamates.[30,31] It allows both the quantitative recovery of Se^{IV} from strong acidic solutions by means of a single extraction[20] and the co-extraction of Pd, which ensures a good thermal stabilization of Se during the atomization process. The solution of Se and the Pd-DDDC complexes in chloroform, kept in contact with the acidic aqueous layer, remains stable for several hours so that extractions can be performed in series into small glass-stoppered tubes.

Because Se^{VI} is not extracted, a reduction step is necessary in order to recover the total amount of Se present in the

Table 3 Effect of the reduction step on the recovery of Se after wet oxidation

Sample	Mass	Total amount of Se found in the digest solution/μg: Without reduction	With reduction
Se^{IV}	1 μg	0.97	0.99
Se^{VI}	1 μg	0.00	0.95
Alfalfa	2 g	0.25	0.27
Alfalfa	2 g	0.22	0.24
Alfalfa	2 g	0.24	0.23
Hevea leaves	1 g	0.41	0.42
Mixed feed	2 g	0.20	0.22
Mixed feed	2 g	0.25	0.24
Mixed feed	2 g	0.33	0.36
Mixed feed	1 g	0.47	0.49
Mixed feed	1 g	0.36	0.36
Mixed feed	1 g	0.31	0.32
Tuna fish (lyophilized)	0.5 g	2.40	2.45

sample digestion solutions. About 95% of Se^{VI} is reduced to Se^{IV} after 30 min in 5 mol dm^{-3} HCl at its boiling point. When a reaction time of 30 min is exceeded, losses of Se may occur owing to the formation of volatile selenium chloride. Data reported in Table 3 show that despite the drastic oxidizing conditions used, the process of decomposing the samples does not change the oxidation state of Se added as Se^{IV} or Se^{VI}, and almost entirely converts the organically bound Se into the Se^{IV} ionic form only. Thus, for feed supplements, the successive application of the method with, and subsequently without, reduction makes it possible to specify whether Se was added as selenite or as selenate compounds.

The addition of ascorbic acid prevents the extraction of Fe, but some other elements are partially or completely recovered in the organic solvent. It has been verified that Cu, which is quantitatively extracted, did not interfere when its concentration in the digest solution was lower than 20 mg l^{-1}. Potential interferences from other matrix components of a great variety of agricultural products have been tested by the addition of Se^{IV} after the digestion of the samples. The mean recovery was found to be 99.4% with a relative standard deviation of 6.5% for more than sixty different materials analysed, such as foods, mixed feeds and plant and animal tissues.

Wet Oxidation of Samples

The destruction of organic matter is one of the most critical stages of any analytical method that is based on a specific chemical reaction of selenite or selenate. Many Se compounds are volatile and can be lost during the process which is required to convert all the organically bound Se into its ionic forms. Thus, a rapid wet oxidation with a mixture of nitric and sulphuric acids leads to poor recoveries. The important point resulting from radiochemical investigations is that losses of Se are related to the extent to which the organic material is allowed to char.[7] The charring of samples indicates the occurrence of reducing conditions, which may induce the formation of gaseous hydrogen selenide. It is therefore necessary to maintain oxidizing conditions at all stages of the decomposition process. This requirement is generally fulfilled when a mixture containing perchloric acid is used. The proposed procedure, involving a pre-oxidation step with nitric acid alone followed by a gradual heating with nitric, sulphuric and perchloric acids until the white fumes of perchloric acid appear, was found to be suitable for the complete destruction of all types of plant and animal tissues tested. The procedure is performed by means of the apparatus described by Pien[6] and Gorsuch[7] which allows refluxing or distillation of nitric acid so that the oxidation potential of the acid mixture can be

Table 4 Comparison of results between conventional and microwave digestions

Sample	Selenium concentration/μg g^{-1}: Conventional digestion	Microwave digestion
Alfalfa	0.140 ± 0.005	0.145 ± 0.005
Hevea leaves	0.42 ± 0.01	0.42 ± 0.01
Mixed feed	0.50 ± 0.01	0.49 ± 0.01
Mixed feed	0.29 ± 0.01	0.29 ± 0.01
Mixed feed	0.19 ± 0.01	0.19 ± 0.01
Tuna fish (lyophilized)	5.05 ± 0.15	4.90 ± 0.20

stabilized or increased. Such a device makes it possible to quickly overcome any occurrence of charring by running back the nitric distillate, drop by drop, into the flask.

This procedure has proved to be reliable but it suffers from being relatively time-consuming and requires the constant presence of a careful analyst. In order to automate the procedure, the use of the Prolabo A-300 open vessel microwave digestion system has been evaluated.

Compared with the previous method, the microwave technique has the main advantage of allowing a strict control over the heating power and over the time during which heating is applied. A reproducible digestion programme can be achieved which includes one or more additions of reagent and increasing the heating power stepwise at timed intervals. Unlike the manual method however, the distillate is lost and it is impossible to intervene while the programme is running, so that the amount of oxidizing mixture necessary to prevent charring must be estimated beforehand. As the amounts of reagents are generally stated for a given programme, the conditions required in order to obtain good results in every instance is related to the use of an adequate sample mass : acid volume ratio.

The digestion programme reported in Table 1 was optimized so as to exactly reproduce all the operating conditions of the conventional procedure. Two variable parameters have to be considered for its successful application. The first is the sample mass which must be between 0.5 and 2 g depending upon both the nature and the content of organic matter in the material. Lipids and sugars are more difficult to destroy without charring than proteins. The second is the type of flask, which depends on the size of the sample. If a large flask is used with small samples, nitric acid may not be entirely removed by the end of the microwave programme, resulting in incomplete breakdown of the organo-selenium compounds. To ensure that white fumes of perchloric acid appear, samples with a mass of less than 1 g should be digested in 50 ml conical flasks, whereas samples weighing between 1 g and 2 g should be digested in 100 ml cylindrical flasks.

There is no significant difference between the results obtained after microwave digestion and those given by the conventional method (see Table 4). Owing to the high Se content of the tuna fish, a 0.5 g sample of this animal tissue was decomposed readily. Larger samples of 2 g of each of the other materials were oxidized without difficulty using both procedures.

Precision and Accuracy

Atomization from the wall of the tube with maximum heating rate and peak height measurements provided the best sensitivity and the highest signal to noise ratio. An absolute sensitivity of about 20 pg of Se (the mass of analyte which provides a defined peak absorbance of 0.0044 A) was achieved, whereas integrated absorbance measurements provided a sensitivity of only 55 pg of Se (*i.e.*, the mass of analyte producing an integrated absorbance signal whose net area is

Table 5 Selenium concentrations in μg g^{-1}, found in IAEA and NIST Reference Materials

Reference material	Certified concentration	Conventional digestion	Microwave digestion
Mussel Homogenate (IAEA, MA-M2-/TM)	2.3 ± 0.3	2.15 ± 0.05	—
Fish Flesh Homogenate (IAEA, MA-A-2/TM)	1.12 ± 0.06*	1.05 ± 0.05	1.08 ± 0.06
Animal Muscle (IAEA, H-4)	0.28 ± 0.03	0.28 ± 0.02	0.28 ± 0.02
Milk Powder (IAEA, A-11)	0.034 ± 0.007	0.031 ± 0.005	0.033 ± 0.005
Bovine Liver (NIST 1577a)	0.71 ± 0.07	0.71 ± 0.02	0.68 ± 0.02
Wheat Flour (NIST 1567a)	1.1 ± 0.2	1.03 ± 0.02	0.85 ± 0.05

* Found by NAA, according to Hansson *et al.*[32]

equal to 0.0044 A s) but a better relative standard deviation when amounts of Se greater than 2 ng were atomized. Consequently, peak area measurements are more suitable to quantify fairly high concentrations of selenium while the peak height mode is more appropriate for very low concentrations. Using the peak height mode, the detection limit of the method, evaluated at twice the standard deviation of the blank, was found to be 0.002 μg g^{-1} of Se for a 2 g sample. This limit can be lowered when more than 30 μl of the organic extract are injected into the furnace, by means, for instance, of a multiple injection technique. The relative standard deviations were found to be 4 and 7% for replicate analyses of two feed samples containing, respectively, 0.5 and 0.03 μg g^{-1} of Se (five determinations each).

The accuracy of the method has been assessed by the analysis of six different Standard Reference Materials from the US National Institute of Standards and Technology (NIST) [formerly known as the National Bureau of Standards (NBS)] and the International Atomic Energy Agency (IAEA). The data were generally obtained from no more than three replicate analyses. The results, reported in Table 5, achieved for the first five materials using either conventional or microwave digestion, are in good agreement with certified Se concentrations. Although the concentration certified for the IAEA Fish Flesh (MA-A-2/TM) was 1.7 ± 0.3 μg g^{-1}, the results obtained here are consistent with the values recently found by Hansson *et al.*[32] using hydride generation atomic absorption spectrometry, and which have been confirmed by neutron activation analysis (NAA). It is therefore clear that the original certified value for this ten year old material is no longer correct. The mean concentration obtained for the Wheat Flour from three replicate analyses using microwave digestion is about 15% lower than that found by the conventional method and is in good agreement with the certified value. The slight discrepancy may be ascribed to the tendency of the material to char. Owing to the finite amount of oxidizing mixture used with the microwave procedure, a sample size of less than 1 g was required in order to avoid any charring, leading to losses of Se. It is likely too that a more efficient refluxing of the nitric acid immediately before the perchloric acid fumes appear would have led to a more complete recovery of Se. The microwave value is, however, very close to the 0.83 μg g^{-1} found for the same material by Shand and Ure[33] using a graphite furnace and a combustion system in which the sample was burned in a stream of oxygen and the volatilized Se collected in acetic acid.

Conclusion

The proposed method is particularly convenient for the accurate determination of Se in a great variety of organic materials over the concentration range 0.01–1.0 μg g^{-1}. The main advantages offered by the fast solvent extraction of Se prior to its atomization are the total suppression of spectral and chemical interferences from the matrix and an increase in sensitivity by preconcentration of the analyte, allowing, respectively, external calibration and very low detection limits. Such a procedure however requires the complete destruction of the organic matter by a wet oxidation technique. This pre-treatment can be automated for routine applications by making use of a microwave digestion apparatus permitting a strict and reproducible control over all the operating conditions without operator intervention, so that overnight digestion of samples is possible. Compared with a conventional wet oxidation procedure, the focused open-vessel microwave digestion system used in this work has been shown to give identical results, provided that great care is taken about important parameters such as microwave power, time, sample size and volume of oxidizing acids.

References

1 Arvy, P., and Lamand, M., *C.R. Acad. Agr. Fr.*, 1983, **69** 489.
2 Lamand, M., *Ann. Nutr. Aliment.*, 1971, **25**, B379.
3 Slavin, W., Carnrick, G. R., Manning, D. C., and Pruszkowska, E., *At. Spectrosc.*, 1983, **4**, 69.
4 Hocquellet, P., *Ann. Falsif. Expert. Chim.*, 1980, **784**, 129.
5 Hocquellet, P., *At. Spectrosc.*, 1985, **6**, 69.
6 Pien, J., *Chimie Anal. (Paris)*, 1956, **38**, 361.
7 Gorsuch, T. T., *The Destruction of Organic Matter*, Pergamon Press, Oxford, 1970.
8 Ediger, R. D., *At. Absorpt. Newsl.*, 1975, **14**, 127.
9 Shan, X., and Hu, K., *Talanta*, 1985, **32**, 23.
10 Liu, P., Wei, L., Matsumoto, K., and Fuwa K., *Anal. Sci.*, 1985, **1**, 257.
11 Shan, X., and Ni, Z., *Acta Chim. Sin.*, 1979, **37**, 261.
12 Jin, L., and Ni, Z., *Can. J. Spectrosc*, 1981, **26**, 219
13 Shan, X., Ni, Z., and Zhang, L, *At. Spectrosc.*, 1984, **5**, 1.
14 Hocquellet, P., *Rev. Fr. Corps Gras*, 1984, **31**, 117.
15 Schlemmer, G., and Welz, B., *Spectrochim. Acta, Part B*, 1986, **41**, 1157.
16 Dědina, J., Frech, W., Lindberg, I., Lundberg, E., and Cedergren, A., *J. Anal. At. Spectrom.*, 1987, **2**, 287.
17 Matousek, J. P., *Prog. Anal. At. Spectrosc.*, 1981, **4**, 247.
18 Chung, C. H., Iwamoto, E., Yamamoto, M., Yamamoto, Y., and Ikeda, M., *Anal. Chem.*, 1984, **56**, 829.
19 Vickrey, T. M., and Buren, M. S., *Anal. Lett.*, 1980, **13**, 1465.
20 Hocquellet, P., *Analusis*, 1978, **6**, 426.
21 Alexander, J., Thomassen, Y., and Langmyhr, F. J., *Anal. Chim. Acta*, 1980, **120**, 377.
22 Saeed, K., and Thomassen, Y., *Anal. Chim. Acta*, 1981, **130**, 281.
23 Manning, D. C., *At. Absorpt. Newsl.*, 1978, **17**, 107.
24 Carnrick, G. R., Manning, D. C., and Slavin, W., *Analyst*, 1983, **108**, 1297.
25 Szydlowski, F. J., *At. Absorpt. Newsl.*, 1977, **16**, 60.
26 Neve, J., and Hanocq, M., *Anal. Chim. Acta*, 1977, **93**, 85.
27 Neve, J., Hanocq, M., and Molle, L., *Anal. Chim. Acta*, 1980, **115**, 133.
28 Tulley, R. T., and Lehman, H. P., *Clin. Chem.*, 1982, **28**, 1448.
29 Norheim, G., Saeed, K., and Thomassen, Y., *At. Spectrosc.*, 1983, **4**, 99.
30 Kamada, T., and Yamamoto, Y., *Talanta*, 1980, **27**, 473.
31 Kumpulainen, J., Raittila, A. M., Lehto, J., and Koivistoinen, P., *J. Assoc. Off. Anal. Chem.*, 1983, **66**, 1129.
32 Hansson, L., Petterson, J., and Olin, A., *Analyst*, 1989, **114**, 527.
33 Shand, C. A., and Ure, A. M., *J. Anal. At. Spectrom.*, 1987, **2**, 143.

Paper 0/04457A
Received October 3rd, 1990
Accepted January 10th, 1991

Enhancement Effects of Dodecyl Sulphates in Flame Atomic Absorption Spectrometry

Daniel Y. Pharr, Henry E. Selnau, Elizabeth A. Pickral and Rhea L. Gordon
Department of Chemistry, Virginia Military Institute, Lexington, VA 24450, USA

Several enhancement models were used to explain the results obtained in the investigation of Al, Ca, Cd, Co, Cr, Cu, Fe, Mn, Ni, Pb, Rb, Sb, Sn, Sr and Zn using flame atomic absorption spectrometry with a pre-mix burner and six different micellar systems: cetyltrimethylammonium bromide, Triton X-100, ammonium dodecyl sulphate, lithium dodecyl sulphate, sodium dodecyl sulphate and potassium dodecyl sulphate. Similarly, 19 metal cations were used in an interference study with sodium dodecyl sulphate.

Keywords: *Flame atomic absorption spectrometry; micelle; surfactant; spectrometry*

The use of surfactants to enhance the analyte signal in flame atomic absorption spectrometry has been reported previously[1–6] and has been compared with the use of organic solvents, which lower the surface tension and promote the generation of smaller droplets in the nebulization process resulting in greater sensitivity.[2] Kodama and co-workers[1,2] have reported on the enhancement of Cr signals and the suppression of interferences in the presence of the surfactant sodium dodecyl sulphate (SDS).

Armstrong *et al.*[4] studied the effects of the SDS enhancement of Cu signals using flame atomic absorption spectrometry and concluded that the aerosol ionic redistribution theory of Borowiec *et al.*[7] could explain the enhancement effects that were reported for Cu and Cr. This theory proposes a mechanism of analyte transport to the hottest part of the flame by the interaction of the spectator ions of the anionic head group of the dodecyl sulphate with the metal cation of the analyte. The enrichment of the analyte occurs on the double layer of the outside surface of the large drops. As these drops divide, a stripping action occurs that effectively concentrates the metal cation in the smaller droplets that are nebulized and carried into the flame, resulting in an increase in the analyte signal.[4] The major evidence given for this conclusion was the decreased amount of Cu that was found in the nebulization waste because of the decreased concentration of the analyte in the larger droplets that go down the drain.

Taga *et al.*[5] reported the enhancement of flame absorption signals for Ti^{IV} and V^{V} using SDS and cetyltrimethylammonium bromide (CTAB). The SDS enhanced the analyte signals 150% for Ti and 180% for V and suppressed the interferences. However, a study of the nebulization waste showed no difference between the waste and the analyte solution.

The present study investigates micellar systems for 15 metals using different cations for the anionic surfactant, dodecyl sulphate. Ammonium, lithium, sodium and potassium dodecyl sulphates were investigated to determine if the salt or matrix effects explain the enhancement of the absorbance signal of the analyte in the presence of SDS.

Experimental

Reagents

Stock metal solutions of 1000 ppm were purchased and used as received (Fisher Scientific). The surfactants SDS (Fisher Scientific), CTAB and Triton X-100 (Sigma) were also used without purification. The ammonium dodecyl sulphate (ADS) and the lithium dodecyl sulphate (LDS) were prepared from dodecanol (Aldrich) and recrystallized twice in water.[8] The potassium dodecyl sulphate (KDS) was prepared from SDS,[9] recrystallized twice and tested for sodium. All other reagents were ACS reagent grade and were used as received. All glassware was cleaned with 10% HNO_3 and rinsed three times with distilled, de-ionized water prior to use. Solutions were prepared for use within 24 h.

Procedure and Apparatus

A Perkin-Elmer Model 370 atomic absorption spectrometer with a pre-mix burner was used for all determinations. An air–acetylene flame was used with a pre-mix burner, and a pre-mix slot burner was used with the dinitrogen oxide–acetylene flame for the Sn study.

Hollow cathode lamps were used as light sources for the atomic absorption of the analyte metals. The height of the optical path above the burner was varied to determine the maximum absorption signal. The oxidizer and fuel flow-rates, slit settings, wavelengths for analysis and hollow cathode lamp current settings used were those recommended by Perkin-Elmer.[10]

All surfactants were used at the concentration that achieved the optimum enhancement of absorbance. This concentration was determined by selecting the highest absorbance value obtained at a constant low concentration of the metal ion at different surfactant concentrations.

Results

Four general patterns were observed. For Co, Fe, Mn, Ni, Sn, Zn [Fig. 1(*a*)] and Ti and V as reported by Taga *et al.*,[5] the absorbance increases gradually and then levels off after the critical micellization concentration (CMC) (6–20 mmol dm^{-3} SDS) has been reached. This pattern supports the theory that enhancement is due to the lowering of the surface tension and changes in viscosity. In Fig. 1(*b*), for Al, Ca, Cd, Cu and Pb, the absorbance exhibits an increase in the signal followed by a decrease to form an asymmetric peak. The intensity of the peak and the optimum surfactant concentration varies for different metals. The optimum absorbance signal for each element was obtained with the following SDS concentrations: 0.20, 0.30, 5.0, 10.0 and 2.0 mmol dm^{-3} for Al, Ca, Cd, Cu and Pb, respectively. Fig. 1(*c*) shows a sudden peak at 10 mmol dm^{-3} SDS and then a plateau for Sb and Fig. 1(*d*) shows a decrease in the absorbance signal for Sr and Rb just below the CMC followed by a rise to a plateau above the CMC.

Dodecyl sulphate surfactants gave the best enhancement effects for most of the metals studied. A cationic surfactant, CTAB, a non-ionic surfactant, Triton X-100, and the anionic surfactants, ADS, LDS, SDS and KDS were all initially studied with Cu, Cr and Pb. In the presence of both CTAB (1.0 mmol dm^{-3}) and Triton X-100 (0.54%), the signals were lower when compared with those obtained in water. The ratio of the values of the Beer's law slope obtained in the micellar

Table 1 Least-squares data for the working curves of analytes

Element	Concentration range (ppm)	Concentration of surfactant in water/ mmol dm^{-3}	Slope/ A ppm^{-1}	Intercept	Correlation coefficient
Al	0.5–20	H_2O	0.0046	−0.01	0.998
		20 (ADS)	0.0041	−0.003	0.986
		10 (LDS)	0.0050	−0.01	0.997
		0.2 (SDS)	0.0046	−0.01	0.999
		10 (KDS)	0.0042	−0.005	0.998
Ca	1–50	H_2O	0.00493	−0.009	0.996
		0.1 (ADS)	0.00557	−0.01	0.991
		0.1 (LDS)	0.00527	−0.005	0.999
		0.3 (SDS)	0.00424	−0.003	0.998
		1.0 (KDS)	0.00539	0.001	1.000
Cd	0.015–2.0	H_2O	0.102	−0.04	0.992
		10 (ADS)	0.117	−0.041	0.985
		11 (LDS)	0.124	−0.044	0.996
		5 (SDS)	0.0983	−0.040	1.000
		11 (KDS)	0.105	−0.040	0.997
Co	0.1–5.0	H_2O	0.0340	−0.001	0.999
		2 (ADS)	0.0353	0.001	1.000
		8 (LDS)	0.0362	0.001	1.000
		10 (SDS)	0.0356	0.004	1.000
		5 (KDS)	0.0418	0.007	0.999
Cr	1–50	H_2O	0.0171	0.020	1.000
		2.0 (ADS)	0.0172	0.058	0.996
		2.0 (LDS)	0.0208	0.140	0.970
		2.0 (SDS)	0.0204	0.110	0.997
		2.0 (KDS)	0.0212	0.130	0.973
Cu	0.04–10	H_2O	0.0429	−0.002	1.000
		2.0 (ADS)	0.0496	−0.005	1.000
		8.0 (LDS)	0.0503	0.000	1.000
		10.0 (SDS)	0.0466	−0.001	1.000
		5.0 (KDS)	0.0516	0.001	1.000
Fe	0.1–5.0	H_2O	0.0107	0.002	0.998
		2.0 (ADS)	0.0339	0.003	0.990
		8.0 (LDS)	0.0245	0.003	0.957
		10.0 (SDS)	0.0102	0.001	0.996
		5.0 (KDS)	0.0360	0.003	0.984
Mn	0.1–3.0	H_2O	0.0637	0.001	0.997
		2.0 (ADS)	0.0654	0.005	1.000
		8.0 (LDS)	0.0532	0.002	0.991
		10.0 (SDS)	0.0737	0.004	0.997
		5.0 (KDS)	0.0860	−0.011	0.993
Ni	0.1–5.0	H_2O	0.0320	−0.006	0.995
		2.0 (ADS)	0.0432	−0.014	0.998
		8.0 (LDS)	0.0416	0.003	0.995
		10.0 (SDS)	0.0332	−0.004	0.990
		5.0 (KDS)	0.0625	0.004	0.996
Pb	1.0–50.0	H_2O	0.00526	0.002	1.000
		2.0 (ADS)	0.00225	0.007	0.995
		2.0 (LDS)	0.00173	0.000	0.977
		2.0 (SDS)	0.00544	0.004	1.000
		2.0 (KDS)	0.00259	−0.001	0.982
Rb	0.1–5.0	H_2O	0.0199	−0.001	1.000
		2.0 (ADS)	0.0235	0.001	1.000
		5.0 (LDS)	0.0240	0.002	0.999
		10.0 (SDS)	0.0260	0.003	0.999
		5.0 (KDS)	0.0337	0.004	0.996
Sb	0.5–60	H_2O	0.00576	0.001	0.998
		2.0 (ADS)	0.00643	−0.004	0.991
		8.0 (LDS)	0.00588	0.006	0.999
		10.0 (SDS)	0.00564	0.002	0.994
		5.0 (KDS)	0.00608	−0.003	0.996
Sn*	15–40	H_2O	0.00196	0.007	1.000
		2.0 (ADS)	0.00245	0.034	1.000
		8.0 (LDS)	0.00241	0.012	1.000
		10.0 (SDS)	0.00208	0.012	0.999
		5.0 (KDS)	0.00260	−0.032	0.999
Sr	0.3–5.0	H_2O	0.0269	−0.007	1.000
		2.0 (ADS)	0.0274	0.001	0.854
		8.0 (LDS)	0.0196	0.001	0.999
		10.0 (SDS)	0.0257	0.003	0.991
		5.0 (KDS)	0.0336	0.003	0.998
Zn	0.04–1.0	H_2O	0.1685	0.003	1.000
		2.0 (ADS)	0.1643	0.004	1.000
		8.0 (LDS)	0.1758	0.000	0.999
		10.0 (SDS)	0.1695	0.004	0.999
		5.0 (KDS)	0.1626	0.004	0.999

* A dinitrogen oxide–acetylene flame is used in the pre-mix slot burner.

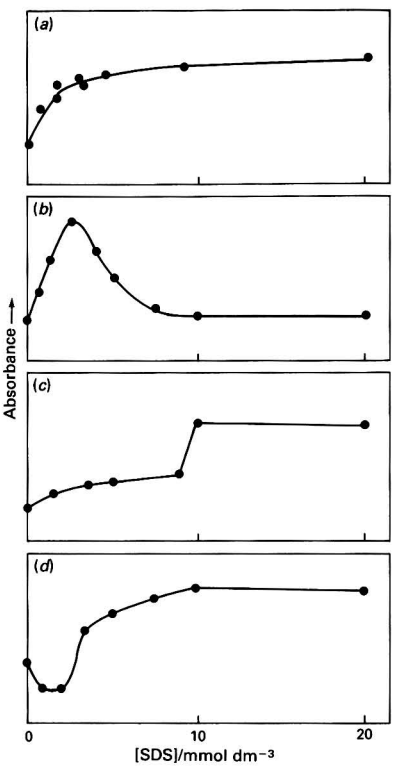

Fig. 1 Optimization of enhancement. (*a*) Pattern for Co, Fe, Mn, Ni, Sn, Ti, V and Zn; (*b*) pattern for Al, Ca, Cd, Cu and Pb; (*c*) pattern for Sb; and (*d*) pattern for Rb and Sr

system and water was used to compare the systems. The slope ratios for Cu were: 0.37 with CTAB and 0.50 with Triton X-100; for Cr: 0.95 with CTAB and 0.96 with Triton X-100; and for Pb 0.07 with CTAB and 0.35 with Triton X-100.

The investigation of the relationship between aspiration rate and viscosity and their effect on the absorbance was studied at two Cu and Cr concentrations in water and SDS. The aspiration rate for the high and low concentrations of the metal ion was similar in water (3.5 ml min^{-1}) and in 10 mmol dm^{-3} SDS (3.9 ml min^{-1}). These results are consistent with those reported by Armstrong *et al.*[4]

A pH study was carried out using the four dodecyl sulphates, ADS, LDS, SDS and KDS, and solutions of the metals Cd (0.80 ppm) and Cu (2.00 ppm) at pH 0.35 (HNO_3), pH 1.0 (0.20 mol dm^{-3} HCl and KCl), pH 2.0 (HCl and KCl), pH 4.0 (potassium hydrogen phthalate and 0.10 mol dm^{-3} NaOH), and pH 7.0 (0.10 mol dm^{-3} KH_2PO_4 and 0.10 mol dm^{-3} NaOH).[10] Each of the absorbance values obtained for the metal was compared with the value obtained in water and the appropriate SDS concentration. (The buffers are a source of other anions and cations.) Both Cd and Cu exhibited similar behaviour showing a 10–13% enhancement of absorbance in surfactant systems with buffers below pH 7 compared with an unbuffered surfactant system. The pH 7.0 buffered surfactant system gave similar values to the unbuffered surfactant system which exhibited an absorption enhancement when compared with the analyte in water.

Table 1 gives the linear regression analysis of the calibration graphs that were obtained for the analyte in the four dodecyl sulphate systems and water. A ratio of the slope for the dodecyl sulphate and aqueous system (enhancement ratio) was used to compare the micellar systems with water (Fig. 2). A minimum of nine data points were used to construct a calibration graph.

Surfactant systems that had an enhancement ratio of greater than 1.20 were considered to exhibit a large enhancement. The KDS system produced an enhanced signal for more elements, including Co, Cr, Cu, Fe, Mn, Ni, Rb, Sn and Sr, than the other surfactant systems. The following elements had a ratio greater than 1.20: Cd, Cr, Fe, Ni, Rb and Sn, for the LDS system; Fe, Ni and Sn, for the ADS system; and only Cr and Rb, for the SDS system.

Moderate enhancement was defined as those systems that had enhancement ratios between 1.1 and 1.2. These included Ca, Cd, Cu, Rb and Sb, for ADS; Cu, for LDS; and Mn, for SDS.

There were several metal analytes that had an enhancement ratio of less than 1.00 which indicates a signal depression in the presence of the surfactant system. The analytes with ratios between 0.95 and 0.99 included Zn, for the ADS system; Cd, Fe, Sb and Sr, for the SDS system; and Zn, for the KDS system. Others included Al (0.89) and Pb (0.43), for the ADS system; Mn (0.84), Pb (0.33) and Sr (0.75), for the LDS system; Ca (0.85), for the SDS system; and Al (0.91) and Pb (0.49), for the KDS system.

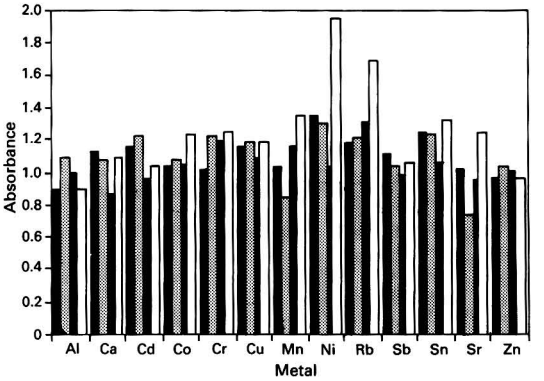

Fig. 2 Comparison of slope ratios of the dodecyl sulphates. Ratio of the dodecyl sulphate slope divided by the slope of the aqueous system for: ■, ADS; ▨, LDS; ▩, SDS; and □, KDS

Discussion

Elements can be categorized by their thermochemical behaviour into three groups.[11] Group A includes elements that do not ionize significantly in flames and that form few or no stable compounds. Their first ionization energy is high while the bond dissociation energy of their monoxides is low. This was the largest group studied; it included Cd, Co, Cu, Fe, Mn, Ni, Pb, Sb and Zn. Group B consists of those elements that have low first ionization energies and do not form refractory compounds. Many of these are usually studied by flame emission spectrometry and they include three of the cations used with the dodecyl sulphate, Li, Na and K. Of this group Sr and Rb were studied. Group C consists of elements that have a low ionization energy but that do form refractory compounds; of this group Al, Ca, Cr and Sn were studied.

Models for Enhancement

There have been several models proposed to explain the enhancement of absorbance signals for Cr and Cu using SDS. The ability of the surfactants to reduce surface tension at the critical micellization concentration (CMC) was first used to explain the atomic absorption enhancement.[1,2] Surfactants such as SDS are known to lower surface tension, thereby generating smaller droplets during the aspiration and nebulization processes. The significant increase in the number of smaller droplets would increase the efficiency of the laminar flow burner, by increasing the amount of the analyte reaching the flame. This theory suggests that a graph of absorbance *versus* concentration would increase up to the CMC and then level off. This behaviour is seen in Fig. 1(*a*) for Co, Fe, Mn, Ni, Sn, Ti, V and Zn. The observed absorbance would be independent of the type of surfactant that was used (cationic, non-ionic or anionic) and of the counter ion that was used with the dodecyl sulphate, if this were the only mechanism involved. However, the positively charged metal ions of the analyte may interfere with the micellar formation.

The aerosol ionic redistribution (AIR) theory of Borowiec *et al.*[7] was first used to explain salt enrichment in ocean spray when compared with ocean water. Armstrong *et al.*[4] have used this theory to explain the enhancement of the absorbance of Cu using SDS. The AIR theory proposes a mechanism of analyte transport to the flame by the interaction of the spectator ions of the anionic sulphate head group of the dodecyl sulphate with the metal cation of the analyte. An enrichment occurs at the double layer on the outside surface of the large drops. As these drops divide, a stripping action occurs that effectively concentrates the metal cation into the smaller droplets that are then nebulized and carried into the flame resulting in an increase in the analyte signal. With concentrations above the CMC, a decreased signal is observed because a higher concentration of micelles in the bulk solution is competing for interaction sites with those involved in the surface stripping action [see Fig. 1(*b*) for Al, Ca, Cd, Cu and Pb]. A cloudy solution for Al and Pb was formed at high SDS concentrations. This solubility problem would explain the decrease in signal at the higher SDS concentrations for these two elements without using the AIR theory.

Salts such as NH_4Cl, $K_2S_2O_8$, K_2SO_4, Na_2SO_3 and Na_2SO_4 were used for the suppression of interferences in the trace-level determination of Cr by Hurlbut and Chriswell.[13] They also reported that these salts caused an increased enhancement of the absorbance signal. The study of salt matrix effects has usually been confined to interference studies. The use of the four different cations (ammonium, lithium, sodium and potassium) with the dodecyl sulphates was used to help determine if there was a metal cation contribution to the signal enhancement. The metal cation could cause enhancement by the prevention of the formation of refractory oxides in the flame or it could act as a releasing agent.

In electrothermal atomic absorption, it is well known that the anionic group can greatly affect the behaviour of the metal during the atomization and vaporization steps. In flame atomic absorption spectrometry the anionic interference of nitrate salts compared with chloride salts has been studied.[2]

Table 2 Waste recovery study for the SDS system. The percentage difference between the absorbance measured in the recovered waste solution and the original analyte–SDS sample that was aspirated

	Element												
	Cd	Co	Cr	Cu	Fe	Mn	Ni	Pb	Rb	Sb	Sn	Sr	Zn
Absorbance difference (%)	−28	−59	−2	−20	−7	−51	−73	−29	−58	−49	−4	−2	+19

Table 3 Interference study of 19 elements. For each analyte and interferent cation two numbers are given; the relative deviation (%) from water water in the presence of the interfering cation and the relative deviation (%) from the SDS system in the presence of the interfering cation. The concentration of the interfering cation was 10 times that of the analyte

		Interfering element									
Element	Concentration(ppm)	Al	Bi	Ca	Cd	Ce	Co	Cr	Cu	Fe	K
Al	20	—	0, −3	6, 99	0, 1	8, − 1	—	—	5, 3	3, 0	10, −8
Ca	2	−97, −86	−1, 4	—	1, 6	0, 5	5, 16	−4, 6	5, 5	10, 15	5, 4
Cd	1	0, 1	−12, 7	−6, 5	—	7, 3	0, 52	1, 2	2, −2	−48, 2	−1, −2
Co	3	—	−6, 2	−1, 9	−23, 0	−2, 6	—	−5, 1	−4, 4	−3, 3	−1, 1
Cr	2	−11, 2	−26, −3	6, −3	0, −3	−21, −8	−26, −5	—	4, 6	−9, −6	6, 0
Cu	20	3, 0	2, 0	3, 5	4, 0	1, −1	4, 2	3, −1	—	2, 0	3, 7
Fe	2	−33, −17	−39, 0	22, −15	39, 8	−17, 0	0, 8	−17, −17	33, 75	—	−11, −17
Mn	2	−2, −9	50, −10	−1, −4	1, −4	16, −4	−4, −5	4, −3	0, 0	7, 0	−1, 0
Ni	2	−10, −48	−16, −4	3, −20	5, −3	−10, −55	−2, −4	−8, −33	42, −14	−8, −12	−5, −13
Pb	4	3, 8	3, −3	6, −25	3, −8	−80, 10	−40, −10	−80, −18	15, −5	−3, −8	0, −8
Rb	4	—	7, −8	−11, 14	6, 3	17, 4	12, 6	16, −4	−51, −22	11, −18	22, −14
Sb	20	2, 12	−96, 8	−22, 9	12, −19	32, 36	−1, 0	15, 33	−80, 5	−4, 17	16, 22
Sn	20	−94, −76	−9, 5	−62, 61	63, 23	1, 53	−92, −400	14, 3	−18, −50	−25, 52	−8, −32
Sr	3	−60, 80	0, 0	−12, −19	11, 7	−9, −15	5, −1	13, −14	−5, −3	0, 4	22, 1
Zn	0.2	—	89, −2	3, −5	86, 7	30, 2	9, 2	70, −10	0, 2	14, 0	9, 2
		Mg	Mn	Na	Ni	Pb	Sb	Sn	Sr	Zn	
Al	20	5, −3	6, 0	11, 5	−2, −7	−3, −3	−3, −5	6, −5	11, 0	—	
Ca	2	18, 30	1, 14	5, 7	−1, −7	7, 4	4, 11	−4, 3	2, 13	0, 17	
Cd	1	1, 6	2, 6	3, −3	3, 52	37, 5	1, 4	2, 7	1, −4	1, 0	
Co	3	−5, 6	−4, 3	−2, −3	−6, 3	−5, 1	−5, 12	4, 5	−1, 10	1, −2	
Cr	2	−13, −23	13, −5	4, −5	−13, −6	−60, −3	9, −2	11, −3	−8, 0	8, −2	
Cu	20	4, −2	5, −2	7, 1	3, −4	4, 4	3, 0	3, 2	3, 3	3, −2	
Fe	2	−33, −25	−39, 25	−1, −33	−28, −17	−33, −25	−28, −33	−33, −17	0, −25	−33, −25	
Mn	2	6, −13	—	−1, −3	1, 0	−3, −5	41, −7	0, 0	1, −24	−1, −4	
Ni	2	−3, −12	−4, −22	−7, −28	—	−11, −41	−7, −29	−11, 0	−32, −29	−1, −17	
Pb	4	12, −5	−15, −15	9, −18	9, −20	—	−6, −3	6, −28	12, 3	12, −13	
Rb	4	22, −10	9, 0	12, −8	15, −10	10, −8	4, −4	10, −13	15, −7	2, −7	
Sb	20	−5,, 9	15, 5	9, 1	1, 5	9, 5	—	20, 13	4, 9	3, 213	
Sn	20	−1, −47	−24, −42	−18, −40	−23, −58	−3, −6	−13, −47	—	−5, 39	13, 21	
Sr	3	−38, −25	−8, −12	8, 1	2, −18	5, 2	5, 2	12, 2	—	9, −11	
Zn	0.2	89, 10	14, 2	80, 2	63, −7	17, −5	14, 10	26, −2	20, 0	—	

The major evidence in support of the AIR theory with regard to Cu was the decrease in the amount of Cu found in the nebulization waste. This decrease was a result of the stripping action, which concentrated the metal cation in the smaller droplets that were carried into the flame, while the larger droplets went down the drain. By collecting and analysing the waste from the analyte–surfactant system, one should observe a decreased absorption signal for the analyte. A series of solutions of the various dodecyl sulphate surfactants was analysed. The absorbance data of the waste solutions were compared with the corresponding absorbance values obtained from the solution that generated the aspirated waste (Table 2). When a 2.0 ppm solution of Cd^{2+} in SDS (5.0 mmol dm^{-3}) gave a signal of 0.264 A, the recovered waste was collected for 1 min and discarded; the subsequent portion was collected and analysed and gave a 28% drop in the signal $[(0.190 - 0.264)/0.264] \times 100$. This is consistent with the AIR theory, *i.e.*, a decrease in waste analyte signal compared with the original analyte–surfactant solution.

For SDS the largest decreases in the waste solution signals occurred with Co, Mn, Ni, Rb and Sb. A moderate decrease of 20, 28 and 29% occurred with Cu, Cd and Pb, respectively. A few metal analytes (Cr, Sn, Sr, Ti, V and Fe) exhibited little or no effect. Surprisingly the waste recovery signal for Zn (+19%) was greater than the solution.

With ADS, LDS and KDS the results were not always consistent with those obtained with SDS. However, waste recovery determination of four metals, using KDS, did give results very similar to the SDS study for Co, Mn, Ni and Rb. For Co and Ni both ADS and LDS were very similar, but for Mn the ADS, LDS and KDS systems all gave a much greater decrease between the waste recovery and the generating analyte than did the SDS. For Rb the ADS, SDS and KDS systems exhibited the same result (−58%), the LDS system had only a 19% decrease. These small inconsistencies with the same metal analyte but with different dodecyl sulphates indicate mechanisms other than those suggested by the AIR theory may be involved.

Salt Study

Three different elements (Ca, Cd and Cu) were studied with salts added to the solution instead of the dodecyl sulphates. These salts had the same four cations (NH_4^+, Li^+, Na^+ and K^+) in concentrations of 1.0, 5.0, 8.0, 10.0, 20.0 and 50.0 mmol dm^{-3} prepared from the following salts; NH_4NO_3, NH_4Cl, $(NH_4)_2SO_4$, LiCl, Li_2SO_4, Na_2SO_4, NaCl, $NaNO_3$, Na_3PO_4, K_2SO_4, KCl and KNO_3, each with 5.00 ppm of Ca, 0.80 ppm of Cd and 2.00 ppm of Cu added. The experimental conditions were the same as those used elsewhere in this work

except that a blank was made for each salt concentration. Many of these salts exhibited an enhancement of the analyte when compared with water.

For Ca, $(NH_4)_2SO_4$ and Li_2SO_4 gave similar enhancements to ADS and LDS. In the presence of K_2SO_4 the signal was enhanced by a ratio of 1.15 while in the presence of KDS it was slightly less at 1.09. For sodium salts (5–50 mmol dm^{-3}) the signal was enhanced by a ratio of 1.01, essentially the same as water, while in the presence of SDS the ratio was only 0.86, *i.e.*, a 14% decrease in signal. The Na_3PO_4 salt was not studied because of the known phosphate anion interferences.

Using a 0.80 ppm Cd solution with the various salts, all salts from 2.0 to 50 mmol dm^{-3} caused an absorption enhancement. The enhancement ratios of 1.34 and 1.31 obtained using ammonium and lithium salts, respectively, were less than those obtained with ADS and LDS, which had ratios of 1.86 and 1.93, respectively.

The potassium salts (KCl and KNO_3) gave values very similar to those obtained with KDS except that at concentrations of $\geq$20 mmol dm^{-3}, they were 15% higher. The ratios obtained using K_2SO_4 were consistently higher ($\approx$15%) for concentrations from 5.0 to 50 mmol dm^{-3}.

Sodium nitrate and Na_3PO_4 caused enhancements similar to SDS. It was found that using NaCl and Na_2SO_4, enhancement ratios of 1.55 and 1.45, respectively, were obtained while for 5.0 mmol dm^{-3} SDS the ratio was 1.36 when compared with water.

The addition of ammonium, lithium and potassium salts to a 2.00 ppm copper standard solution caused enhancements similar to their respective dodecyl sulphates. Potassium sulphate had a slightly greater effect, with an enhancement ratio of 1.54 compared with a ratio of 1.38 for 5.0 mmol dm^{-3} KDS, compared to water. The ratio of 1.19 obtained using SDS was similar to the Na_3PO_4 value, but less than the values using NaCl, $NaNO_3$ and Na_2SO_4, all of which had an enhancement ratio of 1.40 for concentrations of 2–20 mmol dm^{-3}.

Interference Study

Nineteen elements were used in an interference study (Table 3). The concentration of the interfering cation was ten times that of the analyte. For example, an aqueous solution containing 2.00 ppm of Cr was analysed with and without the addition of 20.00 ppm of Al. A decrease of 11% in the absorption signal was observed in the presence of Al. Similarly a 2.00 ppm Cr–SDS solution was analysed with and without the addition of 20.00 ppm of Al. The absorption signal exhibited only a 2% increase in the presence of Al which effectively eliminates Al as an interferent. The other elements that cause interferences in the determination of Cr (Bi, Ce, Co, Fe, Mg, Mn, Ni, Pb, Sb, Sn, Sr and Zn) have, with the exception of Mg, a marked decrease in their interference in the presence of SDS. Similarly the interferences of Fe, Mn, Rb, Sn, Sr and Zn generally decreased in the SDS system compared with water. The absorption signal for Ca in the presence of an interfering cation in the SDS system showed a marked increase while Ni absorbances in the presence of an interfering cation in the SDS system were generally depressed when compared with water. The interfering cations of Bi, Cd, Cr, Mg, Pb and Sn showed a decreased interference for the various analytes studied in the presence of SDS.

Conclusions

The use of an anionic surfactant, dodecyl sulphate, resulted in an increased absorption signal and the masking of interferences for many of the metal ions studied. While the AIR theory may be used to explain the enhancement effects for some of the analytes studied, not all of the metal analytes exhibited the predicted enhancement or the marked decrease of analyte in the nebulization waste. By varying the cationic head group of the surfactant, a significant difference was observed for many of the metal analytes studied. The salt study also showed that certain inorganic salts exhibited a similar behaviour. While this is consistent with the original AIR theory,[7] it is not consistent with the enrichment model of the anionic surfactant systems described by Armstrong *et al.*[4]

There appear to be several competing chemical–physical relationships that may be present in any one system. The dominance of one system or model for one element such as Cr does not mean that all analytes behave in the same manner. The presence of certain metals in a surfactant system may actually affect the bulk properties of that system. This was observed in the changes in viscosity and surface tension during the determination of Al and Pb using SDS.

The complex micellar systems which modify both the nebulization aerosols and the analyte atomization process are only partially understood, however, the analytical applications of these systems and the models used to explain these processes give useful information towards the complete understanding of flame–analyte interactions.

References

1 Kodama, M., Shimizu, S., Sato, M., and Tominaga, T., *Anal. Lett.*, 1977, **10**, 591.
2 Kodama, M., and Miyagawa, S., *Anal. Chem.*, 1980, **52**, 2358.
3 Venable, R. L., and Ballad, R. V., *Anal. Chem.*, 1974, **46**, 131.
4 Armstrong, D. W., Kornahrens, H., and Cook, K. D., *Anal. Chem.*, 1982, **54**, 1325.
5 Taga, M., Takabatake, Y., and Yoshida, H., *Bunseki Kagaku*, 1984, **33**, 439.
6 Farino, J., and Browner, R. F., *Anal. Chem.*, 1984, **56**, 2709.
7 Borowiec, J. A., Boorn, A. W., Dillard, J. H., Cresser, M. S., Browner, R. F., and Matteson, M. J., *Anal. Chem.*, 1980, **52**, 1054.
8 Billman, J. H., and Audrieth, L. F., *J. Am. Chem. Soc.*, 1938, **60**, 1946.
9 Lottermoser, A., and Püschel, F., *Kolloid-Z.*, 1933, **63**, 176.
10 *Analytical Methods for Atomic Absorption Spectrophotometry*, Perkin-Elmer, Norwalk, CT, 1976.
11 *CRC Handbook of Chemistry and Physics*, ed. Weast, R. C., CRC Press, Cleveland, OH, 51st edn., 1971, p. D-104.
12 Magyar, B., *CRC Crit. Rev. Anal. Chem.*, 1986, **17**, 145.
13 Hurlbut, J. A., and Chriswell, C. D., *Anal. Chem.*, 1971, **43**, 465.

Paper 0/02034F
Received May 9th, 1990
Accepted January 3rd, 1991

Use of Flow Injection Flame Atomic Absorption Spectrometry for Slurry Atomization. Determination of Copper, Manganese, Chromium and Zinc in Iron Oxide Pigments

Ignacio López García, Francisca Ortiz Sobejano and Manuel Hernández Córdoba*
Department of Analytical Chemistry, Faculty of Chemistry, University of Murcia, 30071 Murcia, Spain

A procedure for the determination of copper, manganese, chromium and zinc in slurries of commercial iron oxide pigments using flame atomic absorption spectrometry is described. The samples are suspended in water and introduced directly into the spectrometer using a flow injection manifold with air-compensation of the difference between the peristaltic pump flow-rate and the nebulizer uptake rate. In order to avoid matrix effects, calibration is achieved by using slurries prepared from previously analysed iron oxide samples. Excellent agreement was found between the results of the slurry procedure and those obtained by conventional acid-dissolution.

Keywords: *Slurry; atomic absorption spectrometry; flow injection; iron oxide pigment*

The direct introduction of solid samples[1] into a flame for atomic absorption measurements has been studied by several workers as this approach offers a rapid method for the analysis of materials that might normally require pre-treatment using time-consuming digestion or fusion procedures. The analysis of solid samples using atomic absorption spectrometry (AAS) can be carried out either by direct solid sampling or by sampling of slurries. In the former example, experimental difficulties with sample homogeneity, the need for repeated weighings of micro-amounts of sample and the use of devices to introduce a very small amount of sample into the flame accurately are encountered. On the other hand, the use of samples with a fine particle size, suspended in an aqueous or organic medium, appears to be a reliable alternative, as such slurries can be easily handled in the same way as liquid samples. Hence, Fuller and co-workers[2,3] followed this procedure in order to determine trace metals in titanium oxide pigments. Willis[4] studied in detail the analysis of various geological materials and found that the results for one particular element could vary by a factor of two between rocks of widely different types. O'Reilly and Hicks[5] carried out an extensive study on the direct analysis of coal samples, and determined 17 major, minor and trace elements. Other workers have also developed procedures for the determination of several elements in soil,[6] animal tissue[7] and vegetables.[8–10]

The slurry flame AAS procedures are not free from problems. Although the essential condition of a sufficiently small particle size can be met, there is a serious risk of the nebulizer clogging when the suspension is aspirated. In order to avoid this, discrete nebulization[2] and Babington nebulizers[7] have been used.

Flow injection (FI) methodology can be considered a suitable way of avoiding clogging problems when introducing a suspension into the flame. The small volume of the injected sample and the rinsing action of the carrier stream are essential factors which contribute to the success of the procedure. In fact, the approach is similar to using FI for the introduction of samples with high concentrations of dissolved solids into the flame, a recognized[11] advantage of the FI technique.

In this paper, the determination of copper, zinc, manganese and chromium in commercial iron oxide pigments using FI to introduce suspensions of the samples is described. The procedure is rapid, reliable, avoids the sample dissolution step and affords results that agree with those obtained by using conventional dissolution in acid.

Experimental

A Pye Unicam SP1900 atomic absorption spectrometer was used in conjunction with a Hewlett-Packard 7040A recorder. Experiments to demonstrate the absence of background were carried out using a Perkin-Elmer Model 1100B atomic absorption spectrometer with deuterium-arc background correction. The measurements were made at 324.8, 279.5, 213.9 and 357.9 nm for copper, manganese, zinc and chromium, respectively, using conventional hollow cathode lamps. The spectrometers were operated in accordance with the standard conditions recommended by the manufacturers for maximum sensitivity with air–acetylene flames.

The FI manifold has been described previously.[12] A Gilson Minipuls 3 peristaltic pump was used together with an Omnifit injection valve. Sample loops were made of 0.8 mm i.d. polytetrafluoroethylene (PTFE) tubing. All connecting lines were made of 0.5 mm i.d. PTFE tubing. As indicated elsewhere,[12] a three-way connector was included in the manifold in order to provide an inlet for air. This T-piece allows air-compensation of the difference between the nebulizer uptake rate and the pumping flow-rate, thus acting as a 'pre-nebulizer'.

All reagents were of analytical-reagent grade and doubly distilled water was used throughout. Stock solutions of copper, manganese, chromium and zinc (1000 mg l^{-1}) were prepared as recommended in the Perkin-Elmer user's manual. Triton X-100 (octylphenoxypolyethoxyethanol) was obtained from Merck and sodium hexametaphosphate (HMP) from Fluka; these chemicals were used as received.

The commercial iron oxide samples were previously analysed by treating 1 g of sample with a mixture of hot hydrochloric and nitric acid (3 + 1) until total dissolution was achieved. The copper, manganese, chromium and zinc contents were then determined by conventional AAS using the standard additions procedure.

Procedure

Dry the samples in an oven for 1 h at 105 °C. Grind the samples in a ball mill for 5 min and then sieve the powders using a 325 mesh sieve. Weigh 0.5 g of the sieved sample (or 0.1 g for the determination of zinc), add 0.5 g of HMP and make up to 50 ml with water. Stir the mixture magnetically for 10 min. While

* To whom correspondence should be addressed.

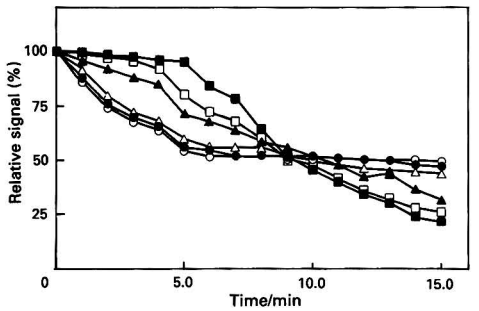

Fig. 1 Effect of HMP: ○, 0.2; ●, 0.4; △, 0.6; ▲, 1.0; □, 1.5; and ■, 2.0% m/v HMP

the suspension is being stirred, fill the sample loop and inject the plug into the FI manifold. Use a 1% HMP solution as carrier. Measure the peak height and compare this with a calibration graph obtained using several previously analysed samples. It is advisable to clean the spray chamber daily using an acidic solution in order to remove any sample residues.

Results and Discussion

As stated above, a reproducible and sufficiently small particle size is the most critical part of the slurry flame AAS approach. Iron oxide pigments are obtained as uniform powders of very small particle size. In order to demonstrate this point, three different commercial samples were suspended in water and shaken by hand for about 5 min. Aliquots of the suspensions were taken and examined using electron microscopy. The electron micrographs showed needle-shaped particles ranging in size from 2 to 5 μm or less, which tended to form small clusters. The particle size was sufficiently small and there was no need for additional grinding. However, as indicated under Experimental, the dry powder forms agglomerates, and, in order to ensure homogeneity and remove any foreign material, the samples were ground for 5 min and dry-sieved through a 325 mesh sieve, discarding the small fraction of larger particle size.

The protective colloid Triton X-100 can be of use in obtaining iron oxide slurries, as has been shown previously for the determination of lead[13] and arsenic[14] by electrothermal AAS. However, for the flame approach described here, several drawbacks were found. As the sensitivity of the flame procedures is less than that of the electrothermal methods, the percentage of sample in the slurry must be higher and more Triton X-100 is needed in order to obtain suitable stabilization. When the surfactant concentration was higher than about 0.20%, the slurries gave rise to abundant foam and small air bubbles were trapped in the sample loop of the FI manifold, making reproducibility worse. Although this problem could be overcome by adding several drops of antifoaming agent ['Antifoam A' (Fluka)] to the slurry, it was also noted that Triton X-100 decreased the absorption signal of copper, both for aqueous solutions and for slurries, and hence this surfactant was not employed.

Better results were obtained using HMP. In order to study the stabilizing characteristics of this reagent, several 2% slurries were prepared in the presence of various amounts of HMP and stirred for 10 min, using a magnetic stirrer. Stirring was then stopped, and 135 μl aliquots were injected into the FI manifold at 1 min intervals and the copper peak height was measured. The results are shown in Fig. 1, where the signals are normalized, *i.e.*, data on the ordinate are the ratios (%) of the signals for the time given on the abscissa to the maximum signal for the slurry being studied. The HMP did not affect the atomic absorption response and no problems from air bubbles were observed for solutions containing up to 1% HMP. The use of 1.5 or 2% HMP solutions gave rise to very small air

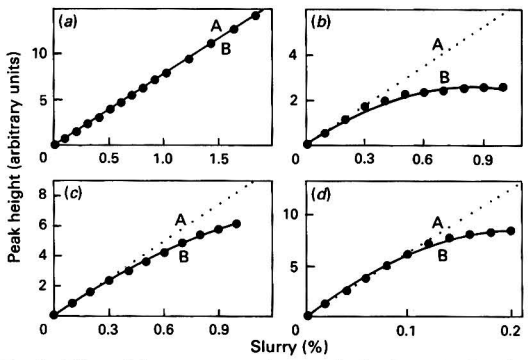

Fig. 2 Effect of the percentage of sample in the slurry. Broken line (A) indicates the response for aqueous solutions. Solid line (B) shows the response for slurries. (*a*) Cu; (*b*) Cr; (*c*) Mn; and (*d*) Zn

bubbles in the coils of the FI manifold. As can be seen in Fig. 1, the stabilizing effect is only partial and even for a 2% HMP concentration the absorbance decreased a few minutes after stirring was stopped. With this in mind, aliquots were taken while the suspension was being continuously stirred and a 1% solution of HMP was used both as carrier and as an aid to partial stabilization of the suspension.

A detailed study on the effect of both the spoiler and impact bead in the nebulizer system, the observation height and the optimum flow of acetylene demonstrated that there were no significant differences between the spraying of slurries and aqueous solutions. Hence, the instrumental parameters of the spectrometer were adjusted in the usual way, using aqueous solutions. Because the instrument used had no background corrector, several experiments were performed on a spectrometer fitted with a deuterium device. Experiments were also carried out using wavelengths other than those of the resonance of the four elements. The results demonstrated the absence of both unspecified and structured background. This is an important advantage because a very simple, low-cost instrument can be used.

In addition, the effect of both sample loop size and pumping rate was studied in the ranges 35–325 μl and 0.5–3.0 ml min^{-1}, respectively. A pumping rate of 2 ml min^{-1} with a 135 μl sample loop was selected as the most suitable. Under these experimental conditions the theoretical sampling frequency was calculated to be 120 samples h^{-1}. The practical sampling frequency using duplicate injections was about 40 samples h^{-1}. It is interesting to note that in the absence of HMP a significant peak tailing effect was observed, leading to a lower sampling frequency. This effect was almost completely suppressed when a 1% aqueous solution of HMP was used as carrier.

Calibration

Under the conditions described above, the absorption signals of the four analytes were reproducible. The main problem to solve was the selection of a suitable calibration procedure. As a first step, in order to obtain reference values to evaluate the various calibration approaches, eight samples of commercial iron oxide pigments were dissolved in acid and the copper, manganese, zinc and chromium contents were determined using the standard additions procedure. One of these commercial samples was also used to prepare several slurries covering the range 0.05–1.5%; the suspensions were injected into the FI manifold and the peak heights of the four analytes were measured. The results are summarized in Fig. 2 where the broken line shows the response obtained when aqueous standard solutions were injected into the FI system under identical experimental conditions. As can be seen from Fig. 2,

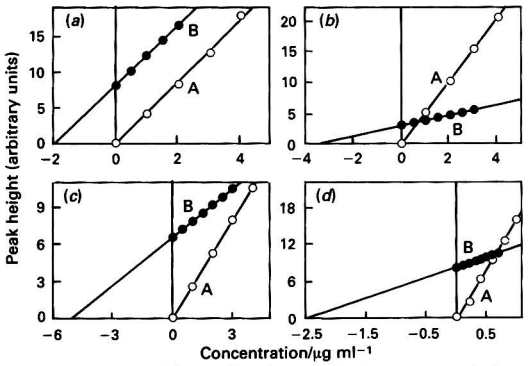

Fig. 3 Standard additions calibration graphs: A, aqueous solutions; and B, 1% slurries; the graph for zinc was obtained with a 0.2% slurry. (*a*) Cu; (*b*) Cr; (*c*) Mn; and (*d*) Zn

Table 1 Comparison of the results for a representative iron oxide sample analysed by the acid-dissolution and suspension procedures

Element	Concentration found by acid-dissolution procedure/ μg g⁻¹*	RSD† (%)	Concentration found by suspension procedure/ μg g⁻¹*	RSD† (%)
Copper	61 ± 3	4.5	65 ± 1	2.4
Chromium	201 ± 7	3.8	205 ± 5	2.6
Manganese	138 ± 5	3.8	130 ± 4	2.9
Zinc‡	221 ± 11	5.2	210 ± 7	3.6

* Mean value ± standard deviation.
† RSD = Relative standard deviation.
‡ Data for zinc were obtained with 0.2% slurries.

the signal obtained for copper is the same, irrespective of whether the metal is introduced into the flame in the form of a slurry or as an aqueous solution, which indicates that direct calibration with aqueous standards is valid. On the other hand, for manganese, zinc and chromium, all of which have lower atomization efficiencies than copper, the analytical signals obtained with slurries differ from those given by aqueous solutions of the same concentration, this effect being more marked as the percentage of sample in the slurry increases. This means that direct calibration can only be successfully carried out for dilute slurries, an unacceptable situation from a practical point of view because of weak signals and poor reproducibility.

In order to confirm these findings, standard additions calibration graphs were obtained for 1% slurries. Fig. 3 shows, as expected, that the slope of the standard additions graph for copper is virtually identical with that obtained for an aqueous solution. In contrast, the slopes of the standard additions graphs for manganese, zinc and chromium differ from those given by aqueous standards. Further, it was observed that the slopes were dependent on the percentage of sample in the slurry, leading to incorrect, low results.

The obvious alternative is to use as standards one or more slurries prepared from the iron oxide samples previously analysed using dissolution in acid followed by conventional AAS measurement as described under Experimental. As the matrix effect described above for the manganese, chromium and zinc signals depends on the percentage of oxide in the slurry, it is necessary for the standard slurries and those of the samples being analysed to be prepared so that they contain the same percentage of oxide. Taking into account the levels of the four analytes in the samples studied, 1% of oxide in the slurries appears to be adequate for the determination of copper, manganese and chromium and 0.2% for zinc.

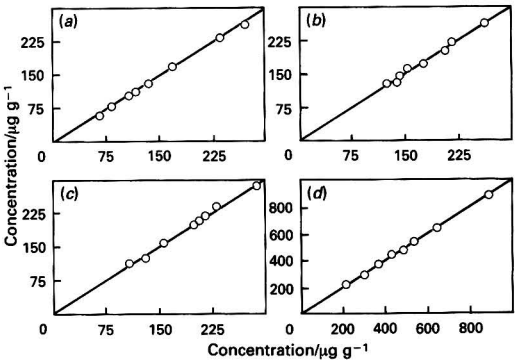

Fig. 4 Comparison of results for eight commercial iron oxide samples. Values on the abscissae were obtained using the slurry procedure. Values on the ordinates were obtained using a conventional acid-dissolution procedure. Solid line indicates 100% correlation. Data for zinc were obtained with 0.2% slurries. (*a*) Cu; (*b*) Cr; (*c*) Mn; and (*d*) Zn

In order to compare the results obtained using suspensions with those given by the conventional acid-dissolution procedure, a representative sample was taken and analysed repeatedly. Hence, five 1% slurries of this sample were prepared and 40 injections of each slurry were carried out, ten for each analyte. The acid-dissolution procedure was also performed five times. The results, summarized in Table 1, show that there is agreement between the procedures and that the precision attained with the suspension approach is similar to that obtained with the acid-dissolution procedure. The same methodology was followed for seven other commercial samples and the results are presented in Fig. 4. The line drawn on each plot is the line of slope equal to 1, corresponding to 100% correlation between the values found using the two procedures.

Conclusion

The results presented here show that slurries can be used successfully in FI-AAS measurements with advantages over conventional procedures involving dissolution in acid. The slurry procedure is rapid, reproducible and accurate. The discrete nature of the FI sample introduction and, in particular, the effective rinsing action of the carrier stream, as pointed out by Fang *et al.*[11] for the comparable situation of analysing samples with a high dissolved solids content, are essential factors in the success of this approach. We believe that the inclusion in the FI manifold of a simple three-way connector with a tip open to the air, which compensates for the difference between the nebulizer uptake rate and the peristaltic pump flow-rate, aids the effective fragmentation of the plug.

Slurry FI-AAS is not a general approach because the samples must have a small particle size. If such a condition is met, as is true for the commercial iron oxides studied here, and no lengthy grinding step is necessary, the approach could be useful for routine purposes.

The authors are grateful to the Spanish Dirección General de Investigación Científica y Técnica (DGICYT) (Project 87-0053) for financial support and to the Electron Microscopy Section of the University of Murcia for the electron micrographs.

References

1 Langmyhr, F. J., and Wibetoe, G., *Prog. Anal. At. Spectrosc.*, 1985, **8**, 193.
2 Fuller, C. W., *Analyst*, 1976, **101**, 961.

3 Fuller, C. W., Hutton, R. C., and Preston, B., *Analyst*, 1981, **106**, 913.
4 Willis, J. B., *Anal. Chem.*, 1975, **47**, 1752.
5 O'Reilly, J. E., and Hicks, D. G., *Anal. Chem.*, 1979, **51**, 1905.
6 Štupar, J., and Ajlec, R., *Analyst*, 1982, **107**, 144.
7 Mohamed, N., and Fry, R. C., *Anal. Chem.*, 1981, **53**, 450.
8 Fagioli, F., Landi, S., Locatelli, C., and Bighi, C., *Anal. Lett.*, 1983, **16**, 275.
9 Fagioli, F., and Landi, S., *Anal. Lett.*, 1983, **16**, 1435.
10 Carrión, N., de Benzo, Z. A., Eljuri, E. J., Ippoliti, F., and Flores, D., *J. Anal. At. Spectrom.*, 1987, **2**, 813.
11 Fang, Z., Welz, B., and Schlemmer, G., *J. Anal. At. Spectrom.*, 1989, **4**, 91.
12 López García, I., Hernández Córdoba, M., and Sánchez-Pedreño, C., *Analyst*, 1987, **112**, 271.
13 López García, I., and Hernández Córdoba, M., *J. Anal. At. Spectrom.*, 1989, **4**, 701.
14 López García, I., and Hernández Córdoba, M., *J. Anal. At. Spectrom.*, 1990, **5**, 647.

Paper 0/04736H
Received October 22nd, 1990
Accepted January 17th, 1991

Separation of Trace Amounts of Silver by Volatilization Prior to Its Determination in Copper Tailings and a Copper Ore by Atomic Absorption Spectrometry

Barbara Różańska
Department of Analytical Chemistry, Warsaw University of Technology, Noakowskiego 3, 00-664 Warsaw, Poland

The volatilization of Ag from samples of complex composition by using various additives was investigated and the optimum conditions were established, *viz.*, additive, Florisil–CaO (5 + 1–10 + 1 m/m); additive : sample mass ratio, 2; heating time, 2 h at 1200 °C; and air flow-rate, 0.17 l min^{-1}. The accuracy and precision of the method for the determination of Ag by flame atomic absorption spectrometry after separation by volatilization from copper tailings and a copper ore were found to be good.

Keywords: *Volatilization technique; additive; copper tailings; silver determination; atomic absorption spectrometry*

The determination of the small amounts of Ag present in copper ores and tailings by flame atomic absorption spectrometry (AAS) requires dissolution of the samples, followed by separation and concentration of the Ag. Because of the complex composition of the samples, both processes tend to be time consuming. Dissolution under pressure in a PTFE bomb with a mixture of HF and HNO_3, and separation by solvent extraction are most frequently used.[1,2]

Volatilization from solid samples appears to be an attractive separation method for trace elements. The procedure is simple and enables the losses of analyte and contamination from the reagents to be minimized.

Methods for the separation of trace elements by volatilization have been reviewed by Tölg[3] and Bächmann.[4] A volatilization technique was mainly used to separate Se, As, Cd, Zn, Tl and Pb, in a stream of oxygen or hydrogen, from relatively non-volatile matrices.[5–9]

Recently, Zhuikov and co-workers[10,11] studied the volatility of elements in oxygen and hydrogen streams at 1000–1200 °C, their interaction with SiO_2 and absorption of the elements on various high-temperature oxide filters in an air or oxygen stream. These workers proposed a method for the separation and concentration of Pt, Ir and Au from geological samples prior to their determination by neutron activation and X-ray fluorescence.[10,11]

In order to increase the yield of analyte volatilization from a sample of complex composition, the addition of suitable substances to the heated sample is often required. The choice of the optimum additives depends on the elements to be volatilized and the composition of the sample. In previous papers, MgO was used in the thermal evolution of Se (SeO_2) from dust and slags produced by the copper industry;[12] alumina, a Florisil–CaO mixture or MgO was used for pyrolytic separation of mercury from industrial samples.[13,14]

Zhuikov and co-workers[10,11] examined several additives and achieved increased yields of Pt (PtO_2) and Ir (IrO_3) by sublimation in the presence of Nb_2O_5, TiO_2 and metallic Nb. The recovery of Ag was not investigated.

The application of volatilization to the separation of trace amounts of Ag has not been reported previously. This work is a continuation of our earlier investigations into the separation of trace elements from industrial samples of complex composition by volatilization. The experimental arrangement is based on apparatus described by Geilmann[5] and Heinrichs and Keltsch.[9]

Experimental

Apparatus

The typical apparatus used for separation by volatilization is shown in Fig. 1. A quartz tube (16 mm i.d.) was connected by a ground joint to a quartz water-cooled condenser. A resistance-type electric furnace was used. The temperature in the sample heating zone can reach 1200–1300 °C and was measured with a 10% Rh–Pt : Pt thermocouple. Air purified by passage through molecular sieves was used as a carrier gas. The flow-rate was regulated by a needle valve and controlled by a flow meter. The sample was placed in an alundum boat.

A Pye Unicam SP-90 series 2 atomic absorption spectrometer and a Thermo Jarrell-Ash S11 atomic absorption spectrometer were also used.

Reagents

All the chemicals used were of analytical-reagent grade.

Stock solution of Ag, 1 mg ml^{-1}. Prepared by dissolving 1.575 g of $AgNO_3$ in water to which 1 ml of concentrated HNO_3 had been added and diluting to 1 l with water.

Alumina (Merck, 1077); specific surface area, 131 m^2 g^{-1}.

Alumina, obtained from the Department of Solid State Technology, Warsaw University of Technology; specific surface area, 190 m^2 g^{-1}.

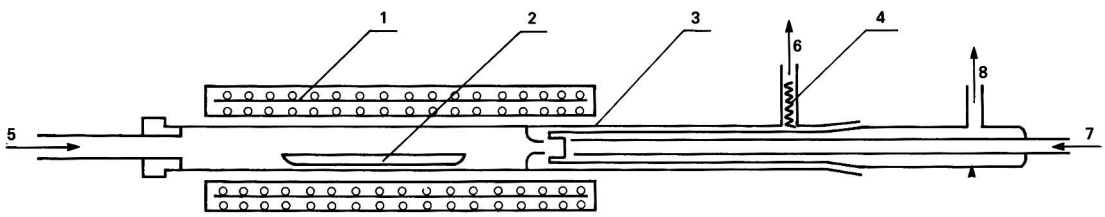

Fig. 1 Experimental arrangement for the volatilization of Ag: 1, electric furnace; 2 alundum boat; 3, quartz tube; 4, Teflon foil; 5, air inlet; 6, air outlet; 7, water inlet; and 8, water outlet

Florisil (magnesium silicate), 60–100 *mesh (Fluka)*.
Calcium oxide (Reachim).

Procedure

A weighed portion of the finely ground sample (about 50 mg) was mixed with the appropriate additives and placed in the alundum boat in the quartz tube and heated for 2 h at 1200 °C in an air stream at a flow-rate of 0.17 l min^{-1}. After cooling the tube and withdrawing it from the furnace, concentrated HNO_3 was transferred by pipette into the condenser through the 'gas inlet' until the finger was completely immersed. After 3 h, the acidic solution was transferred into a quartz beaker, the condenser rinsed with a small amount of concentrated HCl and the solution evaporated to dryness. After cooling, the walls of the beaker were rinsed with 1.5 or 4 ml of 1 mol dm^{-3} HCl and the beaker was covered and gently heated. The solution was transferred into a 2 or 5 ml calibrated flask and diluted to the mark with 1 mol dm^{-3} HCl. Silver was measured by AAS with standards prepared in 1 mol dm^{-3} HCl.

Results

Preliminary experiments were carried out with copper tailings 'C', which is relatively rich in Ag. The determined amounts of Ag were compared with results obtained after an extractive separation. The blanks from the additives were below the limit of detection.

By using the simple experimental arrangement described here, the volatilized Ag was collected not only on the cooled finger surface but also on the surface of the tube condenser. The geometrical parameters of the furnace and the condenser can be optimized but at this stage of the investigation the sole aim was to determine the conditions for quantitative volatilization.

It was found that the efficiency of the volatilization of Ag after heating a sample containing no additives was low (see Table 1).

Because losses of Ag at temperatures higher than 600 °C in the presence of an ashing aid, *viz.*, $Mg(NO_3)_2$, have been reported previously, the addition of $Mg(NO_3)_2$ was examined. The recovery of Ag after heating 50 mg of the sample mixed with 50 mg of $Mg(NO_3)_2$ at 1200 °C for 1 h was 40%. For comparison, after the additon of a fused oxidizing agent, *viz.*, KNO_3, under the same conditions, the volatilization yield was only 5%. In further experiments, the effect of the addition of some refractory compounds such as metal oxides and magnesium silicate, which are known[13,14] to prevent melting of industrial copper samples, was studied (see Table 1).

In order to increase the recovery of Ag, the influence of the addition of substances widely used as carriers in spectrography was examined. Alkali metal and ammonium halides, $CaCO_3$ and CaC_2O_4 (substances decomposed with the evolution of gas), separately or mixed with oxides or graphite in various mass ratios, were tested, but they were found to be less efficient than Florisil–CaO, alumina or silica.

The optimum volatilization conditions were therefore established by using oxides and Florisil mixtures as additives.

The dependence of the recovery of Ag on the additive to sample mass ratio is shown in Fig. 2. The best volatilization yield was obtained at a ratio of 2 for all the additives. At a ratio of 3, a decrease in the recovery was observed, particularly at shorter heating times.

A more detailed examination of the influence of various ratios of components at a constant additive to sample mass ratio is shown in Fig. 3. The mean results for mixtures of Florisil–CaO (5 + 1–10 + 1 m/m) were significantly higher than those obtained with other component ratios, and complete recovery was attained. The combinations of CaO and SiO_2 were not effective.

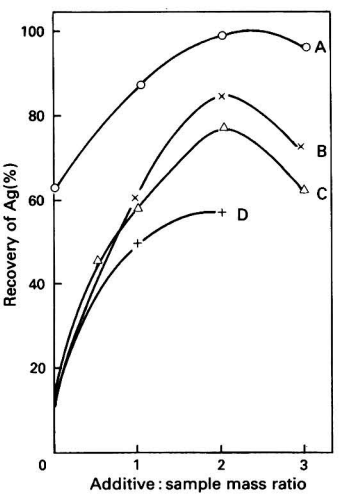

Fig. 2 Dependence of the recovery of Ag on the additive : sample mass ratio. Sample, copper tailings 'C'; temperature, 1200 °C; and air flow-rate, 0.17 l min^{-1}. Additive: A, Florisil–CaO (5 + 1), heating time, 2.5 h; B, Florisil–CaO (5 + 1), heating time, 1 h; C, CaO, heating time, 1 h and D Florisil, heating time, 1 h

Table 1 Influence of the addition of high-temperature oxides and Florisil on the yield of Ag by volatilization. Heating time, 1 h; air stream flow-rate, 0.17 l min^{-1}; sample: copper tailings 'C', 50 mg

Additive	Additive : sample ratio (m/m)	Temperature/ °C	Yield of Ag (%)
None	—	500	5
None	—	1000	8
None	—	1200	10
Florisil	1 : 1	500	8
Florisil	1 : 1	1100	50
Alumina (Merck)	2 : 1	1100	66
Alumina	2 : 1	1100	79
CaO	1 : 2	1100	46
La_2O_3	1 : 2	1100	25
Florisil–CaO (4 + 1)	2 : 1	1100	84
Florisil–La_2O_3 (4 + 1)	2 : 1	1100	83
SiO_2–CaO (4 + 1)	2 : 1	1100	80

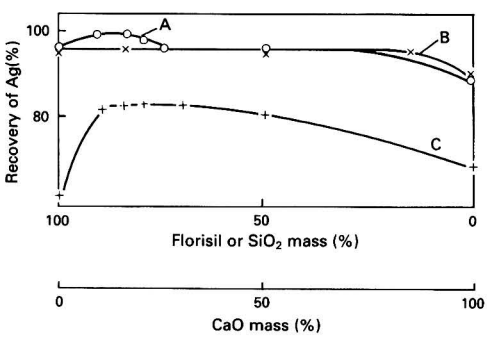

Fig. 3 Dependence of the recovery of Ag on the mass ratio of the additive components. Sample, copper tailings 'C'; additive : sample mass ratio, 2; temperature, 1200 °C; and air flow-rate, 0.17 l min^{-1}. Additive: A, Florisil–CaO, heating time, 2.5 h; B, SiO_2–CaO, heating time, 2.5 h; and C, Florisil–CaO, heating time, 1 h

The use of $CaCO_3$ instead of CaO did not change the yield after heating for 1, 2 and 2.5 h, while the use of lanthanum oxide was less efficient.

Heating at 1200 °C for 2–2.5 h allows a volatilization yield of 96% to be obtained with SiO_2 and Florisil (Fig. 4). With the addition of CaO and Al_2O_3, only a 90% yield can be achieved. By using the chosen mixture of additives, the dependence of the recovery of Ag on the heating temperature (Fig. 5) and the gas flow-rate (Fig. 6) was investigated.

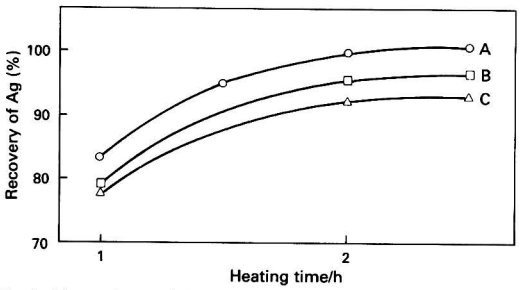

Fig. 4 Dependence of the recovery of Ag on heating time. Sample, copper tailings 'C', 50 mg; additive : sample mass ratio = 2; temperature, 1200 °C; and air flow-rate 0.17 l min^{-1}. Additive: A, Florisil–CaO (5 + 1); B, SiO_2; and C, Al_2O_3

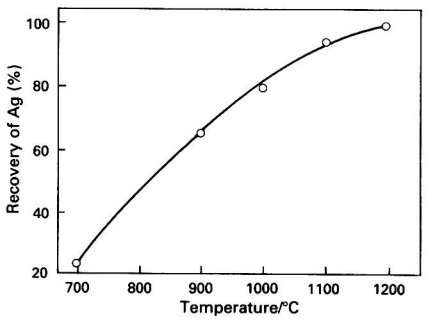

Fig. 5 Influence of heating temperature on the recovery of Ag. Sample, copper tailings 'C', 50 mg; additive, Florisil–CaO (5 + 1); additive : sample mass ratio = 2; and heating time, 2 h

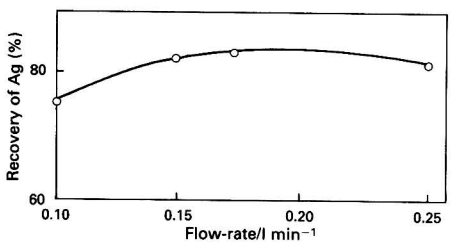

Fig. 6 Influence of air flow-rate on the recovery of Ag. Sample, copper tailings 'C', 50 mg; additive : sample mass ratio = 2; additive, Florisil–CaO (5 + 1); temperature 1200 °C; and heating time, 1 h

Under the optimum conditions, *viz.*, additive, Florisil–CaO (5 + 1–10 + 1 m/m); additive : sample mass ratio, 2; heating time, 2 h; heating temperature, 1200 °C; and air flow-rate, 0.17 l min^{-1}, Ag was volatilized and determined in other copper tailings and a standard reference material, copper–zinc ore (RUS-1) (Table 2).

Discussion

Copper ores and flotation tailings are examples of materials with a complex composition. Sulphides of Fe, Cu and Zn, and minerals such as quartz and plagioclase usually occur in copper ores. Tailings contain considerable amounts of SiO_2 (24–70%), CaO (7–21%), Al_2O_3 (3–8%), MgO (3–10%), Fe (1–2%), Cu (0.05–0.3%), K (2.7–3.1%), S (0.5–3.1%), C (6–7%), organic C (1–2%), Pb, Zn, Na and Mn [$n \times 10^{-3}$% (n = 1–9)] and trace amounts of Ni, Co, Mo, Sb, Sn, As, Cd and Ag.

Volatilization of Ag from samples of complex composition also appears to be a complex process, and several partial processes have to be taken into consideration: (1) thermal decomposition of Ag compounds; (2) evaporation or sublimation of Ag or Ag compounds; (3) transport of Ag vapour or vapours of volatile Ag compounds across a sample bed to the surface; and (4) transport of Ag vapour from the surface. Solids added to the heated sample (additives) could essentially influence the above processes as follows.

Thermal Decomposition of Ag Compounds

According to the data for pure substances,[15] Ag_2SO_4 is among the most stable compounds of Ag. It can be formed from Ag_2S during heating in air at 450 °C, and decomposed at 800–1000 °C:

$$Ag_2SO_4 \rightarrow 2Ag + SO_3 + \tfrac{1}{2}O_2$$

The decomposition of $AgNO_3$ occurs at 600–800 °C, Ag_2CO_3 at 700–800 °C, and dissociation of Ag_2O to Ag at 400 °C. The decomposition reactions of solids, *viz.*, temperature and rates of decomposition and also the mechanism of the reactions, can be affected by the presence of other solids. Reports in the literature also include examples of the decomposition of Ag compounds catalysed by a solid product (*e.g.*, Ag_2O by Ag) or by a solid additive.[16] The reaction mechanism could be changed by the formation of a new phase. The presence of a gaseous reactant product decreases the reaction rate. Reduction of the pressure of SO_3 by formation of the stable compound $CaSO_4$ could accelerate the decomposition of Ag_2SO_4. However, it is difficult to explain the increase in the evaporation yield in the presence of Al_2O_3, as $Al_2(SO_4)_3$ is not thermally stable.

Evaporation or Sublimation of Ag or Ag Compounds

By considering the data for pure substances under vacuum at 1200 °C, and because of the relatively high vapour pressure of Ag (0.2 mmHg[17]) and AgCl (40 mmHg[18]), it can be expected

Table 2 Results of the determination of Ag in copper tailings and a copper–zinc ore (RUS-1)

Sample	$\bar{x}$* (%)	n	RSD†	Literature $\bar{x}$ values‡ (%)	Certified value for Ag (%)
Tailings 'C'	5.50×10^{-3}	6	2.0	5.59×10^{-3}	—
Tailings 'B'	2.46×10^{-3}	4	2.3	2.4×10^{-3}	—
RUS-1	2.76×10^{-3}	4	2.2	2.82×10^{-3}	$2.7 \pm 0.2 \times 10^{-3}$

* Mean value of Ag found.

† RSD = Relative standard deviation.

‡ Results of flame AAS determination after separation of Ag by solvent extraction.[2]

that the thermal evolution of trace amounts of Ag should not be limited by evaporation. The vapour pressure, however, over the complex solid system is different and cannot easily be calculated. The rate of evaporation depends strongly on the surface area and on the melting point of the sample matrix. We have observed an increase in the volatilization yields in the presence of additives that prevent melting. The heated samples contain sulphides, sulphates and carbonates that are easily melted and low melting point silicates (the liquid phase can be seen from relatively low temperatures owing to the eutectic point[19] of the $FeO–SiO_2$ system). The addition of MgO is very effective in preventing the samples from melting; unfortunately, MgO is also the most effective collector of Ag at 1100 °C.[11] Magnesium silicate was found to be a suitable additive for both the copper tailings and the high pyrites sample (RUS-1). The mixtures (or rather solid solutions) of Fe and Mg silicates melt at a temperature higher than 1200 °C. Among alumina–metal oxide binary systems, only Al_2O_3–Cu_2O has a eutectic point below 1200 °C.[20]

When heated in an air stream with additives, the samples of copper tailings form a complex system of oxides, silicates and spinels and do not melt at 1200 °C. The compounds formed depend on the ratio of the components, hence the system is difficult to describe.

The addition of alkali or alkaline earth metal chlorides, assuming conversion of Ag compounds into AgCl, was not effective.

Transport of Ag Vapour or Vapours of Volatile Ag Compounds Across a Sample Bed to the Surface

Diffusion processes and the reaction of Ag vapour with the matrix and with additives are essential for the transport of Ag through the sample bed. According to Zhuikov *et al.*,[11] Ag vapour can be absorbed by CaO in a stream of air at 1000–1100 °C, but the process is reversible at higher temperatures. This might explain the decrease in the volatilization yield with an additive to sample ratio of >2 with a short heating time (Fig. 2).

The complex composition of the samples makes the system so complicated that it is difficult to state which process limits the volatilization of Ag. The choice of additives has to be determined by experiment. The additive suitable for copper tailings 'C', however, was also effective for the other copper tailings and the copper–zinc ore.

The investigation of the volatilization of Ag is also important from the point of view of losses of Ag during the preliminary ignition of the samples, which is often part of the routine analysis of ores and other geological materials containing organic carbon.

Fishkova and Kurskij[21] explained the poor recovery of Ag, after ignition and *aqua regia* ($HCl–HNO_3$, 3 + 1) dissolution of trace amounts of Ag spiked on silica, by formation of sparingly soluble compounds.

On the basis of the results presented here, it is suspected that Ag can be lost by volatilization because the volatilization yields from matrices rich in silica are relatively high.

Conclusion

The proposed method for the separation of Ag prior to its determination by AAS is simple and useful for a short series of samples. Good agreement with the results obtained after extractive separation and with certified values demonstrated that the accuracy of the proposed method was good.

This work was supported by research programme CPBP-01.18.

References

1 Skorko-Trybułowa, Z., Boguszewska, Z., and Różańska, B., *Mikrochim. Acta, Part I*, 1979, 151.
2 Lachowicz, E., *Analyst*, 1987, **112**, 1623.
3 Tölg, G., *Talanta*, 1972, **19**, 1489.
4 Bächmann, K., *Talanta*, 1982, **29**, 1.
5 Geilmann, W., *Fresenius Z. Anal. Chem.*, 1958, **160**, 410.
6 Gielmann, W., and Neeb, K. H., *Fresenius Z. Anal. Chem.*, 1959, **165**, 251.
7 Tölg, G., Meyer, A., Hofer, Ch., and Knapp, G., *Fresenius Z. Anal. Chem.*, 1981, **305**, 1.
8 Tölg, G., Kaiser, G., and Han, H. B., *Anal. Chim. Acta*, 1981, **129**, 9.
9 Heinrichs, M., and Keltsch, M., *Anal. Chem.*, 1982, **54**, 1211.
10 Zhuikov, B. L., Popeko, G. S., and Hyong, F. T., *Zh. Anal. Khim.*, 1986, **41**, 1653.
11 Zhuikov, B. L., Popeko, G. S., and Ortega, H. D., *J. Radioanal. Nucl. Chem. Lett.*, 1987, **117**, 11.
12 Różańska, B., and Różowski, J., *Mikrochim. Acta, Part II*, 1984, 481.
13 Różańska, B., and Lachowicz, E., *Anal. Chim. Acta*, 1985, **175**, 211.
14 Różańska, B., and Domańska, M., *Anal. Chim. Acta*, 1986, **187**, 317.
15 Duval, C., *Inorganic Thermogravimetric Analysis*, Elsevier, Amsterdam, 1963.
16 *Comprehensive Chemical Kinetics. vol. 22, Reactions in the Solid State*, eds. Bamford, C. H., and Tipper, C. F. H., Elsevier, Amsterdam, 1980.
17 Niesmiejanow, A. N., *Zh. Phys. Khim.*, 1959, **33**, 342.
18 *Computer Aided Data Book of Vapour Pressure*, ed. Ohe, S., Data Book Publishing, Tokyo, Japan, 1976.
19 Muan, A., in *High Temperature Oxides*, ed. Alper, A. M., Academic Press, London, 1970, part 1, ch. 7.
20 Ryshkewitch, E., *Oxide Ceramics*, Academic Press, London, 1960.
21 Fishkova, N. L., and Kurskij, A. H., *Zavod. Lab.*, 1989, **55**(8), 34.

Paper 0/04406G
Received October 1st, 1990
Accepted November 22nd, 1990

Determination of Trace Amounts of Copper, Nickel and Zinc in Palladium Compounds by Solvent Extraction Flame Atomic Absorption Spectrometry

Sijka A. Popova, Stefanka P. Bratinova and Christina R. Ivanova
Central Research Laboratory, Higher Institute of Chemical Technology, 1156 Sofia, Bulgaria

A method is described for the determination of trace amounts of Cu, Ni and Zn in diamminedichloropalladium and diamminedinitropalladium by flame atomic absorption spectrometry after an extraction procedure using ammonium pyrrolidin-1-yldithioformate [ammonium pyrrolidinedithiocarbamate (APDC)] as complexing agent and isobutyl methyl ketone (IBMK) as extractant. Another extraction system, NH_4SCN–IBMK, was used for the preliminary removal of Pd which also forms extractable complexes with APDC. Optimum conditions for the selective separation of Pd and for the simultaneous extraction of Cu–, Ni– and Zn–PDC complexes into IBMK were determined. The sensitivity and precision of the proposed method are sufficient for quality control requirements.

Keywords: *Copper, nickel and zinc determination; solvent extraction flame atomic absorption spectrometry; diamminedichloropalladium; diamminedinitropalladium; ammonium pyrrolidin-1-yldithioformate*

Diamminedichloropalladium [$Pd(NH_3)_2Cl_2$] and diamminedinitropalladium [$Pd(NH_3)_2(NO_2)_2$] are used as raw materials in the production of microelectronic systems; hence they have to conform to a high degree of purity necessitating exacting quality control requirements. The content of impurities such as Cu, Ni and Zn in these materials needs to be be controlled and should not exceed 0.001–0.0001%. There are no methods described in the literature for the atomic absorption spectrometric determination of Cu, Ni and Zn in the Pd compounds studied here. Hence there is a need for an accurate method for the determination of Cu, Ni and Zn in $Pd(NH_3)_2Cl_2$ and $Pd(NH_3)_2(NO_2)_2$ with high sensitivity and selectivity. This problem has been solved by using solvent extraction prior to flame atomic absorption analysis. An extraction system extensively used and preferred in atomic absorption analysis is a combination of ammonium pyrrolidin-1-yldithioformate [ammonium pyrrolidinedithiocarbamate (APDC)] as complexing agent and isobutyl methyl ketone (IBMK) as extractant.

The main problem in applying the APDC–IBMK extraction procedure to the determination of Cu, Ni and Zn in Pd compounds is the co-extraction of Pd.[1] This necessitates its prior removal from the system; precipitation is not recommended for this purpose, because of the large amount of Pd involved and the possibility of coprecipitation of Cu, Ni and Zn. It has been recommended that the separation of Pd be carried out by extraction of its rhodanide (sulphocyanide) complex into IBMK.[2,3] Extraction of 99.9% of the Pd into the organic phase from 3–6 mol dm^{-3} HCl can be achieved with a single extraction procedure.[2]

In order to develop a suitable method it is necessary to examine the conditions under which the extraction of Cu, Ni and Zn together with Pd as their rhodanide complexes can be avoided, and to optimize the conditions for the solvent extraction pre-concentration of Cu, Ni and Zn with the use of APDC–IBMK and their subsequent determination by flame atomic absorption spectrometry.

Experimental

Sample Preparation

A 1.000 g sample of $Pd(NH_3)_2Cl_2$ or $Pd(NH_3)_2(NO_2)_2$, previously dried at 105 °C, was dissolved in 10 ml of 1 mol dm^{-3} HCl by heating at about 90 °C for 1 h. After cooling to room temperature, the solution was diluted to 50 ml with de-ionized water.

Reagents

All reagents were of analytical-reagent grade, and de-ionized, doubly distilled water was used throughout.

Ammonium thiocyanate solution, 20%. Previously purified by extraction with APDC–IBMK.

Ammonium pyrrolidin-1-yldithioformate solution, 1%. A 1.00 g amount of the reagent was dissolved in 50 ml of water containing 1 ml of 25% ammonia solution and the solution was diluted to 100 ml. The residue was filtered. The solution was prepared daily.

Sodium hydroxide solution, 25% (*metal-free*). Sodium hydroxide pellets (250 g) were dissolved in 1 l of water and the solution was transferred into a separating funnel. A 1 ml volume of APDC solution was added and the mixture extracted with 20 ml of IBMK. The addition of APDC and extraction was repeated until the extracts were colourless. The solution was stored in a polyethene bottle.

Isobutyl methyl ketone (*Merck*).

Standard solutions of Cu, Ni *and* Zn, 1 mg ml^{-1} *each* (*BDH*).

Working standard solutions of Cu, Ni and Zn were prepared daily by appropriate dilution of the stock standard solutions.

Instrumentation

A Perkin-Elmer Model 3030B atomic absorption spectrometer equipped with hollow cathode lamps for Cu, Ni and Zn as light sources was used. The absorption signals were measured under the conditions shown in Table 1.

A pH-meter (Radiometer) was also used.

Results and Discussion

Conditions for the Separation of Pd

As has been reported previously,[2] virtually complete extraction of Pd as its rhodanide complex can be achieved over a wide range of acidity (3–6 mol dm^{-3} HCl). It is known, however, that Cu, Ni and Zn also form stable rhodanide complexes.[4] This necessitates optimization of the conditions for the selective extraction of Pd into IBMK.

The Ni–rhodanide complex is not extracted into IBMK and remains entirely in the aqueous phase under the optimum conditions for the extraction of Pd as its rhodanide complex (Fig. 1, curve 1). In addition, the Cu– and Zn–rhodanide complexes are not co-extracted with the Pd–rhodanide com-

Table 1 Optimum conditions for the determination of Cu, Ni and Zn in the aqueous and organic phases

Metal	Wave-length/nm	Slit-width/nm	Lamp current/mA	Air flow-rate/ l min^{-1}	Acetylene flow-rate/ l min^{-1}		Aspiration rate/ ml min^{-1}		Linear range of calibration graph/mg l^{-1}
					Aqueous solution	IBMK solution	Aqueous solution	IBMK solution	
Cu	328.1	0.7	15	18.4	4.0	2.6	6	5	0.1–4.0
Ni	232.0	0.2	25	18.4	4.0	2.6	6	5	0.5–6.0
Zn	213.8	0.7	6	18.4	4.0	2.6	6	5	0.1–2.0

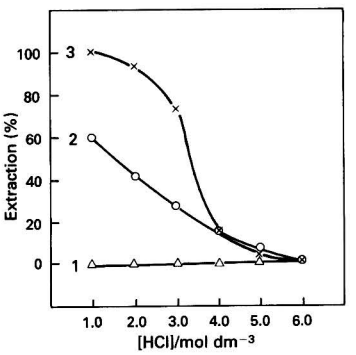

Fig. 1 Effect of hydrochloric acid concentration on the percentage extraction of 1, Ni–; 2, Cu–; and 3, Zn– rhodanide complexes into IMBK: Cu^{II}, 3.10×10^{-5} mol; Ni^{II}, 6.10×10^{-5} mol dm^{-3}; Zn^{II}, 7.65×10^{-6} mol dm^{-3}; aqueous phase, 20 ml; organic phase, 5 ml; and NH_4SCN, 0.4 mol dm^{-3}

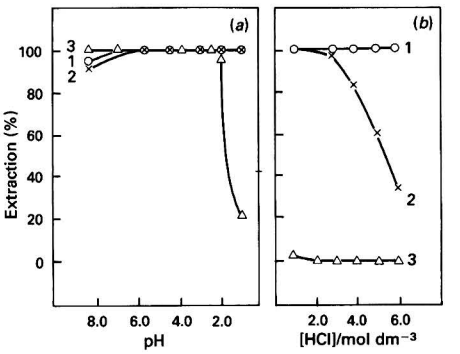

Fig. 2 Effect of (*a*) pH; and (*b*) hydrochloric acid concentration on the percentage extraction of 1, Cu–; 2, Ni–; and 3, Zn–PDC complexes into IBMK: Cu^{II}, 1.55×10^{-5} mol dm^{-3}; Ni^{II}, 3.05×10^{-5} mol dm^{-3}; Zn^{II}, 3.88×10^{-6} mol dm^{-3}; aqueous phase, 40 ml; organic phase, 5 ml; and APDC, 3.00×10^{-3} mol dm^{-3}

plex from a strongly acidic medium (6 mol dm^{-3} HCl) (Fig. 1, curves 2 and 3). Hence, extraction of the Pd–rhodanide complex should be carried out from 6 mol dm^{-3} HCl in order to remove Pd selectively, thus allowing the subsequent determination of Cu, Ni and Zn by flame atomic absorption spectrometry.

It was established that two extractions for 1 min each in the presence of at least a 5-fold molar excess of the reagent (NH_4SCN) with respect to Pd was sufficient for the complete removal of Pd into IBMK.

Determination of Cu and Ni

The medium, after separation of Pd, is strongly acidic (6 mol dm^{-3} HCl). Extraction of Cu–, Ni– and Zn–PDC complexes into IBMK under these conditions has not been fully described in the literature.[5–8] However, it has been shown[9] that these metals form complexes with APDC over a wide pH range (1–14). Reducing the acidity of the solutions to be analysed from 6 mol dm^{-3} to a pH >1 causes additional difficulties, because of the need to introduce large amounts of NaOH, which might lead to contamination. Hence, the possibility of carrying out the extraction procedure from strongly acidic media was investigated. It has been reported[10] that 90% extraction can be achieved from 6 mol dm^{-3} HCl media.

Our investigations, however, do not entirely support these data (Fig. 2). Complete extraction of Cu can in fact be obtained in the range 1–6 mol dm^{-3} HCl. However, in acidic media >3 mol dm^{-3}, the total extraction of Ni into IBMK as its APDC complex is not possible. The extraction procedure must therefore be carried out at HCl concentrations of up to 3 mol dm^{-3} in order to obtain the simultaneous extraction of Cu and Ni. Unfortunately, under these conditions Zn remains entirely in the aqueous phase and hence its determination together with Cu and Ni in the organic phase is not possible.

It was found that the ratio of the volume of the aqueous phase to the volume of the organic phase ($V_a : V_o$) in the range from 2 : 1 to 10 : 1 has no effect on the extent of extraction of Ni and Cu under the optimum conditions for the acidity where the extraction is nearly 100%. Hence, the acidity of the aqueous phase can be decreased by a 2-fold dilution with water.

Total extraction of Cu and Ni as their APDC complexes into IBMK is achieved by using a 10-fold molar excess of the reagent for Cu and a 60-fold molar excess for Ni (Fig. 3). A large excess of the chelating agent is required to allow for decomposition of the reagent in strongly acidic media.[6] A single extraction procedure for a period of 10 s is sufficient because the rate at which the metal chelates are formed and extracted increases as the acidity of the aqueous phase is increased.[7] If the absorption signals for Cu and Ni are measured less than 30 min after the extraction procedure, then separation of the organic layer from the aqueous layer only is required. However, if the absorption signals are measured after more than 30 min it is necessary for the organic phase to be washed with water in order to remove the remaining acid and so prevent it from decomposing the Cu– and Ni–PDC complexes,[6] which would reduce the absorption signals.

Hence, it was established that it is possible to determine Cu and Ni simultaneously in $Pd(NH_3)_2Cl_2$ and $Pd(NH_3)_2(NO_2)_2$ by employing extraction with APDC–IBMK in 3 mol dm^{-3} HCl media after preliminary extraction of Pd into IBMK as its rhodanide complex. As mentioned above, under these conditions Zn remains in the aqueous phase.

For the simultaneous determination of Zn, Cu and Ni, the extraction should be carried out at pH 2. Particular attention has to be paid to the blank; therefore, the base used for

Table 2 Determination of Cu, Ni and Zn in $Pd(NH_3)_2Cl_2$ and $Pd(NH_3)_2(NO_2)_2$

Compound	Method	Cu content (%)	RSD* (%)	Ni content (%)	RSD* (%)	Zn content (%)	RSD* (%)
Determination of Cu *and* Ni *in strongly acidic media* (3 mol dm^{-3} HCl)—							
$Pd(NH_3)_2Cl_2$	Calibration graph	$(2.63 \pm 0.04) \times 10^{-4}$	5.2	$(5.25 \pm 0.04) \times 10^{-4}$	3.6	—	—
	Standard additions	$(2.68 \pm 0.04) \times 10^{-4}$	4.8	$(5.32 \pm 0.04) \times 10^{-4}$	4.8	—	—
$Pd(NH_3)_2(NO_2)_2$	Calibration graph	$(2.72 \pm 0.05) \times 10^{-4}$	6.2	$(7.20 \pm 0.03) \times 10^{-4}$	2.5	—	—
	Standard additions	$(2.67 \pm 0.05) \times 10^{-4}$	7.2	$(7.25 \pm 0.04) \times 10^{-4}$	3.9	—	—
Determination of Cu, Ni *and* Zn *at pH* 2.0—							
$Pd(NH_3)_2Cl_2$	Calibration graph	$(2.75 \pm 0.05) \times 10^{-4}$	7.1	$(5.20 \pm 0.04) \times 10^{-4}$	4.2	$(3.61 \pm 0.04) \times 10^{-4}$	5.1
	Standard additions	$(2.70 \pm 0.05) \times 10^{-4}$	6.8	$(5.27 \pm 0.04) \times 10^{-4}$	4.8	$(3.67 \pm 0.04) \times 10^{-4}$	4.7
$Pd(NH_3)_2(NO_2)_2$	Calibration graph	$(2.67 \pm 0.04) \times 10^{-4}$	5.3	$(7.14 \pm 0.04) \times 10^{-4}$	3.7	$(4.72 \pm 0.04) \times 10^{-4}$	3.9
	Standard additions	$(2.63 \pm 0.04) \times 10^{-4}$	5.5	$(7.19 \pm 0.04) \times 10^{-4}$	5.5	$(4.80 \pm 0.04) \times 10^{-4}$	5.2

* RSD = relative standard deviation.

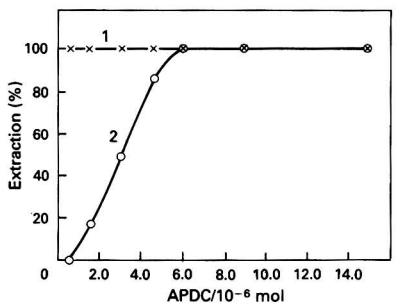

Fig. 3 Effect of the amount of APDC on the extraction of 1, Cu; and 2, Ni into IBMK: Cu^{II}, 1.55×10^{-5} mol dm^{-3}; Ni^{II}, 3.05×10^{-5} mol dm^{-3}; HCl, 3 mol dm^{-3}; aqueous phase, 40 ml; organic phase, 5 ml

adjusting the pH must have been purified previously. As is shown in Fig. 2 the most suitable pH range is 2.0–2.5. At lower pH values the extraction of Zn is decreased considerably, whereas at higher values serious problems arise with the blank even when purified NaOH is used. At pH 2.0–2.5, a period of 10 s is not sufficient for the extraction procedure; a shaking time of 60 s is required. Because the extent of APDC decomposition decreases under these conditions, the minimum amount of the chelating agent required for quantitative extraction is much smaller; however, it is recommended that the procedure be carried out using the same amount of APDC as required for the procedure in strongly acidic media, *viz.*, 3.00×10^{-3} mol dm^{-3}. Absorption signals measured for Cu, Ni and Zn in the organic phase are stable for more than 24 h, hence washing of the organic phase is not necessary.

The following procedures were used for the determination of Cu, Ni and Zn in $Pd(NH_3)_2Cl_2$ and $Pd(NH_3)_2(NO_2)_2$.

Separation of Pd

An aliquot of $Pd(NH_3)_2Cl_2$ or $Pd(NH_3)_2(NO_2)_2$ solution was placed in a 100 ml separating funnel. A 10.3 ml volume of concentrated HCl plus 3 ml of a 20% solution of NH_4SCN were added and the mixture was diluted to 20 ml with water. Then, 5 ml of IBMK were added and the mixture was extracted for 1 min. After the two phases had separated, the organic layer was discarded. The procedure was repeated with another 5 ml aliquot of IBMK and the organic layer was again discarded.

Atomic Absorption Spectrometric Determination of Cu and Ni

The aqueous phase from above was transferred into another separating funnel, and 10 ml of water plus 1 ml of a 1% solution of APDC were added. The mixture was shaken vigorously for about 10 s and allowed to stand for 10 min after which 5 ml of IBMK were added. The mixture was shaken for 30 s and, after the two phases had separated, the aqueous layer was discarded. The organic phase was collected in 5 ml calibrated tubes and diluted to the mark with pure IBMK. The organic layer was aspirated directly into the flame and the absorption signals for Cu and Ni were measured with background correction under the conditions given in Table 1.

Table 3 Recovery of Cu, Ni and Zn added to $Pd(NH_3)_2Cl_2$ and $Pd(NH_3)_2(NO_2)_2$ by flame atomic absorption spectrometry using the APDC–IBMK extraction system

				Recovery	
Element	Found/μg	Added/μg	Expected/ μg	μg*	%*
Cu	2.7	10	12.7	12.4	97.6
Ni	5.2	10	15.2	15.1	99.3
Zn	3.6	10	13.6	13.3	97.8

* Mean of five determinations.

Atomic Absorption Spectrometric Determination of Cu, Ni and Zn

The aqueous phase remaining after the separation of Pd was transferred into 50 ml beakers. An 18 ml volume of 25% NaOH was added and the pH adjusted to 2.0–2.5. One millilitre of a 1% solution of APDC was added and the mixture was transferred quantitatively into another 100 ml separating funnel and diluted to 50 ml with water. A 5 ml aliquot of IBMK was added and the mixture was shaken for 30 s. The aqueous phase was discarded and the organic layer collected in 5 ml calibrated tubes and diluted to the mark with pure IBMK. The organic phase was injected directly into the flame and the absorption signals for Cu, Ni and Zn were measured with the background correction under the conditions given in Table 1.

Standard solutions for calibration graphs were prepared each time by the same extraction procedure, extracting the appropriate volumes of Cu, Ni and Zn solutions each with a concentration of 10 mg l^{-1}. The determination of Cu, Ni and Zn in $Pd(NH_3)_2Cl_2$ and $Pd(NH_3)_2(NO_2)_2$ was carried out by using the calibration graph and standard additions procedures. The results are shown in Table 2. As can be seen, the results obtained using the standard additions method correspond to those obtained using the calibration graph method. In addition, similar results for Cu and Ni were obtained with the two procedures. Hence, the proposed method is accurate and free from interferences.

Recoveries of Cu, Ni and Zn from the two Pd compounds were studied by carrying out standard additions of these metals to $Pd(NH_3)_2Cl_2$ and $Pd(NH_3)_2(NO_2)_2$ during the dissolution procedure. The results obtained for the recovery study are shown in Table 3.

In conclusion, a reproducible and highly sensitive method for the determination of Cu, Ni and Zn by extraction with APDC–IBMK followed by flame atomic absorption spectrometry has been developed. The method was applied to the determination of these elements in $Pd(NH_3)_2Cl_2$ and $Pd(NH_3)_2(NO_2)_2$.

References

1 Sychra, V., Slevin, P. J., Matousek, J., and Bek, F., *Anal. Chim. Acta*, 1970, **52**, 259.
2 Teruo, I., *Bunseki Kagaku*, 1966, **15**, 109.
3 Popova, S. A., and Bratinova, S. P., *J. Anal. At. Spectrom.*, 1990, **5**, 35.
4 Marczenko, Z., *Photometric Determination of Elements*, Mir, Moscow, 1971.
5 Dellien, I., and Persson, L., *Talanta*, 1979, **26**, 1101.
6 Takada, T., *Talanta*, 1982, **29**, 799.
7 Murakami, M., and Takada, T., *Talanta*, 1985, **32**, 513.
8 Murakami, M., and Takada, T., *Talanta*, 1990, **37**, 229.
9 Watson, C. A., *Ammonium Pyrrolidinedithiocarbamate*, Monograph 74, Hopkin and Williams, 1974.
10 Brook, R. R., Hoashi, M., Wilson, S. M., and Zhang R., *Anal. Chim. Acta*, 1989, **217**, 165.

Paper 0/02924F
Received June 28th, 1990
Accepted January 3rd, 1991

Study of the Conversion of Asparagine and Glutamine of Proteins Into Diaminopropionic and Diaminobutyric Acids Using [Bis(trifluoroacetoxy)iodo]benzene Prior to Amino Acid Determination

Dominique Fouques and Jacques Landry
Laboratoire de Chimie Biologique, INRA, INA-PG, F78850 Thiverval-Grignon, France

The treatment of several proteins with [bis(trifluoroacetoxy)iodo]benzene (BTI) was examined as a possible way to determine separately their asparagine and glutamine content, through the quantification of their corresponding 2,3-diaminopropionic and 2,4-diaminobutyric acids. The diamino acid peaks were resolved between those of phenylalanine and lysine after a modification of the chromatographic conditions required for phenylthiocarbamylamino acid analysis. Rate studies performed on three proteins with BTI in the presence of dimethylformamide at 60 °C showed a maximum conversion of amides into diamino acids ranging from 50 to 83% after 4 h of contact, thereby making the direct quantification of amides in protein through the evaluation of diamino acids unsuitable; a fast (30 min) and virtually complete disappearance of glutamine; and a slower (2 h) and only partial (65 ± 6%) disappearance of asparagine.

Keywords: *Protein; glutamine and asparagine; [bis(trifluoroacetoxy)iodo]benzene; phenyl isothiocyanate; high-performance liquid chromatography*

Protein hydrolysis, as routinely performed with 6 mol dm^{-3} HCl for the determination of the amino acid composition of the protein, converts asparagine (asn) and glutamine (gln) into aspartic (asp) and glutamic (glu) acids. These amides are generally included in the sums 'asx' (asp + asn) or 'glx' (glu + gln). They can be separately assayed only from modified samples. Proposed modifications involve the esterification, *i.e.*, reduction, of the free carboxylic acids[1] or the conversion of amides into amines by a Hofmann degradation reaction using [bis(trifluoroacetoxy)iodo]benzene (BTI).[2] In the latter situation, asn and gln are recovered, after hydrolysis of the polypeptide, as diaminopropionic acid (DAPA) and diaminobutyric acid (DABA), respectively. From the foregoing, the quantification of asn and gln in proteins can be performed either from the differences in asx and glx between untreated and BTI treated samples, or from the DAPA and DABA produced. The first alternative was developed by Soby and Johnson[2] who reported determinations of asn and gln consistent with sequence data. The second method was described by Vendrell and Aviles[3] who observed an incomplete conversion of amides into DAPA and DABA but did not provide any quantitative data on yield.

In the present study, the use of BTI and the quantification of the resulting diamino acids, DAPA and DABA, through their phenylthiocarbamyl (ptc) derivatives were further investigated with the aim of establishing appropriate conditions for the determination of the asn and gln content of polypeptides.

Experimental

Materials

Horse heart cytochrome *c*, bovine pancreatic ribonuclease A, bovine pancreatic α-chymotrypsinogen A and oxidized bovine insulin (B chain) were obtained from Sigma. Hen egg-white lysozyme, trifluoroacetic acid (TFA), butyl acetate and BTI [sold as 'iodosobenzene bis(trifluoroacetate)'] were purchased from Merck. Dimethylformamide (DMF), DAPA and DABA were of analytical-reagent grade. Phenyl isothiocyanate (PITC) and triethylamine (TEA) were supplied by Pierce. Sodium acetate and high-performance liquid chromatography (HPLC) grade acetonitrile were obtained from Merck. Nova-Pak (C_{18}, 5 μm, 15 × 0.39 cm i.d.) and Pico-Tag (C_{18}, 4 μm, 15 × 0.39 cm i.d.) analytical columns were from Waters Associates.

BTI Treatment

The polypeptide (50 or 100 μg) dissolved in 60 μl of 0.01 mol dm^{-3} TFA was mixed in an Eppendorf microtube with 60 μl of a freshly prepared BTI solution (0.08 mol dm^{-3}) in acetonitrile or DMF and heated in a water-bath at 35 or 60 °C for between 30 min and 16 h. Samples with DMF were first evaporated under reduced pressure in a SpeedVac concentrator, redissolved in 200 μl of water and extracted three times with an equal volume of butyl acetate. Samples with acetonitrile were directly extracted three times with 200 μl of diethyl ether. The resulting aqueous phases were then evaporated to dryness before acid hydrolysis and amino acid determination were carried out.

Amino Acid Determination

Acid hydrolysis was performed with 6 mol dm^{-3} HCl for 24 h at 110 °C. Amino acids were determined by reversed-phase HPLC after derivatization with PITC.[4] Chromatography was carried out using a Waters Associates system consisting of two pumps (M510), a gradient former (M680) and an absorbance detector operating at 254 nm. The ptc-amino acids were separated on a Nova-Pak coupled with a Pico-Tag column[5]

Table 1 Programme used for ptc-amino acid separation and column washing

Time/min	Flow-rate/ml min^{-1}	A* (%)	B† (%)	Curve No.‡
0.00	1.0	90	10	—
2.25	1.0	90	10	6
5.25	1.0	82	18	5
24.00	1.0	52	48	6
24.50	1.5	0	100	6
29.50	1.5	0	100	6
30.50	1.5	90	10	6
36.00	1.5	90	10	6
36.50	1.0	90	10	6
38.00	Next injection			

* Solvent A: 0.14 mol dm^{-3} sodium acetate containing 0.5 ml l^{-1} of triethylamine and adjusted to pH 6.4 with orthophosphoric acid.
† Solvent B: acetonitrile–solvent A (3 + 2).
‡ Pre-programmed curve profiles, linear (6) or convex (5).

maintained at 40 °C in a water-bath. The elution and regeneration programme is given in Table 1. A Pierce amino acid standard H, to which were added equimolar amounts of methionine sulphone, cysteic acid, DAPA, DABA and norleucine, was used as a reference sample.

Results and Discussion

Separation of Ptc-DAPA and Ptc-DABA

The ptc-DAPA and ptc-DABA were co-eluted between ptc-phe and ptc-lys under the chromatographic conditions described by Bidlingmeyer *et al.*[4] The resolution between ptc-DAPA and ptc-DABA was improved by decreasing the slope of the elution gradient. However, a fall in the slope that was too marked led to an overlapping of the ptc-phe and ptc-DAPA peaks. The optimum separation between ptc-phe, ptc-DAPA and ptc-DABA was achieved with the chromatographic conditions reported in Table 1; the results are shown in Fig. 1.

A procedure allowing DAPA and DABA to be quantified together with 19 other amino acids including cysteic acid and methionine sulphone, at the picomolar level and within a relatively short analysis time (24 min), was designed. Any pre-column method of derivatization would be suitable for DAPA and DABA provided that adequate chromatographic conditions, such as those described for dansyl derivatives,[3] could be found for separating the resultant derivatives. On the other hand, the close resemblance of DAPA, DABA and lysine, which differ only by the number of methylene groups present in their side chains, caused them to be co-eluted in the classical ion-exchange procedure of amino acid determination as noted by Soby and Johnson.[2]

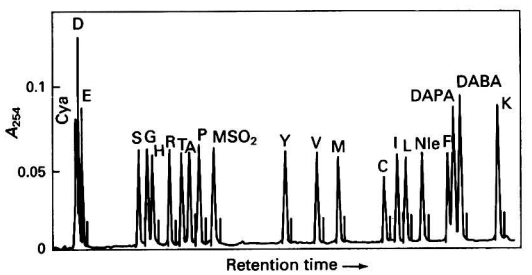

Fig. 1 Separation of ptc-amino acids, including DAPA and DABA. A standard sample containing 500 pmol of each amino acid was injected. Norleucine (Nle) was used as the internal standard. Cya, cysteic acid; MSO_2, methionine sulphone; and the one-letter code is used for other amino acids. Retention times (in minutes) are as follows: Cya, 3.38; D, 3.48; E, 3.66; S, 6.33; G, 6.71; H, 6.99; R, 7.77; T, 8.33; A, 8.68; P, 9.15; MSO_2, 9.79; Y, 13.07; V, 14.57; M, 15.56; C, 17.66; I, 18.25; L, 18.67; Nle, 19.46; F, 20.67; DAPA, 20.93; DABA, 21.25; and K, 23.01

BTI Treatment

Four proteins were treated with BTI for 4 h in the presence of acetonitrile or DMF, at 35 or 60 °C. Bis(trifluoroacetoxy)iodobenzene has been used in the presence of acetonitrile to convert amides of small molecules into amines under mild conditions (at room temperature for 2–5 h)[6] and it has also been employed in the presence of DMF at 35 °C for small peptides,[7,8] and at 60 °C for proteins.[2] As shown in Table 2, the best conversion occurred in the presence of DMF at 60 °C; at this temperature, the solvent had a stronger effect on asparagine than glutamine. In addition, the conversion was not affected when the concentration of BTI was varied from 0.016 to 0.8 mol dm^{-3} (data not shown). Acetonitrile made the extraction procedure simple and induced no interference in the chromatogram. Dimethylformamide caused the presence of additional peaks, the magnitudes of which were related to the concentration of BTI used, and impeded the quantification of DAPA and DABA when a high concentration of BTI (0.8 mol dm^{-3}) was used.

Kinetics of Conversion of Asparagine and Glutamine

Fig. 2 depicts the effects of treatment with BTI on three proteins left in contact with the reagent for between 30 min and 16 h. The effects were assessed through the decrease of asx and glx, and the appearance of DAPA and DABA. The kinetic curves were normalized by expressing the data as the ratio of the experimental value to that predicted from the amino acid sequence. Hence, the ratio for asx or glx must decrease from 1 to a value corresponding to the ratio of asp (or glu) to asx (or glx) calculated from the sequence data for the complete disappearance of asn and gln. Similarly, the ratio for DAPA and DABA must increase from 0 to 1 corresponding to the complete conversion of asn and gln.

The kinetics for the conversion of individual amino acids displayed the same profile regardless of the proteins being studied (Fig. 2). The following information could be obtained from the graphs (Fig. 2). (*i*) The maximum disappearance of glx was reached after about 30 min and that of asx after 2 h. This corresponded to a near complete conversion for gln and partial conversion for asn when the ratios were compared with those anticipated from the sequence data; (*ii*) the appearance of DAPA and DABA was progressive, reaching a plateau after 4 h, however, the levels of appearance were lower than those expected from the disappearance of asn and gln. This discrepancy cannot be ascribed to any interference involving the derivatization with PITC as no significant differences were observed between untreated and BTI-treated proteins regarding stable amino acids other than lysine. Lysine, as shown in Fig. 2, displayed the same behaviour as DAPA and DABA, although its quantification should be independent of the rate of amide degradation.

From the foregoing, BTI was assumed to react with the diamino acids present in the polypeptide or formed during the

Table 2 Influence of BTI reaction conditions on the production of diamino acids

		CH_3CN		DMF		DMF: CH_3CN*
		35 °C	60 °C	35 °C	60 °C	
Cytochrome *c*	DAPA†	1.7‡	2.9	3.0	3.2‡	1.1
	DABA	1.0	2.0	1.6	2.2	1.1
Lysozyme	DAPA	1.7‡	3.0§	4.8‡	5.0	1.7
	DABA	0.7	0.9	1.2	1.1	1.2
Ribonuclease A	DAPA	—	3.3	—	5.6§	1.7
	DABA	—	4.5	—	5.1	1.1
α-Chymotrypsinogen	DAPA	—	5.7‡	—	7.0‡	1.2
	DABA	—	5.6	—	6.0	1.1

* Ratio of the value after reaction in DMF, at 60 °C and after reaction in CH_3CN, at 60 °C.
† DAPA and DABA values were determined based on their ratios to alanine in the hydrolysates and expressed in moles per mole of protein.
‡ Mean of two experiments.
§ Mean of three experiments.

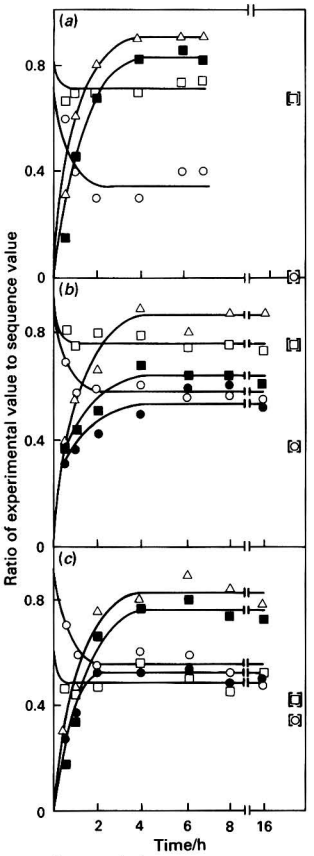

Fig. 2 Time course of asx and glx decrease, and DAPA and DABA increase in BTI treated proteins. (*a*) insulin B; (*b*) cytochrome *c*; and (*c*) ribonuclease A. ○, $(asx)_{treated}/(asx)_{sequence}$; □, $(glx)_{treated}/(glx)_{sequence}$; ●, $DAPA/(asn)_{sequence}$; ■, $DABA/(gln)_{sequence}$; and △, $(lys)_{treated}/(lys)_{sequence}$. [○] and [□] Correspond to expected values for the complete disappearance of asn and gln, respectively. Sequence data are from references 9–11

treatment, to yield intermediate compounds which were unaffected by acid and were gradually converted back into their initial state *i.e.*, that of a diamino acid.

On the other hand, BTI caused the complete disappearance of free gln and asn after 30 min and 2 h of contact, respectively, however, neither DAPA nor DABA was detected.

From Fig. 2, it was deduced that a maximum yield of about 50% for DAPA, 75% for DABA and 85% for lysine after a protein contact time of at least 4 h with BTI could be obtained. The value for the yield of DABA exhibited some variations from one protein to another; the same was probably true for the yield of DAPA. This made the evaluation of these diamino acids unsuitable for assaying asn and gln in proteins. Such an assay can be performed only by estimating the disappearance of asn and gln resulting from the use of BTI, as proposed by Soby and Johnson.[2] However, contrary to the results obtained by those workers[2] the disappearance of asn was found, in the present study, to be incomplete, averaging about 65%.

Additional information on the rate of amide disappearance for four proteins treated with BTI for 4 h in the presence of DMF at 60 °C (as described by Soby and Johnson[2]) is given in Table 3. The results are expressed in two ways. The first relies on the sequence data for the asx (or glx) content in an untreated sample, which minimizes the effect of experimental errors. The second took into consideration experimental values only, which gives a truer picture of the variability of the assay for proteins of unknown sequence. Both methods of

Table 3 Disappearance of asn and gln for four proteins treated with BTI for 4 h (all values in %)

Parameter	Insulin B	Cytochrome *c*	Ribonuclease A	α-Chymotrypsinogen	Mean ± SD*
d_{asn}†	70	66	65	67	67 ± 2
d_{gln}	90	97	89	91	92 ± 4
δ_{asn}‡	60	56	70	62	62 ± 6
δ_{gln}	110	90	96	99	98 ± 8

* SD = standard deviation.

† $d_{asn} = 100[(asx)_S - (asx)_T]/(asn)_S$, S = sequence[9–12] and T = BTI treatment.

‡ $\delta_{asn} = 100[(asx)_{NT} - (asx)_T]/(asn)_S$, NT = no BTI treatment.

expression led to close values for the rates of amide disappearance, in agreement with the mean values deduced from Fig. 2, and confirmed the degradation to be virtually exhaustive for gln and partial for asn. On the other hand the standard deviation was higher when only experimental values were taken into account, suggesting some fluctuations in the determination of asp and glu when using the PITC derivatization. It is known that the yields of ptc-asp and ptc-glu are sometimes variable owing to the presence of material extracted from the glass tube during acid hydrolysis, which perturbs the derivatization.[13]

Conclusion

The results presented here afford a further insight into the use of BTI for the determination of asn and gln in proteins. In this way a direct assay through the evaluation of DAPA and DABA cannot be exploited as the conversion into these diamino acids is incomplete and variable from one protein to another. Therefore, an indirect assay based upon the estimation of degraded amides, as proposed by Soby and Johnson,[2] is required. The disappearance, probably complete for gln irrespective of the protein being studied, is partial for asn, varying in narrow limits from one protein to another. Thus, the determination of asn implies not only an accurate assessment of its disappearance rate and its variability from one protein to another but also a precise quantification of asp. These observations are being investigated further.

References

1 Wilcox, P. E., in *Methods in Enzymology*, ed., Hirs, C. H. W., Academic Press, New York, 1967, vol. II, p. 63.
2 Soby, L. M., and Johnson, P., *Anal. Biochem.*, 1981, **113**, 149.
3 Vendrell, J., and Aviles, F. X., *J. Chromatogr.*, 1986, **358**, 401.
4 Bidlingmeyer, B. A., Cohen, S. A., and Tarvin, T. L., *J. Chromatogr.*, 1984, **336**, 93.
5 Legris-Delaporte, S., and Landry, J., *J. Cereal Sci.*, 1987, **6**, 119.
6 Radhakrishna, A. S., Parham, M. E., Riggs, R. M., and Loudon, G. M., *J. Org. Chem.*, 1979, **44**, 1746.
7 Parham, M. E., and Loudon, G. M., *Biochem. Biophys. Res. Commun.*, 1978, **80**, 1.
8 Parham, M. E., and Loudon, G. M., *Biochem. Biophys. Res. Commun.*, 1978, **80**, 7.
9 Ryle, A. P., Sanger, F., Smith, L. F., and Kitai, R., *Biochem. J.*, 1955, **60**, 541.
10 Margoliash, E., Smith, E. L., Kreil, G., and Tuppy, H., *Nature (London)*, 1961, **192**, 1125.
11 Smyth, D. G., Stein, W. H., and Moore, S., *J. Biol. Chem.*, 1963, **238**, 227.
12 Hartley, B. S., and Kaufmann, D. L., *Biochem. J.*, 1966, **101**, 229.
13 Mora, R., Berndt, K. D., Tsai, H., and Meredith, S. C., *Anal. Biochem.*, 1988, **172**, 368.

Paper 0/05302C
Received November 26th, 1990
Accepted January 23rd, 1991

Analytical Applications of Oxocarbons

Part 3.* Specific Spectrophotometric Determination of Oxalic Acid by Dissociation of the Zirconium(IV)–Chloranilate Complex

Anne-Marie Dona and Jean-François Verchère†
Unité de Recherche Associée 500 du C.N.R.S., Faculté des Sciences, B.P. 118, 76134 Mont-Saint-Aignan, France

Oxalic acid can be determined spectrophotometrically, as it dissociates the chloranilate complex of zirconium(IV) at pH 2. The decrease in the absorbance at 335 nm is proportional to the amount of oxalic acid present. Optimum conditions for the method are described. The sensitivity of the method is high, allowing the determination of 0.035 ppm of oxalic acid. Because of the very high stabilities of the zirconium(IV) complexes of chloranilate or oxalate, few compounds interfere, particularly hydroxy acids. D-Glucose and alditols did not interfere, which could be useful in studies on solutions of biological interest.

Keywords: *Oxalate determination; chloranilate; zirconium(IV); spectrophotometry*

In recent years, there has been an increasing interest in the determination of oxalic acid in biological and non-biological materials.[1] Current methods are based on prior separation by solvent extraction, precipitation or chromatography; oxalate is then determined by amperometry[2] or spectrophotometry.[3] In order to develop less time-consuming procedures, more specific methods have been investigated, based on electrogenerated chemiluminescence[4] or enzymic techniques, using either oxalate decarboxylase[5] or immobilized oxalate oxidase.[6,7]

Few methods are based on spectrophotometry. Although oxalate and its complexes are colourless, absorbance variations can be produced when oxalate reacts with a metal ion, dissociating the coloured complex initially present. Such a method has been developed, for example, by using the uranium–4-(2-pyridylazo)resorcinol (PAR) complex.[8] The absorbance decreased linearly with the oxalate concentration in the range 0–3 ppm, but the method was subject to numerous interferences. In order to increase the selectivity of the procedure, Salinas *et al.*[3] combined separation and spectrophotometry by extracting a mixed vanadate–mandelohydroxamate–oxalate complex into toluene, with the assistance of a phase-transfer reagent (a quaternary ammonium salt). The method allowed the determination of oxalate in urine and blood serum.

We attempted to resolve the problem of specificity in another way, by using a metal ion which would form oxalate complexes with particularly high stabilities compared with other interfering biological species. In this respect, it was considered that carbohydrates would be likely interferents in biological samples. Zirconium(IV) was chosen because the corresponding stability constants[9] appeared to fulfil these conditions, thus avoiding the necessity of extracting oxalate prior to the absorbance measurements. Chloranilate (the ion of 2,5-dichloro-3,6-dihydroxy-1,4-benzoquinone) was chosen as the coloured complex-forming agent, because it belongs[10] to the oxocarbon[11] series. This ensured that it had a high solubility in water and that its complex with zirconium(IV) was highly coloured.[12,13] Finally, the zirconium(IV)–chloranilate complex was less stable than the zirconium(IV)–oxalate complex and could be dissociated within a suitable pH range.

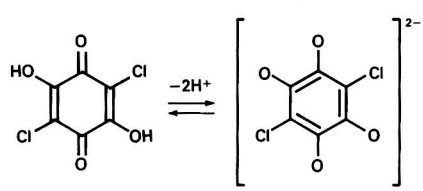

Chloranilic acid (H_2C) Chloranilate ion (C^{2-})

* For Part 2 of this series, see reference 22.
† To whom correspondence should be addressed.

Experimental

All chemicals were of analytical-reagent grade.

Stock solutions of known concentrations of chloranilic acid (Fluka, puriss, 2.5×10^{-3} mol dm^{-3}), zirconyl chloride octahydrate (Fluka, puriss, 0.1 mol dm^{-3}) and oxalic acid (1 g l^{-1}) were prepared by exact weighing and dilution in purified (Millipore) water.

Solutions of the zirconium(IV)–chloranilate complex were prepared by mixing, in the following order, chloranilic acid, hydrochloric acid (1×10^{-3} mol), zirconyl chloride and water. The typical concentration of the complex was 1.67×10^{-4} or 1.67×10^{-5} mol dm^{-3} depending on whether 1 mm or 1 cm cells were used. The volume of the solution (pH $\approx$ 2) was 100 cm^3. The solutions were used after allowing them to stand at room temperature for 24 h.

For the determination of oxalate and interference studies, oxalic acid was added either in solid form or in solution with a micropipette (V_{max} = 1 cm^3). Absorbance measurements were made immediately on a Kontron Uvikon 860 spectrophotometer equipped with 1 mm or 1 cm quartz cells, at ambient temperature. The pH values were measured with a Metrohm 632 pH meter and a combined glass electrode.

Principle of the Method for the Determination of Oxalate

The method is based on the competitive complexation of zirconium(IV) by chloranilate and oxalate. Chloranilic acid (H_2C) is known[12,13] to give a bright magenta solution with a low concentration of zirconium(IV) even in a strongly acidic solution. In the complex(es), the ligand possesses an aromatic structure[14] in which the charges are shared by the oxygen atoms. Accordingly, an intense ultraviolet band is found at 335 nm. On the other hand, oxalic acid also forms stable complexes with zirconium(IV)[9] in acidic media, with the formula $Zr(Ox)_n^{(2n-4)-}$ (n = 1–4). If the concentration and pH are adjusted so that the oxalate complex(es) is(are) more stable than the chloranilate complex(es), the over-all reaction can be displaced to favour the formation of the oxalate species according to the following equation:

$$ZrC_m + nOx \rightleftharpoons Zr(Ox)_n + mC$$

where ZrC_m and $Zr(Ox)_n$ are the chloranilate and oxalate complexes, respectively (charges are omitted for simplicity).

Fig. 1 shows schematically the reactions involved in the process. The spectrum of the zirconium(IV)–chloranilate complex is related to that of the free chloranilate ion, C^{2-}. However, at pH 2, where the main uncomplexed species is the hydrogenochloranilate ion, HC^-, a large absorbance difference is observed at 335 nm. Hence, the dissociation of the zirconium(IV)–chloranilate complex could be monitored as a function of the concentration of oxalic acid, as shown in Fig. 2.

Results and Discussion

Optimum Conditions for the Formation of the Zirconium(IV)–Chloranilate Complex

All initial experiments were carried out with $[H_2C] = 5 \times 10^{-4}$ mol dm^{-3}, which is the optimum concentration when using 1 mm cells. The effect of pH on the formation of the zirconium(IV)–choranilate complex was studied. Maximum complex formation was obtained at a pH of 2.10. At higher pH values, progressive dissociation of the zirconium(IV)–chloranilate complex occurred with the release of C^{2-}. After 2 h at pH >8, no complex could be detected; the spectrum was that of the C^{2-} ion alone. Experiments were carried out to study the reversibility of this dissociation reaction. When the dissociated complex was subjected to an acidic medium (pH = 2), complexation was no longer possible, as the spectra indicated the presence of the free HC^- ion. Hence, zirconium(IV) had been irreversibly transformed, in basic medium, into a species that was unable to react with chloranilic acid at any pH value. It has been reported[15] that zirconium(IV) polymerizes in aqueous solution to a tetrameric hydroxide,[16]

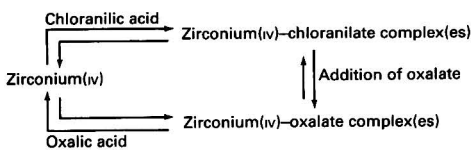

Fig. 1 Principle of the competitive method for the determination of oxalic acid

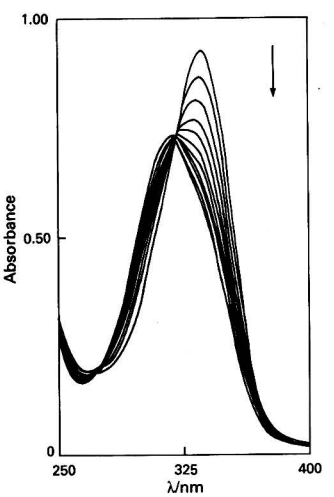

Fig. 2 Variation of the spectrum of a solution of the zirconium(IV)–chloranilate complex as a function of oxalic acid concentration. $[H_2C] = 5 \times 10^{-5}$ mol dm^{-3}; $q = [Zr^{IV}]/[H_2C] = 0.33$; pH = 2.09; and l = 1 cm. The spectra correspond, in the order shown by the arrow, to the concentrations of oxalic acid given in Fig. 4, curve 3

$[Zr_4(OH)_8(H_2O)_{16}]^{8+}$, which is known[17,18] to have a low tendency to undergo complexation. Hence, it was necessary to develop a procedure in which the zirconyl solution would not reach a pH >2.

Therefore, the various reagents must be added in the following order: chloranilic acid, hydrochloric acid and zirconium(IV), and then water to make the solution up to the final volume. It was found that the maximum absorbance was not reached immediately at pH 2. The formation of the complex was slow and the reaction rate increased with the molar ratio q ($q = [Zr^{IV}]/[H_2C]$). Formation of the complex was complete after 5 h for a value of q greater than 0.15.

Stoichiometry of the Zirconium(IV)–Chloranilate Complex

The stoichiometry of the complex was determined by the molar ratio method at a pH of about 2, at which the complex had maximum stability. The results were not very reproducible, because of the slow reaction rate. Care was taken to record the spectra after identical reaction times (24 h) for all the solutions with different values of q.

At pH <0.33, the absorbance increased as a function of q, but the plot was not linear. However, if the points corresponding to q <0.1 were ignored, a satisfactory linear plot was obtained, giving a break for $q = 0.33$ (Fig. 3). The initial sharp increase in the absorbance for q <0.1 might be due to the transient formation of a species containing a larger proportion of chloranilate, possibly with a stoichiometry of 1:4, as zirconium(IV) is known to form octa-coordinated complexes.[9] Nevertheless, the main species characterized under the conditions used here was the 1:3 zirconium(IV)–chloranilate complex.

Attempts were made to verify this stoichiometry by using the molar ratio method in more acidic media (1 or 2 mol dm^{-3} HCl). Unfortunately, the extent of complex formation decreased when the acid concentration was increased, yielding curves instead of linear segments. Tentative determinations of the breaks on such plots gave values for q of 0.40–0.45, which could also be accounted for by a 1:2 stoichiometry for the complex. These results are in contrast to those of Thamer and Voigt[12] which were obtained in very acidic media (2 mol dm^{-3} $HClO_4$), and indicated both a 1:1 and a 1:2 complex. However, our findings in acidic media show that the low stability of the complex does not allow the precise determination of its composition.

On the other hand, Varga and Veatch[19] found that a 1:1 and a 1:3 complex were formed between hafnium(IV) and chloranilic acid in 3 mol dm^{-3} $HClO_4$. Because zirconium and hafnium are elements with very similar properties,[9] it was surprising that complexes of different stoichiometries, *viz.*, 1:2 or 1:3, should be formed under analogous conditions. The results presented here, however, support the formation of

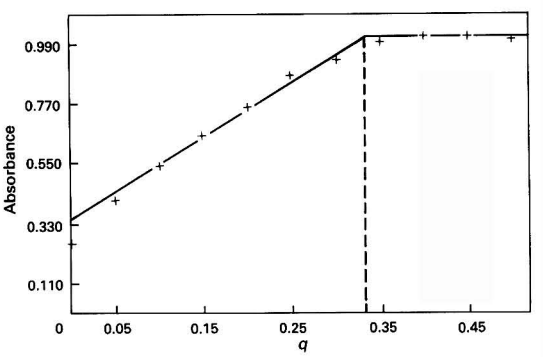

Fig. 3 Absorbance of a solution of the zirconium(IV)–chloranilate complex *versus* the molar ratio q. $[H_2C] = 5 \times 10^{-4}$ mol dm^{-3}; $q = [Zr^{IV}]/[H_2C]$; pH = 2.0; l = 1 mm; and λ = 335 nm

a zirconium(IV) complex with a 1:3 stoichiometry, as was found for hafnium(IV).[19]

It was suggested that chloro complexes of zirconium(IV) could have been formed in this work, thus explaining the differences between our results and those obtained using the non-complexing acid $HClO_4$. Hence two complementary experiments were performed. In the first, the molar ratio method was used with 1 mol dm^{-3} $HClO_4$; this gave a curve similar to that obtained with 1 mol dm^{-3} HCl. In the second, chloride ions, up to a concentration of 0.1 mol dm^{-3}, were added to a solution of the zirconium(IV)–chloranilate complex ($[H_2C] = 5 \times 10^{-4}$ mol dm^{-3}, $q = 0.33$, pH = 2); no change in the absorption spectrum of the complex was observed. It was therefore concluded that the formation of chloro complexes was negligible under the experimental conditions used here.

Determination of Oxalic Acid

Taking into account the above results, the following conditions were chosen: $[H_2C] = 5 \times 10^{-4}$ mol dm^{-3}; $q = 0.33$; pH = 2; path length (l) = 1 mm; and $\lambda = 335$ nm.

Experiments were carried out in which the decrease in the absorbance was monitored as a function of the oxalic acid concentration. The method was very sensitive. For example, a decrease in the absorbance of 0.117 was found for the addition of 0.2 cm^3 of a solution of oxalic acid (1 g l^{-1}) to 100 cm^3 of a solution of the complex (concentration of oxalic acid = 2×10^{-3} g l^{-1}). The sensitivity was defined as the slope of the initial portion of the plot of absorbance *versus* oxalic acid concentration. It was found that the sensitivity was enhanced by using a lower concentration of the coloured complex, because less oxalic acid was necessary for its dissociation.

A second series of measurements were made in which the concentrations of zirconium(IV) and chloranilic acid were reduced by a factor of 10, *i.e.*, $[H_2C] = 5 \times 10^{-5}$ mol dm^{-3}; $q = 0.33$; and $l = 1$ cm. As expected, the sensitivity (S) increased ten times. For $[H_2C] = 5 \times 10^{-4}$ mol dm^{-3}, $q = 0.33$ and $l = 1$ mm, $S = 58.5$ l g^{-1}. For $[H_2C] = 5 \times 10^{-5}$ mol dm^{-1}, $q = 0.33$ and $l = 1$ cm, $S = 590$ l g^{-1}.

Detection Limit

Under the standard conditions (pH = 2), the initial absorbance of a solution of the zirconium(IV)–chloranilate complex containing no oxalic acid, obtained from six replicate determinations, was 0.89 ± 0.02, for $l = 1$ cm. This corresponded to an apparent molar absorptivity (ε) of 17 800 dm^3 mol^{-1} cm^{-1} (calculated for one chloranilate moiety). Hence, the detection limit was defined as the oxalate concentration corresponding to an absorbance value of 0.87, *i.e.*, 0.035 mg l^{-1} or 0.035 ppm. This detection limit is much lower than those reported for earlier methods, *viz.*, 0.5 ppm[3] and 0.4 ppm.[8] This probably resulted from the very high absorptivity of the zirconium(IV)–chloranilate complex.

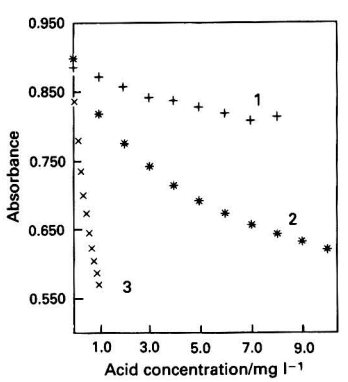

Fig. 4 Absorbance of a solution of the zirconium(IV)–chloranilate complex *versus* the concentration of organic acids. 1, D-Gluconic acid; 2, DL-tartaric acid; and 3, oxalic acid. $[H_2C] = 5 \times 10^{-5}$ mol dm^{-3}; $q = [Zr^{IV}]/[H_2C] = 0.33$; pH = 2.09; $l = 1$ cm; and $\lambda = 335$ nm

Interferences

Examination of the literature on the spectrophotometric determination of oxalate showed that many metal ions interfere. As oxalate can complex with nearly all metal cations, it is obvious that their tolerance limits will be very low in any method. Only the alkali metal ions (Na^+, K^+ and NH_4^+) can be tolerated in appreciable amounts (100 ppm). Alkaline earth metal ions such as Mg^{2+} and Ba^{2+} interfere slightly, but Ca^{2+} precipitates either chloranilate[20] or oxalate and should be removed if present.

The study of the interference of anions is more interesting. Oxo-ions (MoO_4^{2-}, WO_4^{2-}, VO^{2+} and UO_2^{2+}) form coloured complexes[21–24] with chloranilate and hence interfere seriously. Dichromate would oxidize oxalate. Highly complexing agents such as ethylenediaminetetraacetic acid (EDTA) should, of course, be avoided. Of the inorganic anions, only fluoride[9] can be expected to complex with zirconium(IV).

Because the determination of oxalate is generally required for biological studies, the possible interference of biomolecules, such as carbohydrates, polyols and hydroxy acids, was examined. Chloride and sulphate ions, which are reported[9] to form stable complexes with zirconium(IV), were also tested.

A concentration that did not cause more than a 1% change in the absorbance was taken as the tolerance limit. The presence of 20 g l^{-1} of D-glucitol, 20 g l^{-1} of D-mannitol, 20 g l^{-1} of xylitol, 7 g l^{-1} of D-glucose, 5 g l^{-1} of chloride and 0.01 g l^{-1} of sulphate did not interfere with the determination of oxalate.

On the other hand, 5×10^{-3} g l^{-1} of D-gluconic acid caused a 7% decrease in the absorbance, whereas 5×10^{-3} g l^{-1} of DL-tartaric acid caused a decrease of 20% (Fig. 4). This showed that these acids formed fairly stable complexes with zirconium(IV). In order to confirm this, the corresponding sensitivities (S) were calculated under identical conditions: $[H_2C] = 5 \times 10^{-5}$ mol dm^{-3}; $q = 0.33$; pH ≈ 2; and $l = 1$ cm. Values of S of 620, 78 and 15 l g^{-1} were found for oxalic, DL-tartaric and D-gluconic acid, respectively. This gave a relative order of stability of the three complexes which was in agreement with that obtained by an ion-exchange method.[9]

These results show that the stabilities of the complexes of zirconium(IV) decrease as the distance between the carboxyl groups of the hydroxy acids increases. The absence of one (gluconic acid) or two carboxyl groups (polyols) makes the complexes even less stable. The low stabilities of the polyol complexes suggest that the hydroxyl groups play little part in the chelation of zirconium(IV).

Conclusion

The method described here for the determination of oxalate compares favourably with a procedure recently reported by Salinas *et al.*[3] It is essentially simpler, because the extraction step is avoided. The principle is slightly different, as no ternary complex is formed between zirconium(IV), chloranilate and oxalate. The technique is based instead on 'bleaching' of a solution of a coloured complex consecutive to the formation of the more stable oxalate complex. However, the limitations are almost the same, and the list of interfering species is analogous, including those metal ions which can complex with chloranilic acid at pH 2, and the complexing agents of zirconium(IV). It appears, nevertheless, that the proposed method is potentially more sensitive (detection limit 0.035 ppm as opposed to 0.5 ppm), and possesses a higher

specificity if organic interferents are considered. It is particularly significant that carbohydrates and polyols were found not to interfere, and that hydroxy acids interfered only slightly. This might prove useful in studies of solutions of biological interest. As with the related method based on bleaching of the uranium–PAR complex,[8] this might also be useful in the area of water resource research.

The authors thank E. Leconte for technical assistance with part of the experimental work.

References

1 Hodgkinson, A., *Oxalic Acid in Biology and Medicine*, Academic Press, New York, 1977.
2 Fogg, A. G., Alonso, R. M., and Fernandez-Arciniega, M. A., *Analyst*, 1986, **111**, 249.
3 Salinas, F., Martinez-Vidal, J. L., and Gonzalez-Murcia, V., *Analyst*, 1989, **114**, 1685.
4 Rubinstein, I., Martin, C. R., and Bard, A. J., *Anal. Chem.*, 1983, **55**, 1580.
5 Knowles, C. F., and Hodgkinson, A., *Analyst*, 1972, **97**, 474.
6 Nabi Rahni, M. A., Guilbault, G. G., and de Olivera, N. G., *Anal. Chem.*, 1986, **58**, 523.
7 Almuaibed, A. M., and Townshend, A., *Anal. Chim. Acta*, 1989, **218**, 1.
8 Neas, R. E., and Guyon, J. C., *Anal. Chem.*, 1972, **44**, 799.
9 Ryabchikov, D. I., Marov, I. N., Ermakov, A. N., and Belyaeva, V. K., *J. Inorg. Nucl. Chem.*, 1964, **26**, 965.
10 Poirier, J. M., and Verchère, J. F., *Talanta*, 1979, **26**, 341.
11 West, R., and Powell, D. L., *J. Am. Chem. Soc.*, 1963, **85**, 2577.
12 Thamer, B. J., and Voigt, A. F., *J. Am. Chem. Soc.*, 1951, **73**, 3197.
13 Hahn, R. B., and Johnson, J. L., *Anal. Chem.*, 1957, **29**, 902.
14 Andersen, E. K., *Acta Cryst.*, 1967, **22**, 196.
15 Zielen, A. J., and Connick, R. E., *J. Am. Chem. Soc.*, 1956, **78**, 5785.
16 Mak, T. C. W., *Can. J. Chem.*, 1968, **46**, 3491.
17 Connick, R. E., and McVey, W. H., *J. Am. Chem. Soc.*, 1949, **71**, 3182.
18 Devia, D. H., and Sykes, A. G., *Inorg. Chem.*, 1981, **20**, 910.
19 Varga, L. P., and Veatch, F. C., *Anal. Chem.*, 1967, **39**, 1101.
20 Tyner, E. H., *Anal. Chem.*, 1948, **20**, 76.
21 Lee, W. F., Shastri, N. K., and Amis, E. S., *Talanta*, 1964, **11**, 685.
22 Poirier, J. M., and Verchère, J. F., *Talanta*, 1979, **26**, 349.
23 Poirier, J. M., and Verchère, J. F., *J. Inorg. Nucl. Chem.*, 1980, **42**, 1514.
24 Marone, C. B., and Bianchi, G., *An. Quim.*, 1973, **69**, 205.

NOTE—References 10 and 22 are to Parts 1 and 2 of this series.

Paper 0/05144F
Received November 16th, 1990
Accepted January 3rd, 1991

Conductimetric Determination of Some Metal Ions Using Salicylaldoxime as the Reagent

Mitali Sarkar
Department of Chemistry, University of Kalyani, Kalyani 741235, Nadia, India

A simple and sensitive conductimetric method for the determination of copper(II), nickel(II), zinc(II), lead(II), palladium(II), iron(III) and aluminium(III) using salicylaldoxime in an ethanol–water mixture is described. The effect of solvent on the shape of the titration curve is studied; and statistical treatment of the experimental data indicates the method is both precise and accurate.

Keywords: *Conductimetric determination; salicylaldoxime; ethanol–water mixture; metal ion*

As the conductance of a solution relates to the total ionic content, it can be used to follow reactions that result in a change in this quantity.

Conductimetry was first developed as an electrochemical method for studying solutions. As the technique was developed it was used for the analysis of solutions, melts and solids and pure liquids. Conductimetry is one of the most successful yet simple analytical techniques; it can be used for the determination of the titration end-point in neutralization and in precipitation and complex forming reactions in both aqueous and non-aqueous media.[1–6]

In the work described in this paper, a conductimetric study of the interaction of some metal ions with salicylaldoxime in an ethanol–water (2 + 1) mixture has been carried out.

Experimental

All chemicals used were of analytical-reagent grade. Doubly distilled water with a conductivity of 1.58×10^{-4} S m^{-1} was used to prepare 1×10^{-2} mol dm^{-3} stock solutions of aqueous metal chlorides, which were standardized using ethylenediaminetetraacetic acid (EDTA) and metallochromic indicators.[7]

Apparatus

A YSI Model 32M conductance meter (Yellow Springs Instrument Co., Yellow Springs, OH, USA) was used. The measurement range was 1.0–200.0 μS with a maximum error of ± 0.2%. The YSI Model 3417 cell was also used with a conductivity cell constant, K_{cell}, of 100 m^{-1}.

Procedure

A 10.0 ml aliquot of 1×10^{-3} mol dm^{-3} aqueous metal chloride was transferred into a beaker containing 20.0 ml of ethanol. The conductivity cell was immersed in the beaker and 1×10^{-2} mol dm^{-3} ligand solution was added from a microburette. The conductance was measured subsequent to each addition of ligand solution and after thorough stirring. A graph of conductivity *versus* titre was constructed and the end-point determined.

Results and Discussion

Conductimetric titrations were carried out in order to determine the metal-ion concentration. The metal to ligand mole ratio, *i.e.*, the composition of the chelate formed, can be determined from the shape of the titration curve.

By changing the media of the titration, three different examples are described: (*i*) aqueous metal solution titrated with ethanolic ligand solution; (*ii*) ethanolic metal solution titrated with ethanolic ligand solution; and (*iii*) metal solution titrated with the ligand, both in an ethanol–water (2 + 1) mixture. The ligand concentration in each example was about ten times that of the metal solution in order to minimize the dilution effect on the conductivity throughout the titration. A dilution correction[8] was also made using the following equation, assuming that the conductivity is a linear function of dilution:

$$\lambda_{correc} = \lambda_{obs} [(V_1 + V_2)/V_1]$$

where λ is the corresponding electrolytic conductivity, V_1 is the initial volume and V_2 is the volume of added ligand (correc = corrected and obs = observed).

The experiments were carried out in potassium chloride of an ionic strength of 0.1 mol dm^{-3} in order to suppress the effect of the migration of electroactive ions.

Fig. 1 represents the Cu^{II} system and Fig. 2, the Fe^{III} system. The wide curvature (Fig. 1 line A) around the end point, when the aqueous Cu^{II} solution is titrated with the ethanolic ligand solution, can be explained with respect to the formation of a precipitated chelate in the aqueous medium. However, the accuracy of the conductivity value in this region depends on the speed of precipitation, composition and solubility of the precipitate.

An ethanolic Cu^{II} solution was titrated with an ethanolic solution of the ligand (Fig. 1 line B) and a small curvature around the end point was noticed. This is probably a consequence of most of the metal salts studied being insoluble in ethanol. The use of example (*iii*) was discussed to overcome

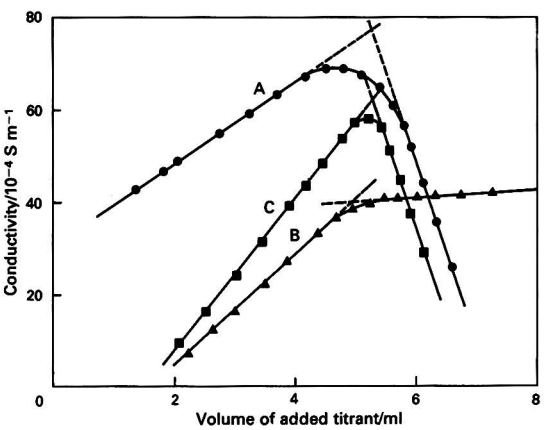

Fig. 1 Conductimetric titration of copper(II) with salicylaldoxime solution. A, aqueous metal solution *versus* ethanolic ligand solution; B, ethanolic metal solution *versus* ethanolic ligand solution; and C, metal *versus* ligand, both in ethanol–water mixture

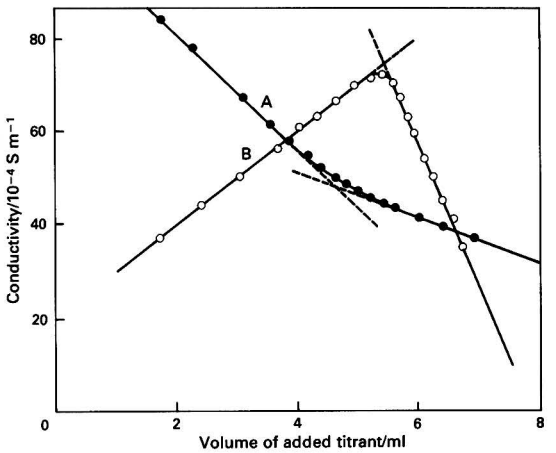

Fig. 2 Conductimetric titration of iron(III) with salicylaldoxime solution in ethanol–water mixture. A, 1×10^{-3} mol dm^{-3} metal *versus* 1×10^{-2} mol dm^{-3} ligand; and B, 1×10^{-2} mol dm^{-3} metal *versus* 1×10^{-1} mol dm^{-3} ligand

the problem of solubility of the chelate and the metal ion, in this example an ethanol–water (2 + 1) mixture is used both for the ligand solution and for the titration medium.

Fig. 1 line C shows the titration curve for a 1×10^{-3} mol dm^{-3} copper(II) chloride solution with a 1×10^{-2} mol dm^{-3} ligand solution in an ethanol–water (2 + 1) mixture. The conductivity increases initially, reaches a maximum and then decreases. The increase in the conductivity before the inflection point is the result of each Cu^{II} ion being replaced by two protons. The protons remain solvated and their interaction with the solvent depends on the ratio of ethanol to water used.[9] The observed maximum conductivity value corresponds to a Cu^{II}–ligand mole ratio of 1 : 2. The reaction can be represented as follows:

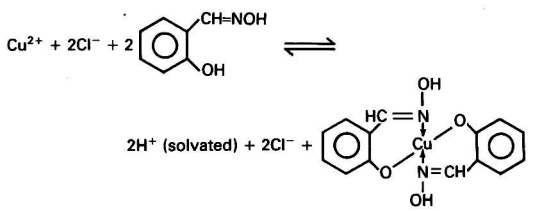

After the equivalence point it is expected that the conductivity should either remain constant (added ligand remains undissociated) or increase slightly (partial dissociation, if any, of the added ligand).

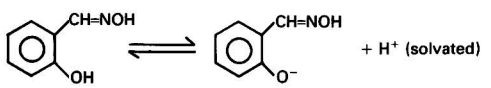

However, the titration curve indicates that after the equivalence point the conductivity of the solution decreases. One assumption is that the protons available in the medium interact with the added ligand solution.

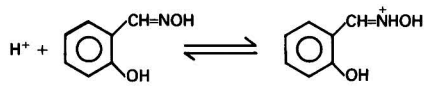

The pH of the solution was measured before and after the end-point. An increase of pH by 0.32 justifies the above

Table 1 Results of conductimetric titrations of metal ions with the ligand in an ethanol–water (2 + 1) mixture

Metal	Mass/g Taken	Mass/g Found	Recovery (%)	Metal–ligand mole ratio
Copper(II)	0.124	0.126	100.8	1:2
	0.290	0.292	100.6	
	0.416	0.418	100.5	
	0.832	0.836	100.5	
	1.040	1.045	100.5	
Zinc(II)	0.621	0.618	99.5	1:2
	0.937	0.931	99.3	
	0.775	0.771	99.5	
Cadmium(II)	0.449	0.447	99.4	1:2
	0.821	0.818	99.6	
	0.574	0.571	99.5	
Lead(II)	0.697	0.702	100.7	1:2
	0.769	0.772	100.4	
	0.976	0.988	100.2	
Iron(II)	0.722	0.720	99.7	1:2
	0.812	0.808	99.5	
	0.921	0.915	99.3	
Iron(III)*	0.724	0.721	99.6	1:1
	0.815	0.811	99.5	
	0.926	0.921	99.5	

* 1×10^{-2} mol dm^{-3} Fe^{III} solution titrated with 1×10^{-1} mol dm^{-3} ligand solution in an ethanol–water (2 + 1) mixture.

Table 2 Linear regression analysis of copper(II)

Mass of copper(II)/g Taken	Mass of copper(II)/g Found	Recovery (%)	Shift or intercept of the regression line	Regression coefficient or or slope of regression line
0.124	0.126	100.8		
0.290	0.292	100.6	0.0335	1.0046
0.416	0.418	100.5		
0.832	0.836	100.5		
1.040	1.046	100.5		

assumption. Furthermore, when 1×10^{-2} mol dm^{-3} of HCl in the ethanol–water (2 + 1) mixture was titrated with 1×10^{-2} mol dm^{-3} of ligand solution a continuous decrease in the conductivity was observed, again, confirming the above assumption. Similar titration curves were observed for the titration of Ni^{II}, Zn^{II}, Pb^{II}, Pd^{II} and Al^{III} with the ligand in the ethanol water (2 + 1) mixture. The observed maximum in the conductivity corresponds with a metal to ligand mole ratio of 1 : 2 in each instance.

Interesting behaviour is observed for the titration of Fe^{III} with the ligand: when 1×10^{-3} mol dm^{-3} of iron(III) chloride is titrated with 1×10^{-2} mol dm^{-3} ligand (L) solution in the ethanol–water (2 + 1) mixture (Fig. 2 line A) the conductivity decreases throughout the titration. Before the end-point, the highly mobile Fe^{III} ions are replaced by the solvated protons and the FeL_2^+ ions and the conductivity decreases rapidly. (The Fe^{III} ion has a greater mobility than the H^+ ion in the ethanol–water mixture, this is evident because the molar conductivity of iron(III) chloride is greater than that of HCl over the same titrant concentration range. After the end-point the decrease in conductivity is smaller. The change in conductivity in this region is attributed to the replacement of H^+ (solvated) by the $[H–L]^+$ ions.

$$Fe^{3+} + 3Cl^- + 2L \rightarrow 2H^+ \text{(solvated)} + 3Cl^- + (FeL_2)^+$$

$$2H^+ \text{(solvated)} + 3Cl^- + FeL_2^+ \rightarrow 2[H\text{–}L]^+ + 3Cl^- + (FeL_2)^+$$

The two rectilinear curves before and after the inflection point meet at the end-point, the mole ratio here corresponds to a 1 : 2 complex for the Fe^{III} chelates.

The change in the shape of the titration curve is of interest, as the Fe^{III} ion concentration is increased ten-fold when titrating against 0.1 mol dm^{-3} ligand solution (Fig. 2 line B). The conductivity first increases and then decreases after the end-point. At this relatively high concentration, $FeCl_3$ may initially be ionized incompletely.

$$FeCl_3 \rightleftharpoons FeCl_2^+ + Cl^-$$

Evidence supporting this dissociation can be found in the literature.[10,11] When the ligand is added in an ethanol–water (2 + 1) mixture, the H^+ (solvated) ions replace the $FeCl_2^+$ ions and the conductivity increases rapidly.

$$FeCl_2^+ + Cl^- + L \rightarrow [FeCl_2L] + Cl^- + H^+ \text{ (solvated)}$$

After the end-point the H^+ ion (solvated) is replaced by the slower moving $[H–L]^+$ ion, therefore, the conductivity decreases. The mole ratio for the Fe^{III} chelate in this instance is found to be 1:1 from the curve at the end-point. In such an instance the vacant metal site in the metal chelate might perhaps be filled by a solvent molecule, however, no direct proof for this is available.

No such variation in the shape of the titration curve and hence the composition of the metal chelate was found for the Cu^{II} system by varying either the metal ion or ligand concentration.

The data obtained from the conductimetric titration is summarized in Table 1. The data show that reproducible results are obtained with a good recovery.

In order to establish whether the proposed method exhibits any fixed or proportional bias, a simple linear regression[12] of the metal concentration was calculated (dependent variable) and the corresponding true concentration (independent variable) was obtained using a programmable calculator. A Student's *t*-test (at a 95% confidence level) was applied to the slope and the intercept of the regression line. The data for the Cu^{II} system are given in Table 2. Statistical analysis of the data shows that the calculated slope and intercept do not differ significantly from the ideal value of unity and zero, respectively. Hence, it can be concluded that there are no systematic differences between the determined and true concentrations over a wide range. Similar calculations were carried out for other metals.

Conclusion

The proposed method is simple and has several advantages over other methods. A buffer is not necessary, in contrast to the conductimetric titration of metal ions with EDTA in buffered media.[7] End-point detection is simple as no background conductivity of the buffer affects the experimental value.[13] Trace amounts of metal ions as low as 0.4 mg dm^{-3} can be determined by this method, even in the presence of interferent salts such as KCl and KNO_3 which might be present at concentrations in excess of ten-fold over the metal ion being determined.

References

1 Lopatin, B. A., *Conductimetry and Oscillometry*, Academy of Sciences of the USSR, 1971, ch. 1, p. 3.
2 Vydra, F., and Karlik, M., *Chem. Listy.*, 1957, **50**, 1749, 1754.
3 Kolthoff, I. M., and Elving, P. J., *Treatise on Analytical Chemistry*, Interscience, New York, 1963, Part I, Vol. 4, p. 2618.
4 Foster, J. N., Hanson, O. C., Hon, J. F., and Muirhead, T. S., *NASA*, 1969, CR-1425, 189.
5 Pasovskaya, G. P., *Zh. Anal. Khim.*, 1957, **12**, 523.
6 Hall, J. L., Gibson, J. A., Jr., Wilkinson, P. R., and Philips, H. O., *Anal. Chem.*, 1954, **26**, 1484.
7 Vogel, A. I., *A Textbook of Quantitative Inorganic Analysis*, English Language Book Society, 3rd edn., 1961, ch IV.
8 Lingane, J. J., *Electroanalytical Chemistry*, Interscience, New York, 2nd ed., 1958, ch. 9, p. 188.
9 Dneprov, G. F., *Uch. Zap. Leningord. Gos. Univ. im. A. A. Zhdanova, Ser Khim. Nauk*, 1953, (13), 56, *Chem. Abstr.*, 1956, **50**, 5373C.
10 Dawson, L. R., and Belcher, R. L., *Trans. Ky. Acad. Sci.*, 1951, **13**, 129.
11 El Aggan, A. M., Bradley, D. C., and Wardlaw, W., *J. Chem. Soc.*, 1958, 2092.
12 Miller, J. C., and Miller, J. N., *Statistics for Analytical Chemistry*, Ellis Horwood, Chichester, 1984, ch. 1, p. 90.
13 West, T. S., *Complexometry With EDTA and Related Reagents*, 3rd edn, BDH Chemicals, 1969, p. 83.

Paper 0/03007D
Received July 4th, 1990
Accepted November 11th, 1990

Extraction and Determination of Manganese(II) in Environmental and Pharmaceutical Samples

N. M. Sundaramurthi and Vijay M. Shinde*
Analytical Laboratory, The Institute of Science, 15 Madame Cama Road, Bombay 400 032, India

A method is proposed for the extraction of manganese(II) from salicylate media by using Aliquat 336 dissolved in xylene as an extractant. The optimum conditions were determined from a critical study of pH, salicylate concentration, Aliquat 336 concentration, diluent and period of equilibration (shaking time). The method permits the separation of manganese from binary mixtures containing commonly associated metal ions. Manganese is determined either by spectrophotometry with 4-(2-pyridylazo)resorcinol or by atomic absorption spectrometry. The method is applicable to the extraction and determination of manganese in environmental and pharmaceutical samples.

Keywords: *Manganese(II) extraction and separation; salicylate solution; liquid ion exchanger; pharmaceutical and environmental samples*

A large number of industries discharge metal-containing effluents into air and water resources without adequate treatment. Contamination of the environment by manganese is currently an area of concern. Although manganese is an essential micro-nutrient, it is a respiratory irritant and a systemic poison when inhaled (as oxides) in excessive amounts. Manganese compounds are known to catalyse the oxidation of sulphur dioxide to sulphur trioxide.[1] In view of this, the determination of manganese is desirable. The proposed method fulfils this requirement.

Few solvent extraction methods are known for manganese. Amines of high relative molecular mass[2–6] have been used for the extraction of manganese(II) from hydrochloric acid and thiocyanate solutions. Extraction of bromo complexes of manganese(II) with Alamine 336[2] and tributyl phosphate[7] and of iodo complexes with Alamine 336[2] and trioctylamine (TOA)[8] have also been reported. Similarly, methyltrioctylammonium chloride,[9] tributyl phosphate,[10] bis(2-ethylhexyl) hydrogen phosphate,[11] long-chain alkylamines[12] and Aliquat 336[13] have been used for the solvent extraction of manganese(II). However, existing methods suffer from several drawbacks, such as a longer extraction time,[2,7,9] temperature control,[2,5,7] emulsification problems[5,7,13] and incomplete extraction.[3,6] Liquid ion exchangers such as Aliquat 336 and TOA have been used in this laboratory for the extraction of titanium(IV), zirconium(IV) and hafnium(IV) from salicylate solution.[14] An extension of this work has shown that it is possible to extract managanese from salicylate solution into Aliquat 336 dissolved in xylene. After stripping from the organic phase, manganese is determined by spectrophotometry with 4-(2-pyridyazo)resorcinol (PAR). The method is simple, rapid and selective and affords separation of manganese from associated metal ions such as cobalt(II), copper(II), mercury(II), iron(III), vanadium(V), chromium(VI) and tungsten(VI) in binary mixtures, and permits the determination of manganese in alloys, pharmaceutical samples and environmental samples.

Experimental

Apparatus and Reagents

Absorbance measurements were carried out on a Unicam SP 500 spectrophotometer with 1 cm silica cells and on a Varian Techtron AA6 atomic absorption spectrometer, and the pH was measured by a Control Dynamics digital pH meter equipped with a combined glass electrode.

The stock solution of manganese(II) was prepared by dissolving 1.1 g of $MnSO_4 \cdot 4H_2O$ in 250 ml of distilled water containing 2 ml of concentrated sulphuric acid. The solution was standardized by titrimetry with ethylenediaminetetraacetic acid[15] and the metal content was found to be 1.068 mg ml^{-1}. The solution was diluted further as required.

Aliquat 336 (methyltrioctylammonium chloride) (Fluka, Buchs, Switzerland) was used without further purification. Solutions of Aliquat 336 (3% m/v) in xylene were shaken with an equal amount of 1 mol dm^{-3} sodium salicylate solution before use.

A buffer solution of pH 10.0 was prepared from ammonium chloride (7 g) and concentrated ammonia solution (57 ml in 1 litre of water).

4-(2-Pyridylazo)resorcinol was used as a 0.1% aqueous solution for the determination of manganese.

All the other chemicals used were of analytical-reagent grade, unless indicated otherwise.

General Extraction Procedure for Manganese(II)

To an aliquot of a solution containing 8 μg of manganese, enough sodium salicylate was added to give a salicylate concentration of 0.05 mol dm^{-3} in a total volume of 25 ml. The pH of the solution was adjusted to 5.0 by the addition of sodium hydroxide solution and hydrochloric acid or by the addition of 6 ml of acetic acid–sodium acetate buffer solution of pH 5.0, then the mixture was shaken for 10 s in a separating funnel with 5 ml of 3% m/v Aliquat 336 solution. After the two phases had separated, the manganese was stripped from the organic phase with two 4 ml portions of 0.01 mol dm^{-3} sulphuric acid. The combined aqueous phases were shaken with 5 ml of xylene to remove the dissolved amine and analysed for manganese either by atomic absorption spectrometry (AAS) or by spectrophotometry after adding 10 ml of buffer solution of pH 10 and 0.5 ml of 0.1% PAR solution.[16]

Results and Discussion

Extraction Conditions

The extraction of manganese(II) was attempted at different pH values (3.2–11.0), sodium salicylate concentrations (0.0125–0.25 mol dm^{-3}) and Aliquat 336 concentrations (0.125–5%), all with xylene as the diluent. Metal ion recovery was calculated either by spectrophotometry or by AAS. It was found that 5 ml of 3% Aliquat 336 in xylene extracts microgram amounts of manganese (0.1–100 μg) quantitatively from 0.05 mol dm^{-3} sodium salicylate at pH 4.0–8.0 (Fig. 1).

* To whom correspondence should be addressed.

Milligram amounts of manganese (1–3 mg) were extracted with 5 ml of 5% Aliquat 336 in xylene from 0.05 mol dm^{-3} sodium salicylate at pH 4.0–8.0. The optimum extraction conditions are reported in Table 1.

Effect of Diluent

The effect of various diluents on the extraction of manganese by the proposed method was investigated. Of the solvents examined, such as benzene, toluene, xylene, hexane, chloroform, carbon tetrachloride and nitrobenzene, the extraction was quantitative with xylene, toluene and hexane; however, xylene was preferred for subsequent work because it afforded clear separation of the two phases.

Period of Extraction

The extraction was very rapid. The period of shaking was varied from 5 to 60 s. The recoveries of metal ions at 5, 7 and 9 s were 61.2, 86.2 and 98.2%, respectively. The extraction was quantitative at 10 s. However, it was found that prolonged shaking had no adverse effect on the extraction of the metal ion.

Table 1 Optimum extraction conditions for manganese(II)

[Mn]	[Salicylate]/ mol dm^{-3}	[Aliquat 336]	Extraction period/s	pH
0.1–100 μg	0.04–0.25	5 ml of a 3% m/v solution	10	4.0–8.0
1.0–3 mg	0.04–0.25	5 ml of a 5% m/v solution	10	4.0–8.0

Table 2 Effect of foreign ions on the extraction of 8 μg of manganese(II)

Tolerance limit*/μg	Foreign ion
400	Nitrite, iodide, tartrate, thiocyanate, nitrate
320	Chloride, thiosulphate
160	Phosphate, fluoride
120	Ag^{I}, Pt^{IV}, Ba^{II}
80	Mg^{II}, Al^{III}, Ti^{IV}, V^{V}, Sb^{III}, U^{VI}
64	Cr^{VI}, Os^{VIII}, Ce^{IV}
40	Ca^{II}, As^{III}, Mo^{VI}, Pd^{II}, Te^{IV}, W^{VI}, Hg^{II}, Bi^{III}, thiourea, oxalate, citrate, sulphate, cyanide
24	Zr^{IV}, Cd^{II}, Hf^{IV}, Au^{III}
8	Fe^{III}, Th^{IV}

* The tolerance limit amount is the average of triplicate analyses.

Nature of the Extracted Species

The log–log plot of distribution ratio *versus* salicylate concentration (at fixed pH and Aliquat 336 concentration) or distribution ratio *versus* Aliquat 336 concentration (at fixed pH and salicylate concentration) yielded a molar ratio of 1 : 2 with respect to both extractant and salicylate. Hence, the extracted species was thought to be an ion-associate of probable composition $[(R_4N^+)_2Mn(OC_6H_4COO)_2^{2-}]$. The anionic nature of the manganese–salicylate complex was confirmed by its adsorption on a column of Dowex 1–X8 anion-exchange resin.

Effect of Foreign Ions

Various amounts of foreign ions were added to a solution containing a fixed amount of manganese(II), and the recommended procedure was followed for the extraction and determination of manganese ions. The tolerance limit was set at the amount of foreign ion required to cause a ±2% error in the recovery of manganese. The results are reported in Table 2. Cobalt(II), nickel(II) and copper(II) (80 μg of each) were eliminated by prior washing with 1 mol dm^{-3} ammonia solution. Interference from zinc(II) and lead(II) was eliminated by selective masking with thiocyanate and thiosulphate, respectively.

Separation and Determination of Manganese(II) in Binary Mixtures

Separation of manganese(II) from binary mixtures containing titanium(IV), iron(III) and aluminium(III) was possible by selective stripping. Manganese was stripped into 0.01 mol dm^{-3} nitric acid, whereas titanium, iron and

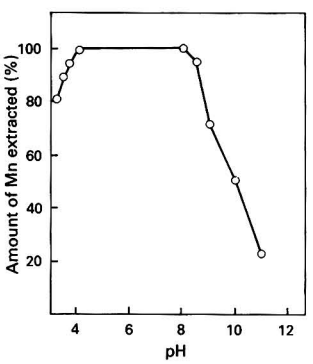

Fig. 1 Extraction of manganese as a function of pH. Mn^{II} = 8 μg; [sodium salicylate] = 0.05 mol dm^{-3}; and [Aliquat 336] = 3% m/v

Table 3 Separation of manganese(II) from binary mixtures

Composition of synthetic mixture*	Manganese: Amount recovered†/μg	Manganese: Standard deviation/μg	Manganese: Relative standard deviation (%)	Added ion: Amount recovered†/μg	Added ion: Standard deviation/μg	Added ion: Relative standard deviation (%)
Mn(8)–Ni(25)	8.0	0.087	1.09	24.8	0.109	0.44
Mn(8)–Cr(16)	8.0	0.055	0.69	16.0	0.141	0.88
Mn(8)–Fe(8)	8.0	0.064	0.79	8.0	0.109	1.37
Mn(8)–Hg(24)	8.0	0.089	1.12	23.9	0.155	0.65
Mn(8)–Co(16)	8.0	0.055	0.69	15.9	0.167	1.05
Mn(8)–Cu(8)	8.0	0.034	0.43	8.0	0.087	1.09
Mn(8)–Ti(100)	8.0	0.040	0.50	99.6	0.179	0.18
Mn(8)–V(100)	8.0	0.045	0.56	99.8	0.224	0.22
Mn(8)–Al(8)	8.0	0.071	0.89	8.0	0.130	1.58
Mn(8)–W(50)	8.0	0.065	0.82	49.6	0.155	0.31
Mn(8)–Bi(80)	8.0	0.089	1.12	79.5	0.178	0.22

* Values in parentheses are the amounts of each metal ion in micrograms.
† Mean of six determinations.

Table 4 Determination of manganese in alloys and pharmaceutical samples

Sample	Certified value	Recovery of Mn by proposed method*	Standard deviation	Relative standard deviation (%)
Alloys—				
High manganese steel (BCS-CRM 494)†	13.55%	13.45%	0.022%	0.17
13% Mn steel (SS 290/2)‡	12.5%	12.4%	0.109%	0.88
Monel alloy 400 (BCS-CRM 363)	1.03%	1.02%	0.014%	1.35
Pharmaceutical samples—				
Supradyn tablet (Roche, India)	500 μg	488 μg	0.547 μg	0.11
Theragran-M tablet (Sarabhai, India)	689 μg	705 μg	0.894 μg	0.13

* Average of six determinations.
† BCS-CRM = British Chemical Standard, Certified Reference Material.
‡ SS = Primary spectroscopic standard.

Table 5 Determination of manganese in environmental samples

Sample	Recovery of Mn by proposed method*	Amount of Mn found by AAS†
Airborne particulate samples—		
Tilak Nagar	0.33 μg m^{-3}	0.33 μg m^{-3}
Khar I	0.25 μg m^{-3}	0.25 μg m^{-3}
Khar II	0.23 μg m^{-3}	0.23 μg m^{-3}
Parel	0.28 μg m^{-3}	0.28 μg m^{-3}
Water samples (Patalganga river water, Maharashtra)—		
Khopoli bridge	248 μg dm^{-3}	250 μg dm^{-3}
Rasayani	140 μg dm^{-3}	142 μg dm^{-3}

* Average of six determinations; manganese determined by spectrophotometry after extraction.
† Manganese determined by atomic absorption spectrometry prior to extraction.

aluminium were stripped with 2 mol dm^{-3} sulphuric acid, 1 mol dm^{-3} hydrochloric acid and 2 mol dm^{-3} hydrochloric acid, respectively. Titanium, iron and aluminium were subsequently determined by spectrophotometry with hydrogen peroxide,[17] 1,10-phenanthroline[17] and Xylenol Orange,[18] respectively. Mercury(II) and bismuth(III) exhibited co-extraction and were separated after first stripping manganese into 0.01 mol dm^{-3} nitric acid and then stripping mercury and bismuth into 1 mol dm^{-3} sulphuric acid. The stripped ions were determined by spectrophotometry with diphenylcarbazide[19] and Xylenol Orange,[17] respectively. Nickel(II), cobalt(II) and copper(II) also co-extracted with manganese(II). They were, however, stripped into 1 mol dm^{-3} ammonia solution and determined by spectrophotometry[17,20] before manganese was stripped and determined as described under General Extraction Procedure for Manganese(II).

The extraction of manganese with the recommended procedure facilitated its separation from chromium(VI), vanadium(V) and tungsten(VI) in binary mixtures as they were not extracted and remained completely in the aqueous phase. The aqueous solution containing chromium, vanadium and tungsten was evaporated to dryness, and the residue treated with perchloric acid to decompose salicylate and finally taken up in water. Chromium, vanadium and tungsten were then determined by spectrophotometry.[17] The results of the separation are reported in Table 3. The recoveries of added ions were ≥99.2%.

Application to the Analysis of Alloys, Pharmaceutical and Environmental Samples

The proposed method was applied to the separation and determination of manganese in various alloys, namely, high manganese steel, 13% manganese steel and monel alloy 400. A 0.1 g amount of each of the alloys was dissolved in 4 ml of concentrated nitric acid, and the solution diluted to 50 ml with water. An aliquot of the solution (0.5 ml of Mn steel and 1 ml of monel alloy solutions) was analysed for manganese by the proposed method. The results are in good agreement with the certificate values (Table 4).

Two different multi-vitamin tablet preparations, namely Supradyn and Theragran-M, were also analysed by the proposed method. The tablets (one of each) were dissolved in 10 ml of 70% perchloric acid, the solution was evaporated to dryness, digested with 5 ml of 0.1 mol dm^{-3} HCl, then filtered and the filtrate made up to volume (10 ml). An aliquot (1 ml) of the solution was used for analysis. The results are reported in Table 4.

Water samples were collected from the Patalganga river (Maharashtra), sampled at Khopoli bridge and Rasayani, as there are many industries around these areas. Each sample (1 l) was concentrated and adjusted to 25 ml, and an aliquot (2 ml) of this solution was extracted by the proposed method. The results of the analysis are presented in Table 5.

Filter-paper strips containing adsorbed manganese particulates from polluted air samples were collected from different suburban areas of Bombay such as Tilak Nagar, Khar and Parel and were supplied by the Air Pollution Monitoring Research Laboratory, Municipal Corporation of Greater Bombay, Khar. The samples were analysed by the proposed method by digesting filter-paper strips (area, 8 cm^2) with 15 ml of 25% nitric acid for about 15 min. After filtration, the entire solutions were used for the extraction and determination of manganese as described under General Extraction Procedure for Manganese(II). The results obtained by the proposed method were confirmed by AAS prior to extraction and were found to be in good agreement (Table 5). The detection limit for manganese was 0.1–100 μg in 25 ml.

The authors thank the University Grants Commission, New Delhi, for financing the project and awarding a fellowship to one of them (N.M.S.).

References

1 *Toxic Metals—Pollution Control and Worker Protection*, ed. Marshall, S., Noyes Data Corporation, NJ, 1976, pp. 184–189.
2 Florence, T. M., and Farrar, Y. J., *Aust. J. Chem.*, 1969, **22**, 473.
3 McClellen, B. E., and Benson, V. M., *Anal. Chem.*, 1964, **36**, 1985.
4 Prabil, R., and Adam, J., *Talanta*, 1973, **20**, 49.
5 Classen, V. P., de Jong, G. J., and Brinkman, U. A. Th., *Fresenius Z. Anal. Chem.*, 1977, **287**, 138.

6 Sato, T., *J. Chem. Tech. Biotechnol.*, 1979, **29**, 39.
7 Morris, D. F. C., Short, E. L., and Slater, D. N., *J. Inorg. Nucl. Chem.*, 1964, **26**, 627.
8 Imata, R., *Niigata-ken Kogai Kenkyusho Kenkyu Hokoku*, 1980, **5**, 69.
9 March, J. G., *Microchem. J.*, 1985, **32**, 338.
10 Agget, J., Evans, D. J., and Hancock, R., *J. Inorg. Nucl. Chem.*, 1968, **38**, 2529.
11 Islam, F., and Biswas, R. K., *J. Bangladesh Acad. Sci.*, 1981, **5**, 61.
12 de Jong, G. J., Kok, W. T., and Brinkman, U. A. Th., *J. Chromatogr.*, 1977, **135**, 249.
13 Gogia, S. K., Singh, O. V., and Tandon, S. N., *Indian J. Chem. Sect. A*, 1983, **22**, 965.
14 Sundaramurthi, N. M., and Shinde, V. M., *Analyst*, 1989, **114**, 201.
15 Vogel, A. I., *A Textbook of Quantitative Inorganic Analysis*, Longman, London, 3rd edn., 1962, p. 453.
16 *Photometric and Fluorometric Methods of Analysis*, ed. Snell, F. D., Wiley, New York, 1978, p. 1028.
17 Marczenko, Z., *Spectrophotometric Determination of Elements*, ser. ed. Chalmers, R. A., Ellis Horwood, Chichester, 1976, pp. 154, 215, 227, 309, 556, 569 and 592.
18 Pritchard, D. T., *Analyst*, 1967, **92**, 103.
19 Balt, S., and van Dalen, E., *Anal. Chim. Acta*, 1962, **27**, 416.
20 Pease, B. F., and Williams, M. B., *Anal. Chem.*, 1959, **31**, 1044.

Paper 0/04129G
Received September 10th, 1990
Accepted January 3rd, 1991

BOOK REVIEWS

Journal of Chromatography: Volume 500
Edited by R. W. Giese, J. K. Haken, K. Macek, L. R. Snyder and E. Heftmann. Pp. ix + 707. Elsevier, Amsterdam, 1990. Price Dfl 220.00. ISSN 0021 9673.

Among the first major scientific journals were those founded by the national chemical societies, *J. Chem. Soc.*, *J. Am. Chem. Soc.*, *Berichte*, and many others. Smaller groups with more specialist interest generated more closely defined journals, *The Analyst, Faraday Trans.*, *Fresenius J. Anal. Chem.*, *etc.* Then in the 1950s and 60s with the post-war resurgence of the chemical industry with the developments in synthetic polymers, pharmaceutical and consumer items, came a sudden flurry of new titles, often from commercial publishers. Some addressed broad areas, such as *Tetrahedron* and *Tetrahedron Lett.* Others were more directed and of these *J. Chromatogr.* must have been one of the most successful.

Founded 32 years ago, in 1958, in response to the developments of what was then only a fledgling technique, the *Journal of Chromatography* has grown in scope and importance and has now reached Volume 500, with new volumes being added at the rate of 37 per year, reflecting the enormous growth and continual importance of separation methods in chemistry over these years.

This hard-bound commemorative volume remembers these early days and the development of chromatography with a collection of photographs collected by Michael Lederer, the Editor of the Journal for many years. These range from scenes of the early editorial office set in the snow of the Swiss alps, the founders and many of the pioneers of chromatography, and ends with the younger generation of the Frei family. Many were taken during the social functions at chromatography symposia around the world and depict the conviviality and friendships within the chromatographic community.

The 500th Volume also contains over 30 original papers with the common feature that each includes as an author a member of the editorial board. The topics as always reflect the wide scope of the journal from SFC, TLC, HPLC and GLC to CZE and with a coverage from the basic understanding of the techniques to their applications.

Roger M. Smith

Field Desorption Mass Spectrometry
László Prókai. *Practical Spectroscopy Series: Volume 9.* Pp. vi + 291. Marcel Dekker. 1990. Price $99.75 (USA and Canada); $119.50 (Export). ISBN 0 8247 8303 4.

Field desorption mass spectrometry (FDMS) became at least partially eclipsed by fast atom bombardment mass spectrometry (FAB-MS) and related techniques following their introduction in the early 1980s, but has enjoyed renewed interest in some areas more recently. This book, Volume 9 in the *Practical Spectroscopy Series*, therefore provides both an excellent introduction to the technique and, for those who used FD in pre-FAB days, a timely reminder of the advantages. The book is divided into four readable chapters: Principles; Experimental Techniques and Methods; General Practice; and Applications. Each chapter contains a comprehensive set of literature references.

Chapter 1 summarizes the current state of knowledge concerning the processes involved in producing ions by both field ionization (the forerunner of FD) and by FD. The treatment is extensive and perhaps more mathematical than some readers would prefer, but by the end of the chapter one is left in no doubt as to the complexity of the processes operating during the FD experiment. Having thus grasped (hopefully) a better understanding of these processes, the practitioner may well feel able to obtain better experimental results.

Probably the most important factor in the successful application of FDMS is the preparation of suitable activated emitters; the author accordingly spends some time in Chapter 2 explaining the most widely used high temperature activation process (using benzonitrile) and then goes on to consider the various alternative methods available. The preparation of emitters from different materials, *e.g.*, silicon emitters and various metal dendrites, is also considered and their advantages and disadvantages are discussed.

Chapter 2 continues with an examination of sample supply techniques and means of controlling the emitter heating current, both important for the production of good quality spectra and concludes with several aspects of instrument design.

In 'General Practice' (Chapter 3) the author discusses the operational details such as sample interactions, the use of additives and derivatization which can all be of considerable assistance in the quest for high-quality spectra. Although FD is more widely known for its ability to provide relative molecular mass information on otherwise intractable molecules, many examples have appeared in the literature where structural information has been derived; this aspect is also discussed and, in common with most areas of this book, illustrated with examples taken from the literature. A comparison of FD with the other common ionization techniques helps to put the technique into perspective, and concludes the chapter.

A comprehensive review of all the applications work to date would probably fill an entire volume of this size, so it comes as no surprise that the author has been selective in his approach. He refers the reader to the annual Analytical Chemistry reviews and the Royal Society of Chemistry Specialist Periodical Reports for more comprehensive coverage of recent applications. Four main areas of application have been selected for attention, *viz.*, biochemical, medical and pharmaceutical applications; environmental analysis; the characterization of fossil fuels and petrochemicals; and the analysis of inorganic and organometallic compounds. These are dealt with in such a way as to give the reader a clear insight into the type of work recently undertaken in each area, with numerous well-chosen examples from the literature.

This reviewer felt that this book provided excellent comprehensive coverage of a much underrated technique. It would prove a valuable addition to the library of any mass spectroscopist involved with, or contemplating involvement with, FDMS.

D. Catlow

Steroid Analysis in the Pharmaceutical Industry: Hormonal Steroids, Sterols, Vitamin D, Cardiac Glycosides
Edited by S. Görög. *Ellis Horwood Series in Analytical Chemistry.* Pp. x + 398. Ellis Horwood. 1990. Price £69.50. ISBN 0 7458 0099 8 (Ellis Horwood); 0 470 21178 4 (Halsted Press).

The primary production of bulk steroids together with secondary formulation has been in operation for the past 40 years, but as Professor Görög rightly observes the majority of publications on steroid analysis originate from medical or academic sources. Clearly there is an element of technical security included in some industrial processes, with perhaps less need for industrial analysts to publish their work, so that this book is a novel enterprise.

The book consists of an introductory chapter which reviews the complicated procedures leading to the production of a new synthetic steroid drug. The second chapter, on the methods

used in steroid analysis, correctly occupies almost half of the book, and begins with spectroscopy. The majority of this section is directed to the newer techniques of NMR and mass spectrometry, because the value of ultraviolet spectrometry has declined since the advent of HPLC, although as the author claims, it can still play a part in structural characterization. Infrared spectrometry is noted for the key role played in the early development of steroid synthesis, at least one company favouring Nujol mulls rather than potassium bromide discs suggested by the author as universally used.

Chromatography is the most important technique for industrial steroid analysis, owing to the excellent separations possible with these stable compounds, but is discussed in less detail because it has featured more widely in other steroid publications. Thin-layer chromatography had a revolutionary impact, compared with paper chromatography which only rates a passing mention. It remains the favoured technique for control of impurities. Gas chromatography is discussed briefly but was overshadowed by the introduction of high-performance liquid chromatography, the specific steroid assay procedure. The more limited applications of protein binding and electroanalytical methods, particularly during research and development of a new synthetic steroid, are also mentioned.

The third chapter is concerned with the structural elucidation of steroids, and begins by stressing that there is normally no limit to the amount of material available, a luxury not always appreciated within the industry. Structure determinations can range from the limited applications of ultraviolet spectrometry for steroids with double bonds (using the Fieser–Woodward rules) to complex X-ray diffractometry, and are illustrated by examples from the author's laboratory. The importance is stressed of identifying by-products and establishing impurity profiles in order to satisfy regulatory authorities.

The fourth chapter is fundamental to the aim of the book and is given prominent space as it concerns analytical control during steroid production. The starting material is of crucial importance and the author puts the emphasis on diosgenin, although hecogenin is also successfully used. In-process control and bulk steroid purity assays are discussed.

Chapter 5 deals with the analytical aspects of the studies both before and after formulation. There are useful tables on formulations although the steroids could have been grouped more logically. Stability testing of formulated (secondary) products is reviewed but stability testing at the primary, bulk-drug stage is hardly mentioned although it is very important when production first begins. The final chapter on steroids in biological media includes a useful reminder that the health control of production staff is also important.

The over-all impression is of a worthwhile addition to the literature on steroids.

P. J. Stevens

CUMULATIVE AUTHOR INDEX

JANUARY–MAY 1991

The XXVII Colloquium Spectroscopicum Internationale

XXVII CSI

1991
NORWAY

will be held in

Grieg Hall, Bergen, Norway
June 9–14 1991

IUPAC

This traditional biennial conference in analytical spectroscopy will once again provide a forum for atomic, nuclear and molecular spectroscopists worldwide to encourage personal contact and the exchange of experience.

Participants are invited to submit papers for presentation at the XXVII CSI, dealing with the following topics:

Basic theory and instrumentation of—

- Atomic spectroscopy (emission, absorption, fluorescence)
- Molecular spectroscopy (UV, VIS and IR)
- X-ray spectroscopy
- Gamma spectroscopy
- Mass spectrometry (inorganic and organic)
- Electron spectroscopy
- Raman spectroscopy
- Mössbauer spectroscopy
- Nuclear magnetic resonance spectrometry
- Methods of surface analysis and depth profiling
- Photoacoustic spectroscopy

Application of spectroscopy in the analysis of—

- Metals and alloys
- Geological materials
- Industrial products
- Biological samples
- Food and agricultural products

Special emphasis will be given to trace analysis, environmental pollutants and standard reference materials.
The scientific programme will consist of both plenary lectures and parallel sessions of oral presentation. Specific times will be reserved for poster sessions.

PRE- AND POST-SYMPOSIA

In connection with the XXVII CSI the following symposia will be organised:

Pre-symposia—

I. GRAPHITE ATOMISER TECHNIQUES IN ANALYTICAL SPECTROSCOPY
June 6–8, 1991, Hotel Ullensvang, Lofthus, Norway.

II. CHARACTERISATION OF OIL COMPONENTS USING SPECTROSCOPIC METHODS
June 6–8, 1991, Hotel Hardangerfjord, Øystese, Norway.

III. MEASUREMENT OF RADIO-NUCLIDES AFTER THE CHERNOBYL ACCIDENT
June 6–8, 1991, Hotel Solstrand, Bergen, Norway.

Post-symposium—

IV. SPECIATION OF ELEMENTS IN ENVIRONMENTAL AND BIOLOGICAL SCIENCES
June 17–19, 1991, Hotel Alexandra, Loen, Norway.

For further information contact:

THE SECRETARIAT
XXVII CSI
HSD Congress-Conference
P.O. Box 1721 Nordnes
N-5024 Bergen, Norway.
Tel. 47-5-318414, Telex 42607 hsd n, Telefax 47-5-324555

FIRST FOLD HERE

THE ANALYST READER ENQUIRY SERVICE
For further information about any of the products featured in the advertisements in this issue, write the appropriate number on the postcard, detach and post.

FOLD HERE

THE ANALYST READER ENQUIRY SERVICE

MAY'91

For further information about any of the products featured in the advertisements in this issue, please write the appropriate number in one of the boxes below.
Postage paid if posted in the British Isles but overseas readers must affix a stamp.

PLEASE USE BLOCK CAPITALS LEAVING A SPACE BETWEEN WORDS *Valid 12 months*

1 NAME

2 COMPANY

PLEASE GIVE YOUR BUSINESS ADDRESS IF POSSIBLE. IF NOT, PLEASE TICK HERE ☐

3 STREET

4 TOWN

5 COUNTY
POST CODE

6 COUNTRY

7 DEPARTMENT
DIVISION

8 YOUR JOB TITLE
POSITION

9 TELEPHONE NO

OFFICE USE ONLY REC'D PROC'D

FOLD HERE

Postage will be paid by Licensee

Do not affix Postage Stamps if posted in Gt. Britain, Channel Islands, N. Ireland or the Isle of Man

BUSINESS REPLY SERVICE
Licence No. WD 106

Reader Enquiry Service
The Analyst
The Royal Society of Chemistry
Burlington House, Piccadilly
LONDON
W1E 6WF
England

ROYAL SOCIETY OF CHEMISTRY

NEW PUBLICATIONS

Non-Chromatographic Continuous Separation Techniques

By: M. Valcárcel and M. D. Luque de Castro, *University of Cordoba*

This unique book provides a systematic and comprehensive description of a series of analytical separation techniques that can be regarded as intermediate alternatives between batch manual and chromatographic techniques. Their ease of automation and miniaturization, flexibility for on-line coupling to most available analytical instruments and high potential for the resolution of real problems in the clinical, pharmaceutical, industrial, environmental and nutritional fields endow them with great, increasing relevance and interest as apparent from the recent spectacular increase in publications devoted to these techniques and the growing availability in commercial equipment. The book covers important continuous techniques such as gas diffusion, continuous distillation, continuous hydrate generation, continuous evaporation, dialysis, liquid–liquid extraction, ion exchange, sorption, electrochemical stripping, continuous precipitation, on-line leaching, field flow fractionation and capillary electrophoresis.
The text is supported by a wealth of figures (120), over 600 literature references and a subject index.

Hardcover xii + 290 pages
234 x 156 mm
Price £42.50
ISBN 0 85186 986 6
June 1991

Electron Spin Resonance Vol 12B

Senior Reporter: M.C.R. Symons, *University of Leicester*
Series: Specialist Periodical Reports

This latest volume contains critical reviews of developments during mid 1989 – mid 1990 in the field of inorganic and bio-inorganic aspects of electron spin resonance.
Brief contents:
Transition Metal Ions, Laser Magnetic Resonance Spectroscopy, ESR of Transition Metal Ions in Zeolites, Metalloproteins, EPR Imaging, Inorganic and Organometallic Radicals, Author Index.

Hardcover xiv + 258 pages
216 x 138 mm
Price £105.00
ISBN 0 85186 891 6
April 1991

Nuclear Magnetic Resonance Vol 20

Senior Reporter: G. A. Webb, *University of Surrey*
Series: Specialist Periodical Reports

Nuclear Magnetic Resonance Vol. 20 reviews the literature published between June 1989 and May 1990.

Contents:
N.M.R. Books and Reviews, Theoretical and Physical Aspects of Nuclear Shielding, Applications of Nuclear Shielding, Theoretical Aspects of Spin–Spin Couplings, Applications of Spin–Spin Couplings, Nuclear Spin Relaxation in Liquids and Gases, Solid State N.M.R., Multiple Pulse N.M.R., Natural Macromolecules, Synthetic Macromolecules, Conformational Analysis, Nuclear Magnetic Resonance of Living Systems, Nuclear Magnetic Resonance Imaging of Living Systems, N.M.R. of Paramagnetic Species, N.M.R. of Liquid Crystals and Micellar Solutions, Author Index.

Hardcover xxii + 602 pages
216 x 138 mm
Price £140.00
ISBN 0 85186 432 5
April 1991

Analytical Applications of Spectroscopy II

Edited by: A. M. C. Davies, *Norwich Near-Infrared Consultancy* and C. S. Creaser, *University of East Anglia*

Analytical Applications of Spectroscopy II provides wide-ranging coverage of recent developments in analytical spectroscopy and particularly the common themes of chromatography – spectroscopy combinations, new techniques and data handling. These themes have played an increasingly important part in advances in spectroscopic techniques and emphasize the multidisciplinary approach of present research.
The book presents an up-to-date review of the major spectroscopic techniques and supplements the information found in the previous volume published in 1988.
Each section includes reviews of key areas of current research, as well as short reports of new developments in those areas, written by spectroscopists who have made major contributions in their respective disciplines.
Brief contents: Introduction, Vibrational Spectroscopy, Microscopy, Mass Spectrometry, Combined Techniques, Chemometrics and Data Handling, Subject Index, Author Index.

Hardcover xii + 324 pages
234 x 156 mm
Price £49.50
ISBN 0 85186 403 1
May 1991

ROYAL SOCIETY OF CHEMISTRY

Information Services

To Order, *Please write to the:*
Royal Society of Chemistry, Turpin Transactions Ltd, Blackhorse Road, Letchworth, Herts SG6 1HN, UK.
or telephone (0462) 672555 quoting your credit card details. We can now accept Access/Visa/MasterCard/Eurocard.

Turpin Transactions Ltd, distributors, is wholly owned by the Royal Society of Chemistry.

For information on other books and journals, *please write to:*
Royal Society of Chemistry, Sales and Promotion Department, Thomas Graham House, Science Park, Milton Road, Cambridge CB4 4WF, UK.

RSC Members *should obtain members prices and order from :*
The Membership Affairs Department at the Cambridge address above.

Circle 006 for further information

ANALAO 116(5) 437–548 (1991) May 1991

The Analyst

The Analytical Journal of The Royal Society of Chemistry

CONTENTS

Typeset and printed by Black Bear Press Limited, Cambridge, England